

**SISSA**

Scuola  
Internazionale  
Superiore di  
Studi Avanzati

Physics Area - PhD course in  
Statistical Physics

**Entanglement, symmetries and  
interfaces in one-dimensional quantum  
systems**

Candidate:  
Luca Capizzi

Advisor:  
Pasquale Calabrese

Academic Year 2022-2023





# List of publications

- [1] **Capizzi Luca**, Ruggiero Paola and Calabrese Pasquale, *Symmetry resolved entanglement entropy of excited states in a CFT*, *J. Stat. Mech.* (2020) 073101.
- [2] Horvath David X., **Capizzi Luca**, and Calabrese Pasquale,  *$U(1)$  symmetry resolved entanglement in free 1+1 dimensional field theories via form factor bootstrap*, *JHEP* 2021, 197 (2021).
- [3] **Capizzi Luca**, and Calabrese Pasquale, *Symmetry resolved relative entropies and distances in conformal field theory*, *JHEP* 2021, 195 (2021).
- [4] **Capizzi Luca**, Horvath David X., Calabrese Pasquale, and Castro-Alvaredo Olalla A., *Entanglement of the 3-state Potts model via form factor bootstrap: total and symmetry resolved entropies*, *JHEP* 2022, 113 (2022).
- [5] **Capizzi Luca**, Castro-Alvaredo Olalla A., De Fazio Cecilia, Mazzoni Michele, and Santamaria-Sanz Lucia, *Symmetry resolved entanglement of excited states in quantum field theory. Part I. Free theories, twist fields and qubits*, *JHEP* 12 (2022) 127.
- [6] **Capizzi Luca**, De Fazio Cecilia, Mazzoni Michele, Santamaria-Sanz Lucia and Castro-Alvaredo Olalla A., *Symmetry resolved entanglement of excited states in quantum field theory. Part II. Numerics, interacting theories and higher dimensions*, *JHEP* 12 (2022) 128.
- [7] **Capizzi Luca**, Mazzoni Michele, and Castro-Alvaredo Olalla A., *Symmetry Resolved Entanglement of Excited States in Quantum Field Theory III: Bosonic and Fermionic Negativity*, *JHEP* 2023, 74 (2023) .
- [8] **Capizzi Luca**, Murciano Sara, and Calabrese Pasquale, *Renyi entropy and negativity for massless Dirac fermions at conformal interfaces and junctions*, *JHEP* 2022, 171 (2022).
- [9] **Capizzi Luca**, Murciano Sara, and Calabrese Pasquale, *Renyi entropy and negativity for massless complex boson at conformal interfaces and junctions*, *JHEP* 2022, 105 (2022).
- [10] **Capizzi Luca** and Eisler Viktor, *Entanglement evolution after a global quench across a conformal defect*, *SciPost Phys.* 14 (2023) 070.
- [11] **Capizzi Luca** and Eisler Viktor, *Zero-mode entanglement across a conformal defect*, *J.Stat.Mech.* 2305 (2023) 053109.
- [12] **Capizzi Luca**, Scopa Stefano, Rottoli Federico and Calabrese Pasquale, *Domain wall melting across a defect*, *EPL* 141 (2023) 31002.

- [13] **Capizzi Luca**, Giachetti Guido, Santini Alessandro, and Collura Mario, *Spreading of a local excitation in a quantum hierarchical model*, [PRB 13, 134210 \(2022\)](#).
- [14] Bonsignori Riccarda, **Capizzi Luca**, and Panopoulos Pantelis, *Boundary Symmetry Breaking in CFT and the string order parameter*, [JHEP 2023, 27 \(2023\)](#).
- [15] **Capizzi Luca**, Murciano Sara, and Calabrese Pasquale, *Full counting statistics and symmetry resolved entanglement for free conformal theories with interface defects*, [arxiv:2302.08209](#).
- [16] **Capizzi Luca**, Vanoni Carlo, Calabrese Pasquale, and Gambassi Andrea, *A hydrodynamic approach to Stark localization*, [arXiv:2303.14059](#).

# Chapter 1

## Introduction

Quantum mechanics is nowadays considered the cornerstone of fundamental physics. During the last century, it has been a guiding line for the formulation of theories aimed to describe a variety of puzzling and counterintuitive phenomena that have been observed in microscopic systems (atoms, particles, cold gases, and so on). While so far a satisfying unifying theory to describe our universe is probably missing, a landscape of quantum models with distinct features has been proposed. A key feature shared by these different formulations is *entanglement*, which is arguably the distinct signature of the quantum world [17, 18]. It tells us that a local probe on a quantum system can have *instantaneous* consequences for arbitrarily distant points. At the very naive level, the presence of these non-local correlations seems to be unavoidable in contrast with relativity, where a maximum velocity of information spreading is present, and with causality: for this reason Einstein was skeptical about quantum theory and used to refer to entanglement as a *spooky action at a distance*[19]. Nowadays, although we know that it is not the case, still the consequences of entanglement are highly counterintuitive, as they are not usually observed in everyday life.

Quantum correlations are at the center of many problems in physics, and apparently disconnected communities, ranging from condensed matter to high-energy, are interested in their characterization. Attempting to compile a comprehensive list of topics where entanglement holds relevance is likely a daunting task, but I will make an attempt nonetheless.

In 1982 Feynman proposed that quantum systems might be efficiently simulated with a computer operating through the rules of the quantum realm [20]. That was a (say, the) input for the development of quantum information theory. During 90s, it was taken into account the possibility of a 'quantum advantage' could arise indeed if 'quantum-bits' (qu-bit) were employed as fundamental pieces of information: these could be atoms, photons, but most importantly they have to be small physical systems where quantum effects play a role. We only mention the famous Shor's algorithm [21], the branch of quantum cryptography [22], quantum teleportation [23], and so on. While many of these protocols were born as 'theoretical possibilities', our ability to manipulate quantum systems has grown up during the last decades, and the dream of Feynman could eventually become a reality in the next few years. Behind these studies, the advantage with respect to the common classical protocols is usually strictly related to the possibility to store and manipulate a large number of highly correlated (entangled) qubits. This is a hard task, as any possible source of noise arising from a coupling with an external environment seems to destroy any possible coherence, making entanglement extremely fragile.

For these reasons, physical systems whose quantum correlations are robust with respect to local perturbation are probably the best candidates to be realistic qubits. Among them, we

mention topological systems [24], as spin liquids, or Quantum Hall phases [25, 26], whose ability to store non-local information (dubbed as topological order) has been considered a promising feature in this respect.

The aforementioned quantum systems/protocols can also be simulated using classical computers. However, this simulation task is typically highly demanding, as expected due to the 'quantum advantage'. Additionally, the efficiency of describing a given quantum system using conventional classical methods is closely tied to the level of entanglement present in the system being simulated. For example, the accuracy of Matrix Product States (MPS) representations, such as the Density Matrix Renormalization group, heavily relies on the amount of entanglement within the system [27]{30}. This explains why these methods effectively describe ground-states of gapped one-dimensional systems with a finite amount of entanglement.

A comprehensive understanding of entanglement is essential in the realm of high-energy physics as it enables the exploration of connections and compatibility between gravity and microscopic quantum principles. Specific examples highlighting this significance are the quantum hole-information paradox, the Bekenstein-Hawking entropy [31, 32] along with the Ryu-Takayanagi formula [33, 34] within the framework of AdS/CFT [35].

## 1.1 What is (NOT) entanglement?

So far, we have discussed mostly areas of physics where entanglement is relevant. However, we have not provided a specific definition of entanglement, nor have we distinguished it from other types of (classical) correlations that we are familiar with. In order to clarify this, I would like to present a simple example to illustrate what entanglement is not.

Imagine there is a bag with two balls inside, one is black, and the other one is white. Two guys, say Mario and Luigi, have to pick a ball each. They do it, they keep the ball in their hand, they take a train, traveling to very distant locations, and eventually, they open their hand to see the color of their ball. If Mario sees a white ball in his hand he immediately knows that Luigi has a black ball in his hand, and viceversa. Superficially, one might argue that information is being transmitted instantaneously in this scenario. However, fortunately, this notion is not taken seriously. It is widely understood that the correlation between the colors observed by Mario and Luigi is merely "apparent" and stems from their incomplete knowledge prior to opening their hands. In reality, the color of each ball was already determined and fixed from the moment they made their selections.

The previous one was an example of classical correlations, and, as we have explained, they cannot be considered as an intrinsic property of a given scenario, and they are related to incomplete information about the systems. Viceversa, in the quantum world a similar, albeit conceptually different, example can be provided to show that certain correlations can be indeed intrinsic, and ultimately quantum. Alice and Bob take two spins  $1/2$  and prepare the system in a singlet state

$$|j-i\rangle = \frac{1}{\sqrt{2}} (|j\neq i, j\neq i\rangle) : \quad (1.1)$$

Each of them picks one of the two spins, keeping it decoupled from the environment, and eventually measures its polarization along a given axis, say the z-axis. When Alice finds a spin-up, she immediately knows that Bob will measure spin down, and viceversa. At first glance, apart from the distinct mathematical formulation of the problem, this scenario may not appear significantly different from the earlier example with Mario and Luigi. However, there exists a crucial dis-

tion: it is possible to demonstrate that the indeterminacy described above arises not merely from Alice and Bob's incomplete knowledge, but from an intrinsic property. In particular, this property stems from the fact that measurements of magnetization can be performed along any direction, but subsequent measurements along two distinct directions do not commute (the order in which they are conducted matters).

The two examples above should be able to show in their simplicity, that there might be issues and subtleties to define properly which correlations are classical and which ones are quantum, and how to quantify/distinguish them. This is where entanglement measures appear and help us to discriminate those cases. We will not enter the details, but we mention that there is a widely accepted definition of what classical correlations are. These are correlations that can be generated by local operation and classical communication (LOCC), and the interested reader can find mathematical details in Ref. [36]. We only mention that the example of Mario and Luigi satisfies those conditions, therefore no quantum correlations are present in that scenario.

When no classical correlations are present, namely for pure states, one might be interested to quantify quantum correlations. This is the purpose of the so-called von Neumann entropy, or simply entanglement entropy [37, 38]: it tells us how much certain (algebra of) complementary observables are correlated among each other in a given pure state. In the case where the system is described by the composition of two subsystems  $A$  and  $B$ , say the Hilbert space is

$$H = H_A \otimes H_B \quad (1.2)$$

and the correlations between  $A$  and  $B$  are concerned, the von Neumann entropy is expressed by

$$S = -\text{Tr}(\rho_A \log \rho_A); \quad (1.3)$$

with  $\rho_A = \text{Tr}_B(\rho_{AB})$ . Here  $\rho_{AB}$  is the state of the system, while  $\rho_A$  is its reduced density matrix. Using the definition above, one can easily verify that in the example of Alice and Bob the von Neumann entropy between the two spins is precisely  $S = \log 2$ ; moreover, one can show that that value is maximal for the system under consideration, therefore we say that the spins are maximally entangled.

If both classical and quantum correlations are present, the story becomes much more complicated. Indeed, tons of inequivalent entanglement measures have been provided in those settings to isolate the quantum contributions (mutual information [39], purity [40], reflected entropy [41]). We spend some words for the negativity [42, 43], important for later purposes. Given a, possibly mixed, state  $\rho_{AB}$  of  $H_A \otimes H_B$ , the logarithmic negativity is defined as

$$E = \log \|\rho_{AB}^{T_A}\|_1 \quad (1.4)$$

With  $\rho_{AB}^{T_A}$  being the partial transposed reduced density matrix and  $\|\cdot\|_1$  the trace norm. With respect to the von Neumann entropy, the negativity allows dealing with spurious classical correlations, say with an additional environment, not contributing to its value: for this reason, it can be considered a good measure of quantum correlations.

The definitions presented earlier can be easily applied to compute the entanglement of systems with a small number of degrees of freedom. However, complications arise when dealing with many-body systems. Firstly, evaluating the provided entanglement measures directly is computationally intensive, limiting investigations to relatively small system sizes (such as spin chains of 15-20 sites). Secondly, and perhaps more significantly, these measures often diverge in the large-scale limit of interest. Therefore, it becomes more meaningful to understand how these measures scale with increasing system size rather than their specific values at a given large size.

Insights into these questions have emerged from the study of quantum field theories (QFT). Specifically, it has been recognized that the entanglement between spatial regions in the vacuum state of a QFT arises from correlations across the boundaries of these regions. The entanglement entropy follows a sub-extensive behavior<sup>1</sup>, adhering to what is known as an "area law" [44, 45]. On the other hand, for typical high-energy states (states with finite energy density), the entropy matches the thermodynamic entropy of the corresponding Gibbs ensemble and exhibits an extensive character.

While this scenario, referred to as the "standard" case, is expected to hold for a broad range of theories, our quantitative understanding primarily stems from 1+1 QFTs. In particular, this understanding is prominent in conformal field theories (CFTs) [46], which describe quantum critical points with relativistic features, and integrable field theories [47, 48], corresponding to specific types of massive deformations.

Most of this thesis will be devoted to the investigation of some specific features of entanglement in the context of one-dimensional quantum systems at, or close to, criticality. For those systems, analytical techniques employed in 1+1 QFTs are fundamental, and they allow investigating properties that are impossible (or, at least, very hard) to establish by first principles.

## 1.2 Structure of the thesis

The primary focus of the first part of this thesis revolves around the fundamental question regarding the relationship between entanglement and (global) symmetries in many-body quantum systems. This inquiry arises from the noteworthy experimental findings reported by Lukin et al. [49], which established that comprehending the finer structure of entanglement, influenced by the presence of symmetry sectors, enables a better understanding of distinct regimes observed in the entanglement dynamics of certain disordered systems. That was the birth of *Symmetry-resolved entanglement*.

Specifically, when investigating systems that conserve the number of particles, corresponding to a U(1) symmetry, entanglement manifests in two distinct forms: number entanglement and configurational entanglement. Number entanglement quantifies the potential variations in the number of particles observed within a specific spatial region, while configurational entanglement measures the abundance of configurations that can be observed with a given number of particles.

Concurrently, theoretical frameworks have been developed by Xavier, Alcaraz, and Sierra in [50] and Goldstein and Sela in [51] to address the challenge of extracting these two contributions separately. These frameworks provide quantitative predictions, particularly in one-dimensional critical systems employing CFT, revealing a characteristic known as *entanglement equipartition*. This property indicates that the contributions to entanglement originating from particle numbers close to the average are equal. The origin of this feature has been traced back to the large amount of quantum fluctuations stored in a critical ground state.

Our initial goal was to explore massive (integrable) field theories in order to gain insight into the subtle changes that occur in symmetry-resolved entanglement slightly away from the critical point. This task is non-trivial as certain properties are shared with the underlying CFT, such as the entropy divergence for small (UV) cut-off, while others depend on the existence of a finite

---

<sup>1</sup>Strictly speaking, the entropy of a QFT is usually finite: roughly this is related to the presence of a finite number of degrees of freedom in any given region. However, it is possible to address this by applying ultraviolet regularization to cure the divergences, followed by extracting the limit of the regularization. It is important to note that the regularization procedure can influence certain quantitative aspects, so-called "universal" characteristics can be deemed physically meaningful.

correlation length, which becomes apparent through the decoupling of entangled points at large distances. To address this challenge, we employ the integrable bootstrap technique to analyze the ground state entanglement of specific QFTs, including free fermions/bosons (Chapter 2) and the 3-state Potts model (Chapter 3). This approach enables us to systematically investigate the large-distance behavior of symmetry-resolved entanglement and make analytical predictions regarding its universal features. Furthermore, we were able to observe the recovery of entanglement equipartition, which arises from the presence of UV divergent fluctuations akin to those observed in CFTs.

Subsequently, we proceed to examine excited states with zero energy density, which can be effectively characterized as perturbations above the ground state. Since many similarities exist between these excited states and the ground state, it is crucial to exercise caution in distinguishing them. Firstly, we direct our attention toward regions that are comparable in size to the system itself. Secondly, since quantum fluctuations in the ground state dominate in QFT<sup>2</sup>, it becomes needed to isolate the contributions stemming from the excitations. To accomplish this, we demonstrate the universality of specific ratios of charged moments. These ratios exhibit well-behaved thermodynamic limits and effectively capture the distinct features of various states.

We explore two distinct classes of states in our analysis. Firstly, in Chapter 4 we examine quasiparticle states, which exhibit an effective decoupling between zero-point fluctuations and excitations. For these states, we can provide simple model-independent semiclassical predictions. Specifically, we offer a general prediction for the ratio of charged moments, which we verify through both analytical and numerical methods in specific cases. By establishing the validity and generality of this mechanism, which has eluded microscopic description thus far, we introduce a unifying framework that holds true in any dimension. This framework relies on minimal assumptions regarding the large-distance behavior of ground state correlation functions, along with algebraic relationships between certain twist operators and local fields.

Next, we shift our focus to analyzing the low-lying states of CFT. In Chapter 5 we introduce a novel concept of a symmetry-resolved measure of indistinguishability for these states, expanding upon our previous examination of symmetry-resolved entropies in Ref. [1]. Interestingly, these states lack a simple semiclassical interpretation, and no decoupling with zero-point fluctuations is observed. Consequently, a case-by-case analysis becomes necessary, and we provide a comprehensive investigation of the lowest energy states of free Dirac massless fermions utilizing bosonization techniques. Additionally, we explore an operator product expansion approach that offers predictive capabilities for small subsystems and allows for establishing generic features across a wide range of states.

The second part of the thesis focuses on examining the entanglement of one-dimensional systems when localized defects are present. Specifically, it investigates the impact of these impurities on systems that would otherwise exhibit translational invariance. A paradigmatic example of the impact was elucidated by Kane and Fisher [52]. It was shown that a local impurity can be a relevant or irrelevant perturbation to a Luttinger Liquid depending on the sign of the interaction. In the absence of interactions, the defect becomes marginal, and non-trivial scale invariant boundary conditions emerge. Striking consequences are present for critical free systems for the entanglement across the defect. In particular, it was first observed numerically and then characterized analytically a logarithmic scaling of the entropy with a prefactor depending on the details of the defect [53{55] and not only on the underlying central charge (as it happens for the homogeneous counterpart, see [46]). While many specific cases have been addressed, and exact

---

<sup>2</sup>Specifically, UV divergences are independent of the state

predictions have been provided, the underlying mechanism is yet not completely understood in a satisfactory manner.

To address the quantum correlations arising from the coupling of multiple one-dimensional critical systems (wires) via a scale-invariant defect, we initially present in Chapter 6 a CFT approach to entanglement entropy and negativity. Previous studies have demonstrated that, for two wires, the characteristics of the defect can be captured by a single parameter representing the transmission. However, the governing factors dictating the entanglement among subsets of wires in the case of multiple wires remained unclear prior to our work. Our objective was to fill this knowledge gap. Specifically, we established that the spectrum of certain projections of the boundary scattering matrix is responsible for this entanglement. We provided explicit predictions for free bosons and fermions, establishing a connection between the above-mentioned spectrum and the entanglement measures.

We move to the dynamics, analyzing two distinct quenches protocols showing macroscopic effects induced by the defect. First, in Chapter 7 we considered a global quench, and we investigate the linear growth of entanglement across a defect. Our original contribution was to show that, due to the coherence between the long-range correlations arising from the defect and the dynamically generated ones, the analytical predictions for the entanglement growth escape any simple naive semiclassical interpretation (in contrast to homogeneous systems, see also Ref. [56]). The mechanism above has been deeply characterized for lattice free fermions, and a quasiparticle picture, which keeps track of interference effects, has been provided. Furthermore, a second original contribution was to formulate the problem in a CFT framework, employing a novel notion of boundary twist fields. This approach allowed us to tackle the dynamics of initial states with thermal properties, and it also looked promising to solve some previous puzzles regarding the equilibrium features.

Lastly, in Chapter 8 we delve into the dynamics resulting from an inhomogeneous initial state, specifically a quench protocol known as domain-wall melting. Initially, we offer a seemingly straightforward and intuitive description of the dynamics, based on the evolution of a local occupation function in the semiclassical phase space. This description proves to be effective in predicting local observables, and we provide analytical predictions for the density profiles. However, when it comes to quantitatively describing the entanglement properties across the interface, this approach fails due to the dynamical generation of long-range correlations at the interface. To overcome this limitation, we introduce a quasiparticle prescription that successfully addresses these issues, enabling us to provide analytical predictions for the entanglement entropy in this scenario.

# Contents

<b>1</b>	<b>Introduction</b>	<b>5</b>
1.1	What is (NOT) entanglement?	6
1.2	Structure of the thesis	8
<b>I</b>	<b>Symmetry resolution of entanglement</b>	<b>15</b>
<b>2</b>	<b>Symmetry resolved entanglement in <math>U(1)</math> free theories</b>	<b>17</b>
2.1	Introduction	17
2.2	Form Factors of Twist Fields for integrable theories	19
2.3	Form factors for free Dirac fermions	22
2.4	Form factors for free complex bosons	24
2.5	Replica diagonalization approach	25
2.6	Two-point function of composite $U(1)$ twist fields	27
2.7	Symmetry resolved Renyi entropies	28
2.8	Concluding remarks	30
2.A	Analytic continuation $n! \rightarrow 1$	30
2.B	Vacuum expectation values	31
<b>3</b>	<b>Symmetry resolved entanglement of the 3-state Potts model</b>	<b>35</b>
3.1	The model	35
3.2	Twist fields and their form factors	38
3.2.1	Form factors of Branch Point Twist Fields	41
3.2.2	Form factors of the Disorder operator $\sigma_1$	41
3.2.3	Form factors of the composite twist fields	43
3.2.4	Checks via $\sigma$ -sum rule	44
3.3	Two-point function of composite $Z_3$ twist fields	46
3.4	Symmetry resolved entanglement	49
3.5	Concluding remarks	51
3.A	Minimal form factor	51
3.B	Computation of $f_{AA}(0; 1; 0)$	52
<b>4</b>	<b>Symmetry- resolved entanglement of quasiparticle states</b>	<b>55</b>
4.1	Introduction and main results	55
4.2	Magnons	58
4.2.1	One-Magnon States	58
4.2.2	Two-magnon states	59

4.3	Form factors approach to 1+1 free theories . . . . .	60
4.3.1	Complex free boson . . . . .	62
4.3.2	Complex free fermion . . . . .	64
4.4	Twist operator approach . . . . .	66
4.4.1	Excited States and Operator Algebra . . . . .	66
4.4.2	Replica construction of the charged moments . . . . .	68
4.4.3	Single-Particle State . . . . .	70
4.5	Numerical Results . . . . .	71
4.5.1	1D Lattice Fermi Gas . . . . .	71
4.5.2	Complex harmonic chain . . . . .	73
4.6	Concluding remarks . . . . .	77
4.A	Form factor computations . . . . .	78
4.A.1	Single-Particle bosonic state . . . . .	78
4.A.2	Single-Particle fermionic state . . . . .	80
<b>5</b>	<b>Symmetry-resolved relative entropies and distances in CFT</b> . . . . .	<b>83</b>
5.1	Introduction and definitions . . . . .	83
5.1.1	Symmetry resolved relative entropies and distances . . . . .	84
5.1.2	Reduced density matrices and charged moments . . . . .	85
5.2	From replicas and charged twist fields to symmetry resolved relative entropies and distances . . . . .	86
5.2.1	Operator product expansion of twist fields . . . . .	87
5.2.2	Charged moments of the excited states . . . . .	89
5.3	Analytical predictions . . . . .	93
5.3.1	Universal function for the pair of states $\psi = V_1$ and $\psi = V_2$ . . . . .	94
5.3.2	Universal function for the pair of states $\psi = i@$ and $\psi = 1$ . . . . .	96
5.4	Symmetry resolution . . . . .	99
5.5	Concluding remarks . . . . .	103
5.A	Correlation functions of primaries for the massless compact boson . . . . .	104
5.B	Numerical methods for the XX chain . . . . .	105
<b>II</b>	<b>Interfaces</b> . . . . .	<b>107</b>
<b>6</b>	<b>Renyi entropy and negativity at conformal interfaces</b> . . . . .	<b>109</b>
6.1	CFT approach . . . . .	109
6.2	Free Fermions . . . . .	112
6.2.1	Boundary states . . . . .	112
6.2.2	Renyi entropies . . . . .	113
6.2.3	Renyi negativities . . . . .	117
6.3	Free Bosons . . . . .	121
6.3.1	Boundary states . . . . .	121
6.3.2	Renyi entropies . . . . .	123
6.3.3	Renyi negativities . . . . .	126
6.4	Numerics for the fermions: Schroedinger junction . . . . .	129
6.4.1	The Renyi entropy between two arbitrary sets of wires . . . . .	131
6.4.2	Entanglement negativity . . . . .	133

6.5	Numerics for the bosons: harmonic chain . . . . .	134
6.5.1	Renyi entropy . . . . .	135
6.5.2	Entanglement negativity . . . . .	136
6.6	Concluding remarks . . . . .	137
6.A	Expectation values of Gaussian operators . . . . .	138
6.A.1	Fermionic case . . . . .	138
6.A.2	Bosonic case . . . . .	140
6.B	A useful determinant . . . . .	142
6.C	Jacobi theta functions . . . . .	143
<b>7</b>	<b>Entanglement across a defect after a global quench</b>	<b>145</b>
7.1	CFT results . . . . .	145
7.1.1	Bulk and boundary twist field . . . . .	146
7.1.2	Global quench . . . . .	149
7.2	Lattice results . . . . .	151
7.2.1	Model and setup . . . . .	151
7.2.2	Quasiparticle picture the for homogeneous case . . . . .	153
7.2.3	Quench with a defect . . . . .	154
7.2.4	Entanglement revivals . . . . .	158
7.3	Concluding remarks . . . . .	160
7.A	Calculation of the slope ratio for $\nu \neq 0$ . . . . .	161
<b>8</b>	<b>Domain wall melting across a defect</b>	<b>165</b>
8.1	The protocol and its hydrodynamic limit . . . . .	165
8.2	Entanglement dynamics . . . . .	168
8.2.1	Subleading behavior . . . . .	171
8.3	Concluding remarks . . . . .	172
<b>9</b>	<b>Outlook</b>	<b>173</b>



## Part I

# Symmetry resolution of entanglement



## Chapter 2

# $U(1)$ symmetry resolved entanglement in free 1+1 dimensional field theories via form factor bootstrap

In this chapter, we delve into the investigation of symmetry resolved entanglement in free massive Dirac and complex boson theories, building upon the findings presented in Ref. [2]. Our primary focus is on analyzing the ground state of these theories and computing the charged moments of an interval. To achieve this, we develop a bootstrap program designed to calculate the form factors of the charged twist fields. We rigorously solve and cross-validate these form factors using the  $\beta$ -theorem. The analytical solutions obtained enable us to express the behavior of the two-point correlation function of charged twist fields in the limit of large distances, facilitating the extraction of symmetry resolved entropies.

### 2.1 Introduction

We consider the ground-state  $|\mathcal{O}\rangle$  of a quantum field theory and, given a spatial subsystem  $A$ , we denote its reduced density matrix (RDM) by

$$\rho_A = \text{Tr}_{\bar{A}}(|\mathcal{O}\rangle\langle\mathcal{O}|); \quad (2.1)$$

that is an operator encoding the entanglement properties between  $A$  and its complement  $\bar{A}$ . In the presence of a global  $U(1)$  symmetry, it is possible to investigate a finer structure of the entanglement via the so-called symmetry resolution of entanglement, a recent idea put forward in Refs. [49, 51, 57, 58]. For instance in a symmetric ground-state, the conserved charge corresponding to the  $U(1)$  symmetry  $\hat{Q}$  commutes with the density matrix  $|\mathcal{O}\rangle\langle\mathcal{O}|$ ; under general circumstances also the restriction of  $\hat{Q}$  to the subsystem  $\hat{Q}_A$ , commutes with the RDM as

$$[\rho_A; \hat{Q}_A] = 0; \quad (2.2)$$

Such commutation implies that  $\rho_A$  admits a decomposition in sectors, associated with the eigenspaces of  $\hat{Q}_A$ . For instance, one can express

$$\rho_A = \sum_{q_A} P(q_A) \rho_A; \quad (2.3)$$

with  $P(q_A)$  being the projector onto the subspace associated to eigenvalue  $q_A$  of  $\hat{Q}_A$ . This fact has the important consequence that also entanglement measures can be decomposed in symmetry sectors as well. For instance, one defines the symmetry resolved Renyi and von Neumann entropies as

$$S_n(q_A) = \frac{1}{1-n} \log \frac{Z_n(q_A)}{Z_1^n(q_A)} ; \quad \text{and} \quad S(q_A) = \lim_{n \rightarrow 1} \frac{1}{n} \frac{Z_n(q_A)}{Z_1^n(q_A)} ; \quad (2.4)$$

with

$$Z_n(q_A) = \text{Tr} ( P_A^{q_A} ) ; \quad (2.5)$$

It is worth to give a physical interpretation of the quantities above as follows. Imagine we have access only to the subsystem  $A$  of our physical system, and we perform a measure of the restricted global charge  $\hat{Q}_A$  (e.g. associated to the number of particle in  $A$ ). In general, the process above alters the initial state and, if the outcome  $q_A$  is observed, the post-measure state would be just  $\frac{P_A^{q_A}}{\text{Tr}(P_A^{q_A})}$ , that is the (normalized) projection of the RDM onto the sector  $q_A$ . Then, the symmetry resolved entropies defined in Eq. (2.4) are nothing but the entropies of the state after the measurement, conditioned to the outcome  $q_A$ . Thus, the knowledge of the symmetry resolved entropies for any possible value of  $q_A$  encodes the residual quantum correlations between  $A$  and  $\bar{A}$  after the measurement protocol.

The calculation of all these symmetry resolved quantities requires in general the simultaneous diagonalisation of  $\rho_A$  and  $\hat{Q}_A$ , an extremely costly task for many-body quantum systems. An ingenious way to circumvent this difficult path passes through the charged moments [51]

$$Z_n(\lambda) = \text{Tr} ( P_A^{q_A} e^{i \lambda \hat{Q}_A} ) ; \quad (2.6)$$

These are related to the main quantity of interest  $Z_n(q_A)$  via Fourier transform, as [51]

$$Z_n(q_A) = \int \frac{d\lambda}{2\pi} Z_n(\lambda) e^{i \lambda q_A} ; \quad (2.7)$$

This approach is particularly powerful for field theoretical calculations in path-integral formalism. In the replica approach, valid for  $n$  integer,  $\text{Tr} P_A^n$  is a partition function on an  $n$ -sheeted Riemann surface  $R_n$ , obtained by joining cyclically the  $n$ -sheets along the subsystem  $A$  [46, 59, 60]. In this language, the charged moments (2.6) correspond to an additional insertion of an Aharonov-Bohm flux on one of the sheets of  $R_n$  [51], giving rise to a charged partition function.

For 1+1 field theories, one can express the partition functions above as expectation values of twist fields in a  $n$ -copy version of the original model. The latter perspective is particularly useful for critical theories, where the dimensions of these fields are exactly known [60, 62], and their two-point function, constrained by scale-invariance, gives immediately the entanglement of one-interval [60]. In addition, for integrable theories away from criticality the form factor bootstrap allows for the calculation of the matrix elements of the branch-point twist field [47, 63, 64], that provides a systematic technique to compute their correlation functions.

In a recent work [65] the  $Z_2$  symmetry resolution of entanglement was investigated for the Ising and Sinh-Gordon Field theories with a form-factor approach. The aim of our work [2] was to generalize those techniques to the case of  $U(1)$  symmetry, and eventually study the symmetry resolution of complex massive free theories. Although these theories have been already analyzed in [66], albeit with different techniques, it was instructive to study them with form factor bootstrap, to shed light on some general properties shared with massive interacting theories. In

particular, we mention that a generalization for the  $U(1)$  symmetry of the sine-Gordon model was considered after our work was completed [67].

In the next sections, we will first go through the bootstrap approach which allows computing the form factors of the standard and  $U(1)$  composite twist fields, that are the building blocks to reconstruct their correlation functions. Then, we will express the two-point functions of those fields in the infrared limit, relating them eventually to the symmetry resolution of an interval.

## 2.2 Form Factors of Twist Fields for integrable theories

In this section, we give a brief introduction to the form-factor theory of the standard twist fields in integrable field theory, following closely Refs. [2, 47]. This is important to introduce some basic ingredients of integrable field theory, and give the building blocks to compute the Renyi entropies, in the replica approach. This construction will be eventually generalized in the other sections to tackle the additional insertion of the  $U(1)$  flux via the notion of  $U(1)$  charged twist fields.

First of all, let us recall that form factors are matrix elements of (semi-)local operators  $O(x; \vec{\eta})$  between the vacuum and asymptotic states, i.e.,

$$F_{1, \dots, n}^O(\#_1; \dots; \#_n) = \langle 0 | O(0; 0) | j\#_1; \dots; \#_n \rangle \quad (2.8)$$

In massive relativistic field theories, the asymptotic states are multi-particle excitations whose dispersion relation is  $(E; p) = (m \cosh \#, m \sinh \#)$ , where  $\#$  is the rapidity, and  $m$  the mass. Moreover, as many particle species are present in principle, we label each specie by an index  $i$ . The multi-particle states are excitations above the vacuum state  $|0\rangle$  as

$$|j\#_1; \#_2; \dots; \#_n\rangle = A_1^Y(\#_1) A_2^Y(\#_2) \dots A_n^Y(\#_n) |0\rangle \quad (2.9)$$

where the operator  $A_i^Y(\#_i)$  creates a particle of specie  $i$  with rapidity  $\#_i$ . In integrable field theories, the creation/annihilation operators satisfy the Zamolodchikov-Faddeev (ZF) algebra, which, for diagonal scattering, reads

$$\begin{aligned} A_i^Y(\#_i) A_j^Y(\#_j) &= S_{i; j}(\#_i, \#_j) A_j^Y(\#_j) A_i^Y(\#_i); \\ A_i(\#_i) A_j(\#_j) &= S_{i; j}(\#_i, \#_j) A_j(\#_j) A_i(\#_i); \\ A_i(\#_i) A_j^Y(\#_j) &= S_{i; j}(\#_j, \#_i) A_j^Y(\#_j) A_i(\#_i) + \delta_{i; j} 2(\#_i, \#_j); \end{aligned} \quad (2.10)$$

Here  $S_{i; j}(\#_i, \#_j)$  denotes the two-particle scattering matrix of particles  $i; j$ , with incoming rapidities  $\#_i; \#_j$  respectively: as a consequence of relativistic invariance, it depends on the rapidity difference only.

We now replicate the theory above  $n$  times. That amounts to the introduction of an additional internal (replica) index  $\alpha = 1; \dots; n$  and each particle specie is now identified by a pair  $(i; \alpha)$ . Since particles in different replicas do not interact by construction, the scattering matrix in the replica model is

$$\begin{aligned} \mathfrak{S}_{(i; \alpha); (j; \beta)}(\#) &= 1; \quad i; j = 1; \dots; n \text{ and } \alpha \neq \beta; \\ \mathfrak{S}_{(i; \alpha); (j; \beta)}(\#) &= S_{i; j}(\#); \quad i; j = 1; \dots; n \text{ and } \alpha = \beta; \end{aligned} \quad (2.11)$$

The resulting model admits a  $Z_n$  symmetry, associated to the cyclic permutation of different replicas, which can be implemented via the introduction of twist fields as we explain below. Given any local field  $\phi_i$  inserted in the  $i$ -th replica, we require that a twist field  $T$  satisfies

$$\begin{aligned} \phi_i(y) T(x) &= T(x) \phi_{i+1}(y) & x < y; \\ \phi_i(y) T(x) &= T(x) \phi_i(y) & x > y; \end{aligned} \quad (2.12)$$

For instance  $T(x)$  introduces a branch-cut over  $[x; \infty)$  where it acts on local fields as a replica shift  $i \rightarrow i+1$ . Similarly, the inverse permutation  $i \rightarrow i-1$  is implemented by another twist field  $\bar{T}$  satisfying

$$\begin{aligned} \phi_i(y) \bar{T}(x) &= \bar{T}(x) \phi_{i-1}(y) & x > y; \\ \phi_i(y) \bar{T}(x) &= \bar{T}(x) \phi_i(y) & x < y; \end{aligned} \quad (2.13)$$

The characterization of these fields can be ultimately formulated in terms of their form factors. These are constrained by the bootstrap equations, whose general expression is [47]

$$F_k^{TJ(\underline{\alpha})}(\underline{\beta}) = S_{(i_1, i_2); (i_{+1}, i_{+2})}(\#_{i_1+1}) F_k^{TJ(\dots; (i_{+1}, i_{+2}); (i_1, i_2); \dots; \#_{i_1+1}; \#_{i_2}; \dots)}; \quad (2.14)$$

$$F_k^{TJ(\underline{\alpha})}(\#_1 + 2i; \#_2; \dots; \#_k) = F_k^{TJ(\dots; (k, k); (1, \wedge^1))}(\#_2; \dots; \#_n; \#_1); \quad (2.15)$$

$$i \underset{\#_0 = \#_0 + i}{\text{Res}} F_{k+2}^{TJ(\dots; (\dots); (\dots))}(\#_0; \#_0; \underline{\beta}) = F_k^{TJ(\underline{\alpha})}(\underline{\beta}); \quad (2.16)$$

$$i \underset{\#_0 = \#_0 + i}{\text{Res}} F_{k+2}^{TJ(\dots; (\dots); (\dots))}(\#_0; \#_0; \underline{\beta}) = \sum_{i=1}^k S_{(\dots); (i, i)}(\#_0) F_k^{TJ(\underline{\alpha})}(\underline{\beta});$$

$$i \underset{\#_0 = \#_0 + iu}{\text{Res}} F_{k+2}^{TJ(\dots; (\dots); (\dots))}(\#_0; \#_0; \underline{\beta}) = \sum_{i=1}^k F_{k+1}^{TJ(\dots; (\dots))}(\#_0; \underline{\beta}); \quad (2.17)$$

where  $\#_{ij} = \#_i \dots \#_j$ ,  $\underline{\beta}$  and  $(\dots)$  are shorthands for  $\#_1; \#_2; \dots; \#_k$  and  $(1, 1); (2, 2); \dots; (k, k)$  respectively;  $\wedge = +1$  and  $\bar{\alpha}$  denotes the anti-particle of species  $\alpha$ . In the last equation  $u$  refers to the position of the pole of the bound state of the particle  $\alpha$  in the S-matrix  $S_{ij}$  and  $i$  is the corresponding pole strength. These equations are natural generalization of the ones for conventional local fields [68{70]. The main difference is the presence of a non-trivial monodromy condition arising from the branch-cut (roughly, a rapidity shift  $\# \rightarrow \# + 2i$  is equivalent to a replica shift  $i \rightarrow i+1$ ). These equations, which are involved in general interacting theories, simplify drastically for complex free boson/fermions. Indeed, no dynamical poles are present (say  $\alpha = 0$ ), the S-matrices do not depend explicitly on the rapidity, and only two species of particles are present (particle/antiparticle respectively).

It is important to mention that, albeit the bootstrap equations severely constraint the form-factors, they admit a plethora of inequivalent solutions. In general this is expected, and it is compatible with the fact that an infinite number of fields share the same features. However, for physical applications one is usually interested in the lighter field with some given properties. In this respect, a very useful tool is the  $\beta$ -theorem [71]. Such a theorem states that the ultraviolet (UV) conformal weight of a field  $O$  is

$$h_{UV} = \frac{1}{4} \int_{\mathcal{H}} d^2x h(x) O(0) i_C; \quad (2.18)$$

where  $\langle x \rangle$  is the trace of the stress-energy tensor and  $\langle \mathcal{O} \rangle$  is the vacuum expectation value of  $\mathcal{O}(x)$ . After expanding the (connected) two-point function  $\langle \mathcal{O}(x) \mathcal{O}(0) \rangle_c$  in the basis of asymptotic states, one eventually gets

$$\langle \mathcal{O} \rangle = \frac{1}{2 \langle \mathcal{O} \rangle} \sum_{n=1}^{\infty} \sum_{j_1, \dots, j_n} \int \frac{d\#_1 \dots d\#_n}{(2\pi)^n n!} E_n^{-2} F_n^{j_1 \dots j_n}(\#_1, \dots, \#_n) F_n^{O_j}(\#_1, \dots, \#_n) \quad (2.19)$$

where  $E_n = \prod_{k=1}^n m_k \cosh \#_k$  and  $F_n^{O_j}; F_n^{j_1 \dots j_n}$  are the form factors of  $\mathcal{O}$ . Consequently, if the dimension of the operator  $\mathcal{O}$  is known, the  $\beta$ -theorem rules out most of the solutions to the bootstrap equations. In particular, in the large rapidity limit  $\#_i \rightarrow 1$ , the growth of a given form factor is utmost  $e^{O_j \#_i}$  with  $y_{\mathcal{O}} = \langle \mathcal{O} \rangle$ . We mention also that, while the exact evaluation of  $\langle \mathcal{O} \rangle$  from (2.19) requires in principle the knowledge of an infinite number of form factors, the series is usually rapidly converging and its truncation up to the two-particle form factors gives already a good estimation.

We summarize below the strategy employed to get the 2-particle form factors for the twist fields in the absence of dynamical poles. The idea is to focus first on the case in which the particles belong to the same replica, say the first one. Here, one can first solve the monodromy condition, finding a minimal solution without zeros and poles, and then add a contribution associated to a kinematic pole (arising when the rapidity difference is  $i$ ). Given that, the other form factors with different replica indices can be easily recovered using the monodromy properties.

The starting point is the monodromy equation for the minimal form factor  $F_{\min}^{Tj(k)(1)(1)}$  determined by Eq. (2.14) and (2.15) as

$$F_{\min}^{Tj(k)(1)(1)} = F_{\min}^{Tj(k)(1)(1)}(\#; n) S; (\#) = F_{\min}^{Tj(k)(1)(1)}(\# + 2in; n) \quad (2.20)$$

Given the integral representation of the S-matrix as

$$S; (\#) = \exp \int_0^{2\pi} \frac{dt}{t} g; (t) \sinh \frac{t\#}{i} \quad (2.21)$$

it is possible to show that the solution for the minimal form factor is

$$F_{\min}^{Tj(k)(1)(1)}(\#; n) = N \exp \int_0^{2\pi} \frac{dt}{t \sinh nt} g; (t) \sin^2 \frac{it}{2} \left( n + \frac{i\#}{2} \right) \quad (2.22)$$

with  $N$  being a normalization constant. Taking into account the equation for the kinematic poles (2.16) one eventually express the two-particle form factor as

$$F_2^{Tj(k)(j)}(\#; n) = \frac{hT \sin \frac{\pi}{n}}{2n \sinh \frac{i(2k-k-1)\#}{2n} \sinh \frac{i(2k-j-1)\#}{2n}} \frac{F_{\min}^{Tj(k)(j)}(\#; n)}{F_{\min}^{Tj(k)(1)(1)}(j; n)} \quad (2.23)$$

with  $hT$  being the vacuum expectation value of the twist field. A similar result is valid for the twist field  $\hat{T}$  and, employing replica symmetry, it is possible to show that

$$F_2^{Tj(k)(j)}(\#; n) = F_2^{\hat{T}j(n-j)(n-k)}(\#; n) \quad (2.24)$$

At this point, it is instructive to write down the explicit solution for complex boson and fermions. The particle content of these theories is given by two species (particle/antiparticle)

labeled by  $\#$ . The scattering matrix does not depend on the species or the rapidity difference, and it is simply given by  $S(\#) = \pm 1$  for bosons/fermions respectively. Since the twist field is neutral wrt the  $U(1)$  symmetry, the only non-vanishing 2-particle form factors are the ones with exactly one particle (+) and one antiparticle (-), expressed as

$$F_2^{Tj(\#):(k)(\#;n)} = \frac{hT \sin \frac{\#}{2n}}{2n \sinh \frac{i(2j-k-1)+\#}{2n} \sinh \frac{i(2k-j-1)-\#}{2n}} \frac{F_{\min}^{Tjj;k}(\#;n)}{F_{\min}^{Tj1;1}(j;n)}. \quad (2.25)$$

The only difference between bosons and fermions is given here by the explicit expression of the minimal form factor. For bosons, we have

$$F_{\min}^{Tj1;1}(\#;n) = 1; \quad (2.26)$$

being the monodromy equation trivial, while the result for fermions is

$$F_{\min}^{Tj1;1}(\#;n) = i \sinh \frac{\#}{2n}; \quad (2.27)$$

For later purposes, in particular for the application of the  $\mathbb{Z}_2$ -theorem, we also need the form factors of the stress-energy tensor. The only non-vanishing ones are the 2-particle form factors, that can be written as

$$F_2^{j(\#):(j)(k)(\#;n)} = \begin{cases} 2m^2 & j = k \\ 0 & j \neq k \end{cases} \quad (2.28)$$

for bosons, and

$$F_{D;2}^{j(\#):(j)(k)(\#;n)} = \begin{cases} i2m^2 \sinh \frac{\#}{2} & j = k \\ 0 & j \neq k \end{cases} \quad (2.29)$$

for fermions, where  $m$  is the mass of the particle/antiparticle. It is worth to notice explicitly that the form factors with particles in different replicas vanish, a property related to the fact that the field does not mix distinct replicas (in contrast to  $T$ ).

### 2.3 Form factors of the composite $U(1)$ twist fields for free Dirac fermions

In this section, we generalize the previous construction of standard twist fields to the  $U(1)$  composite twist fields of Dirac fermions. In particular, we construct a new field  $T(x)$  which acts both shifts the replicas, and it adds an Aharonov-Bohm flux related to the global  $U(1)$  symmetry. This idea can be rephrased in terms of the commutation relation between  $T$  and the fermionic fields as

$$\begin{aligned} i(y)T(x) &= e^{i=n} T(x) i_{+1}(y) & x < y; \\ i(y)T(x) &= T(x) i(y) & x > y; \end{aligned} \quad (2.30)$$

and similarly for  $\bar{T}$

$$\begin{aligned} i(y)\bar{T}(x) &= e^{i=-n} \bar{T}(x) i_{-1}(y) & x > y; \\ i(y)\bar{T}(x) &= \bar{T}(x) i(y) & x < y; \end{aligned} \quad (2.31)$$

Here,  $\psi_i(x)$  is the fermion field in the  $i$ -th replica, and a flux  $e^{i=2\pi}$  is introduced between the  $i$ -th and the  $i+1$ -th replica. This choice is dictated by the requirement, that the total phase picked up by the particle when turning around the  $n$ -sheeted branch-point has to be  $e^{i=2\pi}$ . For  $n=1$ ,  $T$  becomes the  $U(1)$  twist-eld of the Dirac theory, that will be denoted here as  $V$ .

We now specialize the bootstrap equations to the  $U(1)$  composite twist-eld as

$$F_k^T \left( \frac{j(\cdot)}{\cdot} \right) (\#) = \mathcal{S}_{(i_i);(i_{+1} \dots i_{+1})} (\#_{i,i+1}) F_k^T \left( \frac{j(\cdot)}{\cdot} \right) (\#_{i,i+1}; \#_i; \dots); \quad (2.32)$$

$$F_k^T \left( \frac{j(\cdot)}{\cdot} \right) (\#_1 + 2; \#_2; \dots; \#_n) = e^{i=2\pi} F_k^T \left( \frac{j(\cdot)}{\cdot} \right) (\#_2; \dots; \#_n; \#_1); \quad (2.33)$$

$$i \operatorname{Res}_{\#_0 = \#_0 + i} F_{k+2}^T \left( \frac{j(\cdot)}{\cdot} \right) (\#_0; \#_0; \#) = F_k^T \left( \frac{j(\cdot)}{\cdot} \right) (\#); \quad (2.34)$$

$$i \operatorname{Res}_{\#_0 = \#_0 + i} F_{k+2}^T \left( \frac{j(\cdot)}{\cdot} \right) (\#_0; \#_0; \#) = e^{i=2\pi} \prod_{i=1}^k \mathcal{S}_{(i_i);(i_i)} (\#_0) F_k^T \left( \frac{j(\cdot)}{\cdot} \right) (\#); \quad (2.35)$$

where  $\# = -1$  refers to particle/antiparticle, while  $\# = 1; \dots; n$  is the replica index. The presence of the  $U(1)$  flux is ultimately related to a mutual locality index, which enters the bootstrap equations and modifies the monodromy properties (wrt  $T$ ).

We present below the solution for the two-particle form factors, which is non-vanishing only if a particle and an anti-particle are present ( $T$  is  $U(1)$  neutral, as  $T$ ). For instance, the solution for  $n=1$  was known from earlier investigations [72{74],

$$F_2^V \left( \frac{j(\cdot)}{\cdot} \right) (\#; \cdot) = \frac{i2 \sin \frac{\#}{2} e^{\frac{\#}{2}} \sinh \frac{\#}{2}}{\sinh \#}; \quad (2.36)$$

In the limit  $\# \rightarrow 0$ , the  $U(1)$  field  $V$  becomes the identity fields, and consequently its two-particle form factors vanish, which is compatible with Eq. (2.36).

To get the solution at  $n > 1$ , we follow the same approach adopted for the standard twist-elds, and we focus on the case of particle/antiparticles belonging to the first replica. For the minimal form factor, we have to solve the monodromy condition

$$F_{\min}^T \left( \frac{j(\cdot)}{\cdot} \right) (\#; n) = F_{\min}^T \left( \frac{j(\cdot)}{\cdot} \right) (\#; n) = e^i F_{\min}^T \left( \frac{j(\cdot)}{\cdot} \right) (\# + 2; n); \quad (2.37)$$

A solution is given

$$F_{\min}^T \left( \frac{j(\cdot)}{\cdot} \right) (\#; n) = i e^{\frac{\#}{2n}} \sinh \frac{\#}{2n}; \quad (2.38)$$

which is compatible with (2.27) in the limit  $\# \rightarrow 0$ . We now need to modify the minimal solution, to take into account the presence of kinematic poles. For instance, the physical form-factor should have a pole at  $\# = i; 2in - i$  with residue  $ihTi; ie^i hTi$  respectively, as expressed by the bootstrap Eqs. (2.34)(2.35). In our work, we provided the solution

$$F_2^T \left( \frac{j(\cdot)}{\cdot} \right) (\#; n) = \frac{ihTi \sin \frac{\#}{n}}{2n \sinh \frac{i-\#}{2n} \sinh \frac{i+\#}{2n}} \frac{\cos \frac{\#}{2n} \sinh \frac{\#}{2n}}{\sin \frac{\#}{2n}} \frac{\sin \frac{\#}{2n} \cosh \frac{\#}{2n}}{\cos \frac{\#}{2n}} e^{\frac{\#}{2n}}; \quad (2.39)$$

which is compatible both with the limit  $\# \rightarrow 0$ , which gives the form-factor of the standard twist-eld  $T$ , and the known results for  $n=1$ . The other form factors with two different replica indices are similarly recovered using the monodromy equations and the final result is

$$F_2^T \left( \frac{j(\cdot)}{\cdot} \right) (\#; n) = \begin{cases} e^{i(k-j)=n} F_2^T \left( \frac{j(\cdot)}{\cdot} \right) (2i(k-j) - \#; n) & \text{if } k > j; \\ e^{i(j-k)=n} F_2^T \left( \frac{j(\cdot)}{\cdot} \right) (2i(j-k) + \#; n) & \text{otherwise.} \end{cases} \quad (2.40)$$

As already mentioned, the solutions to the bootstrap equations are not unique, and we tested the validity of our results with  $\beta$ -theorem. Indeed, from (2.19) we get the UV conformal weight of  $T$  (half of its scaling dimension) as

$$T = \frac{n}{32} \frac{\int_1^Z \frac{F_2^{j(1)}(\#) F_2^{T(j(1))(1)}(\#; n) + F_2^{T(j(1))(1)}(\#; n)}{\cosh^2(\#/2)} d\#}{2m^2 h T i} : \quad (2.41)$$

The integral can be computed explicitly and the result is

$$T = \frac{1}{24} \left( n - n^{-1} \right) + \frac{1}{2n} \frac{1}{2} ; \quad (2.42)$$

which is compatible with the known UV result [51].

## 2.4 Form factors for free complex bosons

In this section, we treat the case of the complex boson, and we provide a solution to the 2-particle form factor of the composite  $U(1)$  twist field. The main difference with fermions is the scattering phase, that is just  $+1$ . Thus, the bootstrap equations are eventually expressed by

$$F_k^T \frac{j(\_)}{\_}(\#) = F_k^T \frac{j(\_); \dots; (i+1, i+1); \dots; (i, i); \dots; (\dots; \#_{i+1}; \#_i; \dots; \_)}{\_} ; \quad (2.43)$$

$$F_k^T \frac{j(\_)}{\_}(\#_1 + 2i; \#_2; \dots; \#_k) = e^{i\pi n} F_k^T \frac{j(\_); \dots; (k, k); \dots; (1, 1); \dots; (\_)}{\_}(\#_2; \dots; \#_n; \#_1); \quad (2.44)$$

$$i \operatorname{Res}_{\#_0 = \#_0 + i} F_{k+2}^T \frac{j(\_); \dots; (\_)}{\_}(\#_0; \#_0; \#) = F_k^T \frac{j(\_)}{\_}(\#); \quad (2.45)$$

$$i \operatorname{Res}_{\#_0 = \#_0 + i} F_{k+2}^T \frac{j(\_); \dots; (\_)}{\_}(\#_0; \#_0; \#) = e^{i\pi n} F_k^T \frac{j(\_)}{\_}(\#); \quad (2.46)$$

We mention that the solutions for the case  $n=1$  are known [75]. In particular, one gets the (bosonic)  $U(1)$  field  $V$  whose 2-particle form factors as

$$F_2^V \frac{j(1)(1)}{\_}(\#; \_) = \sin \frac{\#(\_)}{2} \frac{e^{\frac{\#(\_)}{2}}}{\cosh \frac{\#}{2}}; \quad \_ \in [0; 2\pi]; \quad (2.47)$$

We now proceed with the case  $n > 1$ , following the same logic applied for the fermions. In this case, the monodromy equations for the minimal form factors are

$$F_{\min}^T \frac{j(1)(1)}{\_}(\#; n) = F_{\min}^T \frac{j(1)(1)}{\_}(\#; n) = e^{i\pi} F_{\min}^T \frac{j(1)(1)}{\_}(\# + 2in; n); \quad (2.48)$$

An ansatz for the minimal solution satisfying the previous equation is

$$F_{\min}^T \frac{j(1)(1)}{\_}(\#; n; \_) = e^{\frac{\#(\_)}{2n}} \cosh \frac{\#}{2n}; \quad (2.49)$$

Then, we have to modify this solution taking into account the kinematic poles, as done for fermions. We proposed the following expression

$$F_2^T \frac{j(1)(1)}{\_}(\#; n; \_) = \frac{h T i \sin \frac{\#}{n}}{2n \sinh \frac{i\#}{2n} \sinh \frac{i\#+}{2n}} \frac{\cos \frac{\#}{2n} \cosh \frac{\#}{2n}}{\cos \frac{\#}{2n}} \frac{\sin \frac{\#}{2n} \sinh \frac{\#}{2n}}{\sin \frac{\#}{2n}} e^{\frac{\#(\_)}{2n}}; \quad (2.50)$$

which is compatible with the known results for  $\beta \neq 0$  and  $n \neq 1$ . Finally, we express the other form-factors as

$$F_2^{T(j);(k)}(\#; \eta) = \begin{cases} e^{i(k-j)=n} F_2^{T(j);(k)}(\#; \eta) & \text{if } k > j; \\ e^{i(j-k)=n} F_2^{T(j);(k)}(\#; \eta) & \text{otherwise;} \end{cases} \quad (2.51)$$

exploiting the monodromy relations. The validity of our ansatz was checked by the  $\beta$ -theorem as

$$T = \frac{n}{32} \frac{\int_{-\infty}^{\infty} d\# \frac{F_2^{j;1}(\#) F_2^{T(j);(k)}(\#; \eta) + F_2^{T(j);(k)}(\#; \eta)}{\cosh^2(\#-2)} = \frac{2}{24} \left( n - n^{-1} + \frac{1}{2n^2} \right) \frac{1}{2} ; \quad 2[0;2] ; \quad (2.52)$$

which is compatible with the exact UV result [66].

## 2.5 Replica diagonalization approach

In this section, we provide an alternative derivation of the two-particle form factors of the composite  $U(1)$  twist fields, based on the diagonalisation in the space of replicas [76]. This technique has been already employed in [77] for the computation of the form factors of the standard branch-point twist fields. It works well for free theories when the  $S$ -matrix does not depend explicitly on the rapidities, and it is more closely related to the approach of Ref. [66]. We will briefly summarize this formalism, discussing the case in which a non-vanishing flux is inserted. This provides an additional non-trivial check of our results, besides  $\beta$ -theorem.

Let us consider the creation operator  $A_{j;}^Y(\#)$  of a particle/antiparticle in the  $j$ -th replica. The cyclic symmetry of replicas can be diagonalised moving to a "replica Fourier space"

$$\hat{A}_{k;}^Y(\#) = \frac{1}{\sqrt{n}} \sum_{j=0}^{n-1} e^{i\frac{2kj}{n}} A_{j;}^Y(\#); \quad (2.53)$$

where we identified the replica indices  $j \sim j + n$  and  $k \sim k + n$ . In order to account for the correct (anti)commutation relations (and hence  $S$ -matrix) of bosons and fermions, the index  $k$  should be either integer or half-integer according to the following rules

- for bosons ( $S(\#) = 1$ )  $k = 0; \dots; n - 1$ ;
- for fermions ( $S(\#) = -1$ )  $k = \frac{n-1}{2}; \dots; \frac{n-1}{2}$ .

We mention that while different prescriptions can be found in the literature for the diagonalisation in the replica space [47, 66, 76, 78], they are all related to each other by unitary transformations and in the end, the diagonal modes simply get a phase. Since here we are only interested in the absolute value squared of the form factors, this issue is irrelevant to our purpose. The advantage of this approach is that the composite twist field  $T$  does not mix different Fourier modes. We denote its non-vanishing 2-particle form factor as

$$F_{k;}(\#) = \langle 0 | T(0) \hat{A}_{k;}^Y(\#) \hat{A}_{k;}^Y(0) | 0 \rangle; \quad (2.54)$$

which satisfies the bootstrap equations

$$F_{k; (\# + 2i)} = e^{i\frac{2k}{n}} F_{k; (\#)}; \quad (2.55)$$

$$\text{Res}_{\# = i} F_{k; (\#)} = i(1 - e^{i\frac{2k}{n}}) hT i; \quad (2.56)$$

$$F_{k; (\#)} = S(\#) F_{k; (\#)}; \quad (2.57)$$

These equations are similar to the ones satisfied by the  $U(1)$  twist field  $V$  [62], studied in [79]: the only difference is the monodromy phase, which is  $e^{i\frac{2k}{n}}$  (rather than  $e^i$ ). We thus can employ the known results for boson and fermions [79] to get the solution of our problem. After that, we can eventually express the physical form-factor via Fourier transform as follows

$$\begin{aligned} \langle 0 | jT(0) A_{j;+}^Y(\#) A_{j; }^Y(0) | 0 \rangle &= \\ \langle 0 | jT(0) \prod_{k=1}^{\infty} A_{k;+}^Y(\#) e^{i\frac{2kj}{n}} \prod_{k=0}^{\infty} A_{k; }^Y(\#) e^{i\frac{2kj}{n}} | 0 \rangle &= \frac{1}{n} \sum_k F_{k;+}(\#); \end{aligned} \quad (2.58)$$

For the fermions, we get the solution

$$F_{k;+}(\#) = ihT i \sin \frac{k}{2n + \frac{k}{n}} \frac{e^{\# = 2n + k \# = n}}{\cosh \frac{\#}{2}}; \quad (2.59)$$

and using the relation

$$\prod_{k=\frac{n-1}{2}}^{\frac{n-1}{2}} d^k = \frac{e^{i\frac{n-2}{2}} e^{i\frac{n-2}{2}}}{e^{i\frac{n-2}{2}} e^{i\frac{n-2}{2}}} = \frac{\sin \frac{n}{2}}{\sin \frac{n}{2}}; \quad (2.60)$$

we get the sum over the modes as

$$\langle 0 | jT(0) A_{1;+}^Y(\#) A_{1; }^Y(0) | 0 \rangle = \quad (2.61)$$

$$ihT i \frac{e^{\# = 2n}}{2n \sinh \frac{i+\#}{2n} \sinh \frac{i-\#}{2n}} \left( e^{2n \sinh \frac{\#}{2n}} + e^{i = 2n \sinh \frac{\#}{2n}} \right); \quad (2.62)$$

and this provides an alternative derivation of the FF in Eq. (2.39). We also mention that the same expression can be derived starting from the ansatz

$$\langle 0 | jT(0) A_{1;+}^Y(\#) A_{1; }^Y(0) | 0 \rangle = hT i \frac{e^{\# = 2n}}{2n \sinh \frac{\# + i}{2n} \sinh \frac{\# - i}{2n}} \left( C_0 e^{\# = 2n} + C_1 e^{\# = 2n} \right); \quad (2.63)$$

compatible with the monodromy equations, and choosing  $C_0, C_1$  such that the kinematic poles are

$$\text{Res}_{\# = i} \langle 0 | jT(0) A_{1;+}^Y(\#) A_{1; }^Y(0) | 0 \rangle = ihT i; \quad (2.64)$$

$$\text{Res}_{\# = 2n - i} \langle 0 | jT(0) A_{1;+}^Y(\#) A_{1; }^Y(0) | 0 \rangle = ie^i hT i; \quad (2.65)$$

We now apply the same technique to the complex boson, starting from the solution of the bootstrap equations

$$F_{k;+}(\#) = hT i \sin \frac{k}{2n + \frac{k}{n}} \frac{e^{\# = 2n + k \# = n \# = 2}}{\cosh \frac{\#}{2}}; \quad (2.66)$$

The sum over the modes is easily done using

$$\sum_{k=0}^{\infty} e^{ik} = \frac{e^{in} - 1}{e^i - 1} = e^{i\frac{n}{2}} \frac{\sin \frac{n}{2}}{\sin \frac{1}{2}}; \quad (2.67)$$

and the form-factor for the boson is thus expressed as

$$\langle 0 | j_T(0) A_{1,+}^{\vee}(\#) A_{1,-}^{\vee}(\#) | 0 \rangle = i h T i \frac{e^{\#-2n} - e^{-\#-2n}}{2n \sinh \frac{\#+i}{2n} \sinh \frac{\#-i}{2n}} e^{i=2n} e^{-i=2n} \sinh \frac{\#}{2n} \quad (\text{c.c.}) ; \quad (2.68)$$

which corresponds to the result (2.50). As for fermions, the same result can be recovered starting from the ansatz

$$\langle 0 | j_T(0) A_{1,+}^{\vee}(\#) A_{1,-}^{\vee}(\#) | 0 \rangle = h T i \frac{e^{\#-2n} - e^{-\#-2n}}{2n \sinh \frac{\#+i}{2n} \sinh \frac{\#-i}{2n}} C_0 e^{\#-2n} + C_1 e^{-\#-2n} ; \quad (2.69)$$

and fixing  $C_0, C_1$  compatibly with the kinematic poles.

## 2.6 Two-point function of composite $U(1)$ twist fields

In this section, we compute the large-distance limit of the 2-point function of the composite  $U(1)$  twist fields, exploiting the analytic results of the previous sections. In particular, as we see below, the first correction to the asymptotic factorization is given by a 2-particle contribution, which is determined as a function of the corresponding form factor.

Inserting a resolution of the identity in terms of the quasi-particle states, we approximate

$$\begin{aligned} \langle h T(0) \bar{\psi}(\cdot) | h T(i^2) \sum_{j,k=1}^{\infty} \frac{d\#_1 d\#_2}{(2\pi)^{2j!}} j F_2^{T(j+)(j)}(\#_1, \#_2; n) j^2 e^{-m(\cosh\#_1 + \cosh\#_2)} \\ + \sum_{j,k=1}^{\infty} \frac{d\#_1 d\#_2}{(2\pi)^{2j!}} j F_2^{T(j)(j+)(k)}(\#_1, \#_2; n) j^2 e^{-m(\cosh\#_1 + \cosh\#_2)} \\ = h T(i^2) \left[ 1 + \frac{n}{4} \sum_{j=1}^{\infty} d\# f(\#; n) K_0(2m \cosh(\frac{\#-2}{2})) \right] ; \end{aligned} \quad (2.70)$$

where  $K_0(z)$  is a Bessel function, and  $f(\#; n)$  is a universal function defined as

$$\begin{aligned} h T(i^2) f(\#; n) = \sum_{j=1}^{\infty} j F_2^{T(j+)(j)}(\#; n) j^2 + j F_2^{T(j)(j+)(j)}(\#; n) j^2 \\ = \sum_{j=0}^{\infty} j F_2^{T(j)(j+)(1)}(2ij, \#; n) j^2 + \sum_{j=0}^{\infty} j F_2^{T(j+)(j)}(2ij, \#; n) j^2. \end{aligned} \quad (2.71)$$

Here, the terms with more than two particles have been neglected, as their contribution goes exponentially to zero faster than the two-particle one when  $m \rightarrow +\infty$ . Instead, there are no one-particle contributions as the corresponding form factors are zero (since the particle/antiparticles are charged, while the twist field is neutral). It is worth to notice that the integral appearing in

(2.70) localizes at  $\# = 0$ , and only the behavior of  $f(\#; n)$  at small  $\#$  is relevant. In particular, for later convenience, we write down the approximation

$$\frac{1}{2} \int_{-\infty}^{\infty} d\# K_0(2m \cosh \frac{\#}{2}) \frac{\#^{2k}}{2} = \frac{k + \frac{1}{2}}{2^{3-2k}} \frac{e^{-2m}}{(m)^{k+1}} (1 + O((m)^{-1})); \quad (2.72)$$

which comes directly from the asymptotic expression  $K_0(z) \sim e^{-z} \frac{1}{\sqrt{z}}$  (see [80]) valid in the large  $z$  limit.

We focus first on the case  $n > 2$  integer, which gives for both bosons and fermions

$$hT(0) \overline{F}(\cdot) i = hT(i)^2 \left( 1 + \frac{n e^{-2m}}{4 m} \right); \quad (2.73)$$

Here we used the Taylor expansion of  $f(\#; n)$  at  $\# = 0$ , and the approximation (2.72) (for  $k = 0$ ), keeping only the dominant contribution given by  $f(0; n)$ . Similarly, it is possible to consider the case  $n = 1$ , and we get

$$hT(0) \overline{F}(\cdot) i = hT(i)^2 \left( 1 + 2 \sin^2 \frac{1}{2} \frac{e^{-2m}}{4 m} \right); \quad (2.74)$$

We notice that the next-to-leading term depends on  $\#$  explicitly only for  $n = 1$ , which is a specific feature of the form factors of our theories.

So far we considered  $n$  integer, but in principle, we can make an analytic continuation over  $n$ , that is relevant for the computation of the von Neumann entropy. This task has been performed in [47] for the standard twist field, and the main result was the discovery of a singular limit  $n \rightarrow 1$ . Using a similar approach, we obtain that  $f(\#; n)$  becomes a singular distribution in the limit  $n \rightarrow 1$ , and one is not allowed anymore to Taylor expand around  $\# = 0$ . More precisely, we found for both bosons and fermions (see Appendix 2.A)

$$\lim_{n \rightarrow 1} \frac{\partial}{\partial n} f(\#; n) = 2 \cos(\#) + \text{non-singular part}^Q; \quad (2.75)$$

which immediately gives

$$\frac{\partial}{\partial n} hT(0) \overline{F}(\cdot) i \Big|_{n=1} = \frac{1}{4} \cos K_0(2m) = \cos \frac{\rho_-}{8} \frac{e^{-2m}}{m}; \quad (2.76)$$

up to corrections of order  $O\left(\frac{e^{-2m}}{m}\right)$ . These formulas, based solely on the form factor bootstrap, are the main results of our work and perfectly match with the results of Ref. [66], derived by completely different means.

## 2.7 Symmetry resolved Rényi entropies

In this section, we use the results of the previous section to express the charged moments of an interval and eventually compute the symmetry resolved entropies. We consider the interval  $A = [0; \cdot]$  and, following [66], we express the charged moments as

$$Z_n(\cdot) = \text{Tr} \left[ \rho_A^{\otimes n} \hat{\rho}_A \right] = \int \rho_n^{\otimes n} hT(0) \overline{F}(\cdot) i; \quad (2.77)$$

where  $\epsilon$  is a UV regulator, and  $d_n$  is the scaling dimension of the composite  $U(1)$  twist field

$$d_T = 2 - \tau = \begin{cases} \frac{1}{12} n - n^{-1} + \frac{2}{(2)^{2n}}; & \text{Dirac fermions;} \\ \frac{1}{6} n - n^{-1} - \frac{2}{(2)^{2n}} + \frac{j}{2n}; & \text{complex bosons;} \end{cases} \quad (2.78)$$

valid for  $2 \leq n \leq \infty$ .  $c_n$  are non-universal normalization constants, that we discard from now on.

Following Ref. [66], we can write the logarithm of the charged moments for both fermions/bosons as

$$\begin{aligned} \log Z_n(\epsilon) &= \log Z_n^{(0)}(\epsilon) + \frac{ne^{2m\epsilon}}{4m} + \dots; \\ \log Z_1(\epsilon) &= \log Z_1^{(0)}(\epsilon) + \frac{e^{2m\epsilon}}{2m} \sin^2 \frac{\epsilon}{2} + \dots; \\ \frac{d}{dn} \log Z_n(\epsilon) &= \frac{d}{dn} \log Z_n^{(0)}(\epsilon) + \frac{1}{4} \cos K_0(2m\epsilon) + \dots; \end{aligned} \quad (2.79)$$

where  $\log Z_n^{(0)}(\epsilon)$  is the  $\epsilon$ -independent term

$$\log Z_n^{(0)}(\epsilon) = \frac{1}{6} n - n^{-1} + \frac{2}{2^{2n}} \log(m^n); \quad \text{Dirac fermions;} \quad (2.80)$$

$$\log Z_n^{(0)}(\epsilon) = \frac{1}{3} n - n^{-1} - \frac{2}{2^{2n}} + \frac{j}{n} \log(m); \quad \text{complex bosons;} \quad (2.81)$$

and the non-universal contributions of order  $O(1)$  (in the limit of small UV cut-off  $\epsilon$ ) are neglected explicitly.

From Eq. (2.79) the symmetry resolved von Neumann and Renyi entropies can be straightforwardly computed following [66]. We only report here the leading and sub-leading contributions to the entropies as

$$\begin{aligned} S_n(q_A) &= S_n + \frac{1}{2} \log \log(m^n)^{-1} + O(1) \text{ for Dirac fermion;} \\ S_n(q_A) &= S_n + \log \log(m^n)^{-1} + O(1) \text{ for complex boson;} \end{aligned} \quad (2.82)$$

for  $n \geq 1$ . The total Renyi and von Neumann entropy has the following large  $n$  behaviour

$$\begin{aligned} S_n &= \frac{c}{6} n - n^{-1} \log(m^n)^{-1} - \frac{n}{n-1} \frac{e^{2m\epsilon}}{4m} + \dots \quad n > 1; \\ S_1 &= \frac{c}{3} \log(m^n)^{-1} - \frac{1}{4} K_0(2m\epsilon) + \dots; \end{aligned} \quad (2.83)$$

where the non-universal constants are again neglected explicitly and  $c$  is the central charge ( $c = 1; 2$  for complex fermions and bosons, respectively). We recall that the result for  $S_1$  is already known from Ref. [47]; in particular, the correction  $-\frac{1}{4} K_0(2m\epsilon)$  is the double of what was found in the Ising field theory: this comes from the presence of two particles species in the Dirac theory, compared to Ising.

At leading order, one observes the equipartition of entanglement, namely  $S_n(q_A)$  does not depend explicitly on  $q_A$ . Still, the equipartition is broken when the cut-off  $\epsilon$  is finite compared to the other relevant length scales  $m^{-1}; \dots$ . A careful analysis has been performed in [66], and the terms which break equipartition can be written as a power series in  $\frac{1}{\log(m^n)^{-1}}$ .

Finally, we mention that the total von Neumann entropy can be decomposed as [39]

$$S_1 = \sum_{q_A} \rho(q_A) S(q_A) - \sum_{q_A} \rho(q_A) \log \rho(q_A) = S^c + S^f; \quad (2.84)$$

where  $\rho(q_A) = Z_1(q_A)$  equals the probability of finding  $q_A$  as the outcome of a measurement of  $\hat{Q}_A$ . The contribution  $S^c$  is called configurational entanglement entropy, and it measures the average entropy of each charge sector [49, 81]. The fluctuation (or number) entanglement entropy  $S^f$ , which instead takes into account the entropy due to the fluctuations of  $\hat{Q}_A$  [49, 82, 84].

## 2.8 Concluding remarks

In our work we applied the 1+1D bootstrap approach to compute the form factors of the composite  $U(1)$  branch-point twist fields which are directly related to symmetry resolved entropies. The technique was initiated in Ref. [65] for discrete symmetries and we generalised here to a  $U(1)$  conserved charge. For simplicity, we focused on free theories, namely the free massive Dirac theory and the free massive complex boson theory, both of which admit a global  $U(1)$  symmetry. We found solutions to the bootstrap equations that we test in some inequivalent ways. In particular, we used the  $\beta$ -theorem to check the compatibility with known CFT results, and we use replica diagonalization to recover our formulas. These calculations were a warm-up toward interacting integrable theories, as the whole machinery of form factor bootstrap was applied with the minimum amount of technical complications (absence of non-diagonal scattering, absence of bound-states, etc.).

Some general conclusions appear independent of the details of the underlying field theory, and they are manifest within the language of form factors. For instance, we found that the charged moments go to a constant in the limit of large intervals ( $m \rightarrow 1$ ), which is compatible with the asymptotic factorization of  $U(1)$  twist fields and their non-vanishing vacuum expectation value. The exponential subleading corrections arising in this limit, which is the focus of this work, are instead ruled by the lightest excitations above the vacuum. These features are related to a description of the theory in terms of massive asymptotic particles, and do not rely on the explicit absence of interactions. We interpret the factorization described above as a sort of 'area-law' of symmetry-resolved entanglement, related to the localization of quantum correlations around the entangling points: here the typical correlation length is given by the inverse mass  $m^{-1}$ .

## 2.A Analytic continuation $n \rightarrow 1$

The analytic continuation of  $f(\#; n)$ , defined by (2.71), is a subtle issue. In the absence of  $U(1)$  flux, say for  $\epsilon = 0$ , it was shown in Ref. [47] that the limit  $n \rightarrow 1$  is singular, and the convergence  $f(\#; n)$  is non-uniform, which is better understood in the language of distributions.

In particular, a contribution proportional to  $\delta(\#)$  arises in the derivative  $\lim_{n \rightarrow 1} \frac{\partial}{\partial n} f(\#; n)$ . We found a similar mechanism for  $\epsilon \neq 0$ , that we summarize below.

We first claim that it is possible to express

$$f(\#; n) = \tanh \frac{\#}{2} \operatorname{Im} F_2^{T, j(+1)(-1)}(2\# + i; n) + F_2^{T, j(-1)(+1)}(2\# + i; n) \\ e^{i\#} F_2^{T, j(+1)(-1)}(2\# + i2n - i; n) - e^{i\#} F_2^{T, j(-1)(+1)}(2\# + i2n - i; n) ; \quad (2.85)$$

where  $T$  is normalized as  $\langle hT \rangle = 1$ : this assumption is irrelevant for the final expression  $f(\#; n)$ , as the latter does not depend on the field normalization, and it only simplifies the notation. The relation above can be derived from the definition (2.71) by expressing the sum as a contour integral on the complex plane, as explained in details in [2, 47]. From the explicit expression (2.85) it is possible to recognize a pathological behaviour in the double limit  $n \rightarrow 1$  and  $\# \rightarrow 0$ . Namely, in this limit  $\tanh \frac{\#}{2} \rightarrow 0$  while the 2-particle form factors diverge due to the kinematic residue of  $F_2^{T, j(1)(1)}(\#; n)$  at  $\# = i; 2i, n - i$ . We carefully analyze this limit, and we express the leading contributions as

$$f(\#; 1 + \epsilon) \sim \frac{\#}{2} \frac{i}{2\#} \frac{ie^i}{2\# - 2i} + \frac{i}{2\#} \frac{ie^{-i}}{2\# - 2i} + \text{c.c.}; \quad (2.86)$$

valid for  $\#; \epsilon$  small. We first observe that at  $\# = 0$  the result depends discontinuously on  $n$ , and

$$f(0; 1 + \epsilon) = \begin{cases} (1 - \cos \epsilon) & = 0; \\ 1 - \epsilon & \neq 0; \end{cases} \quad (2.87)$$

Then, we analyse the derivative wrt  $n$ , that is

$$\frac{\partial f(\#; n)}{\partial n} \sim \# \sin \frac{2\#}{(\#^2 + 2)^2}. \quad (2.88)$$

While the support of the function above shrinks, as it is localised around the region  $j \approx \#$ , the typical value of  $\partial_n f(\#; n)$  diverges there: in particular, the integral

$$\int_1^Z \frac{\partial f(\#; n)}{\partial n} d\# \quad (2.89)$$

is finite, which means that  $\partial_n f(\#; n)$  converges to a  $\delta$ -distribution in the limit  $n \rightarrow 1$ . Fixing carefully the normalization constant, we eventually reach to

$$\lim_{n \rightarrow 1} \frac{\partial}{\partial n} f(\#; n) \sim 2 \cos(\#) \delta(\#); \quad (2.90)$$

We mention that (2.90) is not an exact relation, as it was derived using only the most leading singularities of the form factors. Indeed, corrections to (2.90) given by smooth (non-singular) terms are present, and their explicit expression differ for fermions and bosons. However, their contribution to the two-point function decays faster to zero for  $m \rightarrow 1$ , and then (2.90) rules the dominant infrared behavior in the limit  $n \rightarrow 1$ .

## 2.B Vacuum expectation values

The determination of the vacuum expectation value (VEV) is generally a difficult task, and for the standard/composite twist field it has been derived only for free theories [47, 65, 85]. The main issue is that the form-factor bootstrap approach is able to characterize a field up to proportionality constants, and it does not give any recipe to compute the VEVs. Indeed, to fix the field normalization one needs to impose a condition in the UV limit, i.e. requiring

$$\lim_{t \rightarrow 0} \langle hT(0) \mathcal{F}(\cdot)_{ij} \rangle e^{2\epsilon t} = 1; \quad (2.91)$$

that is difficult to express in terms of form-factors. In this appendix, we derive the VEV  $T$  for the  $U(1)$  free theories, with a logic similar to 2.5, making use of the diagonalization in the space of replicas.

We focus on fermions first, using the ideas of Refs. [47, 65, 76, 86]. Let us denote the fermion fields living on the  $j$ th replica by  $\psi_j$ . We consider the multiplet of  $n$  fields  $(\psi_1; \dots; \psi_n)$ , and we look for the matrix whose action in the space replica corresponds to the  $U(1)$  composite twist field. Since the total phase picked up by the twist field when turning around the entire Riemann surface is  $e^i$ , the transformation matrix can be obtained by multiplying the transformation matrix of the conventional fields [76] by  $e^{i/n}$ , as done in Ref. [66]. Accordingly, the following representation is obtained

$$= e^{i/n} \begin{pmatrix} 0 & 0 & 0 & 0 & \dots & 0 & (1)^{n+1} & 1 \\ 1 & 0 & 0 & 0 & \dots & 0 & 0 & 0 \\ 0 & 1 & 0 & 0 & \dots & 0 & 0 & 0 \\ 0 & 0 & 1 & 0 & \dots & 0 & 0 & 0 \\ \vdots & \vdots & \vdots & \vdots & \ddots & \vdots & \vdots & \vdots \\ 0 & 0 & 0 & 0 & \dots & 0 & 0 & 0 \\ 0 & 0 & 0 & 0 & \dots & 1 & 0 & 0 \end{pmatrix}. \quad (2.92)$$

The transformation matrix has to be diagonalised for the determination of the VEV [47]. The eigenvalues of can be written as  $e^{2k/n} e^{i/n}$ , with

$$k = \frac{n-1}{2}; \dots; \frac{n-1}{2} \quad (2.93)$$

being an integer/half-integer for  $n$  odd/even. The eigenvectors of correspond to some new fermionic fields  $\psi_k$ , which pick a phase under the action of . Indeed, one easily shows that they satisfy canonical anticommutation relations  $\{\psi_k(x), \psi_{k'}(x')\} = \delta_{k,k'} \delta(x-x')$ ,  $\{\psi_k(x), \psi_{k'}(x')\} = 0$  and  $\{\psi_k(x), \psi_{k'}(x')\} = 0$ . Since these fields are not mixed among each by , it follows [66] that the composite  $U(1)$  twist field can be factorised as

$$T = \prod_{k=(n-1)/2}^{(n-1)/2} T_k \quad (2.94)$$

Here  $T_k$  is a twist-field acting non-trivially on the mode  $\psi_k$  with a phase  $e^{2k/n} e^{i/n}$ , that is the corresponding eigenvalue of the twist matrix . Since  $T_k$  correspond to single-replica  $U(1)$  twist fields, their VEV can be computed with the results of [87] as

$$\langle h \bar{\psi}_k \psi_k \rangle = \frac{m}{2} \frac{(k-n/2)^2}{G(1-k/n) G(1+k/n)}; \quad (2.95)$$

where  $G(x)$  is the Barnes G-function. Hence, for the  $n$ -replica Dirac theory we get

$$\langle h T \rangle = \prod_{k=\frac{n-1}{2}}^{\frac{n-1}{2}} \langle h \bar{\psi}_k \psi_k \rangle = \frac{m}{2} \prod_{k=\frac{n-1}{2}}^{\frac{n-1}{2}} \frac{1}{G(1-\frac{2k+n}{2n}) G(1+\frac{2k+n}{2n})}; \quad (2.96)$$

which can be equivalently expressed as

$$hTi = \frac{m}{2} \exp \left[ \int_0^1 dt \frac{\sinh t \cosh \frac{t}{n}}{2 \sinh \frac{t}{n} \sinh^2 t} \right] \left( \frac{n}{12} + \frac{2}{(2n)^2} \right) e^{2t} \quad (2.97)$$

using the integral representation of the Barnes G-function.

For the case of the complex boson, we can proceed in a similar fashion, and our eventual computation expresses the VEV of the composite branch-point twist field as a product of VEVs for conventional  $U(1)$  twist fields. Contrary to the case of the free Dirac theory, however, we now face an important subtlety when defining those VEVs in the complex boson theory. For instance, this theory is not compact and as a consequence the short-distance behaviour of the theory and the proper definition of the VEV is non-trivial [85], because of the presence of a zero mode. Consequently, the explicit value of the VEV is non-universal, in the sense that depends on the employed normalisation. This problem was carefully discussed in Ref. [85], where an expression for the VEV was actually proposed based on a natural regularisation of the fields and on the angular quantisation scheme, and we adopt these conventions.

To proceed, we need the transformation matrix  $T$ , whose action in the multiplet  $(\psi_1, \dots, \psi_n)$  corresponds to the composite twist field. We write it as [66]

$$T = e^{i\bar{n}} \begin{pmatrix} 0 & 0 & 0 & 0 & 0 & 1 \\ 1 & 0 & 0 & 0 & 0 & 0 \\ 0 & 1 & 0 & 0 & 0 & 0 \\ 0 & 0 & 1 & 0 & 0 & 0 \\ \vdots & \vdots & \ddots & \ddots & \vdots & \vdots \\ 0 & 0 & 0 & 0 & \ddots & 0 \\ 0 & 0 & 0 & 0 & 1 & 0 \end{pmatrix}; \quad (2.98)$$

and its eigenvalues are  $e^{i2k-n} e^{i\bar{n}}$ , with

$$k = 0, \dots, n-1; \quad (2.99)$$

Similarly to the Dirac case, one can introduce new Bose fields, which satisfy the canonical commutation relations  $[\psi_k(x); \psi_{k'}^\dagger(x)] = \delta_{k,k'}$ ,  $[\psi_k(x); \psi_{k'}(x)] = 0$  and  $[\psi_k^\dagger(x); \psi_{k'}^\dagger(x)] = 0$  and diagonalize the action of  $T$ . Again, we decompose again  $T$  as (2.94), and, employing the results of [85], we write down

$$h\bar{T}i = N (me^\epsilon)^{\frac{1}{2n}} \exp \left[ \int_0^1 dt \frac{\sinh t \ln(\cosh t)}{(4t^2 + 2) \cosh^2 t} \right] \cos \frac{t}{2} \sinh t + 2t \sin \frac{t}{2} \cosh t; \quad (2.100)$$

with  $\epsilon = \frac{k}{n} + \frac{1}{2n}$ ,  $\epsilon$  the Euler's constant, and  $N$  given by

$$N = \exp \left[ \frac{1}{3}(\epsilon + \ln 2) + \frac{1}{2}(\ln(2)) \right] \int_0^1 dt e^{-t} \frac{\sinh t}{(e^t - 1)(\cosh t - 1)} + \frac{1}{3}; \quad (2.101)$$

Eventually, one gets the VEV of  $T$  of the bosonic  $n$ -replica theory as

$$\begin{aligned}
 \langle hT_i \rangle = \prod_{k=0}^{N-1} \langle h_k \rangle = N^n (me^\epsilon)^{\frac{1}{6}(n-\frac{1}{n})} \frac{2}{(2)^{2n} + (2)^n} \exp \left[ \frac{1}{2} \int_0^{2\pi} dt \frac{\sinh t \ln(\cosh t)}{(4t^2 + \pi^2) \cosh^2 t} \right. \\
 \left. + \frac{2it}{2n} \cos \frac{2i(n+1)t + 2itj}{2n} \right] + \\
 + \frac{+2it}{2n} \cos \frac{(n+2i(n+1)t) + (n+2it)j}{2n} + \\
 + \frac{2it}{2n} \sin \frac{(n-2it)(n-1) + j}{2n} + \\
 + \frac{+2it}{2n} \sin \frac{(n+2it)(n-1) + j}{2n} : \quad (2.102)
 \end{aligned}$$

## Chapter 3

# $Z_3$ symmetry resolved entanglement of the 3-state Potts model via form factor bootstrap

In this chapter, based on [4], we apply the form factor bootstrap approach to the twist fields in the 3-state Potts model. This is an integrable interacting massive quantum field theory with a global  $Z_3$  symmetry, which is unbroken in the paramagnetic phase. Its ground state can be thus analyzed with the lens of symmetry resolved entanglement, and we provide exact results giving the solutions of the bootstrap equations. Our predictions are carefully checked using  $\epsilon$ -theorem.

### 3.1 The model

In this section, we review the scattering theory of the  $q$ -state Potts model for  $0 < q < 4$ , firstly analyzed in [88], and we focus on  $q = 3$  [89, 90]. We first formulate the property of this model, following closely [91], in its ferromagnetic phase, where excitations are multi-kink states interpolating different vacua. Then, we discuss the paramagnetic phase, which is the main focus of our work.

The  $q$ -state Potts model admits  $q$  distinct vacua, labeled by an index  $\alpha = 1, \dots, q$ . A generic  $p$ -kink state is written as

$$|j, K_{\alpha_1}(\theta_1) K_{\alpha_2}(\theta_2) \dots K_{\alpha_p}(\theta_p)\rangle \quad \text{with} \quad \alpha_i \in \{1, \dots, p\}, \quad \theta_i = 1, \dots, p; \quad (3.1)$$

where  $\theta_i$  are the rapidity variables, and  $K_{\alpha}(\theta)$  which represent an elementary kink interpolating between vacua  $\alpha$  and  $0$ . Such a state is "neutral" if  $\alpha_0 = \alpha_p$  and "charged" if  $\alpha_0 \neq \alpha_p$ . Since the model is integrable the scattering theory is fully determined by the two-particle scattering amplitudes. In addition, the permutation symmetry under exchange of the vacua implies that there are only four independent functions that need to be computed namely the Zamolodchikov-Faddeev (ZF) [92, 93] algebra may be written as

$$\begin{aligned} K_{\alpha}(\theta_1) K_{\beta}(\theta_2) &= S_0(\theta_1, \theta_2) \sum_{\gamma \in \{1, \dots, p\}} K_{\gamma}(\theta_2) K_{\alpha}(\theta_1) + S_1(\theta_1, \theta_2) K_{\beta}(\theta_2) K_{\alpha}(\theta_1) \quad \alpha \neq \beta; \\ K_{\alpha}(\theta_1) K_{\beta}(\theta_2) &= S_2(\theta_1, \theta_2) \sum_{\gamma \in \{1, \dots, p\}} K_{\gamma}(\theta_2) K_{\alpha}(\theta_1) + S_3(\theta_1, \theta_2) K_{\beta}(\theta_2) K_{\alpha}(\theta_1); \end{aligned} \quad (3.2)$$

where  $\delta_{ij} = \delta_{i-j}$  and the first term in the relations above indicates that the scattering is generally non-diagonal. The amplitudes  $S_i(\theta)$  with  $i = 0;1;2;3$  are constrained by a number of equations related to physical requirements such as unitarity. These equations can be solved analytically, giving

$$\begin{aligned} S_0(\theta) &= \frac{\sinh \frac{2i}{3} \sinh \left( \frac{i}{3} \right)}{\sinh \frac{i}{3}} S(\theta); \\ S_1(\theta) &= \frac{\sin \frac{2}{3} \sinh \left( \frac{i}{3} \right)}{\sin \frac{i}{3} \sinh \frac{2i}{3}} S(\theta); \\ S_2(\theta) &= \frac{\sin \frac{2}{3} \sinh \frac{i}{3}}{\sin \frac{i}{3} \sinh \frac{i}{3}} S(\theta); \\ S_3(\theta) &= \frac{\sin \frac{i}{3}}{\sin \frac{i}{3}} S(\theta); \end{aligned} \tag{3.3}$$

in terms of the variable  $\rho$  which is related to  $q$  as

$$\rho = 2 \sin \frac{i}{3} : \tag{3.4}$$

From this definition, it follows that  $q$  is only an integer for very particular values of  $i$ , but we mention that it is possible to make sense of the model even for generic  $i$  [88]. For  $i = \frac{3}{2}$  we have  $q = 4$  and the resulting theory has 4 particles and  $S$ -matrices which can be identified with those of the  $D_4$ -minimal Toda theory. Similarly,  $i = 1$  corresponds to  $q = 3$ ,  $i = \frac{3}{4}$  to  $q = 2$  (the Ising model) and  $i = \frac{3}{5}$  to  $q = 1$ . The function  $S(\theta)$  may be expressed as an infinite product of gamma functions or also through an integral representation given by

$$S(\theta) = \frac{\sinh \frac{i}{3}}{\sinh \left( \frac{i}{3} \right)} e^{A(\theta)}; \tag{3.5}$$

with

$$A(\theta) = \int_0^{\infty} \frac{dt \sinh \frac{t}{2} \left( 1 - \frac{1}{\cosh \frac{t}{2}} \right) \sinh \frac{5t}{3}}{t \sinh \frac{t}{2} \cosh \frac{t}{2}} \sinh \frac{t}{i}; \tag{3.6}$$

For  $i = 1$ , and in particular  $q = 3$ , the function  $S(\theta)$  has no poles on the physical sheet. However, the amplitudes  $S_0(\theta)$  and  $S_1(\theta)$  have a pole at  $\theta = \frac{2i}{3}$  in the direct channel corresponding to the formation of a bound state, which is itself an elementary kink  $K$  with three point coupling

$$\left( \begin{matrix} K \\ KK \end{matrix} \right)^2 = - \sinh \frac{2}{3} e^{A(\frac{i}{3})}; \tag{3.7}$$

Correspondingly, the amplitudes  $S_2(\theta)$  and  $S_3(\theta)$  have a pole in the cross-channel at  $\theta = \frac{i}{3}$ . We mention that for  $i > 1$  additional poles arise, and the particle spectrum becomes more involved, but this is beyond our purpose, and we do not discuss it further.

From now on, we focus on  $q = 3$ , corresponding to  $i = 1$ , where the  $S$ -matrices reduce to [88]{90]

$$S_1(\theta) = \frac{\sinh \frac{1}{2} + \frac{2i}{3}}{\sinh \frac{1}{2} - \frac{2i}{3}} \quad S_2(\theta) = \frac{\sinh \frac{1}{2} + \frac{i}{3}}{\sinh \frac{1}{2} - \frac{i}{3}} \quad \text{and} \quad S_3(\theta) = 0; \tag{3.8}$$

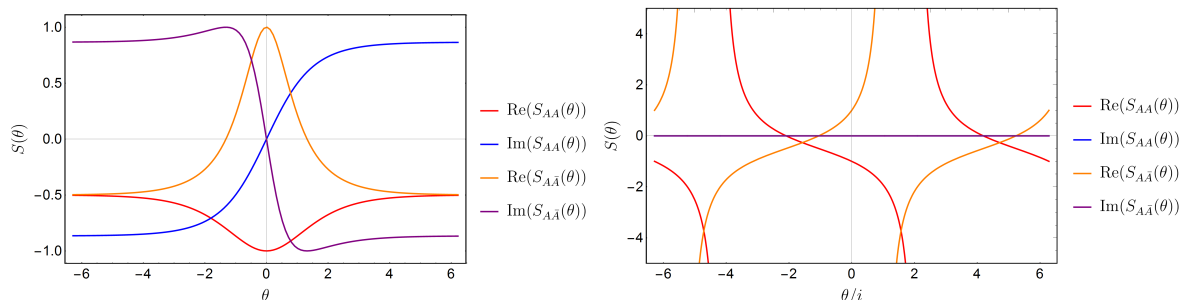


Figure 3.1: Left: Scattering amplitude for real rapidity difference ( $\text{Im}(\theta) = 0$ ) in the 3-state Potts model. When  $\theta = 0$  we have  $S_{AA}(\theta = 0) = 1$  and  $S_{A\bar{A}}(\theta = 0) = -1$ , while for  $j \neq j' + 1$  the scattering amplitude goes to a constant. Right: Scattering amplitude for imaginary values of the rapidity difference ( $\text{Re}(\theta) = 0$ ) in the 3-state Potts model. The imaginary part is vanishing and the amplitudes develop dynamical poles associated with the presence of a bound state.

So far, we discussed the ferromagnetic phase only, but it is worth giving some additional details for the 3-state Potts model in the other phases. The model can be seen as a perturbed CFT [91], with Euclidean action given by

$$S = S_{\text{CFT}} + \int d^2x \phi(x) \quad (3.9)$$

The underlying conformal field theory [94], obtained for  $\theta = 0$  (critical phase), is the tricritical 3-state Potts model, that is the minimal model  $\mathcal{M}(6;5)$  of central charge  $c = 4/5$ . The energy density field  $\phi(x)$  is identified with the primary field  $\phi_{2,1}$  with conformal dimensions

$$(\phi; \phi) = \left( \frac{2}{5}; \frac{2}{5} \right); \quad (3.10)$$

and it is a relevant perturbation driving the system away from the critical point: depending on the sign of  $\theta$ , one has the paramagnetic or ferromagnetic phase. Here, we comment more on the paramagnetic (or disordered) phase (see [95, 96]), in contrast with the analysis of the ferromagnetic phase given at the beginning of this section. For what concerns scattering properties, the choice of the phase makes little difference, as we will see below. Instead, it amounts to a change in the way we identify the fundamental particles of the theory. In the paramagnetic phase, we consider particles as fundamental excitations above a vacuum  $|0\rangle$ , that is the only ground-state unbroken under  $Z_3$ . Multiparticle states are then constructed in terms of particles belonging to one of two species, denoted here  $A$  and  $\bar{A}$ , related by charge conjugation. The scattering is diagonal and the only non-trivial scattering phases are the transmission amplitudes

$$S_{AA}(\theta) = S_{\bar{A}\bar{A}}(\theta) = \frac{\sinh \frac{1}{2}(\theta + \frac{2i}{3})}{\sinh \frac{1}{2}(\theta - \frac{2i}{3})}; \quad S_{A\bar{A}}(\theta) = S_{\bar{A}A}(\theta) = \frac{\sinh \frac{1}{2}(\theta + \frac{i}{3})}{\sinh \frac{1}{2}(\theta - \frac{i}{3})}; \quad (3.11)$$

whose expression is identical in the ferromagnetic phase (3.8). The latter amplitudes are related by crossing symmetry  $S_{AA}(\theta) = S_{\bar{A}\bar{A}}(i - \theta)$ . Moreover, since the theory is invariant under charge conjugation and parity symmetry, then  $S_{AA}(\theta) = S_{\bar{A}\bar{A}}(\theta)$  and  $S_{A\bar{A}}(\theta) = S_{\bar{A}A}(\theta)$ .

A dynamical pole is present for  $S_{AA}(\theta)$  with associated residue

$$\text{Res}_{\theta = i\frac{2}{3}} S_{AA}(\theta) = (A_{\bar{A}A})^2 = i^{\frac{2}{3}}; \quad (3.12)$$

which corresponds to the bound state formation process

$$A + A \rightarrow A; \quad (3.13)$$

In Fig. 3.1 we plot the S-matrix as a function of the rapidity difference along the real and the imaginary axis respectively. An important feature is that  $S_{AA}(0) = -1$  which implies fermionic statistics; for this reason, we call  $S_{AA}(\theta)$  a fermionic-type scattering matrix. Instead  $S_{AA}(0) = 1$  and similarly  $S_{AA}(\theta)$  are bosonic-type scattering matrices.

Critical to our analysis is the global  $Z_3$  symmetry, present in this theory. It is generated by the following action on the particles

$$A \rightarrow e^{2i/3} A; \quad A \rightarrow e^{i/3} A; \quad (3.14)$$

We can then associate a  $Z_3$ -charge to each particle, which is additive and equals  $+1$  for species  $A$ , and  $-1$  for species  $\bar{A}$ , while the ground state  $|0\rangle$  is neutral. Note that the charge is conserved in the process (3.13), since

$$(+1) + (+1) = -1 \pmod{3}; \quad (3.15)$$

In the 3-state Potts model there are order and disorder fields which are either local or semi-local w.r.t. the  $Z_3$  symmetry. We call them  $\phi_1(x)$ ;  $\psi_1(x)$  respectively. While  $\phi_1(x)$  is local w.r.t. the particles and has the meaning of a magnetization operator (say a local order parameter),  $\psi_1(x)$  is non-local and acts nontrivially introducing an Aharonov-Bohm flux of value  $e^{i2\pi/3}$  for each space point  $y > x$ . In other words,  $\psi_1(x)$  is the twist field associated with  $Z_3$  symmetry. The conjugate fields are  $\bar{\phi}_1(x)$  and  $\bar{\psi}_1(x)$  and the latter gives an Aharonov-Bohm flux of value  $e^{-i2\pi/3}$ . The two order/disorder operators  $\phi_1$ ;  $\psi_1$  share the same conformal dimensions

$$(\phi_1; \bar{\phi}_1) = (\psi_1; \bar{\psi}_1) = \left(\frac{1}{15}; \frac{1}{15}\right); \quad (3.16)$$

which dictate the ultraviolet behaviour of their correlation functions. At criticality, these fields are identified with the primary field  $\phi_{23}$  of the minimal model  $\mathcal{M}(6;5)$  [97]. Away from criticality, one can relate the paramagnetic and ferromagnetic phase via the Kramers-Wannier duality, which exchanges the role of the order and disorder operators. This last observation is useful as it implies that we can compare results for the disorder operator in the paramagnetic phase to those for the order operator in the ferromagnetic phase, discussed in [91].

## 3.2 Twist fields and their form factors

In this section, we introduce and characterize the twist fields of the (replica) Potts model, giving analytical predictions for their 2-particle form factors. We remind that these fields are non-local or semi-local with respect to other fields in the theory, a property that translates into non-trivial equal-time commutation relations. For our purpose, three different types of twist fields have to be considered:

- the branch-point twist fields,  $T_n$  and its conjugate  $\bar{T}_n$ , associated with cyclic permutation symmetry  $Z_n$  among copies in the  $n$ -replica model. These fields play a central role in the characterization of the Renyi entropy and, via analytical continuation  $n \rightarrow 1$ , the entanglement entropy.

- The disorder fields  $\sigma_1$  associated with the global  $Z_3$  symmetry of the 3-state Potts model.
- The composite twist fields  $T_n; \bar{T}_n$  that from the fusion of the previous fields, originally described in [98{101} gives rise to composite twist fields  $T_n$  and  $\bar{T}_n$ . These fused fields play a central role in the computation of the symmetry resolved entanglement entropies, as described in [51].

The exchange relations for standard branch-point twist field in a replica QFT are [47]

$$T_n(x)O_i(y) = O_{i+1}(y)T_n(x) \quad \text{for } y > x; \quad (3.17)$$

$$= O_i(y)T_n(x) \quad \text{for } x > y; \quad (3.18)$$

where  $O_i$  is a local field of the  $i$ -th replica ( $i = 1; \dots; n$ ). Similarly  $\bar{T}_n(\mathbf{x})$ , the hermitian conjugate of  $T_n(x)$ , is associated with the inverse cyclic permutation, and its exchange relations are

$$\bar{T}_n(x)O_i(y) = O_{i-1}(y)\bar{T}_n(x) \quad \text{for } y > x; \quad (3.19)$$

$$= O_i(y)\bar{T}_n(x) \quad \text{for } x > y; \quad (3.20)$$

Let us now consider an operator  $V(x)$  which introduces an Aharonov-Bohm flux  $e^i$  in the region  $y > x$ . For the moment, we assume being generic, keeping in mind that the allowed values in the 3-state Potts model are  $i = 0$  (corresponding to the identity operator) and  $i = 2 \Rightarrow 3$  (corresponding to  $\sigma_1$ ). Doing so, the generator of the symmetry  $e^{iQ_A}$  of the subsystem  $A = [0; \cdot]$  can be identified by

$$e^{iQ_A} = V(0)(V)^y(\cdot); \quad (3.21)$$

The mutual locality between  $V$  and another operator  $O$  is identified by the relation

$$O(y; \bar{t})V(x; t) = e^{i \circ} V(x; t)O(y; \bar{t}); \quad (3.22)$$

or, when using the radial quantisation picture,

$$O(0;0)V(e^{i2}z; e^{i2}z) = e^{i \circ} O(0;0)V(z;z); \quad (3.23)$$

We refer to  $i \circ$  as the charge of the operator  $O$  for the symmetries under consideration. The fusion between the standard twist field  $T_n$  and  $V$  gives rise to the so-called composite twist fields which can be defined very precisely in CFT [98{100}

$$:T_n V:(y) := r^2 \lim_{x' \rightarrow y} \int_{x'}^y dx \, y^{j^2} \left(1 \frac{1}{n}\right)^{\sum_{j=1}^n} T_n(y) V_j(x); \quad (3.24)$$

where  $V_j(x)$  is the copy of field  $V(x)$  living in replica  $j$ ,  $\int$  represents normal ordering and the power law involves the conformal dimension of the field  $V$  (for spinless fields, this is half of the scaling dimension  $h$  given earlier). For the  $Z_3$  symmetry of the Potts model, where  $i = 0; 2 \Rightarrow 3$  we identify

$$V_0 = 1; \quad V_{2=3} = \sigma_1; \quad (3.25)$$

Similarly, the composite twist fields of the replica theory will be denoted by

$$\begin{aligned} T_n^O(\mathbf{x}) &:= :T_n \sigma_1(\mathbf{x}) & \text{and} & \quad T_n^0(\mathbf{x}) := T_n(\mathbf{x}); \\ \bar{T}_n^O(\mathbf{x}) &:= : \bar{T}_n \sigma_1(\mathbf{x}) & \text{and} & \quad \bar{T}_n^0(\mathbf{x}) := \bar{T}_n(\mathbf{x}); \end{aligned} \quad (3.26)$$

With the exchange relations (3.17) at hand, one can formulate the branch-point twist fields form factor equations in integrable QFTs (IQFTs) [64, 75, 77, 98, 102, 111], which generalize the standard form factor programme for local fields [70, 73]. These equations were first given in [47] for diagonal theories and then in [63] for non-diagonal ones. Here, we discuss the paramagnetic phase of the Potts model, giving a complementary description to previous studies [91] that focused on the ferromagnetic phase. In this phase, the ground state  $|0\rangle$  is unique, and the asymptotic states are multiparticle-excitations: two species of particle are present, and we denote them as  $A; \bar{A}$ . The forthcoming approach is very similar to the one considered for complex free theories in [2], and the only novelty is the explicit presence of interactions encoded in a non-trivial scattering matrix. We denote the form factors of a (semi-)local operator  $O(x; \vec{t})$ , that are matrix elements between the vacuum and asymptotic states, as

$$F_{1 \dots k}^O(\vec{t}_1; \dots; \vec{t}_k) = \langle 0 | O(0; 0) | j_1 \vec{t}_1; \dots; j_k \vec{t}_k \rangle \quad (3.27)$$

The dispersion relation of the particles is parametrized as  $(E; \vec{p}) = (m_i \cosh \eta; m_i \sinh \eta)$ , where  $i$  indicates the particle species ( $A$  or  $\bar{A}$  for us) and  $\eta$  is the rapidity. Any multi-particle state can be constructed from the vacuum state  $|0\rangle$  as

$$| j_1 \vec{t}_1; j_2 \vec{t}_2; \dots; j_k \vec{t}_k \rangle = Z_1^{j_1}(\vec{t}_1) Z_2^{j_2}(\vec{t}_2) \dots Z_k^{j_k}(\vec{t}_k) |0\rangle \quad (3.28)$$

where  $Z^j$ s are particle creation operators; in particular, the operator  $Z_i^j(\vec{t}_i)$  creates a particle of species  $i$  with rapidity  $\vec{t}_i$ . The creation and annihilation operators  $Z_i^j(\vec{t})$  and  $Z_i(\vec{t})$  satisfy the ZF algebra [92, 93] which (in the case of diagonal scattering) reads

$$\begin{aligned} Z_i^j(\vec{t}_i) Z_j^k(\vec{t}_j) &= S_{i,j}(\vec{t}_{ij}) Z_j^k(\vec{t}_j) Z_i^j(\vec{t}_i); \\ Z_i(\vec{t}_i) Z_j(\vec{t}_j) &= S_{i,j}(\vec{t}_{ij}) Z_j(\vec{t}_j) Z_i(\vec{t}_i); \\ Z_i(\vec{t}_i) Z_j^k(\vec{t}_j) &= S_{i,j}(\vec{t}_{ij}) Z_j^k(\vec{t}_j) Z_i(\vec{t}_i) + \delta_{i,j} 2^{-\vec{t}_{ij}} \delta(\vec{t}_i - \vec{t}_j); \end{aligned} \quad (3.29)$$

where  $S_{i,j}(\vec{t}_{ij})$  denotes the two-body S-matrices of the theory as function of rapidity differences. For any given integrable QFT we consider the  $n$ -replica model, that is understood as follows: the internal degrees of freedom of the particles are parametrized with a pair

$$(\vec{t}; i); \quad i = 1; \dots; n \quad (3.30)$$

where  $i$  is a replica index and  $\vec{t}$  labels the species of the original model. The scattering matrix is then

$$\mathfrak{S}_{(i; \vec{t}_i)(j; \vec{t}_j)}(\vec{t}) = \begin{cases} S_{i,j}(\vec{t}) & i = j \\ 1 & i \neq j \end{cases} \quad (3.31)$$

namely particles in different replicas do not interact. To make our notations easier we introduce the multi-index, following [47]

$$a_i = (\vec{t}; i); \quad (3.32)$$

together with

$$\bar{a}_i = (\vec{t}; -i); \quad (3.33)$$

where  $\bar{a}_i$  denotes the anti-particle of  $a_i$ . We now aim to characterize the 2-particle form factors for the three types of twist fields previously introduced.

### 3.2.1 Form factors of Branch Point Twist Fields

The bootstrap equations for form factors of  $T_n$ , denoted by  $F_{\underline{a}}(\underline{\cdot}; n)$ , are

$$F_{\underline{a}}(\underline{\cdot}; n) = S_{a_i a_{i+1}}(i; i+1) F_{\dots a_i \dots a_{i+1} a_i a_{i+2} \dots}(\dots; i+1; i; \dots; n); \quad (3.34)$$

$$F_{\underline{a}}(\dots; i+2; i; \dots; k; n) = F_{a_2 a_3 \dots a_k a_1}(\dots; k; i+1; n); \quad (3.35)$$

$$i \operatorname{Res}_{\substack{\circ \\ \circ+i}} F_{a_0 a_0 \underline{a}}(\substack{\circ \\ \circ}; \substack{\circ \\ \circ}; n) = F_{\underline{a}}(\underline{\cdot}; n); \quad (3.36)$$

$$i \operatorname{Res}_{\substack{\circ \\ \circ+i}} F_{a_0 a_0 \underline{a}}(\substack{\circ \\ \circ}; \substack{\circ \\ \circ}; n) = \prod_{l=1}^{\gamma^k} S_{a_0 a_l}(\circ) F_{\underline{a}}(\underline{\cdot}; n); \quad (3.37)$$

$$i \operatorname{Res}_{\substack{\circ \\ \circ+i u}} F_{(\dots; \circ)(\dots; \circ) \underline{a}}(\substack{\circ \\ \circ}; \substack{\circ \\ \circ}; n) = \substack{\circ \\ \circ} F_{(\dots; \circ) \underline{a}}(\substack{\circ \\ \circ}; n);$$

where  $\underline{\cdot}$  and  $\underline{a}$  are shorthands for  $(\dots; i; \dots; k)$  and  $(\dots; i+1)(\dots; i+2)(\dots; k)$  respectively, where  $\substack{\circ \\ \circ} = A; A$ . We emphasize that two particles of type  $A$  can form bound state  $A$ , or the other way round, and this is encoded in the bound state equation (3.37), a feature that is absent in free theories. It is easy to see, however, that, since  $T_n$  is  $Z_3$  neutral, both the one-particle form factors and the 2-particle one with equal species ( $(A; A)$  or  $(A; A)$ ) are vanishing. As a consequence, the first non-trivial form factor, excluding the VEV, is the particle-antiparticle one ( $(A; \bar{A})$ ) which is not affected by bound state poles. For this reason, the strategy we adapt to construct the solution of the bootstrap equations is similar to the one employed for complex free theories.

Following Ref. [47] it is easy to write down the two-particle FF of the BPTF  $T_n$  for particles in the same copy (say 1), which reads as follows

$$F_{(A;1)(\bar{A};1)}(\dots; n) = \frac{h \bar{h} i \sin \frac{\pi}{n}}{2n \sinh \frac{i+}{2n} \sinh \frac{i-}{2n}} \frac{h(\dots; n)}{h(i; n)}; \quad (3.38)$$

where  $h \bar{h} i$  is the vacuum expectation value (VEV) of  $T_n$  and  $h(\dots; n)$  is an entire function known as the minimal form factor which we present in Appendix 3.A. From  $F_{(A;1)(\bar{A};1)}(\dots; n)$  we obtain  $F_{(A;j)(\bar{A};k)}(\dots; n)$ , via the monodromy conditions, as

$$F_{(A;j)(\bar{A};k)}(\dots; n) = \begin{cases} F_{(A;1)(\bar{A};1)}(2i(k-j); \dots; n) & \text{if } k > j; \\ F_{(A;1)(\bar{A};1)}(2i(j-k)+; \dots; n) & \text{otherwise,} \end{cases} \quad (3.39)$$

and

$$F_{(A;j)(\bar{A};k)}(\dots; n) = F_{(A;j)(\bar{A};k)}(\dots; n) \quad (3.40)$$

The form factors of the other field  $\bar{T}_n$ , denoted by  $\bar{F}$ , can be simply obtained from those of  $T_n$  [47] through the relation

$$\bar{F}_{(A;j)(\bar{A};k)}(\dots; n) = F_{(A;n-j)(\bar{A};n-k)}(\dots; n); \quad (3.41)$$

coming from the property  $\bar{T}_n(x) = (T_n(x))^{\mathcal{Y}}$ .

### 3.2.2 Form factors of the Disorder operator $\tau_1$

In this subsection we consider the form factor equations for the field  $\tau_1$ , the disorder operator associated to the flux  $e^{2\pi/3}$ . This can be seen as a particular case of the composite twist field  $T_n^{-1}$  when just a single replica is present ( $n = 1$ ). As mentioned before, we provide results for

the disordered phase of the model, which are related to those in the ordered phase under the exchange of order/disorder operator ( $\sigma_1 \leftrightarrow \tau_1$ ) [91].

The disorder operators  $\tau_1$  are  $Z_3$  invariant, so the form factors  $F_{AA}(\cdot) F_{AA}(\cdot)$  vanish by symmetry; from now on we focus on the particle-antiparticle form factors. The monodromy equation is

$$F_{AA}^1(\cdot + 2i) = e^{\frac{2i}{3}} F_{AA}^1(\cdot); \quad (3.42)$$

since a mutual locality index  $e^i = e^{i2=3}$  among  $A$  and  $\tau_1$  is present. The unitarity equation is

$$F_{AA}^1(\cdot) S_{AA}(\cdot) = F_{AA}^1(\cdot) \quad (3.43)$$

A kinematical residue is present at  $\cdot = i$  and it is related to the VEV  $h_{\tau_1 i}$  via

$$\text{Res}_{\cdot=i} F_{AA}^1(\cdot) = i(1 - e^{\frac{2i}{3}}) h_{\tau_1 i}; \quad (3.44)$$

while no dynamical poles are present<sup>1</sup>. Similar equations hold if one exchanges  $A \leftrightarrow \tau_1$ , keeping in mind that the only difference would be the mutual locality index  $e^{i2=3}$  between  $A$  and  $\tau_1$ . A solution to these equations is given by<sup>2</sup>

$$F_{AA}^1(\cdot) = h_{\tau_1 i} \sin \frac{e^{-\frac{\delta}{3}} h(\cdot; 1)}{3 \cosh \frac{\delta}{2} h(i; 1)}; \quad (3.45)$$

$$F_{AA}^1(\cdot) = h_{\tau_1 i} \sin \frac{e^{\frac{\delta}{3}} h(\cdot; 1)}{3 \cosh \frac{\delta}{2} h(i; 1)}; \quad (3.46)$$

where the minimal form factor  $h(\cdot; 1)$  is the  $n = 1$  case of the function analysed in Appendix 3.A. The structure of this solution can be easily justified: the minimal form factor solves the equations

$$h(\cdot; 1) = S(\cdot) h(\cdot; 1) = h(2i - \cdot; 1); \quad (3.47)$$

that is, the form factor equations in the absence of the semi-locality phase  $e^{\frac{2i}{3}}$ . The factors  $r(\cdot) := \frac{e^{-\frac{\delta}{3}}}{\cosh \frac{\delta}{2}}$  then account for this phase by satisfying

$$r(\cdot) = r(\cdot) = e^{\frac{2i}{3}} r(2i - \cdot); \quad (3.48)$$

and finally the denominator  $\cosh \frac{\delta}{2}$  ensures the presence of a kinematic pole at  $\cdot = i$  whilst the constant factors ensure the correct normalisation of the residue at the pole. For  $\delta \rightarrow \infty$  it is possible to show that

$$h(\cdot; 1) \sim e^{\frac{j}{3}}; \quad |j| \rightarrow \infty \quad (3.49)$$

thus, our solution has the following asymptotics

$$\lim_{|j| \rightarrow \infty} F_{AA}^1(\cdot) = \text{const.}; \quad (3.50)$$

<sup>1</sup>Note that this equation is different from the corresponding equation for branch-point twist operators where instead there are two separate kinematical residues. The case  $n = 1$  is indeed special, and the limit  $n \rightarrow 1$  gives rise to a fusion of two poles: the residue of the resulting pole is just the sum of the two original residues (present for  $n > 1$ ).

<sup>2</sup>This solution is inspired from the solution of the complex non-compact free boson, which is discussed in [77]

that is in complete agreement with results of [91, 112] and the general form of the momentum space cluster property. For the other disorder operator  $\sigma_1$  similar considerations apply. A way to get easily the form factors of  $\sigma_1$  is exploiting the charge-conjugation symmetry, meaning that  $\sigma_1$  is the charge-conjugated field of  $\sigma_1$  and so its form factors can be obtained by interchanging  $A \leftrightarrow \bar{A}$  in the previous formula.

### 3.2.3 Form factors of the composite twist fields

Here, we characterize the form factors of the composite twist fields in the  $n$ -th replica model (with  $n \geq 2$ ). Similarly to Refs. [2, 65, 67], it is possible to write down the bootstrap equations for these novel twist fields. Importantly, these equations take into account the presence of an additional Aharonov-Bohm flux  $e^{i2\pi/3}$  inserted between the first and the  $n$ -th replica. This is a slightly different choice wrt the approach employed for  $U(1)$  theories in Refs. [2, 67], where the total flux  $e^i$  was fractionalized, and a flux  $e^{i\pi/n}$  was present among any pair of consecutive replicas. This is a technical point, still, while most of the physical quantities of interest are not affected by this specific convention, the bootstrap equations are slightly modified compared to (2.45). For instance, the form factors of  $T_n$  denoted by  $F_{\underline{a}}(\cdot; n)$  satisfy

$$F_{\underline{a}}(\cdot; n) = S_{a_i a_{i+1}}(\cdot; i+1) F_{\dots a_i \dots a_{i+1} a_i a_{i+2} \dots; n}(\cdot; i+1; i; \dots; n); \quad (3.51)$$

$$F_{\underline{a}}(\cdot; 1+2; i; \dots; k; n) = F_{a_2 a_3 \dots a_k a_1}(\cdot; i; \dots; k; 1; n) \begin{cases} e^{i\pi/2=3} & i = n \\ 1 & \text{otherwise} \end{cases} \quad (3.52)$$

$$i \operatorname{Res}_{\substack{o= \\ o+i}} F_{a_0 a_0 \underline{a}}(\cdot; o; \cdot; n) = F_{\underline{a}}(\cdot; n); \quad (3.53)$$

$$i \operatorname{Res}_{\substack{o= \\ o+i}} F_{a_0 a_0 \underline{a}}(\cdot; o; \cdot; n) = \prod_{l=1}^k S_{a_0 a_l}(\alpha) F_{\underline{a}}(\cdot; n) \begin{cases} e^{i\pi/2=3} & o = n \\ 1 & \text{otherwise} \end{cases};$$

$$i \operatorname{Res}_{\substack{o= \\ o+iu}} F_{(\cdot; o)(\cdot; \vartheta) \underline{a}}(\cdot; o; \cdot; n) = F_{(\cdot; o) \underline{a}}(\cdot; n); \quad (3.54)$$

with all notations compatible with the ones for the branch-point twist fields discussed earlier. As for the disorder operator  $\sigma_1$ , and  $T_n$  as well, the composite twist field  $T_n$  is  $Z_3$  neutral and the first non-trivial form factor is the particle/antiparticle one.

Under these considerations, the Watson's equations for the 2-particle form factors in the first replica can be summarised as

$$F_{(A;1)(\bar{A};1)}(\cdot; n) = S_{AA}(\cdot) F_{(A;1)(\bar{A};1)}(\cdot; n) = e^{i\pi/2=3} F_{(A;1)(\bar{A};1)}(2in; \cdot; n); \quad (3.55)$$

The kinematic residue equation (3.53) is

$$i \operatorname{Res}_{=i} F_{(A;1)(\bar{A};1)}(\cdot; n) = h \bar{h} i \quad (3.56)$$

with  $h \bar{h} i$  being the VEV. Similarly, as previously discussed for the twist field  $T_n$ , the form-factors with arbitrary replica indices can be recovered as

$$F_{(A;j)(\bar{A};k)}(\cdot; n) = \begin{cases} F_{(A;1)(\bar{A};1)}(2i(k-j); \cdot; n) & \text{if } k > j; \\ F_{(A;1)(\bar{A};1)}(2i(j-k)+\cdot; n) & \text{otherwise;} \end{cases} \quad (3.57)$$

A solution to these equations is given by

$$F_{(A;1)(\bar{A};1)}^+(\cdot; n) = i h \bar{h} i \frac{e^{-\bar{\alpha}}}{2n \sinh \frac{+i}{2n} \sinh \frac{i}{2n}} = \frac{i}{e^{\bar{\alpha}} \sinh \frac{i}{2n}} \quad (\text{c.c.}) \quad \frac{h(\cdot; n)}{h(i; n)}; \quad (3.58)$$

which, apart from the different pole structure, is very much reminiscent of the solution (3.45). Here  $h(i; n)$  is the minimal form factor discussed in Appendix 3.A.

Similar conclusions hold for the form factor  $F_{(A;1)(\bar{A};1)}^+(i; n)$  (antiparticle/particle) except for the kinematical residue value at  $\theta = 2in - i$  which is given by

$$\text{Res}_{\theta=2in-i} F_{(A;1)(\bar{A};1)}^+(i; n) = ie^{-2i} = 3h_{\bar{h}}^* i: \quad (3.59)$$

In this case, the solution is

$$F_{(A;1)(\bar{A};1)}^+(i; n) = ih_{\bar{h}}^* i \frac{e^{6n}}{2n \sinh \frac{i}{2n} \sinh \frac{i}{2n}} e^{\frac{i}{6n} \sinh \frac{i}{2n}} + (\text{c.c.}) \frac{h(i; n)}{h(i; n)}: \quad (3.60)$$

We mention that, while so far we assumed  $n \geq 2$  integer explicitly, we can analytically continue these results over  $n$ . In particular, in the limit  $n \rightarrow 1$  the poles at  $\theta = i; 2i - in$  of the form factors  $F_{(A;1)(\bar{A};1)}^+(i; n)$  and  $F_{(A;1)(A;1)}^+(i; n)$ , defined by Eqs. (3.58) and (3.60), combine to produce a single pole with residue given by the sum of the two residues present for  $n \notin 1$ . As expected, the form factors found above give in this limit the solutions for  $n=1$  previously obtained.

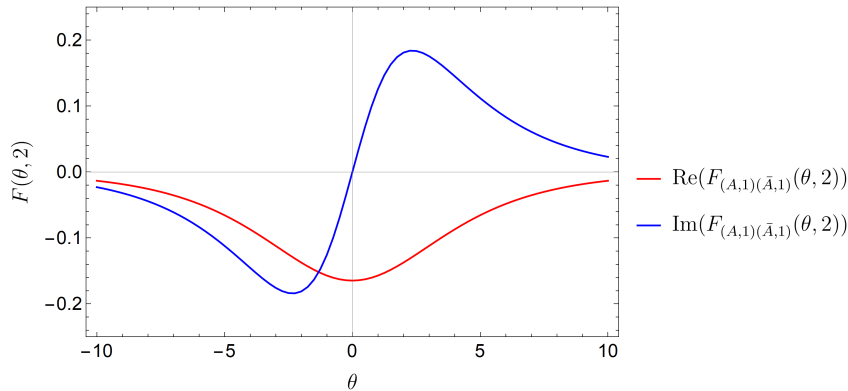


Figure 3.2: Two-particle form factors of the standard twist field  $T_n$  for  $n = 2$  replicas. This figure shows the real and the imaginary parts of the  $AA$  form factor, which equal those of  $A\bar{A}$ , for real values of the rapidity difference  $\theta$ . They both go to zero when  $\theta \rightarrow 1$ .

In Figs. 3.2 and 3.3 we show the behaviour of the two-particle form factor for  $T_n$  and  $T_n^+$  respectively as a function of  $\theta$  for  $n = 2$ ; our plots are normalized by the VEV of the fields (say we set them equals to 1). While for the standard twist field the correspondent form factor is vanishing in the limit  $\theta \rightarrow 1$ , it approaches an asymptotic non-zero value for  $T_n^+$ , as expected from clustering.

### 3.2.4 Checks via $\Delta$ -sum rule

In this subsection, we check the compatibility of our solutions for the 2-particle form factors with the  $\Delta$ -theorem. The method, and the logic, are the same that have been applied for complex free theories in [67]. The only crucial difference is that, while for free theories, the stress-energy tensor

has only two-particle form factors, this is not the case for the Potts model. Consequently, we do not have all the ingredients to write down an exact version of the  $\Delta$ -theorem. However, we keep only the 2-particle contribution, which is expected a good estimation of the correct result

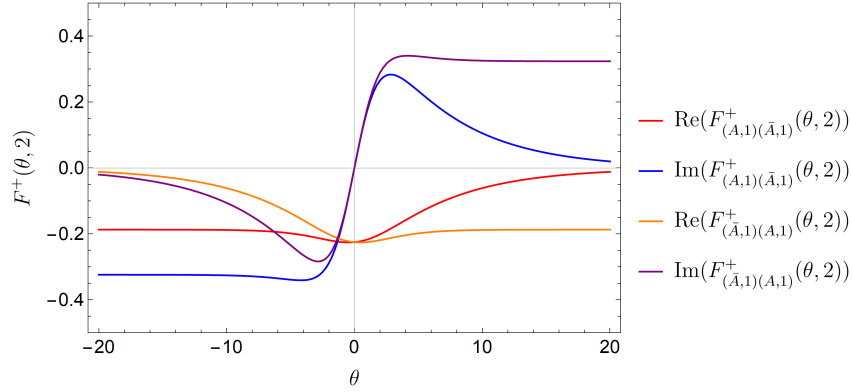


Figure 3.3: Two-particle form factors of the composite twist field  $T_n^+$  for  $n = 2$  replicas. This figure shows the  $AA$  and  $\bar{A}\bar{A}$  form factors, which are different, for real values of the rapidity difference  $\theta$ . They converge to a non-zero constant as  $|\theta| \rightarrow \infty$  respectively.

(see e.g. [47] for the BPTF of the sinh-Gordon model). According to this approximation, we write down the UV conformal weight  $\Delta_O$  of a field  $O$  as

$$\Delta_O = \frac{1}{32} \frac{1}{2hOm^2} \int_1^Z d \frac{1}{\cosh^2 \frac{x}{2}} \times F_{a;a^O}(\alpha) F_{a;a^O}^O(\alpha); \quad (3.61)$$

where we used the fact that the two-particle form factors of  $\psi$  vanish for different replica indices [47]. The only non-vanishing two-particle form factors of  $\psi$  are

$$F_{(A;1)(A;1)}(\alpha) = F_{(A;1)(A;1)}(\alpha) = 2 m^2 \frac{h(\alpha; 1)}{h(i; 1)} \quad (3.62)$$

and they are normalised such that  $F_{(A;1)(A;1)}(i) = 2 m^2$ .

We now apply the  $\alpha$ -theorem to the twist fields, and we get

$$\Delta_n = \frac{n}{32} \frac{1}{2m^2 h \bar{h} i} \int_1^Z d \frac{1}{\cosh^2 \frac{x}{2}} (F_{(A;1)(A;1)}(\alpha) F_{(A;1)(A;1)}(\alpha; n) + F_{(A;1)(A;1)}(\alpha) F_{(A;1)(A;1)}(\alpha; n)); \quad (3.63)$$

with  $\Delta_n$  being the conformal weight of  $T_n$ . This result has to be compared with the CFT prediction, which reads as follows [51, 100]

$$\Delta_n = \Delta_n + \frac{c}{24} n \frac{1}{n} \quad (3.64)$$

where  $\Delta_n$  is the weight of  $T_n$  [61, 62] and of  $\psi$  respectively, while  $c = 4\pi^2$  is the central charge.

Figs. 3.4 and 3.5 show this comparison for standard and composite twist fields respectively, where the integral appearing in Eq. (3.63) has been performed numerically. The data are very close to the CFT value, but discrepancies are expected to be present since we are neglecting higher particle form factors.

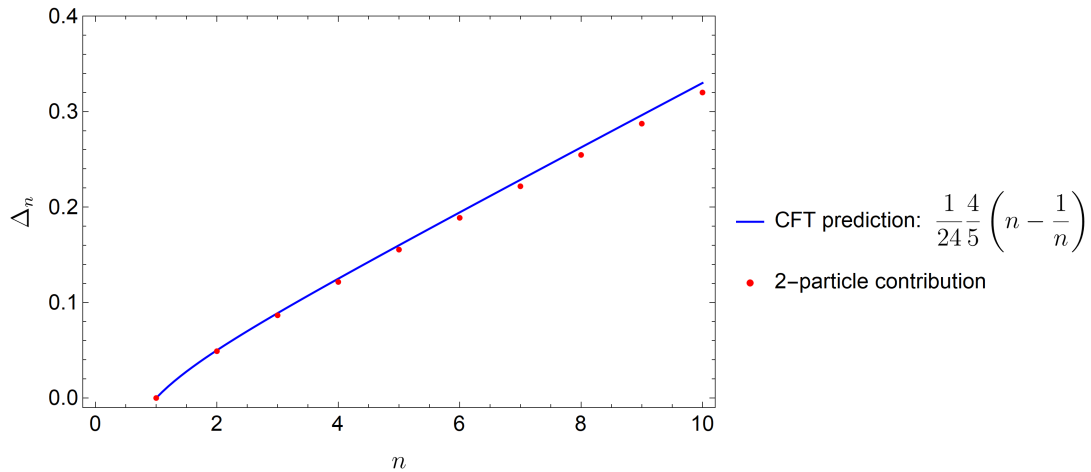


Figure 3.4: Conformal dimension of  $T_n$  as obtained from the  $\beta$ -theorem (red dots) compared to the exact CFT formula (blue dots).

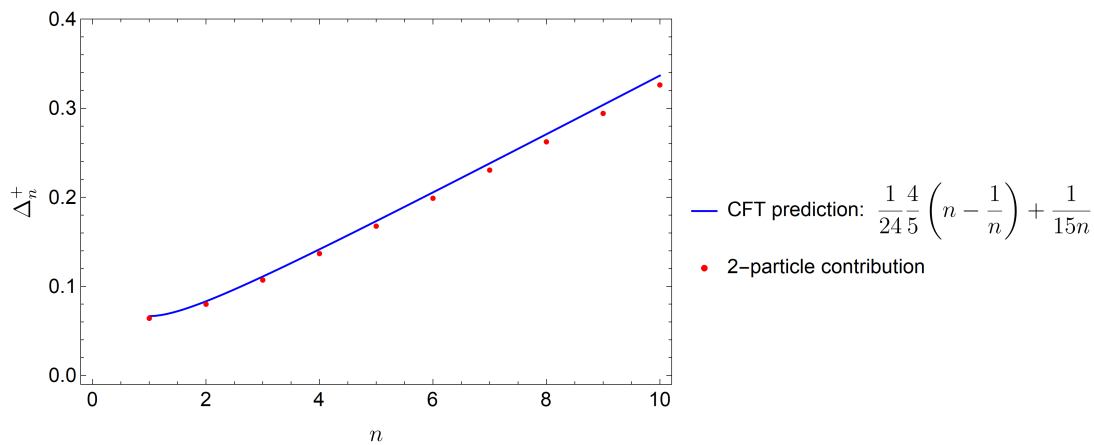


Figure 3.5: Conformal dimension of the composite twist field  $T_n^+$  as obtained from the  $\beta$ -theorem (red dots) compared to the exact CFT formula (blue dots).

### 3.3 Two-point function of composite $Z_3$ twist fields

In this section, we analyze the long-distance behaviour of the correlation function of composite twist fields, using our predictions for their form factors. We give a prediction valid for any  $n$  in the limit  $m \rightarrow 1^-$ , and then we focus on two singular cases  $n = 1$  and  $n = 2$ .

We first expand the correlation function  $\langle \bar{T}_n(0) T_n(\cdot) \rangle$  in the quasiparticle basis keeping only

the two-particle contribution, and we get

$$\begin{aligned}
& h\bar{h}(0)\bar{f}_n(\cdot)ihT_ni^2 + \sum_{j,k=1}^n \int_{-1}^1 \frac{d^2z}{(2\pi)^2} jF_{(A;j)(A;k)}(z;n)j^2e^{-m(\cosh_1+\cosh_2)} \\
& + \sum_{j,k=1}^n \int_{-1}^1 \frac{d^2z}{(2\pi)^2} jF_{(A;j)(A;k)}(z;n)j^2e^{-m(\cosh_1+\cosh_2)} \\
& = h\bar{h}i^2 + \frac{n}{4} \sum_{\alpha:A:A} \int_{-1}^1 d^2z f_\alpha(z;n)K_0(2m\cosh(\frac{z}{2}))^\alpha :
\end{aligned} \tag{3.65}$$

Above,  $K_0(z)$  is the modified Bessel function and the functions  $f_\alpha(z;n)$  are implicitly defined as

$$f_{AA}(z;n)h\bar{h}i^2 = \sum_{j=1}^n jF_{(A;1)(A;j)}(z;n)j^2 = \sum_{j=0}^{n-1} jF_{(A;1)(A;1)}(z;n)j^2; \tag{3.66}$$

and similarly for  $f_{AA}(z;n)$ . We remind that, due to the  $Z_3$  symmetry in the current theory  $f_{AA}(z;n) = f_{AA}(z;n) = 0$  and  $m_A = m_{\bar{A}} = m$  (particles and antiparticles have equal mass). Then, expanding the integral in Eq. (3.65) at leading order in the limit  $m \gg 1$  we get

$$h\bar{h}(0)\bar{f}_n(\cdot)ihT_ni^2 = 1 + \frac{n}{2} f_{AA}(0;n) \frac{e^{-2m}}{m}; \tag{3.67}$$

where we used the fact that  $f_{AA}(0;n) = f_{AA}(0;n)$ .

For  $n = 1$  and  $\alpha = 0$  the twist field becomes the identity operator and  $f_{AA}(z;1;0) = f_{AA}(z;1;0) = 0$ . However, for  $\alpha \neq 0$  we have that  $f_{AA}(z;1;1) \neq 0$ , as the (composite) twist field becomes the disorder operator  $\sigma_1$  that is non-trivial. Had we chosen a different convention for the flux insertion, the form factors  $F_{(A;i)(A;j)}(z;n)$  would have differed by the presence of a phase for distinct replica indices  $i \neq j$ . Indeed, the relation (3.57) would have been modified, due to an additional phase coming from the monodromy among distinct replicas (see [2] [65] for further details). Nevertheless, since here we are only interested in the squares of the form factors, the presence of this additional phase is irrelevant.

In Fig. 3.6 we plot  $f_{AA}(0;n) + f_{AA}(0;n) = 2f_{AA}(0;n)$  as a function of  $n$  for  $n$  integer, for both  $\alpha = 0$  and  $\alpha = 1$  (which are identical). From the figure, it is evident that  $f_{AA}(0;n)$  converges to a  $\alpha$ -independent constant when  $n \gg 1$ . We were able to compute analytically this constant (see Appendix 3.B for the details). The result is

$$2f_{AA}(0;1;1) = \frac{16}{2} \frac{\Gamma(5/6)\Gamma(2/3)}{\Gamma(4/3)\Gamma(1/6)} {}_5F_4 \left( \begin{matrix} 1/2, 1/2, 5/6, 5/6, 1/1 \\ 1/2, 1/2, 3/2, 3/2 \end{matrix} ; 1 \right) = 0.575153; \tag{3.68}$$

and the derivation is very similar to the sinh-Gordon analysis presented in [47].

Finally, we consider the singular limit  $n \rightarrow 1$ , that requires an analytic continuation over the integers. The main subtlety is the occurrence of a  $\alpha$ -singularity in the derivative  $\frac{d}{dn} f_{AA}(z;n)|_{n=1}$ , coming from the collision of kinematical poles. The mechanism is well understood in the absence of flux, and a careful analysis of the Ising and sinh-Gordon model has been performed in [47, 64]. The generalization in the presence of the flux follows the same logic of  $U(1)$  free theories

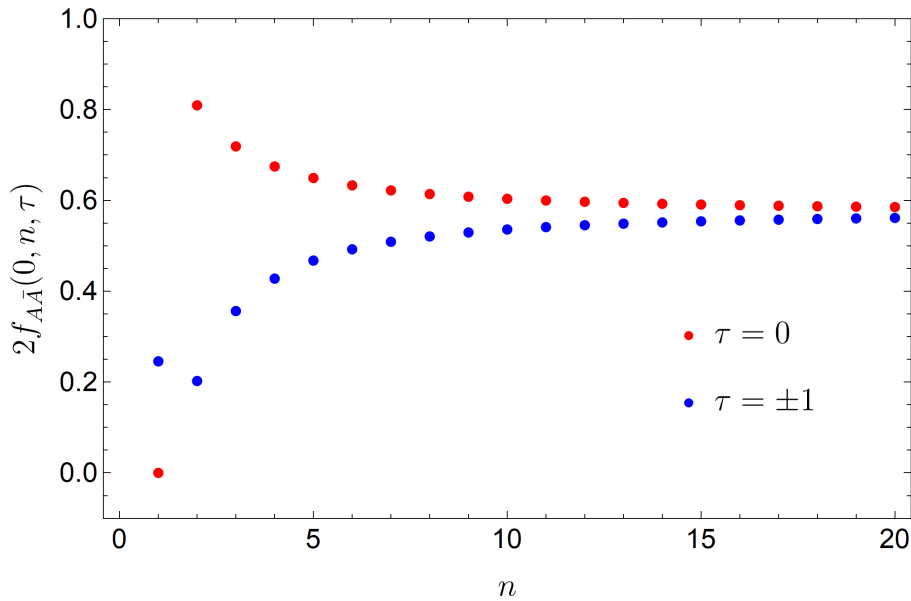


Figure 3.6:  $2f_{AA}(0; n; \tau)$  is shown as a function of  $n$  both for the standard ( $\tau = 0$ ) and CTFs ( $\tau = \pm 1$ ). As expected, its asymptotic value in the limit  $n \rightarrow \infty$  does not depend on  $\tau$ .

[67], that we briefly summarize below. We first represent the sum in (3.66) as a contour integral. Namely, we relate the value of the integral

$$\frac{1}{2\pi i} \int_C dz \cot(\pi z) F_{(\tau;1)(\tau;1)}(2i; j; n) j^{2\tau} \quad (3.69)$$

where the contour is a rectangle with vertices  $(0^+ - iL; n - 0^+ - iL; n - 0^+ + iL; 0^+ + iL)$ , to the value of  $F_{(\tau;1)(\tau;1)}(2i; j; n)$  using the residue theorem. The integral is in general hard to compute, but if we just focus on the singular limit  $n \rightarrow \infty$  for which the kinematic poles collide, then we get

$$F_{(\tau;1)(\tau;1)}(2i; j; n) = \frac{\tanh^2 \frac{\pi}{2}}{2} \text{Im} F_{(\tau;1)(\tau;1)}(i - 2; j; n) e^{i\pi\tau} F_{(\tau;1)(\tau;1)}(i(2n-1) - 2; j; n) + (\text{reg. terms}); \quad (3.70)$$

where  $e^{i\pi\tau}$  is the Aharonov-Bohm phase picked by the particle  $\tau$ , and we assume the normalization  $\hbar \tau i = 1$  for simplicity. Taking the derivative in  $n$  and then the limit  $n \rightarrow \infty$  in the previous expression, we eventually get

$$\lim_{n \rightarrow \infty} \frac{d}{dn} F_{(\tau;1)(\tau;1)}(2i; j; n) = \frac{2}{2} \cos \left( \frac{\pi}{2} \right) + (\text{smooth } n\text{-dependent part}); \quad (3.71)$$

If one specializes this prediction to the 3-state Potts model, where just two species of particles  $A$  and  $\bar{A}$  are present, picking a phase  $\tau = 2/3$ , we get

$$\lim_{n \rightarrow \infty} \frac{d}{dn} f_{AA}(\tau; n; 1) = \frac{2}{2} \cos \frac{2\pi}{3} + (\text{smooth } n\text{-dependent part}); \quad (3.72)$$

Inserting this result in the two-point function of composite twist field, we finally get

$$\frac{d}{dn} \frac{\langle \mathcal{T}_n^{\#}(0) \mathcal{T}_n^{\#}(\infty) \rangle}{\langle \mathcal{T}_n^{\#}(\infty) \rangle^2} \sim \frac{1}{4} \cos \frac{2\pi}{3} K_0(2m); \quad (3.73)$$

valid in the limit of large  $m^{-1}$ .

One final remark on Eq. (3.71) is probably needed. As we stated before, it encodes the two-particle contribution only, and its singular behaviour does not really depend on the S-matrix, but it comes from the kinematic poles of the particle-antiparticle form factors. For a QFT with no one-particle contributions, one can generalize (3.73) as

$$\frac{d}{dn} \frac{\langle \text{tr} T_n^+(0) \text{tr} T_n^+(\ell) \rangle}{\langle \text{tr} T_n^+ \rangle^2} \sim \frac{1}{8} X \cos(K_0(2m^{-1}\ell) + \dots \text{ indep. terms}) + \dots; \quad (3.74)$$

with  $m^{-1}$  being the mass of particle and the  $e^{i\theta}$  its monodromy phase. However, in generic QFTs one-particle contributions can be present, which would be leading for large distances. In particular, this is possible in the presence of a neutral particle, appearing as a virtual bound state in a particle/antiparticle scattering. An explicit example for this mechanism has been carefully discussed in the sine-Gordon model in Ref. [67].

### 3.4 Symmetry resolved entanglement

In this section, we relate the 2-point function of composite twist fields, previously characterized, to the  $Z_3$  symmetry resolved entropy of an interval  $A = [0; \ell]$ . We mention that similar analysis has been already performed [113] for the same model in the critical regime, which corresponds to the limit of vanishing mass  $m^{-1} \rightarrow 0$ . Here we instead are interested in the long distance behaviour, for instance the limit of  $m^{-1} \rightarrow 1$  with  $m$  kept fixed, where our approach is predictive.

The technique employed is closely related to the  $U(1)$  symmetry resolution, where the connection between charged partition functions and symmetry resolved entanglement was established [114,120]. We denote by  $|j\rangle$  the ground-state of the Potts model in the paramagnetic phase, and  $\rho_A$  is its RDM on  $A = [0; \ell]$ . Due to the  $Z_3$  symmetry of the state, the RDM commute with the reduced generator of the symmetry, a property encoded in the relation

$$\rho_A = e^{iQ_A} \rho_A e^{-iQ_A}; \quad Q = 0; \quad 2 = 3 \quad (3.75)$$

in analogy with the  $U(1)$  case [51]. It follows that  $\rho_A$  admits a block decomposition in charge sectors, whose associated projectors are

$$P_q; \quad q = 0; \quad 1; \quad (3.76)$$

After introducing the symmetry resolved partition function

$$Z_n(q) = \text{tr}(\rho_A^n P_q); \quad (3.77)$$

we define the symmetry resolved Renyi and von Neumann entropies as follows

$$S_n(q) = \frac{1}{1-n} \log \frac{Z_n(q)}{Z_1(q)^n}; \quad \text{and } S(q) = - \frac{d}{dn} \log \frac{Z_n(q)}{Z_1(q)^n} \Big|_{n=1}; \quad (3.78)$$

The crucial observation is that the symmetry resolved partition functions are related to the charged moments via (discrete) Fourier transform as

$$Z_n(q) = \text{Tr}(\rho_A^n P_q) = \frac{1}{3} \sum_{k=0}^{X-1} Z_n \left( \frac{2k}{3} \right) e^{i \frac{2kq}{N}} \quad (3.79)$$

where the charged moments  $Z_n(\alpha)$  are defined via

$$Z_n(\alpha) = \text{Tr} \left[ \sum_A e^{iQ_A} \right] \quad (3.80)$$

Similarly, for the  $U(1)$  case, the charged moments corresponds directly to the 2-point function of twist fields [51] as follows

$$Z_n(\alpha) = \langle \mathcal{T}_n(0) \mathcal{T}_n(\alpha) \rangle \quad \text{with} \quad \alpha = \frac{2}{3} \quad (3.81)$$

for the subsystem  $[0, \alpha]$ . Here, the constant  $\alpha$  plays the role of UV regulator, and we suppose that  $\alpha; m^{-1}$  so that the scaling limit is reached. Putting everything together, one eventually obtains

$$Z_n(\alpha) = \frac{1}{3} \langle \mathcal{T}_n(0) \mathcal{T}_n(\alpha) \rangle + 2 \cos \frac{2}{3} \alpha \langle \mathcal{T}_n^+(0) \mathcal{T}_n^+(\alpha) \rangle \quad (3.82)$$

since by charge conjugation symmetry of the state  $Z_n(\alpha=2/3) = Z_n(\alpha=1/3)$ . At leading order in our analysis, namely in the limit of small cut-off, we can approximate

$$Z_n(\alpha) \approx \frac{1}{3} Z_n(0) \quad (3.83)$$

In this limit, the dependence on  $\alpha$  is lost and the symmetry resolved entropy becomes

$$S_n(\alpha) \approx S_n \log 3 \quad (3.84)$$

showing an explicit equipartition of charge. Beyond this approximation, a dependence on  $\alpha$  is found. We investigate the first corrections to Eq. (3.84) coming from the lowest powers of the regulator. For  $n > 1$  we obtain the following

$$S_n(\alpha) = S_n \log 3 + \frac{1}{1-n} 2 \cos \frac{2}{3} \alpha \frac{\langle \mathcal{T}_n^+(0) \mathcal{T}_n^+(\alpha) \rangle}{\langle \mathcal{T}_n(0) \mathcal{T}_n(\alpha) \rangle} + o(\alpha^{4-n}) \quad (3.85)$$

The case  $n=1$  has to be analyzed carefully, since logarithmic corrections appear. Let us thus expand  $S_1(\alpha)$ , keeping just the correction of order  $O(\alpha^{4-n})$  and  $O(\alpha^{4-n} \log \alpha)$

$$\begin{aligned} S_1(\alpha) &= \frac{1}{2} \log Z_n(\alpha) + \log Z_1(\alpha) \\ &= S_1 \log 3 + 2 \cos \frac{2}{3} \alpha \frac{\langle \mathcal{T}_1(0) \mathcal{T}_1(\alpha) \rangle}{\langle \mathcal{T}_1^+(0) \mathcal{T}_1^+(\alpha) \rangle} \\ &\quad + \log \frac{\langle \mathcal{T}_1^+(0) \mathcal{T}_1^+(\alpha) \rangle}{\langle \mathcal{T}_1(0) \mathcal{T}_1(\alpha) \rangle} + o(\alpha^{4-n}) \end{aligned} \quad (3.86)$$

Although in the previous expression enters the normalization constants of the fields, which have not been fixed, they contribute just as  $\alpha$ -independent constant. Moreover, since we are interested in the large  $m$  limit, we can just keep

$$\frac{\langle \mathcal{T}_1^+(0) \mathcal{T}_1^+(\alpha) \rangle}{\langle \mathcal{T}_1(0) \mathcal{T}_1(\alpha) \rangle} \approx \frac{\langle \mathcal{T}_1^+(0) \mathcal{T}_1^+(\alpha) \rangle}{\langle \mathcal{T}_1(0) \mathcal{T}_1(\alpha) \rangle} \quad (3.87)$$

as the only  $\alpha$ -dependent term; the reason is that the next-to-leading order large  $m$  correction to  $\langle \mathcal{T}_1(0) \mathcal{T}_1(\alpha) \rangle$  is of order

$$\langle \mathcal{T}_1(0) \mathcal{T}_1(\alpha) \rangle \approx \langle \mathcal{T}_1^+(0) \mathcal{T}_1^+(\alpha) \rangle + O\left(\frac{e^{-2m\alpha}}{m}\right) \quad (3.88)$$

whereas the contributions from (3.87) are proportional to  $K_0(2m')$ . Therefore, at leading and next-to-leading order for large  $m'$  we can write

$$S_1(q) = S_1 \log 3 - 2 \cos \frac{2q}{3} + j h_{1ij}^2 + \log + \frac{1}{4} \cos \frac{2}{3} - 1 K_0(2m') + (\text{indep. terms}) + o + \frac{e^{-2m'}}{m'} : \quad (3.89)$$

### 3.5 Concluding remarks

In this work, we apply the form factor bootstrap approach to compute the two-particle form factors of  $Z_3$  composite branch point twist fields in the 3-state Potts model, that is an interacting integrable quantum field theory in 1+1 dimensions. Our main analytical result is an expression for the leading and next-to-leading large-distance behaviour of the symmetry resolved Rényi and von Neumann entropies of the paramagnetic ground-state. Despite the explicit presence of interactions, some features are shared with  $U(1)$  free theories, albeit most of the quantitative predictions rely on the exact form of the scattering matrix. In this context, the main finding is the singular limit  $n \rightarrow 1$ , that turns out to be dependent on the pole structure of the form-factor only, and the predictions share the same functional form observed for free theories. This mechanism was established in the absence of the flux (leading to 'model-independent' correction of the von Neumann entropy [121]), and we found its generalization when the flux is present.

Finally, we mention that, in principle, our techniques employed to investigate other geometries (two or more intervals), or other entanglement measures (negativity, relative entropies, etc.). Also, our analysis can be slightly adapted to deal with other integrable models displaying internal symmetries as the integrable perturbations of the parafermionic  $Z_N$  theories [122].

### 3.A Minimal form factor

In this appendix we analyze the behavior of the minimal form factor  $h(\cdot; n)$  in the replica 3-state Potts model. As in the previous appendix and following closely [47], we start with an integral representation of the S-matrix

$$S_{AA}(\cdot) = \frac{\sinh \frac{\cdot}{2} + i \frac{\cdot}{6}}{\sinh \frac{\cdot}{2} - i \frac{\cdot}{6}} = \exp \int_0^{\cdot} \frac{dt}{t} \frac{\sinh \frac{2t}{3}}{\sinh t} \frac{2 \sinh \frac{2t}{3}}{\sinh t} : \quad (3.90)$$

Then, the only solution (up to a multiplication constant) which does not have zeros or poles in the region  $\text{Im} \cdot \in (0; 2\pi n)$  and satisfies the bootstrap axioms

$$h(\cdot + 2\pi i n; n) = h(\cdot; n); \quad h(\cdot; n) S_{AA}(\cdot) = h(\cdot; n); \quad (3.91)$$

is given by

$$h(\cdot; n) = \exp \int_0^{\cdot} \frac{dt}{t} \frac{2 \sinh \frac{2t}{3}}{\sinh t} \sin^2 \frac{it}{2} \frac{i}{n + \frac{i}{2}} : \quad (3.92)$$

It is easy to prove that for real  $\cdot$  the integral is convergent, since the integrand scales as  $t^{-1} e^{-t/3}$  and no singularity is present in the limit  $t \rightarrow 1$ . However, for  $\cdot = i j$  the integrand goes as  $t^{-1} e^{-t/3 + t j}$  for large  $t$ , that is, it is no longer convergent for  $\text{Im}(\cdot) = 3$ .

For real  $\beta$  in the limit  $\beta \rightarrow +1$  a more careful but standard estimate of the integral gives

$$\int_0^1 \frac{dt}{t \sinh(\beta t)} \frac{2 \sinh \frac{2}{3} t}{\sinh t} \sin^2 \frac{it}{2} \approx \frac{4}{3\beta} \int_0^1 \frac{dt}{t^2} \sin^2 t = \frac{4}{3\beta} \quad (3.93)$$

The approximate equality holds at order  $O(\beta^{-1})$ , and so the asymptotic growth of the minimal form factor is

$$h(\beta; n) \sim e^{-3\beta n}; \quad \beta \rightarrow +1 \quad (3.94)$$

Finally, we would like to present the mixed product representation of  $h(\beta; n)$  that we have used in our numerical work. Expanding  $\frac{1}{\sinh t} = \sum_{n=0}^{\infty} e^{-2nt} + \frac{e^{-2Nt}}{\sinh t}$  as

$$\frac{1}{\sinh t} = 2 \sum_{n=0}^{\infty} e^{-2nt} + \frac{e^{-2Nt}}{\sinh t} \quad (3.95)$$

and using the integral representation of the  $\zeta$ -function

$$\zeta(z) = \exp \int_0^1 \frac{dt}{t} \frac{e^{-tz} - e^{-t}}{1 - e^{-t}} + (z-1) \int_0^1 e^{-t} dt; \quad (3.96)$$

the integral (3.92) gives, after a lengthy but straightforward calculation

$$h(\beta; n) = \sum_{m=0}^N \frac{\Gamma\left(\frac{2m+n+\frac{1}{3}}{2n}\right)^2 \Gamma\left(\frac{2m}{2n} - \frac{i}{2n} + \frac{5}{3}\right) \Gamma\left(\frac{2m+2n+i}{2n} + \frac{5}{3}\right)}{\Gamma\left(\frac{2m+n+\frac{5}{3}}{2n}\right)^2 \Gamma\left(\frac{2m}{2n} - \frac{i}{2n} + \frac{1}{3}\right) \Gamma\left(\frac{2m+2n+i}{2n} + \frac{1}{3}\right)} \quad (3.97)$$

$$\exp \int_0^1 \frac{dt}{t \sinh(\beta t)} e^{-2t(N+1)} \frac{2 \sinh \frac{2}{3} t}{\sinh t} \sin^2 \frac{it}{2} \approx \frac{4}{3\beta} \quad (3.98)$$

For real rapidity difference  $\beta$  the integral representation (3.92) converges, as we commented before, so the mixed-product form is not really needed. However, for numerical work, Eq. (3.98) is really useful since the integral factor in (3.98) becomes exponentially suppressed for large  $\beta$ .

### 3.B Computation of $f_{AA}(0; 1; 0)$

We present here an analytic computation of the value of the function  $f_{AA}(\beta; n; \beta)$  at  $\beta = 0$ ,  $n = 1$  and  $\beta = 0$  in the 3-state Potts model. As seen in Fig. 3.6 the result is independent of  $\beta$ , so we simply choose the simplest case  $\beta = 0$  and follow closely the calculation presented in [47] for the sinh-Gordon model. We start from the definition

$$f_{AA}(0; n; 0) = f_{AA}(0; n; 0) = \frac{1}{h_{T_n}^2} \sum_{j=0}^{N-1} |F_{(A;1)(A;1)}(2i+j; n)|^2 \quad (3.99)$$

where the form factor  $F_{(A;1)(A;1)}(\beta)$  is given by

$$F_{(A;1)(A;1)}(\beta; n) = h_{T_n} \frac{\sin \frac{\beta}{n}}{2n \sinh \frac{i}{2n} \sinh \frac{\beta+i}{2n}} \frac{h(\beta; n)}{h(i; n)} \quad (3.100)$$

<sup>3</sup>We can also choose to expand the factor  $\frac{1}{\sinh(\beta t)}$ , leading to an equivalent representation.

Figure 3.7: Plot of the minimal form factor in the  $n$ -th replicated theory for imaginary values of the rapidity. For different values of  $n$  ( $n = 1; 2; 3$ ) the real and the imaginary part, which is vanishing, are shown.

In the sum (3.99), the  $j$ -th and  $(n - j)$ -th terms are identical by periodicity. This means that, in the large  $n$  limit, one can replace the sum by the series

$$\begin{aligned}
 f_{AA}(0; n; 0) &= \frac{1}{jhT_n} \sum_{j=0}^{n-1} j F_{(A;1)(A;1)}(2i j; n) j^2 j F_{(A;1)(A;1)}(0; n) j^{2A} \\
 &= \frac{1}{jhT_1} \sum_{j=0}^{\infty} \lim_{n \rightarrow \infty} j F_{(A;1)(A;1)}(2i j; n) j^2 j F_{(A;1)(A;1)}(0; n) j^{2A} \quad (3.101)
 \end{aligned}$$

that is rapidly converging. The limit inside the sum above can be computed, as we explain below. Let us consider the different factors involved in  $F_{(A;1)(A;1)}(i; n)$ . We have

$$\frac{\sin \frac{i}{n}}{2n \sinh \frac{i}{2n} \sinh \frac{-i}{2n}} \sim \frac{2}{(2i j - i)(2i j + i)}; \quad (3.102)$$

and

$$\frac{h(2i j; n)}{h(i; n)} \sim \frac{\exp \int_0^1 \frac{dt}{t} \frac{2 \sinh(\frac{2t}{3})}{\sinh t} e^{-2tj}}{\exp \int_0^1 \frac{dt}{t} \frac{2 \sinh(\frac{2t}{3})}{\sinh t} e^{-t}} = \frac{\frac{5}{6} + j}{\frac{1}{6} + j} \quad (2 \rightarrow 3); \quad (3.103)$$

Putting all the pieces together, we get

$$f_{AA}(0; 1; 0) = \frac{8}{2} \sum_{j=0}^{\infty} \frac{1}{(2j-1)^2 (2j+1)^2} \frac{\frac{5}{6} + j}{\frac{1}{6} + j} \frac{2^{\frac{3}{2}}}{2^{\frac{4}{3}}} \frac{4}{2} \frac{2^{\frac{5}{6}}}{2} \frac{2^{\frac{3}{2}}}{2^{\frac{4}{3}}}; \quad (3.104)$$

The result is given in terms generalized hypergeometric functions defined as

$${}_pF_q \left( \begin{matrix} a_1, a_2, \dots, a_p \\ b_1, b_2, \dots, b_q \end{matrix}; z \right) = \sum_{k=0}^{\infty} \frac{(a_1)_k (a_2)_k \dots (a_p)_k}{(b_1)_k (b_2)_k \dots (b_q)_k} \frac{z^k}{k!}; \quad (3.105)$$

where  $(a)_k = \frac{(a+k)!}{a!}$  is the Pochhammer symbol. The sum of both particle orderings  $f_{AA}(0; 1; 0) + f_{AA}(0; 1; 0) = 2f_{AA}(0; 1; 0)$  then gives

$$2f_{AA}(0; 1; 0) = \frac{16^2 (5=6)^2 (2=3)}{2^2 (4=3)^2 (1=6)} \quad (3.106)$$

${}^5F_4 \quad \begin{matrix} 1=2; & 1=2; & 5=6; & 5=6; & 1; & 1 \\ 1=2; & 1=2; & 3=2; & 3=2 & & \end{matrix} \quad 1=2 \quad ' \quad 0:575153$

## Chapter 4

# Symmetry- resolved entanglement of quasiparticle states

In this chapter, based on two works [5, 6], we study the symmetry-resolved entanglement of states resulting from exciting a finite number of quasiparticles above the ground state in free quantum field theory. Previous works pointed out the universality of the excess of entanglement entropy these states have compared to the ground state value, and simple formula depending only on the number of excitations were obtained. Here, we show that a similar mechanism is found for the symmetry-resolved entanglement, and we provide analytical predictions for the ratio of charged moments.

We organize this chapter as follows. In Sec. 4.1 we provide a brief introduction, summarizing the main results. In Sec 4.2 we discuss simple states, arising as magnon excitations of spin chains, where our formula can be recovered with elementary methods. A non-trivial case where our results hold, that is for (free) massive field theories, is discussed in Sec. 4.3 via form factor techniques. A unifying framework which recovers all the previous cases, and covers in principle any quantum system admitting quasi-particle excitations, is presented in Sec. 4.4. We test numerically the validity of our formulae in Sec. 4.5, where lattice free (fermionic and bosonic) chains are discussed. We finally provide some final remarks in Sec. 4.6.

### 4.1 Introduction and main results

Before entering the core of this chapter, we set some notations, following closely [5, 6] (that slightly differ from chapter 2), and give a summary of our main finding.

Let  $|\psi\rangle$  be a pure state of a many-body system and let us define a spatial into two complementary regions  $A$  and  $A^c$  so that the Hilbert space of the theory  $\mathcal{H}$  also decomposes into a tensor product  $\mathcal{H}_A \otimes \mathcal{H}_{A^c}$ . Then the reduced density matrix associated to subsystem  $A$  is obtained by tracing out the degrees of freedom of subsystem  $A^c$  in

$$\rho_A = \text{Tr}_{A^c}(|\psi\rangle\langle\psi|) \quad (4.1)$$

and the von Neumann and  $n$ th Rényi entropy of a subsystem  $A$  are defined as

$$S = -\text{Tr}_A(\rho_A \log \rho_A) \quad \text{and} \quad S_n = \frac{\log(\text{Tr}_A \rho_A^n)}{1-n} \quad (4.2)$$

where  $\text{Tr}_A Z_A^n := Z_n = Z_1^n$  can be interpreted as the normalised partition function of a theory constructed from  $n$  non-interacting copies or replicas of the original model. As is well known, the von Neumann entropy can be obtained as the limit  $S = \lim_{n \rightarrow 1} \frac{1}{n} S_n$ .

We assume that the theory has a global  $U(1)$  symmetry generated by a charge operator  $Q$  satisfying

$$Q = Q_A \otimes I + I \otimes Q_A; \quad (4.3)$$

Whenever the state  $|j\rangle$  has a definite value of the charge, one can show that  $\langle Q_A; A \rangle = 0$ . The latter relation brings to a block-diagonal decomposition of  $Z_A$  in the charge sectors of the restricted charge  $Q_A$  labeled by  $q$ . Given the projector  $P(q)$  onto the sector with charge  $q$ , we define

$$Z_n(q) = \text{Tr}_A (Z_A^n P(q)); \quad (4.4)$$

and we express the symmetry resolved entropies as

$$S_n(q) = \frac{1}{n} \log \frac{Z_n(q)}{Z_1^n(q)} \quad \text{and} \quad S(q) = \lim_{n \rightarrow 1} S_n(q); \quad (4.5)$$

As discussed in [51] these quantities can best be obtained in terms of their Fourier modes, the charged moments  $Z_n(\mathbf{q}) = \text{Tr}_A (Z_A^n e^{2i\mathbf{Q} \cdot \mathbf{A}})$  as

$$Z_n(q) = \int_{-\frac{1}{2}}^{\frac{1}{2}} d\mathbf{q} Z_n(\mathbf{q}) e^{2i\mathbf{q} \cdot \mathbf{q}}; \quad (4.6)$$

We mention that a  $2$  factor of difference is present wrt Chapter 2, that is only a notational choice for later convenience.

When the system is described by a certain hamiltonian  $H$  which commutes with  $Q$ , then (in the absence of spontaneous symmetry breaking) the eigenstates  $|\psi\rangle$  have a definite value of the  $U(1)$  charge, and one can symmetry-resolve their entanglement. This is the case for the ground-state, already discussed in Chapter 2, but also for the states with vanishing energy density, that are the focus of this chapter.

More precisely, we consider a one-dimensional quantum system in a ring of length  $L$ , we take the subsystem  $A$  to be an interval of length  $\ell$ , and we consider the limit in which  $\ell; L \rightarrow 1$  with the ratio  $r = \ell/L$  being fixed. We also assume that the number of particles, together with the associated momenta, are fixed in the limit above. This leads to an excited state with finite energy difference compared to the ground-state, that has vanishing energy-density by definition. In a series of works [77, 104, 106] it was first shown using form factor techniques that the entropy difference of these excited states took a remarkably simple expression, with a striking intuitive semiclassical interpretation. In particular, it has been observed a sort of 'decoupling' between zero-point fluctuations, associated to the ground-state entanglement, and the quasi-particle entanglement, depending only on the probability of observing the particles in the given subregion  $A$ . While the original derivation refers to massive free quantum field theories in 1+1 dimensions, it was argued in [104] (and illustrated on the example of one and two magnon states) that the formulae should hold much more generally, for interacting and even higher-dimensional theories as long as a notion of localised excitations and stable quasi-particle exists. These claims have been substantiated through additional recent results. In particular, a series of works by Rajabpour and collaborators [123, 128] has expanded previous work in various directions. Similar formulae have

<sup>1</sup>In [106] the same formulae were shown to hold for free bosons in any dimension if  $r$  is replaced by the ratio of generalised volumes.

also been found for interacting higher-dimensional theories in [129] and even in the presence of an external potential, arising from a semiclassical limit [130]. Indeed, the formulae found in [104] were not entirely unexpected as they can be derived for semiclassical systems [131], however their wide range of applicability, well beyond the semiclassical regime, as well as their derivation in the context of QFT were new. Finally, we mention that violations to those formulae were observed in [132] at the critical point (free CFTs) for low-lying excited states with energy proportional to  $1=L$ : for those states, the semiclassical picture and the 'decoupling' of zero-point fluctuations just did not apply, while a proper field theoretic characterization was needed to capture quantitatively their entanglement.

Within the hypothesis discussed so far, we were able to find some universal results that we summarize below. Let  $Z_n(L; \cdot; \cdot)$  be the charged moments of the symmetry resolved with Renyi entropy of a connected region of length  $\ell$ , in a pure state  $|j\rangle_L^n$  of an  $n$ -replica theory in finite volume  $L$ . Then, the ratio of moments

$$\lim_{L \rightarrow \infty} \frac{Z_n(L; rL; \cdot)}{Z_n^0(L; rL; \cdot)} =: M_n(r; \cdot); \quad (4.7)$$

between the state  $|j\rangle_L^n$  and the ground state  $|0\rangle_L^n$ , in the infinite volume limit with  $r$  fixed, is given by a universal formula, which depends very simply on  $r$  and  $\cdot$ . There are two particularly useful cases from which more general formulae can be constructed. When  $|j\rangle_L^n = |j1\rangle_L^n$  is a state of a single particle excitation with  $U(1)$  charge  $e$  we have that

$$M_n^1(r; \cdot) = e^{2i} r^n + (1-r)^n; \quad (4.8)$$

whereas for a state of  $k$  identical excitations of charge  $e$  we have that

$$M_n^k(r; \cdot) = \sum_{j=0}^k [f_j^k(r)]^n e^{2ij}; \quad (4.9)$$

where  $f_j^k(r) := \binom{k}{j} r^j (1-r)^{k-j}$  and  $\binom{k}{j} = \frac{k!}{j!(k-j)!}$  is the binomial coefficient. Formula (4.9) is the building block for all other results (formula (4.8) is the  $k=1$  case of (4.9)). A generic state comprising  $s$  groups of  $k_i$  identical particles of charge  $e_i$  will have

$$M_n^{k_1^1 \dots k_s^s}(r; \cdot) = \prod_{i=1}^s M_n^{k_i^i}(r; \cdot); \quad (4.10)$$

For  $\cdot = 0$ , these formulae reduce to those found in [77, 104, 106] and the universality of moment ratios can be expressed as the universality of entropy difference. However, universality is not implied for the difference of symmetry resolved Renyi entropies, due to the Fourier transform which relate them to the charged moments. As an example, for the one-particle state  $|j1\rangle_L^n$  the symmetry resolved Renyi entropies are ( $n > 1$ )

$$S_n^1(r; q) = \frac{1}{1-n} \log \frac{Z_n^1(r; q)}{(Z_1^1(r; q))^n} = \frac{1}{1-n} \log \frac{Z_n^0(q) r^n + Z_n^0(q) (1-r)^n}{(Z_1^0(q) r + Z_1^0(q) (1-r))^n}; \quad (4.11)$$

showing that the ground-state partition function  $Z_n^0(q)$  enters non-trivially. In the general case of higher-particle excitations, the expressions become more cumbersome, and we will only discuss a few specific examples. Instead, we aim to establish the validity of our universal results (4.9) in some paradigmatic systems.

## 4.2 Magnons

In the works [77, 104, 105] several models and approaches were considered, including the study of the entanglement of certain states of magnons. In the present context, such states are useful as they provide a simpler way of obtaining our formulae for the ratios of charged moments, in fact much simpler than those of QFT. Here we generalize those computations taking into account the presence of  $dJ(1)$  associated to the number of particles.

The main idea behind this construction is somewhat similar in spirit to the qubit picture [5, 77], namely, that the entanglement content of quasiparticles can be easily understood if one factors out the zero-point fluctuations. In other words, instead of considering the full quantum theory where the quasiparticles are constructed on top of a nontrivial ground state, which in general has its own entanglement content, we consider a simpler theory in which particles are constructed above a trivial ground state. It turns out that the entanglement of this simpler model keeps track of the exact entanglement of the quasiparticle and discards explicitly the entanglement of the true ground state.

### 4.2.1 One-Magnon States

We firstly focus on a single magnon state on the lattice, belonging to the one-particle sector of a quantum spin- $\frac{1}{2}$  chain of length  $L$ . This state can be written as

$$|j\rangle = \frac{1}{L} \sum_{j=1}^L e^{ipj} |jj\rangle; \quad (4.12)$$

where  $|jj\rangle$  is the state of a localised magnon in position  $j$ . If one requires periodic boundary conditions, the momentum  $p$  has to be quantized as follows

$$p \in \frac{2\pi}{L} \mathbb{Z}; \quad (4.13)$$

We introduce the action of the symmetry operator  $e^{2iQ}$ , where  $Q$  is associated with the internal symmetry of particle number. For our purposes we just need to specify its action on the vacuum state  $|0\rangle$ , the state without particles, and on the one-particle sector. We focus on the sublattice  $A = \{1, 2, \dots, \lfloor \frac{L}{2} \rfloor\}$  and we aim to characterize the restricted symmetry generator  $e^{2iQ_A}$ , that is

$$e^{2iQ_A} |0\rangle = |0\rangle; \quad e^{2iQ_A} |jj\rangle = e^{2i \chi_{j \in A}} |jj\rangle; \quad (4.14)$$

where  $\chi_{j \in A}$  gives 1 if  $j$  is in  $A$  and 0 otherwise. The reduced density matrix of the region  $A$  is

$$\rho_A = \text{Tr}_B (|j\rangle \langle j|) = \frac{1}{L} \sum_{j, j' \in A} e^{ip(j-j')} |jj\rangle \langle j'j'| + (1-r) |0\rangle \langle 0|; \quad (4.15)$$

These two terms appearing in the formula above are interpreted as the contributions associated to the presence/absence of the particle in subsystem  $A$ , respectively. For later convenience, we compute

$$e^{2iQ_A} \rho_A^n = \frac{1}{L^n} \sum_{j, j' \in A} e^{ip(j-j')} |jj\rangle \langle j'j'| + (1-r)^n |0\rangle \langle 0|; \quad (4.16)$$

a relation which is compatible the U(1) symmetry of the RDM  $\rho_A$  that is  $[\rho_A; e^{2iQ_A}] = 0$ . After a straightforward calculation, one gets

$$\text{Tr}_A \left[ \frac{1}{L} \sum_{j,j' \in 2A} e^{ip(j-j')} \rho_{j,j'} \right] = r^n; \quad \text{Tr}_A \left( (1-r)^n \rho_{j_0, j_0} \right) = (1-r)^n; \quad (4.17)$$

with  $r = \lambda/L$ . Putting the previous pieces together, we arrive at the final result

$$\text{Tr}_A e^{2iQ_A} = r^n e^{2i} + (1-r)^n; \quad (4.18)$$

which provides the exact charged moments of a single magnon state.

#### 4.2.2 Two-magnon states

In the following, we consider a state of two magnons with the same charge and given quasimomenta  $p, p^0$ . This example is interesting as it allows us to test the robustness of our prediction in the presence of interactions, encoded in a non-trivial scattering phase. Given a pair of quasimomenta  $p$  and  $p^0$ , we express the state as

$$|j, i\rangle = \frac{1}{L} \sum_{j,j'} S_{j,j'} e^{ipj + ip^0 j'} |j, j^0\rangle; \quad (4.19)$$

where  $S_{j,j'}$  is a scattering matrix and  $|j, j^0\rangle$  is the state with two localised magnons at sites  $j$  and  $j^0$ . The choice of the matrix  $S$  is not really relevant for our purpose, but for the sake of concreteness we set

$$S_{j,j^0} = \begin{cases} e^{i\theta} & \text{for } j > j^0, \\ 1 & \text{for } j < j^0, \\ 0 & \text{for } j = j^0, \end{cases} \quad (4.20)$$

using the same conventions as in [104]. For the sake of concreteness, we write down explicitly the action of the restricted symmetry operator  $e^{2iQ_A}$  on the two-particle sector as

$$e^{2iQ_A} |j, j^0\rangle = e^{2i(j + j^0)} |j, j^0\rangle; \quad (4.21)$$

Following [104], we decompose the RDM  $\rho_A = \text{Tr}_A (|j, i\rangle \langle j, i|)$  as

$$\rho_A = \frac{1}{L} \left( \rho_A^{(0)} + \rho_A^{(1)} + \rho_A^{(2)} \right); \quad (4.22)$$

where  $\rho_A^{(0)}$  is the vacuum contribution (no particles in  $A$ ),  $\rho_A^{(1)}$  is the one-particle contribution (one particle in  $A$  and one in  $A$ ) and  $\rho_A^{(2)}$  is the two-particle contribution (both particles in  $A$ ). The introduction of the flux gives rise to the following relation

$$\text{Tr}_A e^{2iQ_A} = \frac{1}{L^n} \left( \rho_A^{(0)} + \rho_A^{(1)} e^{2i} + \rho_A^{(2)} e^{4i} \right); \quad (4.23)$$

that is useful to evaluate the charged moments. No approximation was made up to this point, but the explicit expressions of  $\rho_A^{(j)}$ , given in [104], are cumbersome and not particularly enlightening

for our purpose. However, one can show that in the limit  $L \rightarrow \infty$  and  $\ell = L/n$ ;  $p \neq p^0$  kept fixed,  $\text{Tr}_A \left( \binom{j}{A} \right)^n$  simplifies drastically:

$$\text{Tr}_A \left( \binom{2}{A} \right)^n \sim L^n r^{2n}; \quad \text{Tr}_A \left( \binom{0}{A} \right)^n \sim L^n (1-r)^{2n}; \quad \text{Tr}_A \left( \binom{1}{A} \right)^n \sim 2L^n r^n (1-r)^n; \quad (4.24)$$

Putting all the pieces together one finally gets

$$\text{Tr}_A \left( \sum_A e^{2iQ_A} \right)^n \sim r^{2n} e^{4i} + 2r^n (1-r)^n e^{2i} + (1-r)^{2n} = (r^n e^{2i} + (1-r)^n)^2; \quad (4.25)$$

This computation shows that, in this particular scaling limit, the interaction between the two particles has no effect on the final result, and the total charged moment is just a product of two single-particle charged moments (which is compatible with the lack of correlations between the two particles).

A different result is obtained if  $p = p^0$  is kept fixed. In that case, the magnons are indistinguishable and correlations are no more negligible. Similar calculations lead to

$$\text{Tr}_A \left( \binom{2}{A} \right)^n \sim L^n r^{2n}; \quad \text{Tr}_A \left( \binom{0}{A} \right)^n \sim L^n (1-r)^{2n}; \quad \text{Tr}_A \left( \binom{1}{A} \right)^n \sim 2^n L^n r^n (1-r)^n; \quad (4.26)$$

so that

$$\text{Tr}_A \left( \sum_A e^{2iQ_A} \right)^n \sim r^{2n} e^{4i} + 2^n r^n (1-r)^n e^{2i} + (1-r)^{2n}; \quad (4.27)$$

which no longer factorizes into one-magnon contributions. We can explain the discrepancy between the cases  $p \neq p^0$ , and  $p = p^0$  as follows. In the first case, it is possible to observe a single particle in  $A$  with momentum  $p$  or with momentum  $p^0$ , and they are distinct events. In contrast, in the second case there is only an event associated with the presence of a single particle in  $A$ , and one gets a sort of 'Bose-Einstein' statistics for the number of particles. These considerations generalize easily to the case of multi-magnon states, and similar calculations lead directly to our prediction (4.9).

### 4.3 Form factors approach to 1+1 free theories

In this section, we investigate the excited states of the complex  $\mathcal{N}(1)$  free quantum field theories in 1+1 dimensions (complex bosons and Dirac fermions). We make use of the twist fields to express the charged moments, in the same spirit of Chapter 2, and we evaluate their correlation functions via the form factor expansion. The analysis, which is rather technical compared to the magnon states, shows the explicit decoupling of the non-trivial zero-point fluctuations related to the vacuum expectation values of the twist fields.

For concreteness, we consider a system of length  $L$  with periodic boundary conditions and the subsystem  $A$  is an interval of length  $\ell$ . Given any state  $|j\rangle_i$  of the system, we can express the moment of the associated RDM as

$$\text{Tr} \left( \rho_A^n \right) = \int \langle j | T_n(0) \mathcal{T}_n(\ell) | j \rangle^n; \quad (4.28)$$

where  $T_n; \mathcal{T}_n$  are the branch-point twist field of the  $n$ -replica model with conformal dimension [47, 60][62]:

$$h_n = \frac{c}{24} n + \frac{1}{n} \quad \text{with } c \text{ the central charge} \quad (4.29)$$

Here  $\mathbb{1}$  is a short-distance non-universal cut-off and  $|j, i\rangle$  is the replicated state. Given  $|j_0\rangle$  the ground-state of the system, one can express the ratio of moments as

$$\frac{\langle \mathbb{1} | T_n(0) \bar{T}_n(\mathbb{1}) | j, i \rangle^n}{\langle \mathbb{1} | T_n(0) \bar{T}_n(\mathbb{1}) | j_0 \rangle^n}; \quad (4.30)$$

that is expected to be a universal function of  $\mathbb{1} = L$  (and  $|j, i\rangle$ ,  $n$  as well) in the limit  $L \rightarrow \infty$  with  $\mathbb{1} = L$  kept fixed. We remind that the dependence on  $L$  is implicit in the states  $|j, i\rangle; |j_0\rangle$ , that are states of the Hilbert space of the finite size system of length  $L$ . The generalization to the charged moments, that are the key objects for the symmetry resolution, is straightforward, and it amounts to replace  $T_n$  with the  $U(1)$  composite twist fields  $T_n$ . The latter are obtained via point-splitting procedure as

$$T_n(y) := T V : (y) = n^2 \lim_{x \rightarrow y} \frac{1}{x! y!} \prod_{j=1}^n T_n(y) V^j(x); \quad (4.31)$$

where  $V$  is the  $U(1)$  symmetry field associated with the insertion of an Aharonov-Bohm with phase  $e^{2i}$ . Here  $V^j(x)$  represent the insertion of the symmetry field at the  $j$ -th replica. We denote by  $\Delta_n$  the conformal dimension of the composite twist fields and, as shown in [98, 100], its value is

$$\Delta_n = \Delta + \frac{1}{n}; \quad (4.32)$$

with  $\Delta$  being the dimension of  $V$ , which depends on the theory under analysis (and differs explicitly for complex bosons/fermions). Following [51], we express the charged moments  $\phi_i$  as

$$\text{Tr}_A e^{2iQ_A} = \langle \mathbb{1} | T_n(0) \bar{T}_n(\mathbb{1}) | j, i \rangle^n; \quad (4.33)$$

The main result of this section is the finding that the ratio of charged moments admits a universal large volume limit

$$M_n(r; \mathbb{1}) = \lim_{L \rightarrow \infty} \frac{\langle \mathbb{1} | T_n(0) \bar{T}_n(rL) | j, i \rangle^n}{\langle \mathbb{1} | T_n(0) \bar{T}_n(rL) | j_0 \rangle^n} \quad (4.34)$$

which is a function of the ratio  $r$ , the charge  $Q$  and the state  $|j, i\rangle$ , and whose value is summarized in the introduction.

A key technical problem, that was solved in [77], is the question of how to evaluate finite volume form factors of the branch-point twist field. The same question arises here for the composite  $U(1)$  twist field. Although a finite volume form factor programme for generic local fields exists [133, 134] this cannot be directly employed for twist fields (its extension to this case is still an open problem). In the absence of such a programme, an alternative approach can be used for complex free theories, where the internal  $U(1)$  symmetry on each replica can be exploited to diagonalise the action of the (composite) branch point twist field [135]. The idea is that we can find a factorisation

$$T_n = \prod_{p=1}^n T_{p+}; \quad \bar{T}_n = \prod_{p=1}^n T_p; \quad (4.35)$$

for complex free bosons and

$$T_n = \prod_{p=\frac{n-1}{2}}^{\frac{n-1}{2}} T_{p+}; \quad \bar{T}_n = \prod_{p=\frac{n-1}{2}}^{\frac{n-1}{2}} T_p; \quad (4.36)$$

for complex free fermions, of the CTFs where the factors  $T_{p+}$  are (single replica)  $U(1)$  twist elds inserting a ux  $e^{2i(p+)=n}$ . These  $U(1)$  twist elds are nothing but the  $U(1)$  symmetry elds  $V$  whose conformal dimension is

$$\begin{aligned} &= \frac{2}{2}; && \text{for free fermions;} \\ &= \frac{j \cdot j}{2} && \text{for free bosons} \end{aligned} \quad (4.37)$$

where  $2 [ ; ]$ .

The elds  $T_{p+}$  satisfy the usual equal-time exchange relations fo  $U(1)$  elds, which involve what is termed a factor of local commutativity  $T_{p+} = \exp(2i(p+)=n)$ , that is, the phase that a eld  $\psi(x)$  with charge 1 accrues when taking a trip around the twist eld. As reviewed in [77], this factor is the key ingredient in determining the form factors of these elds.

The computation presented in [77] for the total entanglement entropy may be easily extended to the case of the ratio  $M_n(r; )$  in excited states. First of all, a word is due regarding the excited state  $j \cdot i$ . In general, any state in the replica QFT can be characterised in terms of the rapidities and quantum numbers of the excitations above the ground state. Considering a free complex theory, we may define creation operators  $(a_j^i)^{\psi}(\cdot)$  where  $=$  is the  $U(1)$  charge of the particle,  $j = 1; \dots; n$  is the replica number, and  $i$  is its rapidity. Unlike the works [77, 104{106] where complex theories were considered only in order to access results for real ones, here we are interested in obtaining results for complex models as they carry the  $U(1)$  symmetry we are interested in. For this reason, the type of excited states that we want to consider is in fact simpler and more natural than those studied in previous works. The type of  $k$ -particle excited state that we are interested in consists of  $n$  identical copies of a standard  $k$ -particle state

$$j \cdot i^n = \prod_{j=1}^n (a_j^1)^{\psi}(\cdot_1) (a_j^2)^{\psi}(\cdot_2) \dots (a_j^k)^{\psi}(\cdot_k) j \cdot i^n; \quad (4.38)$$

where  $i$  are the rapidities,  $j_i$  the copy numbers and  $i =$  specifies the charge that is created by the action of the creation operator  $(a_j^i)^{\psi}(\cdot_i)$ . We first discuss the bosonic case, and then we will analyze the fermions.

#### 4.3.1 Complex free boson

In order to represent the state, it is convenient to move to a basis where the composite twist eld action is diagonal, that is the idea of replica diagonalization. In this basis, the state can be expressed in terms of creation operators  $a_p^{\psi}(\cdot)$  and  $b_p^{\psi}(\cdot)$  associated with the two bosonic species (particles/antiparticles). They are related to the creation operators in the standard basis as [77]

$$a_p^{\psi}(\cdot) = \prod_{j=1}^n e^{\frac{2ijp}{n}} (a_j^+)^{\psi}(\cdot) \quad \text{and} \quad b_p^{\psi}(\cdot) = \prod_{j=1}^n e^{\frac{2ijp}{n}} (a_j^-)^{\psi}(\cdot); \quad (4.39)$$

where  $p = 1; \dots; n$  labels the Fourier modes of the replica space.

As an example, let us consider the case of a single particle excitation. We will write the replicated state as  $j \cdot i^n$  where  $=$  represents the  $U(1)$  charge of boson type. In the original basis, this would simply be the state  $(a_1)^{\psi}(\cdot) (a_2)^{\psi}(\cdot) \dots (a_n)^{\psi}(\cdot) j \cdot i^n$ , that is a state where a

single complex boson of rapidity  $\theta$  and charge  $q$  is present in each replica. Going to the Fourier basis, such a state takes the form

$$|1^+ \rangle^n = \prod_{f \in N^+} A_n(f \in N^+ | g) \prod_{p=1}^{\Upsilon^n} [a_p^\Upsilon(\theta)]^{N_p^+} |0^+ \rangle^n; \quad |1^- \rangle^n = \prod_{f \in N^-} A_n(f \in N^- | g) \prod_{p=1}^{\Upsilon^n} [b_p^\Upsilon(\theta)]^{N_p^-} |0^- \rangle^n; \quad (4.40)$$

where the indices  $f \in N^\pm = \{f \in N_1^\pm; N_2^\pm; \dots; N_n^\pm\}$  are bosonic occupation numbers in each sector, and they are constrained by the condition that they must add up to  $n$

$$\sum_{p=1}^{\Upsilon^n} N_p = n; \quad (4.41)$$

The numerical coefficients  $A(f \in N^\pm | g)$  can be obtained systematically from the relationships (4.39) and their inverses. We now expand the 2-point correlation of the composite twist field in the excited state  $|j \in i \rangle^n$  as follows

$$\langle j \in i | T_n(0) \bar{T}_n(\theta) | 1^+ \rangle^n = \prod_{f \in N^+} \prod_{g \in M^+} A_n(f \in N^+ | g) A_n(f \in M^+ | g) \prod_{p=1}^{\Upsilon^n} \langle 0 | [a_p^\Upsilon(\theta)]^{N_p^+} T_{p+}(\theta) T_p(\theta) [a_p^\Upsilon(\theta)]^{M_p^+} | 0 \rangle; \quad (4.42)$$

$$\langle j \in i | T_n(0) \bar{T}_n(\theta) | 1^- \rangle^n = \prod_{f \in N^-} \prod_{g \in M^-} A_n(f \in N^- | g) A_n(f \in M^- | g) \prod_{p=1}^{\Upsilon^n} \langle 0 | [b_p^\Upsilon(\theta)]^{N_p^-} T_{p+}(\theta) T_p(\theta) [b_p^\Upsilon(\theta)]^{M_p^-} | 0 \rangle; \quad (4.43)$$

The expansion above shows explicitly a factorization in contributions coming associated with Fourier modes that are not mixed among each other.

To proceed further, we sum over a complete set of states between the two  $\mathbb{d}(1)$  fields, as detailed in Appendix 4.6. A particular subtlety of this kind of computation is that, because of finite volume, the momenta/rapidities of excitations are quantised. In particular, as explained in [77], as the twist fields connect untwisted and twisted sectors, non-trivial quantization conditions for the momenta arise, depending on  $p$  and  $n$  and ultimately related to the monodromy of the fields. For instance, we have:

$$P(\theta_i) = m \sinh \theta_i = 2 J_i \frac{2(p+)}{n}; \quad J_i \in 2\mathbb{Z}; \quad (4.44)$$

where  $\theta_i$  are understood as rapidities of particles of type  $i$  respectively, which would be present in the sum over intermediate states. In contrast, the rapidity  $\theta$  of the 'physical' particle is quantised through  $P(\theta) = 2l$  for  $l \in 2\mathbb{Z}$ , as it is associated to the untwisted sector. Note the quantity  $\frac{p+}{n}$  is never an integer for  $2 \in [\frac{1}{2}; \frac{1}{2}]$  and  $p \notin n$ . This guarantees that only non-diagonal form factors (that is, matrix elements involving only distinct right and left states) will be involved in the computation of the leading large-volume contribution to (4.42).

Once a sum over a complete set of states is inserted in (4.42) the problem reduces to the computation of matrix elements of the  $U(1)$  fields  $T_{p+}$ . Such matrix elements have been known

for a long time, but they were re-derived in [2, 77]. Because of the free nature of the theory, all the matrix elements can be expressed in terms of the basic building blocks being the two-particle form factors

$$f_{p+}^n(\tau) = \langle 0 | T_{p+}(\tau) a_p^\dagger(\tau_1) b_p(\tau_2) | 0 \rangle = \sin \frac{(p+)}{n} \frac{e^{\left(\frac{p+}{n} - \frac{1}{2}\right) \tau}}{\cosh \frac{\tau}{2}}; \quad (4.45)$$

where  $\langle 0 | T_{p+}(\tau) | 0 \rangle$  is the vacuum expectation value of  $T_{p+}$  and  $\tau = \tau_1 - \tau_2$ . In summary, all results obtained in [77] follow through for the composite twist fields with the replacement  $p \rightarrow p+$ . In particular, the ratio of the moments for an excited state of one excitation are nearly identical to formula (4.19) in [77], and the final result is

$$M_n^1(r) = \sum_{f, N, g} j A_n(f, N, g) j^2 \prod_{p=1}^Y (N_p!) [g_{p+}^n(r)]^{N_p} = e^{2i} r^n + (1-r)^n; \quad (4.46)$$

with

$$g_p^n(r) := 1 - \left(1 - e^{\frac{2ip}{n}}\right) r; \quad (4.47)$$

For free bosons, this can be generalised to states containing  $k$  identical excitations (with equal rapidities) to find (4.9). Moreover, for states containing  $k$  different particles (with different rapidities and any combination of charges  $i$ ) the result is factorized

$$\begin{aligned} M_n^{1 \dots 1 k}(r) &= \sum_{s=1}^Y \sum_{f, N, g} j C_n(f, N, g) j^2 \prod_{p=1}^Y N_{p;s}^+! N_{p;s}! g_{p+}^n(r)^{N_{p;s}^+} g_p^n(r)^{N_{p;s}} \\ &= \prod_{j=1}^k e^{2i_j} r^n + (1-r)^n; \end{aligned}$$

In these formulae  $C_n(f, N, g)$  and  $A_n(f, N, g)$  are numerical coefficients which are determined by the form of the state in the diagonal basis. Both results are special cases of (4.10), and the details of the derivation are reported in Appendix 4.6.

### 4.3.2 Complex free fermion

For complex free fermions the computation is very similar, but states involving identical excitations are forbidden and the relationship between the original creation operators and those in the diagonal base is also slightly different. We first express the Fourier modes of the creation operators as

$$a_p^\dagger(\tau) = \prod_{j=1}^n e^{\frac{2ijp}{n}} (a_j^\dagger)^\tau(\tau) \quad \text{and} \quad b_p(\tau) = \prod_{j=1}^n e^{\frac{2ijp}{n}} (a_j)^\tau(\tau) \quad (4.48)$$

where now  $p = \frac{n-1}{2}; \dots; \frac{n-1}{2}$  and the operators  $(a_j)^\tau(\tau)$  anticommute for distinct values of  $j$ , the replica index. The explicit expression of the particle-antiparticle form factor associated to the  $U(1)$  twist field (see Ref. [136]) is

$$f_{p+}^n(\tau) = \langle 0 | T_{p+}(\tau) a_p^\dagger(\tau_1) b_p(\tau_2) | 0 \rangle = i \sin \frac{(p+)}{n} \frac{e^{\left(\frac{p+}{n} - \frac{1}{2}\right) \tau}}{\cosh \frac{\tau}{2}}; \quad (4.49)$$

with  $\rho_+$  being the VEV  $T_{\rho_+}(0)$ .

Then, we make explicit the replicated state consisting of a single particle excitation that is, as for the boson

$$1^{+n} = \prod_{j=1}^n (a_j^+)^\nu(j) j0i^n = \prod_{j=1}^n \rho_{\frac{n-1}{2}} \frac{X^{n-1}}{X^2} !^{jp} a_p^\nu(j) j0i^n; \quad (4.50)$$

$$1^{-n} = \prod_{j=1}^n (a_j^-)^\nu(j) j0i^n = \prod_{j=1}^n \rho_{\frac{n-1}{2}} \frac{X^{n-1}}{X^2} !^{jp} b_p^\nu(j) j0i^n \quad (4.51)$$

with  $! = e^{\frac{2i}{n}}$  the  $n$ -th root of unity. Thanks to the fermionic anticommutation relations, the expression above gives a much simpler structure compared to the bosonic case, once expanded. For instance, for  $n = 2$  we have

$$1^{+2} = \frac{1}{2} (ia^{\nu}_{\frac{1}{2}}(j) - ia^{\nu}_{\frac{1}{2}}(j)) (a^{\nu}_{\frac{1}{2}}(j) - a^{\nu}_{\frac{1}{2}}(j)) j0i^2 = ia^{\nu}_{\frac{1}{2}}(j) a^{\nu}_{\frac{1}{2}}(j) j0i^2; \quad (4.52)$$

and similarly for  $n = 3$

$$1^{+3} = ia^{\nu}_1(j) a^{\nu}_1(j) a^{\nu}_1(j) j0i^3; \quad (4.53)$$

In general, one easily show that for generic  $n$  the one-particle replicated state is

$$1^{+n} = e^{i \prod_{p=\frac{n-1}{2}}^{\frac{n-1}{2}} a_p^\nu(j) j0i^n}; \quad 1^{-n} = e^{i \prod_{p=\frac{n-1}{2}}^{\frac{n-1}{2}} b_p^\nu(j) j0i^n} \quad (4.54)$$

with  $e^i$  a phase that is irrelevant to our purpose.

At this point, to compute the two-point function of twist fields, we make use of the factorisation (4.36) and we expand over a complete set of states. The details are presented in Appendix 4.6, and, eventually, one arrives to the final result

$$M_n^1(r; y) = \prod_{p=\frac{n-1}{2}}^{\frac{n-1}{2}} g_p^n(r) = \prod_{p=\frac{n-1}{2}}^{\frac{n-1}{2}} \frac{h}{1 - (1 - e^{\frac{2i(p+\dots)}{n}})r}^i; \quad (4.55)$$

It is possible below to write down the product as a more compact expression, which provides the analytical continuation for non-integer values of  $n$ , as we show below. Indeed, thanks to the expression

$$\prod_{p=\frac{n-1}{2}}^{\frac{n-1}{2}} (x - e^{\frac{2ip}{n}} y) = x^n + (-y)^n; \quad (4.56)$$

that is the factorization of the polynomial  $(x^n + y^n)$ , one arrives to

$$\prod_{p=\frac{n-1}{2}}^{\frac{n-1}{2}} g_p^n(r) = e^{2i} r^n + (1 - r)^n; \quad (4.57)$$

This is the same formula we found for the boson in the case of one-particle excited states. Similarly, it is possible to consider distinct excitations (say particles with distinct momenta) and the results presented in the previous subsection would be recovered. Finally, we emphasize that excitations made by multiple particles with the same quantum numbers are just ruled out in fermionic systems due to the Pauli exclusion principle.

## 4.4 A unified framework: higher dimensions and the twist operator approach

So far we have derived the behaviour of the charged moments of quasiparticle excited states making use of two different formalisms: the form factor expansion in 1+1 integrable QFTs, and the analysis of magnon states on the lattice. Unfortunately, the applicability of those techniques strongly relies on assumptions not directly related to the range of validity of our final results. For instance, the form factor approach we employed is specific to 1+1 theories and makes use of relativistic invariance. Moreover, an elementary lattice approach for the magnon states is not able to capture the zero-point (ground-state) fluctuations, thus does not clarify how the latter are decoupled from the entanglement of quasi-particle in the limit we are considering.

In this section, we consider a generic QFT in any dimension, and we give a unified framework to derive our results. To this aim, we employ the notion of twist operators, generalizing the branch point twist fields which are special of 1+1 dimensional QFT [47, 60]. Our method follows the ideas [106], where the excitations of the free massive boson in dimensions have been extensively analysed and their Renyi entropy was computed in terms of graph partition functions. In this section we slightly generalise the formalism of [106], to take into account the insertion of the twist operator and the possible presence of interactions, which are not expected to validate the results as long as quasi-particle excitations exist. As a proof of concept, a simple calculation of symmetry resolved entanglement of a single-particle excited state is shown. The key ingredients we need are the description of the excited states as local operators acting on a vacuum state and their commutation relation with a twist operator, which generalizes the composite branch point twist field to higher dimensional settings. The only strong assumption we make in our derivation is the presence of a finite correlation length for the vacuum correlation function (say, a finite gap is present above the ground-state). We mention that the latter assumption is not really a necessary condition, since the emergence of the universal entanglement content is also expected for some high-energy states in massless theories (see [126, 128], for the analysis of the gapless XY chain). However, we keep this assumption here mostly to avoid technical complications in some intermediate passages, leaving the analysis of massless theories to future investigations.

We anticipate here that our formulae (4.8)-(4.10) are unchanged in higher dimensional theories, up to the identification

$$r = \frac{V_A}{V}; \quad (4.58)$$

which is the ratio of volumes between subsystem  $A$  and the total system.

### 4.4.1 Excited States and Operator Algebra

Let us consider a vacuum state  $|0\rangle$  of a Hilbert space  $H$ , together with an algebra  $A$  of operators representing the physical observables<sup>2</sup>, acting on  $H$  and having  $|0\rangle$  as a cyclic vector (we refer [137] for a modern review of this algebraic viewpoint of entanglement in QFT). This allows us to represent any state  $|j\rangle$  of the Hilbert space as

$$|j\rangle = O|0\rangle \quad \text{with} \quad O \in A; \quad (4.59)$$

We would like to assume further that the vacuum state is translation invariant, namely that it is invariant under a certain faithful representation of the translation group in  $d$  dimensions. Strictly

<sup>2</sup>In the case of a single real boson,  $A$  is just the algebra of generated by the field  $\phi(x)$  and its conjugated momentum  $\pi(x)$ .

speaking, since we consider a finite-size system, we have to slightly modify this requirement. Specifically, we put our system on a  $d$ -dimensional torus  $M$  of volume  $V$  and we require that  $|j\rangle$  is invariant under the isometries of the torus. Other boundary conditions can be considered too, but they do not change the picture in the scaling limit we are interested in. We also require locality of the observables, asking that  $\mathcal{A}$  is generated by  $\int_M \mathcal{O}(x) dx$ , which can be applied at any point of  $M$ . For any  $\mathcal{O}(x)$ , one can construct its Fourier transform  $\mathcal{O}(p)$  as

$$\mathcal{O}(p) = \int_M d^d x e^{i p x} \mathcal{O}(x); \quad (4.60)$$

that is the building block for the following set of translation invariant states

$$|O_1(p_1) \dots O_k(p_k) j\rangle; \quad (4.61)$$

The state above corresponds physically to  $k$  particles distributed on  $M$  with momenta  $\{p_j\}_{j=1, \dots, k}$ , and the choice of the  $\mathcal{O}_j$  may depend on the particle species and quantum numbers. In particular, up to quantization of momenta, these states are eigenstates for free theories or integrable theories.

This construction is similar to the usual way of generating particle states in free theories, acting with creation operators on the vacuum on a Fock space. However, the real advantage of our formulation is that it is directly related to local observables, a property which is fundamental to correctly define entanglement measures (encoded in the commutation relations among local fields and twist operators).

Let us take a set of orthogonal fields  $\mathcal{O}_j$ , so that the correlation function  $\langle \mathcal{O}_i^y(x) \mathcal{O}_j(x^0) \rangle$  vanishes for  $i \neq j$ . In other words the fusion

$$\mathcal{O}_i^y \mathcal{O}_j = \delta_{ij} \mathbb{1} \quad (4.62)$$

is present only if  $i = j$  and their operator product expansion (OPE) can be expressed formally as

$$\mathcal{O}_i^y(x) \mathcal{O}_j(x^0) = \delta_{ij} \langle \mathcal{O}_i^y(x) \mathcal{O}_i(x^0) \rangle |j\rangle + \dots; \quad (4.63)$$

where we neglected explicitly the contributions coming from less relevant operators. The exact evaluation of the correlation function above can be hard for a generic theory, but the assumption of a finite gap  $m$  ensures that it vanishes exponentially for  $|x - x^0| \gg m^{-1}$ . This is the only property we really need in our subsequent discussion.

We now construct a smeared version of the modes  $\mathcal{O}(p)$ , having support in a subsystem only, that is a region of space. To each spatial region  $A \subset M$  and field  $\mathcal{O}(x)$ , we associate

$$\mathcal{O}_A(p) = \int_A d^d x e^{i p x} \mathcal{O}(x); \quad (4.64)$$

Given any two regions  $A$  and  $A^0$ , we compute<sup>3</sup>  $\mathcal{O}_A^y(p) \mathcal{O}_{A^0}(p^0)$ , making use of some approximations. First, we consider only the most relevant term in the fields OPE, namely

$$\mathcal{O}_A^y(p) \mathcal{O}_{A^0}(p^0) = \int_A d^d x \int_{A^0} d^d x^0 e^{i p x} e^{i p^0 x^0} \langle \mathcal{O}_i^y(x) \mathcal{O}_i(x^0) \rangle |j\rangle; \quad (4.65)$$

<sup>3</sup>One should note that hermitian conjugation and Fourier transform do not commute. Indeed, we have that  $\mathcal{O}_A^y(p) = (\mathcal{O}_A(p))^y$ .

Second, since we are working in the limit of small correlation length (compared to the geometry), the leading contribution comes from the insertion of the fields at small distances, which is present if  $x, x^0$  are close to each other and they both belong to  $A \setminus A^0$ , this observation motivates the change of variables  $x^0 = x^0 - x$ , and the subsequent approximation

$$O_A^y(p) O_{A^0}(p^0) \sim \int_{A \setminus A^0} d^d x e^{i(p-p^0)x} \int_M dx^0 e^{ip^0 x^0} \langle j | O^y(0) O(x^0) | j \rangle \quad (4.66)$$

The second integral (over  $x^0$ ) may be difficult to compute and in principle it could require a UV regularisation for  $|x^0| < m^{-1}$ . However, it does not depend on the region  $A \setminus A^0$  and in our computation appears only as a multiplicative constant. In conclusion, we end up with

$$O_A^y(p) O_{A^0}(p^0) \sim V_{A \setminus A^0}^{-1} \mathcal{C}_{p,p^0} \quad (4.67)$$

where  $V_{A \setminus A^0}$  is the volume of  $A \setminus A^0$  and the proportionality constant do not depend on the regions, which is the main result of this subsection.

It is natural to ask how our discussion above would be modified for a vanishing gap  $m = 0$ . The main change is in the scaling of correlations functions: exponential localization of the correlation function in a region of typical length  $m^{-1}$  does not hold any longer, due to the long algebraic tails of the correlation functions. We conjecture that, as long as the momenta are fixed in the infinite-volume limit, the main conclusion (4.67) is unchanged. A qualitative argument is that in this case the inverse momentum, say the De Broglie length, plays the role of typical length scale. In order to make this consideration more precise, let us analyse Eq. (4.66) for a 1+1D CFT, where  $O$  is a field of conformal dimension  $\Delta$ . We focus on the following integral

$$\int_M dx^0 e^{ip^0 x^0} \langle j | O^y(0) O(x^0) | j \rangle; \quad (4.68)$$

which we regulate both in the UV, with a cutoff  $\epsilon$ , and in the IR, with a cutoff  $L$ , as follows

$$\int_{\epsilon}^L dx e^{ipx} \frac{1}{x^{4-\Delta}} + (\text{c.c.}); \quad (4.69)$$

This integral can be explicitly computed. However, the important feature is that for  $\Delta > 0$ ,  $p > 0$  and  $\epsilon > 0$  all fixed, the integral converges to a finite value when  $L \rightarrow \infty$ . This is no longer the case if  $\Delta = 1 = L$  in the infinite-volume limit. In practice, this means that for small momentum and scaling dimension  $0 < \Delta < 1$  the considerations we made so far regarding the scaling at large sizes cannot be applied. As a matter of fact, for free CFTs the scaling dimensions of the fundamental fields are smaller than 1: the fermionic field has dimension  $\Delta = 1/2$  while the derivative of a compact boson has dimension 1. While the latter considerations are not mathematically rigorous, they are sufficient to explain why in gapless theories the low-energy states, or multiparticle states with small momenta difference, are not well captured by our predictions. Indeed, for such states the excess entanglement was computed in [132, 138] in some specific cases, and is clearly different from the formulae of [77, 104].

#### 4.4.2 Replica construction of the charged moments

Consider now a replica theory, consisting of  $n$  copies of the original theory. For any state  $|j\rangle$  we consider its replicated version  $|j\rangle^{\otimes n}$ . Our goal is to define a composite  $U(1)$  twist operator,

which generalises the composite branch point twist field as defined in [51], to higher dimensional theories. In particular, its expectation value over  $j$ -th replica gives exactly the charged moments  $Z_n(\cdot)$  we are interested in.

This type of operator was already considered in the literature, at least in the absence of the flux insertion (see for example [106, 139, 141]), but here we are mostly interested in its relationship with the algebra of local operators.

The first point we have to clarify regards the symmetry, and its action on the space of fields. Starting from  $e^{2iQ}$ , the global generator of  $U(1)$  symmetry in the non-replicated theory, we say that  $O(x)$  has charge  $q$  if

$$e^{2iQ} O(x) e^{-2iQ} = e^{2iq} O(x); \quad (4.70)$$

Since one can decompose the space of fields as irreducible representations of  $U(1)$ , it is sufficient analysis to charged fields with a given charge. Going back to the replicated theory, we consider the algebra of replicated observables  $\mathcal{A}^n$  as the algebra generated by the tensor product of observables in  $\mathcal{A}$ . Thus, to any field  $O(x) \in \mathcal{A}$ , we associate  $O^j(x) \in \mathcal{A}^n$  defined as

$$O^j(x) = \underbrace{1 \otimes \dots \otimes 1}_{j-1} \otimes O(x) \otimes \underbrace{1 \otimes \dots \otimes 1}_{n-j}; \quad (4.71)$$

where  $O(x)$  lives only in the  $j$ -th replica. Consider a spacial region  $A$ , and its complement  $A^c$ . We define a composite twist operator  $T_A$  which implements the structure of the  $n$ -sheets, cyclically connected, Riemann surface with the additional  $U(1)$  flux. As for a composite twist field in a 1+1 QFT, it does so via its commutation relations with any local charged field  $O^j(x)$ , which we require to be

$$T_A O^j(x) = \begin{cases} e^{2iq} O^{j+1}(x) T_A & x \in A; \\ O^j(x) T_A & x \in A^c; \end{cases} \quad (4.72)$$

According to this choice, the flux is inserted only between the  $n$ -th and the first replica. We mention that (4.72) does not identify unambiguously  $T_A$ , rather a space of twist operators satisfying those relations. While in principle this could be an issue and further properties has to be specified to characterize  $T_A$ , in practice (4.72) is sufficient to give predictions in our regime.

We would like to emphasize that a similar definition has already appeared in the context of 1+1D integrable QFTs (see [2, 4, 65, 67]). In particular, for  $A = [0; \cdot]$ , one can identify

$$T_A = T_n(0) \mathcal{T}_n(\cdot); \quad (4.73)$$

and the commutation relations for  $T_A$  can be expressed as commutation relations for the composite twist fields  $T_n$ .

With all the ingredients given so far, we are now ready to relate the twist operator to the symmetry resolved entanglement. The charged moments  $Z_n(\cdot)$  are given by

$$Z_n(\cdot) = \frac{\langle \mathcal{H}_j T_A \mathcal{H}_j \rangle_i^n}{\langle \mathcal{H}_j \rangle_i^n}; \quad (4.74)$$

The above definition, together with the commutation relations (4.72) and the OPE of Eq. (4.67), turns out to be enough to prove the explicit analytical expression of the ratio of charged moments between  $j$ -th replica and the ground state (4.7). We now show how these ideas come together for a simple example.

## 4.4.3 Single-Particle State

Here, we analyse an excited state  $|j\rangle_i$  made of a single quasiparticle with momentum  $p$  generated by a charged field  $O$ . Its explicit expression is given by

$$|j\rangle_i = O(p)|j0\rangle_i; \quad (4.75)$$

and the replicated version is just

$$|j\rangle_{i^n} = O^1(p) \cdots O^n(p)|j0\rangle_{i^n}; \quad (4.76)$$

For the sake of convenience, we split

$$O^j(p) = O_A^j(p) + O_{\bar{A}}^j(p); \quad (4.77)$$

so that the commutation relations with  $T_A$  become more transparent. Indeed, using just (4.72) one can express

$$\begin{aligned} T_A |j\rangle_{i^n} &= T_A (O_A^1(p) + O_{\bar{A}}^1(p)) \cdots (O_A^n(p) + O_{\bar{A}}^n(p)) |j0\rangle_{i^n} = \\ &= (O_A^2(p) + O_{\bar{A}}^1(p)) \cdots (O_A^1(p)e^{2i\phi} + O_{\bar{A}}^n(p)) T_A |j0\rangle_{i^n}; \end{aligned} \quad (4.78)$$

Up to now, everything is exact. For an approximate evaluation of  ${}^n\langle j|T_A|j\rangle_{i^n}$  we make use of the OPE contraction in (4.67), neglecting explicitly the less relevant terms. Among all the terms which are generated once the sums are expanded, all but two are vanishing, and they give

$$\begin{aligned} {}^n\langle j|T_A|j\rangle_{i^n} &\sim e^{2i\phi} \int \langle O_A^y(p) \cdots O_A^1(p) O_A^2(p) \cdots O_{\bar{A}}^n(p) O_{\bar{A}}^1(p) T_A |j0\rangle_{i^n} \\ &+ \int \langle O_{\bar{A}}^y(p) \cdots O_{\bar{A}}^1(p) O_{\bar{A}}^1(p) O_{\bar{A}}^2(p) \cdots O_{\bar{A}}^n(p) T_A |j0\rangle_{i^n} \\ &/ e^{2i\phi} \int V_A^n + (V - V_A)^n \frac{{}^n\langle j|T_A|j\rangle_{i^n}}{{}^n\langle j0|j0\rangle_{i^n}}; \end{aligned} \quad (4.79)$$

Similarly, we can evaluate the norm  ${}^n\langle j|j\rangle_{i^n}$ , which does not require the splitting of  $O^j(p)$ , as

$${}^n\langle j|j\rangle_{i^n} = \int \langle O_A^y(p) \cdots O_A^1(p) O^1(p) \cdots O^n(p) |j0\rangle_{i^n} / V^n; \quad (4.80)$$

In the evaluation of the ratio

$$\frac{{}^n\langle j|T_A|j\rangle_{i^n}}{{}^n\langle j|j\rangle_{i^n}} \quad (4.81)$$

the proportionality constant (which is non-universal and could be absorbed in a redefinition of the field) cancels out, and one can write

$$\frac{{}^n\langle j|T_A|j\rangle_{i^n}}{{}^n\langle j|j\rangle_{i^n}} \sim e^{2i\phi} \int r^n + (1 - r)^n \frac{{}^n\langle j|T_A|j0\rangle_{i^n}}{{}^n\langle j0|j0\rangle_{i^n}} \quad (4.82)$$

with  $r = \frac{V_A}{V}$ . In the expression above, the first piece is universal while the second is not, but it is just the  $n$ th charged moment of the ground-state. Indeed, taking the ratio of the two charged moments, we finally arrive to the desired result

$$M_n(r; \phi) = \frac{{}^n\langle j|T_A|j\rangle_{i^n}}{{}^n\langle j|j\rangle_{i^n}} \frac{{}^n\langle j0|j0\rangle_{i^n}}{{}^n\langle j0|T_A|j0\rangle_{i^n}} \sim e^{2i\phi} \int r^n + (1 - r)^n; \quad (4.83)$$

Results for multiparticle states can be obtained in a similar fashion, just more terms would arise and one should distinguish the cases with equal/distinct momenta.

To conclude, the striking simplicity of these results relies especially on the truncation of the OPE in (4.63), which is expected to become exact in the limit  $m^d V \rightarrow 1$ . We further expect that for finite  $m^d V$  further contributions in the OPE can be recast as a (possibly non-integer) power series in  $(m^d V)^{-1}$ , which generalises the explicit  $(mL)^{-1}$  power expansion that is obtained for 1+1D free theories using form factor techniques [5]. In massless theories, for the cases our results apply, we instead conjecture corrections as a power series in  $(m^d V)^{-1}$ .

The explicit evaluation of these corrections, which are expected to be momentum and QFT-dependent, and any possible issues regarding the convergence of these power series are all beyond our purpose.

## 4.5 Numerical Results

In this section, we present numerical results for two very different discrete models. First we consider a 1D lattice Fermi gas, which has critical features but also possesses highly excited states whose entanglement is well described by our formulae, and then we look at the harmonic chain, whose scaling limit is a massive free boson. Whereas for the first model we can only consider distinct excitations, due to Pauli principle, for the second we consider also states of identical excitations. The good agreement found confirms the more general picture that these kinds of formulae hold under the broad assumption of 'localised' excitations. These are present both in gapped systems due to finite mass scale/correlation length, and in critical systems, when the De Broglie wave length of the excitations (which is inversely proportional to their momentum) is sufficiently small compared to subsystem size.

### 4.5.1 1D Lattice Fermi Gas

Here, we analyse a particle-hole excited state of a 1D lattice Fermi gas, comparing our analytical predictions with the numerical data. Even though the model is critical, it was realised in [125] that certain highly energetic quasiparticle excitations still have a universal entanglement content. More precisely, if one assumes that a set of quasiparticles with small enough De Broglie wavelengths (compared to the typical geometric lengths) is present and their momenta are sufficiently separated, then the quasiparticles will be essentially uncorrelated with each other and with respect to zero-point fluctuations. We refer the interested reader to [123, 128] for further details about the universal entanglement content of quasiparticles in critical systems.

Here we briefly review the numerical techniques involved in the characterisation of fermionic Gaussian states [142] and their application to the computation of symmetry resolved measures. We start by considering the Hamiltonian of free spinless fermions on a circle of length  $L$ .

$$H = \frac{1}{2} \sum_j \left( f_{j+1}^\dagger f_j + f_j^\dagger f_{j+1} \right) + \sum_j \epsilon_j f_j^\dagger f_j; \quad (4.84)$$

where  $\epsilon_j$  is the chemical potential and  $f_{j=1, \dots, L}$ ,  $f_{j=1, \dots, L}^\dagger$  are the fermionic operators obeying the standard anticommutation relations

$$f_j f_j = f_j^\dagger f_j^\dagger = 0; \quad f_j f_j^\dagger = f_j^\dagger f_j = \delta_{jj}; \quad (4.85)$$

When  $j < 1$  the theory is gapless, and the ground state is a Fermi sea with Fermi momentum  $k_F = \arccos(\frac{1}{2})$ . The two-point function evaluated in the ground-state at Fermi momentum  $k_F$  takes the following form

$$C_0(j; j^0) = \langle f_j^\dagger f_{j^0} \rangle_0 = \frac{\sin k_F (j - j^0)}{L \sin \frac{(j - j^0)}{L}}. \quad (4.86)$$

Here, we analyse the quasiparticle excited state described by the following two-point function

$$C(j; j^0) = C_0(j; j^0) + \frac{1}{L} e^{i(k_F + \frac{\pi}{4})(j - j^0)} - \frac{1}{L} e^{i(k_F - \frac{\pi}{4})(j - j^0)}. \quad (4.87)$$

It corresponds to the insertion of a fermion of momentum  $k = k_F + \frac{\pi}{4}$  above the ground state and the removal of another fermion (or equivalently, the insertion of a hole) at  $k = k_F - \frac{\pi}{4}$ . The choice of the momentum shift  $\frac{\pi}{4}$  is not important in the continuum limit, where the only necessary condition is that  $k - k_F$  remains finite when  $L \rightarrow \infty$ . We now have to specify the symmetry of the model. The Hamiltonian (4.84) is invariant under an internal  $U(1)$  symmetry associated to the number of fermions generated by

$$Q = \sum_j f_j^\dagger f_j, \quad (4.88)$$

and it clearly satisfies the locality condition  $Q = Q_A + Q_{\bar{A}}$ , with

$$Q_A = \sum_{j \in A} f_j^\dagger f_j; \quad Q_{\bar{A}} = \sum_{j \in \bar{A}} f_j^\dagger f_j. \quad (4.89)$$

As subsystem  $A$  we consider the segment of length  $\ell$ , that is the sites  $j = 1, \dots, \ell$  and investigate its entanglement properties with the complementary region  $\bar{A}$  containing sites  $j = \ell + 1, \dots, L$ . We denote by  $C_0^A$  and  $C^A$  the  $\ell \times \ell$  matrices resulting from projection of the matrices  $C_0$  and  $C$  (defined by Eqs. (4.86) and (4.87) respectively) onto subsystem  $A$ , keeping only  $j = 1, \dots, \ell$  as spacial indices. Following [1] we express the charged moments of the particle-hole state and the ground state by means of the determinants

$$\text{Tr}_A \left( \rho_A^n e^{2iQ_A} \right) = \det \left( C^A \right)^n e^{2i} + (1 - C^A)^n; \quad (4.90)$$

$$\text{Tr}_A \left( \rho_{A;0}^n e^{2iQ_A} \right) = \det \left( C_0^A \right)^n e^{2i} + (1 - C_0^A)^n; \quad (4.91)$$

with  $\rho_A$  and  $\rho_{A;0}$  the respective reduced density matrices. According to our analytical predictions, we expect that the ratio of the charged moments takes the following universal form

$$\frac{\text{Tr}_A \left( \rho_A^n e^{2iQ_A} \right)}{\text{Tr}_A \left( \rho_{A;0}^n e^{2iQ_A} \right)} \sim (r^n e^{2i} + (1 - r)^n) (r^n e^{-2i} + (1 - r)^n); \quad (4.92)$$

that is, the expression for two distinct excitations with charges  $\pm 1$ , which contribute to the charged moment with an Aharonov-Bohm phase  $e^{2i}$ . We write  $\sim$  to indicate that equality is only expected in the scaling limit of the lattice model.

To test the validity of Eq. (4.92) we consider two entanglement measures, namely the excess of (total) Rényi entropy and the so-called (following the terminology of [1]) "excess of variance".

<sup>4</sup>In the work [1] another particle-hole state satisfying  $\sum_j (k_j - k_F) = 1 = L$  was analysed. The entanglement measures of that low-lying state turned out to be captured instead by CFT predictions, due to the strong correlation effects between the particle/hole and the zero-point fluctuations.

The excess of entropy is recovered from our formulae for  $\beta = 0$  and for two distinct excitations takes the simple form

$$S_n = \frac{1}{1-n} \log \frac{\text{Tr}_A(\rho_A^n)}{\text{Tr}_A(\rho_{A;0}^n)}, \quad \frac{\log(r^n + (1-r)^n)^2}{1-n} : \quad (4.93)$$

We denote the variance<sup>5</sup> associated to  $\rho_A$  as

$$h_{Q_A^2 i_n} = \frac{\text{Tr}_A(\rho_A^n Q_A^2)}{\text{Tr}_A(\rho_A^n)} - \left( \frac{\text{Tr}_A(\rho_A^n Q_A)}{\text{Tr}_A(\rho_A^n)} \right)^2 = \frac{1}{(2i)^2} \frac{d^2}{d^2} \log \frac{\text{Tr}_A(\rho_A^n e^{2iQ_A})}{\text{Tr}_A(\rho_A^n)} \Big|_{=0} : \quad (4.94)$$

Similarly, we denote by  $h_{Q_A^2 i_{n;0}}$  the variance of the ground state  $\rho_{A;0}$ . From (4.92) it then follows that the excess of variance is given by

$$h_{Q_A^2 i_n} - h_{Q_A^2 i_{n;0}} = \frac{2r^n(1-r)^n}{(r^n + (1-r)^n)^2} : \quad (4.95)$$

A way to physically interpret the result of Eq. (4.95) is to regard this excess of variance as twice the contribution associated to a single quasiparticle, since particles and antiparticles contribute in the same way. The latter is just the variance of a Bernoulli random variable with success probability given by

$$p = \frac{r^n}{r^n + (1-r)^n} ; \quad (4.96)$$

namely the probability one associates to the presence of a quasiparticle  $i_A$  computed with the density matrix  $\rho_A$ . Since the variance of a Bernoulli variable with probability  $p$  is just  $p(1-p)$ , we get Eq. (4.95).

In Fig. 4.1 we report the numerical values of  $S_n$  and  $h_{Q_A^2 i_n} - h_{Q_A^2 i_{n;0}}$ , computed from (4.90) and (4.91) using exact diagonalisation of the correlation matrices  $C_A; C_{A;0}$ , and our analytical predictions. We keep  $L$  fixed, analysing different values of  $r = \beta/L$ . Our choice is motivated by the expectation that these plots should be universal at large  $L$ , meaning different data obtained with different  $L$  should collapse to the same universal prediction (independent of lattice details as  $k_F$ ) when  $L \rightarrow \infty$ . As we see from the plots in Fig. 4.1, the match between numerics and analytics is really good.

#### 4.5.2 Complex harmonic chain

Here we consider a complex massive free boson. Unlike the 1D Fermi gas, this model and its lattice version allow us to test formulae for states containing two or more identical excitations. Our numerical computation is based on the wave-functional method introduced in [77] (see Appendix A of that paper) that has been generalized in [6] in the presence of  $\mathfrak{u}(1)$  flux. We do not review all the details the method, that are found in [6]. Instead, we summarize below the idea behind.

The crucial observation regarding the free boson is that, while its ground-state is Gaussian state and its entropy can be characterized efficiently [143], this is not the case for its excited states. One can overcome this issue via the replica-trick, describing the  $n$ -th Renyi entropies

<sup>5</sup>The choice of this terminology comes from the fact that for  $n = 1$  the physical variance of the charge is obtained. For  $n > 1$  this variance has not a direct physical meaning, nevertheless it is still useful for the understanding of the symmetry resolved entanglement.

Figure 4.1: Numerical data versus analytical prediction for the particle-hole excited state described by the correlation function (4.87). The data is for  $k_F = \pi/2$ ,  $L = 200$  and different values of  $n$  for  $r = \pi/2 \in [0; 1]$ . Left: Excess Rényi entropy checked against Eq. (4.93). Right: Excess variance, checked against Eq. (4.95). The numerical results are in very good agreement with the analytical formulae.

as an expectation value of a twist operator over the excited state. The latter can be further expressed as an expectation value over the ground-state, where additional fields are inserted, that is indeed a Gaussian state and can be described efficiently via the Wick theorem. In the end, in order to compute the Rényi entropies of the excited states, one needs to perform the following procedure

- Construct the Gaussian measure associated with the insertion of the  $\mathcal{U}(1)$  twist in the replica model. This step is performed numerically, and it gives rise to an  $N \times N$  matrix which encodes all the possible Wick contractions, with  $N$  being the number of sites of the chain.
- Describe the excited-state expectation value of the twist operator as an expectation value over the Gaussian measure constructed above. This gives rise to many Wick contractions, which are evaluated numerically and summed over.

The method above can be applied for any lattice realization of the free boson, but we perform numerics in a one-dimensional chain. In particular, we start from the hamiltonian

$$H = \int_0^L dx \left[ \frac{1}{2} \dot{\phi}^2 + \frac{v^2}{2} (\partial_x \phi)^2 + m^2 \phi^2 \right]; \quad (4.97)$$

with periodic boundary conditions, and we regularize over a lattice with  $L$  sites, namely the lattice spacing is  $\Delta x = 1$ . This amounts to discretize the Laplace operator as

$$\partial_x^2 \phi(x) \approx \frac{\phi(x+1) + \phi(x-1) - 2\phi(x)}{(\Delta x)^2}. \quad (4.98)$$

The latter can be diagonalized in Fourier space and the set of momenta is

$$p \in \left\{ \frac{2\pi}{L} n \mid n = 0, \dots, L-1 \right\}; \quad (4.99)$$

Figure 4.2: Numerical data (triangles) versus analytical predictions (dashed lines) for  $M_2^{1+1+}(r; \theta)$  (top row) and  $M_2^{2+}(r; \theta)$  (bottom row). We consider  $n = 2$ , system size  $L = 30$  with  $m = 0:1$ . The left/right panels in each row show the real/imaginary part of the function. In both rows we take values of the  $ux = 0; 0:1; \dots; 0:5$ . The numerics for the top row figures employ momenta  $p_1 = \frac{2\pi}{5}$ ;  $p_2 = 2\pi = 5$  whereas for the bottom row we took equal momenta  $p_1 = p_2 = \frac{2\pi}{5}$ .

giving rise to the dispersion relation

$$E_p = \sqrt{m^2 + 2 \sin^2 \frac{p}{2}}; \quad (4.100)$$

from which the relativistic relation  $E_p^2 = m^2 + p^2$  is obtained when  $p \ll 1$ . We study the entanglement of a single interval of length  $\ell < L$  and we evaluate the ratio of charged moments as functions of  $r = \ell/L$ .

In Fig. 4.2 we compare results for two kinds of two-particle excited states: those of particles with identical charges and either distinct or equal momenta  $p_1$  and  $p_2$ . Our analytical predictions for  $M_n(r; \theta)$  are

$$\begin{aligned} M_n^{1+1+}(r; \theta) &= (r^n e^{2i\theta} + (1-r)^n)^2; \quad p_1 \neq p_2; \\ M_n^{2+}(r; \theta) &= r^{2n} e^{4i\theta} + 2^n (1-r)^n r^n e^{2i\theta} + (1-r)^{2n}; \quad p_1 = p_2; \end{aligned} \quad (4.101)$$

In our numerics we have chosen  $L = 30$ , and we also fix the mass scale to  $m = 0:1$ , which corresponds to a typical correlation length of  $\xi = m^{-1} = 10$  sites. Finally, we choose either  $p_1 = p_2 = \frac{2\pi}{5}$  or  $p_1 = \frac{2\pi}{5}$  and  $p_2 = 2\pi$ , both in units of the lattice spacing.

Similarly, Fig. 4.3, we consider the following three-particle excited states: a state of three equal momenta, that is  $p_1 = p_2 = p_3$ , a state of two equal momenta among the three, that is

Figure 4.3: Numerical data (triangles) versus analytical predictions (dashed lines) for  $M_2^{3+}(r; \mu)$  (top row),  $M_2^{2+1+}(r; \mu)$  (central row), and  $M_2^{1+1+1+}(r; \mu)$  (bottom row). We consider  $n = 2$ , system size  $L = 30$  with  $m = 0:1$ . The left/right panels in each row show the real/imaginary part of the function. In each row we take values of the  $\mu$   $= 0; 0.1; \dots; 0.5$ . The numerics for the top row figures employ momenta  $p_1 = p_2 = p_3 = \pi$ , for the central row  $p_1 = p_2 = \pi; p_3 = 3\pi$ , whereas for the bottom row we took  $p_1 = \pi; p_2 = 3\pi; p_3 = 5\pi$ .

$p_1 = p_2 \neq p_3$ , and a state with three distinct momenta, that is  $p_1; p_2; p_3$  distinct. In this case the analytical predictions are

$$M_n^{3+}(r; \mu) = r^{3n} e^{6i} + 3^n r^{2n} (1-r)^n e^{4i} + 3^n r^n (1-r)^{2n} e^{2i} + (1-r)^{3n}; \quad p_1 = p_2 = p_3; \quad (4.102)$$

and

$$\begin{aligned} M_n^{2+1+}(r; \mu) &= M_n^{2+}(r; \mu) (r^n e^{2i} + (1-r)^n); \quad p_1 = p_2 \neq p_3; \\ M_n^{1+1+1+}(r; \mu) &= (r^n e^{2i} + (1-r)^n)^3; \quad p_1 \neq p_2 \neq p_3; \end{aligned} \quad (4.103)$$

The set of momenta is  $p_1 = p_2 = p_3 = 1$  for the first excited state,  $p_1 = p_2 = 2; p_3 = 3$  for the second state, and  $p_1 = 1; p_2 = 3; p_3 = 5$  for the third one.

In all our figures we chose non-negative values of  $\mu$ . Given the formulae above, taking  $\mu < 0$  is equivalent to complex conjugation with  $\mu$  positive, so the figures for negative  $\mu$  are identical except for a change of sign in the imaginary part of all functions. We have also considered the value  $\mu = 0$  (in green) which is the limit where there is no flux. As expected, in this case our formulae recover those for the excess Rényi Entropies in [77, 104], which are symmetric in  $n$  and have vanishing imaginary part. Despite the fact that the correlation length is not particularly small with respect to the system's size  $L$  ( $\ell \approx 0.33L$ ), we took highly energetic states (momenta being fixed in the large-volume limit) and we thus expect the validity of our predictions.

In both Fig. 4.2 and 4.3, we plot the numerical data (triangles) against analytical predictions ((4.101) and (4.103)) as functions of  $r$  fixing  $n = 2$  for several values of  $\mu$  between 0 and  $\frac{1}{2}$ , which correspond to  $\ell = 1$ , respectively. At these two points, the ratio becomes purely real. The figures show excellent agreement between numerical data and analytical predictions.

## 4.6 Concluding remarks

We gave predictions for the symmetry resolved entanglement of quasi-particle state, extending the results of [77] (in the absence of the flux). For instance, via many different approaches, we showed the universality of the ratio of charged moments between the excited state and the ground-state. We also found that the difference of symmetry resolved Rényi entropies does not lead in general to any universal result (in contrast to the difference of standard entropies considered in [77]).

Besides the precise form of our predictions, one of the main achievement of our work was the development of a general framework to tackle the problem. In particular, we showed how few simple algebraic properties between some twist operators and the local fields lead directly to our results. This approach turns out to be far more simple and predictive wrt the brute force form factor expansion (first considered in [77]), and it also looks really promising for further possible applications (other entanglement measures, dynamics).

Some questions are still open. We mentioned that for CFTs (say massless free theories) even if the low-lying excited states do not follow our predictions, some finite energy excitations are expected to do so. If that is true, it means that while the edge of the spectrum of CFTs is truly theory dependent, some general features at finite energy might be universal, similarly as it happens in the middle of the spectrum (finite energy density). It would be interesting to analyse this mechanism, trying to understand a possible universality for the correlations functions of heavy states in CFTs.

Another question regards the possibility of characterizing the entanglement of excited states in the middle of the spectrum for theories without a clear quasi-particle description (say non-integrable). Generically, one expects that the properties of those states might be captured by Gibbs ensembles, but it is not clear which assumptions are actually needed and if the twist operator formalism might shed light on these questions.

## 4.A Form factor computations

In this Appendix, we present the form factor computation of the ratio of charged moments for the free complex free theories. Beside some technical steps related to the involved combinatorics structure, we anticipate the importance of two elements that enter the computation: the (modified) quantization condition for the quasi-particle momenta in the twisted sector and the universality of the kinematic poles. These ingredients lead directly, after tedious algebra, to the universal predictions (4.9).

### 4.A.1 Single-Particle bosonic state

The two-point function in Eq. 4.42 can be computed by inserting a sum over a complete set of states between the  $U(1)$  fields as follows:

$$\begin{aligned} \langle 1^+ | T_n(0) \bar{T}_n(\cdot) | 1^+ \rangle^n &= \sum_{fN^+g} \sum_{fM^+g} A_n(fN^+g) A_n(fM^+g) \prod_{p=1}^n \prod_{m=0}^{\infty} \prod_{fJ} \prod_{gJ} \prod_{r=1}^n \frac{1}{m^+! m^-!} \\ & \langle n | \langle j | [a_p(\cdot)]^{N_p^+} T_{p^+}(0) a_p(\cdot)^\dagger b_p(\cdot)^\dagger | 0 \rangle^n \langle n | \langle j | a_p(\cdot)^\dagger b_p(\cdot)^\dagger T_p(\cdot) [a_p(\cdot)]^{M_p^+} | 0 \rangle^n ; \end{aligned} \quad (4.104)$$

and similarly for  $j \perp i$  (the anti-particle state). The matrix elements involved are the finite-volume ones. However, as explained in [133, 134] they differ from the infinite-volume ones by exponentially small corrections in the system-size, thus from now on we do not make this explicit distinction. Therefore, following closely [77], we express the two-point function as

$$\begin{aligned} \langle 1^+ | T_n(0) \bar{T}_n(\cdot) | 1^+ \rangle^n &= \sum_{fN^+g} \sum_{fM^+g} A_n(fN^+g) A_n(fM^+g) \prod_{p=1}^n \prod_{m=0}^{\infty} \prod_{fJ} \prod_{gJ} \frac{1}{m^+! m^-!} \quad (4.105) \\ & \frac{e^{i \sum_{j=1}^{m^+} P(\cdot)_+ + \sum_{r=1}^{m^-} P(\cdot)_-} M_p^+ P(\cdot)}{\prod_{j=1}^{N_p^+ + M_p^+} \text{LE}(\cdot) \prod_{j=1}^{m^+} \text{LE}(\cdot)_+ \prod_{r=1}^m \text{LE}(\cdot)_-} F_{N_p^+ + m^+ + m}^{n;p}(\cdot) \\ & F_{M_p^+ + m^+ + m}^{n;p;n}(\cdot); \end{aligned}$$

being  $\hat{E}_j = \epsilon_j + i$ ,  $E(\cdot) = m \cosh$  and  $P(\cdot) = m \sinh$  the single-particle energy/momentum respectively, and the  $F$ -functions are just the finite-volume form factors (details can be found in [77]). The complete formula for the form factors above was given in [77] and they can be fully expressed as sums of products of two-particle form factors: they are non-vanishing for  $N_p^+ = M_p^+ = m^+ - m^-$ , and zero otherwise.

If the same intermediate rapidity  $\cdot_j^+$  is paired up with the rapidity of the excited state from the in- and out-states, the dominant contribution in the form factor product will come from

kinematic poles. In other words, if  $\{j^+\}$  two-particle form factors will appear as follows:

$$F_{N_p^+ + m^+ + m}^{n;p} ( \{j^+\} \dots \{m^+\}; \{ \wedge^+ \} \dots \{ \wedge^+ \} ) = N_p^+ f_{p^+}^n ( \{j^+\} \wedge^+ ) \quad (4.106)$$

$$F_{N_p^+ + m^+ + m}^{n;p} ( \{j^+\} \dots \{j^+\}_{j-1} \{j^+\}_{j+1} \dots \{m^+\}; \{ \wedge^+ \} \dots \{ \wedge^+ \} )$$

$$F_{M_p^+ + m^+ + m}^{n;p;n} ( \{ \dots \} \dots \{ \wedge^+ \}_1 \dots \{ \wedge^+ \}_{m^+} ) = M_p^+ f_{n(p^+)}^n ( \wedge^+_{j^+} ) \quad (4.107)$$

$$F_{M_p^+ + m^+ + m}^{n;p;n} ( \{ \dots \} \dots \{ \wedge^+ \}_1 \dots \{ \wedge^+ \}_{j-1} \{ \wedge^+ \}_{j+1} \dots \{ \wedge^+ \}_{m^+} );$$

where the number of  $\wedge^+ ( )$  in the arguments of the form factors in the right-hand side term are now  $N_p^+ - 1 (M_p^+ - 1)$ . The main property of the matrix elements in (4.104) that determines the final formula for (4.42) is the infinite volume limit of the terms such as

$$\sum_{J^+ \geq 2Z} \frac{f_{p^+}^n ( \{j^+\} \wedge^+ ) f_{n(p^+)}^n ( \wedge^+ ) e^{i(P(j^+) - P(\wedge^+))}}{\cosh \cosh^+}$$

$$(mL)^2 \sum_{J^+ \geq 2Z} \frac{\sin^2 \frac{(p^+)}{n}}{2} \frac{e^{2ir (J^+ - l + \frac{p^+}{n})}}{(J^+ - l + \frac{p^+}{n})^2} = (mL)^2 g_{p^+}^n (r); \quad (4.108)$$

with  $g_{p^+}^n (r)$  the functions defined in (4.47) and the indices  $J^+; l$  are integers resulting from the quantisation conditions of the rapidities of intermediate states (4.44) and of the rapidity of the physical one-particle state  $P(\wedge^+) = 2l$  with  $l \geq Z$ . In other words, the exact calculation simplifies once only the leading terms, coming from almost equal incoming/intermediate momenta, are kept and the form factors approximated close to their poles.

Once all possible contractions with a rapidity of the excited in- and out- state have been carried out, the leading contribution is expressed as a sum over the intermediate quantum number  $J$  and comes from the terms with  $M = N$ . It can be written as

$$\langle n-1^+ | T_n(0) \mathbb{T}_n(\wedge^+) | 1^+ \rangle^n = \sum_{fN^+g} j A_n (fN^+g) j^2 \sum_{p=1}^N N_p^+! g_{p^+}^n (r) \sum_{q^+=0}^{N_p^+} \sum_{m=0}^{q^+} \frac{1}{q^+! m!} \sum_{fJ, g2Z} \quad (4.109)$$

$$\frac{e^{i \sum_{j=1}^{q^+} P_{j^+}(\wedge^+) + \sum_{r=1}^m P_r(\wedge^+)}}{Q_{q^+}^{j^+} L^2 E(\wedge^+) Q_{r=1}^m L^2 E(\wedge^+) } F_{q^+ + m}^{p;n} ( \{j^+\} \dots \{q^+\}_{j^+} \{j^+\}_{j^+} \dots \{m\} ) F_{q^+ + m}^{n;p;n} ( \wedge^+_{j^+} \dots \wedge^+_{q^+}; \wedge^+_{j^+} \dots \wedge^+_{m^+} ) \quad (4.110)$$

with  $q^+ = m^+ - N_p^+$ . Dividing by the vacuum two-point function  $\langle 0 | T_{p^+}(0) \mathbb{T}_{p^+}(\wedge^+) | 0 \rangle$ , we eventually obtain the formula (4.46) for the ratio of moments for a one-particle state. We finally point out that the approximations employed in the intermediate steps, become exact in the limit  $L; \hbar \rightarrow 1$  with  $\hbar=L$  and  $m$  fixed as explained in [77]. In contrast, one has to be more careful whenever the typical correlation length  $m^{-1}$  and the size  $L$  are compatible. In that case, while the general approach can be still employed, it is extremely hard to make quantitative predictions due to the presence of many subtleties that play a role: difference between finite and infinite volume form factors, explicit form factors needed (not only their value close to the kinematic poles), etc.

## 4.A.2 Single-Particle fermionic state

Below, we present the explicit computation of the two-point function of composite twist fields in an excited state consisting of a single positively-charged particle. The logic and most of the intermediate steps are in common with the bosonic case, but some technical differences arise. Thanks to the factorisation (4.36), we first cast the two-point function as

$$\begin{aligned}
& \langle \mathbb{T}_n(0) \mathbb{T}_n(\tau) \rangle_{1^+}^n \\
&= \frac{1}{\sqrt{2}} \sum_{p=\frac{n-1}{2}}^{\frac{n-1}{2}} \langle \mathbb{h} \mathbb{0} | a_p(\tau) T_{p^+}(0) T_p(\tau) a_p^\dagger(0) | \mathbb{0} \rangle \\
&= \frac{1}{\sqrt{2}} \sum_{p=\frac{n-1}{2}}^{\frac{n-1}{2}} \sum_{s=0}^{\frac{n-1}{2}-p} \sum_{f, J_i, g} \frac{1}{s!(s+1)!} \langle \mathbb{h} \mathbb{0} | a_p(\tau) T_{p^+}(0) a_p^\dagger(1) \cdots a_p^\dagger(s+1) b_p^\dagger(s+2) \cdots b_p^\dagger(2s+1) | \mathbb{0} \rangle \\
&\quad \langle \mathbb{h} \mathbb{0} | a_p(1) \cdots a_p(s+1) b_p(s+2) \cdots b_p(2s+1) T_p(0) a_p^\dagger(\tau) | \mathbb{0} \rangle e^{i \sum_{i=1}^{2s+1} P(i) P(\tau)} \\
&= \frac{1}{\sqrt{2}} \sum_{p=\frac{n-1}{2}}^{\frac{n-1}{2}} \sum_{s=0}^{\frac{n-1}{2}-p} \sum_{f, J_i, g} \frac{j F_{2s+2}^{p^+, n}(\tau; \dots; s+1; \tau + i; s+2; \dots; 2s+1) j^2}{s!(s+1)! \text{LE}(\tau) \prod_{i=1}^{2s+1} \text{LE}(i)} e^{i \sum_{i=1}^{2s+1} P(i) P(\tau)} \quad (4.111)
\end{aligned}$$

where the resolution of the identity is inserted. Notice that since the excitations are fermionic, the quantization of the Bethe number can be  $J_i = 2Z$  or  $J_i = 2Z + \frac{1}{2}$ : for the sake of simplicity, we will consider the case where these numbers are integer, an assumption that does not play any significant role in this context.

The non-vanishing contributions in the large  $L$  limit come from the terms in the previous expression in which the rapidity of the particle is contracted with  $\tau_i, i = 1, \dots, s+1$ . The  $s+1$  possible contractions in  $F_{2s+2}^{p^+, n}$  give rise to:

$$\begin{aligned}
& F_{2s+2}^{p^+, n}(\tau; \dots; s+1; \tau; s+2; \dots; 2s+1) \\
& \quad f_{p^+}^n(\tau_i) F_{2s}^{p^+, n}(\tau; \dots; i; \dots; s+1; s+2; \dots; 2s+1) \quad (4.112)
\end{aligned}$$

and close to the kinematical pole we approximate

$$f_{p^+}^n(\tau_i) \sim \frac{mL \sin \frac{(p^+)}{n} \cosh e^{\frac{i(p^+)}{n}}}{(J_i^+ - l + \frac{p^+}{n})} \quad (4.113)$$

Finally, we can separately perform the  $s+1$  summations over the quantum numbers  $J_i^+$  as

$$\begin{aligned}
& \sum_{J_i^+ = 2Z} \frac{j f_{p^+}^n(\tau_i) j^2 e^{i(P(i) P(\tau))}}{Lm \cosh Lm \cosh i} \\
& \sum_{J_i^+ = 2Z} \frac{\sin^2 \frac{(p^+)}{n} e^{2i r (J_i^+ - l + \frac{p^+}{n})}}{2(J_i^+ - l + \frac{p^+}{n})^2} = g_{p^+}^n(r); \quad (4.114)
\end{aligned}$$

and, therefore, we obtain

$$\begin{aligned}
 & \langle 1^+ | T_n(0) T_n(\cdot) | 1^+ \rangle^n \\
 = & \prod_{p=\frac{n-1}{2}}^{\frac{n-1}{2}} g_{p+}^n(r) \prod_{s=0}^{\frac{n-1}{2}} \frac{1}{(s!)^2} \prod_{f, J_i, g} j F_{2s}^{p+; n}(\lambda_1; \dots; \lambda_s; \lambda_1; \dots; \lambda_s) j^{2s} \prod_{i=1}^s \frac{e^{i P(\lambda_i) + P(\lambda_i)}}{LE(\lambda_i) LE(\lambda_i)} \\
 = & \langle 1^+ | T_n(0) T_n(\cdot) | 1^+ \rangle^n \prod_{p=\frac{n-1}{2}}^{\frac{n-1}{2}} g_{p+}^n(r) \tag{4.115}
 \end{aligned}$$

where we re-labelled the rapidities of the intermediate states:  $\lambda_1 = \lambda_{s+2}; \dots; \lambda_s = \lambda_{2s+1}$ . We can perform the product over  $p$ , and we get the ratio of charged moments

$$M_n^{1+}(r; \cdot) = \prod_{p=\frac{n-1}{2}}^{\frac{n-1}{2}} g_{p+}^n(r) = (1+r)^n + e^{2i} r^n \tag{4.116}$$

An analogous result can be obtained for a negatively charged particle, up to the replacement  $r \rightarrow 1/r$ .



## Chapter 5

# Symmetry-resolved relative entropies and distances in low-lying excited states of a CFT

In this chapter, based on [3], we introduce the notion of symmetry-resolved subsystem trace distance and relative entropies. In particular, we consider the low-lying excited states of a critical one-dimensional system at finite size  $L$ , with an energy proportional to  $1/L$ , and we develop a systematic approach using CFT techniques. We provide analytical expressions for free massless Dirac fermions in some cases, making use of bosonization techniques. Moreover, we exploit the OPE expansion of composite twist fields to provide very general results when the subsystem size is much smaller than the total system.

### 5.1 Introduction and definitions

In this section, we review the notion of relative entropies and trace distances, and then we propose a definition for their symmetry resolution, as done in [3]. For this purpose, we first consider two (mixed) states defined by their density matrix  $\rho$  and  $\sigma$  and we aim to measure 'how much they are different'. In this respect, the most studied quantity so far is surely the relative entropy [144]

$$S(\rho \parallel \sigma) = \text{Tr}(\rho \log \rho) - \text{Tr}(\rho \log \sigma); \quad (5.1)$$

for two (reduced) density matrices  $\rho$  and  $\sigma$ . The relative entropy is often interpreted as a measure of the distinguishability of quantum states. The relative entropy attracted a lot of interest from the field theory community, see e.g. [145, 161], also, but not only, for its relation with the modular Hamiltonian [162, 163] and quantum null energy condition [164].

However, the relative entropy has a major drawback. Indeed, a proper measure of the difference between states should be a distance in a mathematical sense, meaning it should be non-negative, symmetric in its inputs, equal to zero if and only if its two inputs are the same, and should obey the triangular inequality. Unfortunately, the relative entropy does not match these requirements, as it is not symmetric in its entries. An important family of distances, all satisfying the above rules, is given by the Schatten distances

$$D_n(\rho, \sigma) = \frac{1}{2^{1-n}} \text{Tr}(\rho^n - \sigma^n); \quad (5.2)$$

where  $n \geq 1$  is a generic real parameter. Here  $\| \cdot \|_n$  stands for the  $n$ -norm, see below. It is well known that the trace distance  $D(\rho; \sigma) = \frac{1}{2} \| \rho - \sigma \|_1$  (i.e. (5.2) for  $n = 1$ ) has several properties that make it special and more effective compared to the others values of  $n$  and even compared to other distances, see e.g. the examples and discussions in Refs. [39, 165, 168].

In our work, we considered the reduced density matrices of a subsystem, say an interval of length  $\ell$ , associated to different low-energy excited states of a critical system, and we aimed to distinguish them. In particular, we wanted to understand the differences among these states in the  $U(1)$  symmetry sectors of a given subsystem. To do so, we put together several pieces of a puzzle already present in the literature, namely: (I) the construction of the RDM in excited states of a CFT [132, 138], (II) the replica trick for relative entropies [146, 157, 159] and distances [167, 169], (III) the symmetry resolution of these density matrices via charged moments [50, 51].

### 5.1.1 Symmetry resolved relative entropies and distances

In this section, we recap the notion of symmetry resolution of entanglement measures and provide new definitions for the measures of the subsystem distinguishability of two states within the symmetry sector. Namely, we define symmetry resolved relative Renyi entropies and subsystem Schatten distances

We start with a quantum theory with a Hilbert space  $\mathcal{H}$  that admits a decomposition in sectors as follows

$$\mathcal{H} = \bigoplus_q \mathcal{H}_q; \quad (5.3)$$

where  $q$  is an index labelling the sector  $\mathcal{H}_q$ . Although we are mainly interested in sectors arising from irreducible representations of a group associated with global symmetries (say  $U(1)$  parametrizes the value of a  $U(1)$  charge), this is not yet a required assumption. Let us denote by  $\mathcal{P}_q$  the linear projector onto the sector  $\mathcal{H}_q$  under consideration. For any density matrix satisfying  $\text{tr}(\mathcal{P}_q \rho) > 0$ , we can define a conditioned density matrix  $\rho(q)$  as

$$\rho(q) = \frac{\mathcal{P}_q \rho \mathcal{P}_q}{\text{tr}(\mathcal{P}_q \rho)}; \quad (5.4)$$

where the denominator ensures the normalisation  $\text{tr}(\rho(q)) = 1$ . Whenever  $[\rho, \mathcal{P}_q] = 0$ , it holds  $\mathcal{P}_q \rho \mathcal{P}_q = \rho \mathcal{P}_q = \mathcal{P}_q \rho$ . Hereafter, we focus on symmetric states, i.e. such that  $[\rho, \mathcal{P}_q] = 0$ , so that we can decompose the density matrix in a block diagonal form

$$\rho = \bigoplus_q p(q) \rho(q); \quad p(q) = \text{tr}(\mathcal{P}_q \rho); \quad (5.5)$$

where  $p(q)$  is the probability of the  $q$  sector. In the previous chapters, we only considered the Renyi entropies of those matrices  $\rho(q)$ , dubbed as symmetry-resolved entropies, but in principle other entanglement measures can be considered as well. For instance, given two density matrices  $\rho$  and  $\sigma$ , we define the symmetry-resolved relative entropy (5.1) for each sector  $q$ , i.e.,

$$S(k)(q) = S(\rho(q) | \sigma(q)) = \text{tr}(\rho(q) \log \rho(q)) - \text{tr}(\rho(q) \log \sigma(q)); \quad (5.6)$$

as a measure of distinguishability between the states in that sector. In terms of the total density matrices and projectors,  $S(k)(q)$  may be written as

$$S(k)(q) = \frac{\text{tr}(\rho^k \mathcal{P}_q)}{\text{tr}(\rho \mathcal{P}_q)^k} + \frac{\text{tr}(\sigma^k \mathcal{P}_q)}{\text{tr}(\sigma \mathcal{P}_q)^k} - \log \frac{\text{tr}(\rho \mathcal{P}_q)}{\text{tr}(\sigma \mathcal{P}_q)}; \quad (5.7)$$

From the expression above, one shows that the symmetry resolved relative entropies satisfy the sum rule

$$S(k) = \sum_q p(q) S(k)(q) + \sum_q p(q) \log \frac{p(q)}{p(q)}; \tag{5.8}$$

where

$$p(q) = \text{tr}(\rho(q)); \quad p(q) = \text{tr}(\rho(q)); \tag{5.9}$$

Following Refs. [146, 157, 159], the relative entropy can be obtained as the replica limit  $n \rightarrow 1$  of the  $n$ -th Renyi entropy of the sector  $q$  as

$$S_n(k)(q) = S_n(\rho(q)k(q)) = \frac{1}{1-n} \log \frac{\text{tr}(\rho(q)k(q)^{n-1})}{\text{tr}(\rho(q)^n)} = \frac{1}{1-n} \log \frac{\text{tr}(\rho(q)^{n-1}k(q))(\text{tr}(\rho(q)))^{n-1}}{\text{tr}(\rho(q)^n)(\text{tr}(\rho(q)))^{n-1}}; \tag{5.10}$$

We mention that other more physical forms of Renyi relative entropies exist, see e.g. [157], but from a replica perspective they just represent an inessential complication.

On the same line, we can define the symmetry resolved Schatten  $n$ -distance  $D_n(\rho; \sigma)$  as

$$D_n(\rho; \sigma)(q) = D_n(\rho(q); \sigma(q)) = \frac{1}{2^{1-n}} \sum_i k_i(q) \sigma_i(q) k_i; \tag{5.11}$$

where the  $n$ -norm of the operator is

$$k_i = \left( \sum_j \rho_j^i \right)^{1/n}; \tag{5.12}$$

with  $\rho_j$  being the eigenvalues of  $\rho$ . We recall that for finite dimensional Hilbert spaces, not all distances are equivalent, and thus one has in general different notions of indistinguishability of states. Moreover one has to be particularly careful on how the states are regularised in the continuum limit, otherwise the distance can diverge or going to zero in an undesired way, see e.g. Refs. [167, 169] for practical examples. Unfortunately, the natural definition (5.11) of distances between sectors is untreatable analytically (and also very difficult numerically). For this reason, we introduce also another notion of (still unnormalised) symmetry resolved distance as

$$D_n^0(\rho; \sigma)(q) = \frac{1}{2^{1-n}} \sum_i k_i(q) \sigma_i(q) k_i = \frac{1}{2^{1-n}} (\text{tr}(\rho(q) \sigma(q)^n))^{1/n}; \tag{5.13}$$

As we shall see,  $D_n^0$  is analytically treatable and it is related to the total  $n$ -distance by the following sum rule

$$\sum_q (D_n^0(\rho; \sigma)(q))^n = (D_n(\rho; \sigma))^n; \tag{5.14}$$

### 5.1.2 Reduced density matrices and charged moments

Until this point, everything is valid for arbitrary density matrices, independently of their origin. Here we are interested in entanglement properties and so to the case when the density matrices correspond to spatial subsystems of a larger system in a pure state  $|\psi\rangle$ , with  $\rho_A = \text{tr}_B |\psi\rangle\langle\psi|$ . Such spatial bipartition induces the decomposition of the Hilbert space  $H = H_A \otimes H_B$  so that the reduced density matrix of the subsystem is

$$\rho_A = \text{tr}_B(|\psi\rangle\langle\psi|); \tag{5.15}$$

Now we consider a system having an internal  $U(1)$  symmetry, meaning that the state commutes with a local charge operator  $Q$  [51]  $[\rho; Q] = 0$ . Taking the partial trace of the previous relation, one gets

$$[\rho_A; Q_A] = 0; \quad (5.16)$$

i.e.  $\rho_A$  has a block diagonal form with blocks corresponding to the eigenvalues  $q$  of  $Q_A$ . An effective way to write the projectors  $\rho_q$ , particularly useful for field theory calculations, is through Fourier transform

$$\rho_q = \int \frac{d\theta}{2\pi} e^{i\theta Q_A} \rho e^{-i\theta Q_A}; \quad (5.17)$$

The reason why this technique, introduced in Ref. [51], is powerful is that it provides a formalism which connects non local objects, as the symmetry-resolved entanglement measures, to local quantities, as correlation functions in a replicated theory. Generalizing the method of [51], one can introduce charged composite moments for the relative entropies and trace distances, whose Fourier transforms are eventually related to the quantity of interest. For the relative entropy between two RDMs  $\rho_A$  and  $\sigma_A$ , we just need to compute the following charged moments

$$\text{tr}(\rho_A^n e^{i\theta Q_A}); \quad (5.18)$$

and its Fourier transform

$$\text{tr}(\rho_A^n e^{i\theta Q_A}) = \int \frac{d\theta}{2\pi} e^{-i\theta q} \text{tr}(\rho_A^n e^{i\theta Q_A}) \quad (5.19)$$

readily provides the Renyi relative entropies defined as in Eq. (5.10).

We now consider the subsystem Schatten distance, whose replica trick is based on the expansion of  $\text{tr}(\rho_A - \sigma_A)^n$  as

$$\text{tr}(\rho_A - \sigma_A)^n = \sum_S \binom{n}{|S|} \text{tr}(\rho_{1_S} - \sigma_{1_S})^{|S|} \text{tr}(\rho_{(n)_S} - \sigma_{(n)_S})^{n-|S|}; \quad (5.20)$$

where the summation  $S$  is over all the subsets of  $S_0 = \{1, \dots, n\}$ ;  $|S|$  is the cardinality of  $S$  and  $\rho_{j_S} = \rho_A$  if  $j \in S$  and  $\sigma_A$  otherwise. This expression coincides with the Schatten distance only for  $n$  even. All other (real) values of  $n$ , including the important  $n = 1$  being the trace distance, are obtained taking the analytic continuation from the sequence of even  $n = n_e$ , as explained in [167, 169]. Crucially, each term in the sum appearing in the rhs of Eq. (5.20) is related to a partition function on an  $n$ -sheeted Riemann surface. In the presence of a flux, Eq. (5.20) is trivially generalised as

$$\text{tr}(\rho_A - \sigma_A)^n e^{i\theta Q_A} = \sum_S \binom{n}{|S|} \text{tr}(\rho_{1_S} - \sigma_{1_S})^{|S|} \text{tr}(\rho_{(n)_S} - \sigma_{(n)_S})^{n-|S|} e^{i\theta Q_A}; \quad (5.21)$$

whose Fourier transform is exactly  $D_n^0(q)$  in Eq. (5.13) for even  $n$ . It should be now clear why the distance in Eq. (5.13) is easily computed by replicas, while (5.11) is not.

## 5.2 From replicas and charged twist fields to symmetry resolved relative entropies and distances

In the replica approach, the moments of the RDM,  $\text{Tr} \rho_A^n$ , are evaluated for any  $(1+1)$ -dimensional quantum field theory as partition functions over the  $n$ -sheeted Riemann surface  $\mathcal{R}_n$  in which the  $n$

## 5.2. FROM REPLICAS AND CHARGED TWIST FIELDS TO SYMMETRY RESOLVED RELATIVE ENTROPIES

sheets (replicas) are cyclically joined along the subsystem  $A$  [46, 60]. Similarly [51], the charged moments find a geometrical interpretation by inserting an Aharonov-Bohm flux through such surface, so that the total phase accumulated by the field upon going through the entire surface is  $e^i$ . Then the partition function on such modified surface gives the charged moments.

This partition function can be equivalently rewritten in terms of the correlator of twist fields in the replicated theory. Those fields are characterized by the commutation relations with local observables, and for a  $U(1)$  bosonic field theory, they read as as [47, 51, 60]

$$T_{n_i}(x; \dots)_j(x^0; \dots) = \begin{cases} T_{j+1}(x^0; \dots) e^{i \int_{x^0}^x T_{n_i}(x; \dots)} & \text{if } x < x^0, \\ T_j(x^0; \dots) T_{n_i}(x; \dots) & \text{otherwise.} \end{cases} \quad (5.22)$$

Similarly, one introduces the field  $\bar{T}_{n_i} = T_{n_i}^y$  that introduces a flux  $e^{-i}$  between the 1st and the  $n$ -th replica, and it implements the replica permutation  $j \rightarrow j-1$ . We will refer to  $T_{n_i}$  for  $i \in \mathbb{Z}$  as the charged (or composite) twist field while to  $T_n = T_{n;0}$  as the standard twist field. For later purpose, it is useful to work out the OPE of the charged twist fields, and we do it in the following subsection.

### 5.2.1 Operator product expansion of twist fields

In this subsection, we first review the construction of the OPE of standard twist fields (following Refs. [170, 172]), and then we generalise these results to charged twist fields.

Let us consider a given CFT of central charge  $c$ , and we focus on its holomorphic sector (the antiholomorphic sector is similarly treated). We write the full set of primaries as

$$\{O_a\}_{a \in \mathcal{G}} \quad (5.23)$$

We refer to  $CFT_n$  as the theory built with  $n$  replicas of the original CFT with central charge is  $nc$  (say  $CFT_n = CFT^{(n)}$ ). A full set of operators which are primary w.r.t all  $n$  copies of  $CFT_n$  is

$$\{O_{a_1}^{i_1} \dots O_{a_n}^{i_n}\}_{g} \quad (5.24)$$

where the upper index is a replica index. This  $CFT_n$  has a permutation symmetry  $Z_n$  which can be promoted to a global symmetry, leading to the construction of the orbifolded theory  $CFT_n = Z_n$ . The field content of the latter is different from the one of  $CFT_n$  and, in particular, the twist fields appear as local operators (a clear and complete treatment of the orbifold construction in the context of entanglement can be found in [173]). Roughly, the twist field  $T_n(z)$  is defined such that its insertion in the spacetime of the orbifolded theory corresponds to an opening of a branch-cut in the time slice  $[z; 1]$  which connects the  $j$ -th replica to the  $j+1$ -th [46]. The conformal dimension of  $T_n$  is read off from three-point function  $\langle h T_n(z) \bar{T}_n(z^0) T(w) \rangle$  with  $\bar{T}_n = T_n^y$  and the stress-energy tensor of  $CFT_n$

$$T = \sum_{j=1}^n T^j; \quad (5.25)$$

where  $T^j$  is a short notation for  $T \otimes \dots \otimes T$  ( $n$  times) (the stress-energy tensor of the  $j$ -th replica). Through unfolding procedure induced by the transformation  $(z) = z^{1/n}$  one gets [46]

$$\frac{\langle h T_n(0) \bar{T}_n(1) T(z) \rangle}{\langle h T_n(0) \bar{T}_n(1) \rangle} = h \sum_{j=1}^n \frac{d}{dz} \left[ T \left( e^{-i \frac{2j}{n}} \right) + \frac{cn}{12} f; z \right] = \frac{c}{24z^2} \left( n - \frac{1}{n} \right); \quad (5.26)$$

which is equivalent to say that the scaling dimension of the twist field is  $h_{T_n} = \frac{c}{24} n - \frac{1}{n}$ . Moreover, since  $\mathcal{T}_n = T_n^y$ , the following fusion is present

$$[T_n] [\mathcal{T}_n] = [1]; \quad (5.27)$$

and then all the descendants of the conformal tower of the identity are generated in the OPE of  $T_n; \mathcal{T}_n$ . Similarly, we conclude that the primary (nonidentity) operator  $O_a^j$  is not present in the OPE twist fields, because its one-point function  $h_{O_a^j}(z)$  on the plane is zero. However, if  $[O_{a_j}] [O_{a_k}] = [1]$  (implying that  $O_{a_j}$  and  $O_{a_k}$  have the same conformal dimension  $h_{a_j} = h_{a_k}$ ), the following fusion is present

$$[T_n] [\mathcal{T}_n] = [O_{a_j}^j O_{a_k}^k]; \quad (5.28)$$

and the unfolding leads to

$$\frac{h_{T_n}(0)\mathcal{T}_n(1)(O_{a_j}^j O_{a_k}^k)(z=1)}{h_{T_n}(0)\mathcal{T}_n(1)} = \frac{1}{n^{h_{a_j}+h_{a_k}}} h_{O_{a_j}^j}(z=e^{i\frac{2j}{n}}) O_{a_k}^k(z=e^{i\frac{2k}{n}}); \quad (5.29)$$

Here products of operators at coinciding points are intended as applied on different sheets on the unfolded theory, see Ref. [173] for details. All the other fusions between the twist fields and the other primaries of the replicated theory can be obtained from  $m$ -point functions of primaries in the unreplicated theory.

For the charged twist fields, the discussion follows the same logic, but some additional caveats arise. Let us first identify the primary operator  $V(z)$  of the original theory which generates the  $U(1)$  symmetry we are interested in, i.e. it inserts an additional flux  $e^j$ , in the time-slice  $2[z; +1)$ . The composite twist field  $T_{n;}$  is constructed by fusing together  $T_n$  and  $V^{j=n}$ , which means that it is the lightest operator appearing in the OPE  $T_n(z)V^{j=n}(0)$  (see e.g. [98, 99, 113, 174]). We use the convention that the additional flux is inserted between the  $n$ -th and the first replica, but other equivalent choices do not affect the following discussion in any relevant part.

Once one unfolds the theory, the charged twist fields generate additional insertions of  $V; V$ , that were absent for the standard twist fields. In particular, we can employ the latter property to compute the dimension of the modified twist field [51]

$$\frac{h_{T_{n;}}(0)\mathcal{T}_{n;}(1)T(z)}{h_{T_n}(0)\mathcal{T}_n(1)} = \frac{h_V(0)V(1) \prod_{j=1}^n \frac{d}{dz} T(e^{i\frac{2j}{n}}) + \frac{cn}{12} f; z g}{h_V(0)V(1)} = \frac{h_V}{n} + h_{T_n}; \quad (5.30)$$

so

$$h_{T_{n;}} = \frac{h_V}{n} + h_{T_n}; \quad (5.31)$$

As we explain below, the fusion rule  $T_{n;}(T_n)^y$  is eventually reconstructed from  $(m+2)$ -point function of  $m$  primaries  $O_{a_k}^k$  and the two symmetry operators  $V(0); V(1)$ . In particular, it holds

$$\frac{h_{T_{n;}}(0)\mathcal{T}_{n;}(1)(O_{a_j}^j O_{a_k}^k)(z=1)}{h_{T_n}(0)\mathcal{T}_n(1)} = \frac{1}{n^{h_{a_j}+h_{a_k}}} h_V(0) O_{a_j}^j(z=e^{i\frac{2j}{n}}) O_{a_k}^k(z=e^{i\frac{2k}{n}}) V(1); \quad (5.32)$$

which is the generalization of (5.29) in the presence of a nontrivial flux. An important difference is found with the standard twist fields, namely, a single primary operator  $O_{a_j}^j$  might

## 5.2. FROM REPLICAS AND CHARGED TWIST FIELDS TO SYMMETRY RESOLVED RELATIVE ENTROPIES

appear in the OPE  $T_{n;}(z) \mathcal{F}_{n;}(0) \sim (T_{n;}(z))^y$ ; this is indeed the case whenever the three-point function  $\langle hV(0) \mathcal{V}(1) \mathcal{O}_{a_i}(1) \rangle$  is non-vanishing.

Summing up, the OPE  $T_{n;}(z) \mathcal{F}_{n;}(0)$  restricted to the conformal tower of the identity is

$$T_{n;}(z) \mathcal{F}_{n;}(0) = \langle hT_{n;}(z) \mathcal{F}_{n;}(0) \rangle + z^2 \frac{2h_{T_{n;}}}{nc} \sum_{j=1}^{\infty} T^j(0) + \dots; \quad (5.33)$$

where  $\langle hT_{n;}(z) \mathcal{F}_{n;}(0) \rangle = \frac{1}{z^{2h_{T_{n;}}}}$  is the normalized correlator among twist fields computed in the vacuum. Similarly, the restriction of the OPE in the space of primaries  $\mathcal{O}^j$  reads

$$T_{n;}(z) \mathcal{F}_{n;}(0) = \langle hT_{n;}(z) \mathcal{F}_{n;}(0) \rangle + \frac{z^{h_{\mathcal{O}^j}}}{n^{h_{\mathcal{O}^j}}} C_{\mathcal{O}^j} \sum_{j=1}^{\infty} \mathcal{O}^j(0) + \dots; \quad (5.34)$$

and  $C_{\mathcal{O}^j}$  is the OPE coefficient of the fusion  $[V] [V] \rightarrow [\mathcal{O}^j]$  in the unreplicated theory.

### 5.2.2 Charged moments of the excited states

The last ingredient we need is the CFT description of the low-energy excited states. In this section, we address this task, and eventually we express the charged moments of those excited states as correlation functions in the original CFT.

Given a local field  $\mathcal{O}(x; \tau)$ , it is possible to construct an excited state  $|j\rangle$  inserting  $\mathcal{O}$  at past infinite imaginary time as

$$|j\rangle = \lim_{\tau \rightarrow -\infty} \mathcal{O}(x; \tau) |0\rangle; \quad (5.35)$$

where  $|0\rangle$  is the vacuum of the CFT. In particular, given the scaling dimension of  $\mathcal{O}$ , the energy of the excitation  $|j\rangle$  is

$$E = \frac{2}{L}; \quad (5.36)$$

This mapping is known as state-operator correspondence (see, e.g., the textbook [97] for details). The corresponding field-theoretic representation of the density matrix  $\rho = |j\rangle \langle j|$  presents two insertions of  $\mathcal{O}$  at  $z = x + i\epsilon = i1$ .

We now assume periodic boundary conditions along the space direction, so that the worldsheet is an infinite cylinder of circumference  $L$ . We focus on the subsystem  $A = [0; \ell]$  (embedded in the system  $[0; L]$ ) and, for later purpose, we introduce the dimensionless ratio

$$x = \frac{\ell}{L}; \quad (5.37)$$

This is particularly useful, since the quantities we are interested depend on the lengths  $\ell; L$  via  $x$ .

Given the excited states, we are now interested in their (charged) moments, and the construction is summarized below. Hereafter, we omit explicitly the subscript  $A$  for notational convenience, denoting by  $\text{tr}_B(|j\rangle \langle j|)$  the reduced density matrix associated with the state  $|j\rangle$ , referring to the subsystem  $A$  only when strictly necessary.

For an arbitrary operator  $\mathcal{O}$ ,  $\text{tr}(\mathcal{O}^n)$  is obtained sewing cyclically along  $A$ ,  $n$  of the cylinders defining the reduced density matrix. Following Ref. [132], we introduce the quantity ratio

$$F^{(n)}(x) = \frac{\text{tr}(\mathcal{O}^n)}{\text{tr}(\mathbb{1}^n)}; \quad (5.38)$$

with  $\rho_1$  being the ground-state reduced density matrix. This allows to 'simplify' the UV divergent entanglement contributions of the ground-state, so that  $F^{(n)}(x)$  depends eventually only on dimensionless parameters. In particular, one obtains [132, 138]

$$F^{(n)}(x) = \frac{\prod_{k=1}^n \langle \mathcal{Y}(z_k) \mathcal{Y}(z_k^+) \rangle_{R_n}}{h(z_1) \langle \mathcal{Y}(z_1^+) \rangle_{R_1}^n}; \quad (5.39)$$

where  $z_k$  corresponds to the points at past/future in time respectively of the  $k$ -th copy of the system ( $k = 1; \dots; n$ ) in  $R_n$  ( $R_1$  is just the cylinder). Clearly, the normalisation factor of the field does not matter because it cancels out in the ratio (5.39); moreover,  $F^{(1)}(x) = 1$  since the trace of the density matrices is 1.

The correlation functions appearing so far are evaluated over the Riemann surface  $R_n$ . However, it is convenient to 'unfold' the Riemann surface, going back to a geometry without branch-cuts. Thus, we apply the conformal mapping [138]

$$w(z) = i \log \frac{\sin \frac{(z-u)}{L}}{\sin \frac{(z-v)}{L}}; \quad (5.40)$$

and the Riemann surface  $R_n$  is transformed into a single cylinder. At this point, one has to transform also the field under a conformal mapping, a task that in general is involved (especially for higher descendants [97]). However, if we focus on primary states, describing the lowest-energy excitations, the transformation law becomes simply

$$\langle \mathcal{W}(w); \mathcal{W}(w) \rangle = \left( \frac{dz}{dw} \right)^h \left( \frac{dz}{dw} \right)^h \langle \mathcal{Z}(z); \mathcal{Z}(z) \rangle; \quad (5.41)$$

with  $(h; h)$  the conformal weights of  $\mathcal{Z}$ . Hence, for primary operators, one can easily express  $F^{(n)}(x)$  in terms of correlation functions over the cylinder. The final result reads [138]

$$F^{(n)}(x) = n^{-2n(h+h)} \frac{\prod_{k=1}^n \langle \mathcal{W}(w_k) \mathcal{W}(w_k^+) \rangle_{\text{cyl}}}{h(w_1) \langle \mathcal{W}(w_1^+) \rangle_{\text{cyl}}^n}; \quad (5.42)$$

where  $w_k$  are the points corresponding to  $z_k$  through the map  $w(z)$ , i.e.

$$w_k = \frac{(1+x)+2(k-1)}{n}; \quad w_k^+ = \frac{(1-x)+2(k-1)}{n}; \quad \text{with } k = 1; \dots; n; \quad (5.43)$$

We mention that in the literature it is possible to find also some extension to descendant states [175, 177] and boundary theories [178, 179].

The generalisation in the presence of the flux has been worked out in our previous work [1]. Following this reference, we introduce a generating function associated to  $\phi^i$ ,

$$P_n(\lambda) = \frac{\text{tr}(\rho_n e^{iQ})}{\text{tr}(\rho_n)} \quad (5.44)$$

<sup>1</sup>We stress that to make sense of  $U(1)$  symmetry resolution for  $j \neq i$ , we have to be sure that the state has a definite value of the charge. This is indeed the case if the corresponding field  $\phi^i(z)$  has a given charge, namely it transforms under an irreducible representation of  $U(1)$ .

## 5.2. FROM REPLICAS AND CHARGED TWIST FIELDS TO SYMMETRY RESOLVED RELATIVE ENTROPIES

and the ratio

$$f_n(\cdot) = \frac{p_n(\cdot)}{p_n^1(\cdot)}. \quad (5.45)$$

The key idea behind the definitions above was to isolate explicitly the dependence on the flux  $e^j$ , that is the important information for the symmetry resolution. A field theoretic expression for  $f_n(\cdot)$  can be recovered, and it is eventually expressed as a correlation function of the fields  $\psi$  and  $V$ . Using the same conventions of Eq. (5.39) for the insertions of  $\psi$  and  $V$ , we have

$$f_n(\cdot) = \frac{\prod_{k=1}^n \int_{R_n} V(u_1) V(v_1) \psi(z_k) \psi(z_k^+)}{h \prod_{k=1}^n \int_{R_n} V(u_1) V(v_1) \psi(z_k) \psi(z_k^+) i_{R_n}}: \quad (5.46)$$

Here  $u_1$  and  $v_1$  are the points where the flux is inserted (coinciding with the branch points), which are identified with the points 0 and  $\infty$  of the first replica.

As a last step, we have to express the charged moments necessary for the relative entropies and subsystem distances are in Eqs. (5.18) and (5.21). They can all be written in terms of  $\text{tr}(e^{jQ} \rho_1 \dots \rho_n)$  with properly chosen density matrices  $\rho_i$ . The corresponding correlation functions are then the ones for the neutral moments reported in [146, 169] with the additional insertion of two charge operators  $V$ . Given some RDMs  $\rho_j = \text{tr}_B(j \rho_j i_h j)$ , the charged moments of interest are conveniently parametrised as

$$\frac{\text{tr}(e^{jQ} \rho_1 \dots \rho_n)}{\text{tr}(e^{jQ} \rho_1)} \frac{\text{tr}(\rho_1)}{\text{tr}(\rho_1 \dots \rho_n)} = \frac{\prod_{k=1}^n \int_{\mathcal{C}} V(0) V(\infty) \psi(z_k) \psi(z_k^+)}{h \prod_{k=1}^n \int_{\mathcal{C}} V(0) V(\infty) \psi(z_k) \psi(z_k^+) i_{\mathcal{C}}} = \frac{\prod_{k=1}^n \int_{\text{cyl}} V(i_1) V(i_1) \psi(w_k) \psi(w_k^+)}{h \prod_{k=1}^n \int_{\text{cyl}} V(i_1) V(i_1) \psi(w_k) \psi(w_k^+) i_{\text{cyl}}}: \quad (5.47)$$

The points  $z_k; w_k$  correspond respectively to the infinite past/future points in the  $k$ -th sheet of the Riemann surface ( $k = 1; \dots; n$ ). Their explicit expression is read off from Eq. (5.43), i.e.

$$z_k = \exp \left[ i \frac{2(k-1)}{n} + \frac{i(1-x)}{n} \right]; \quad w_k = \frac{2(k-1)}{n} + \frac{(1-x)}{n}; \quad (5.48)$$

The locations of these operator insertions in the  $z$  and  $w$  planes are reported in Fig. 5.1.

In the calculation of relative entropies and distances, we are dealing with just two (primary) fields at a time, says  $\psi$  and  $\bar{\psi}$ , and we need to work with combinations of the form  $m_1 m_2 m_3 \dots$ . Hence, each partition  $S = (m_1; \dots; m_k)$  of  $n$  ( $m_1 + \dots + m_k = n$ ) is related to a product of RDMs according to the rule

$$S = (m_1; \dots; m_k) ! A_S^{m_1 m_2 m_3 \dots} \quad (5.49)$$

Figure 5.1: Points where the operators are inserted in the correlations  $\langle V \dots V \rangle_{\mathcal{D}} = \langle \prod_{k=1}^n \sigma_k \rangle_{\mathcal{D}}$  in Eq. (5.47). We report  $n = 3$  for the two geometries, planar (left) and cylindrical (right).

We define also the following quantities

$$p_S(\mathcal{D}) = \frac{\text{tr}(A_S e^{iQ})}{\text{tr}(A_S)}; \quad f_S(\mathcal{D}) = \frac{p_S(\mathcal{D})}{p_n^1(\mathcal{D})}. \quad (5.50)$$

With a slight abuse of notation, we will refer to  $p_S(\mathcal{D})$  as probability generating function. Although  $p_S(\mathcal{D})$  is normalised as  $p_S(\mathcal{D} = 0) = 1$ , it is not guaranteed that  $A_S$  is hermitian, nor that it has non-negative spectrum.

However, none of these complications is a problem for our aims and we can safely define

$$p_S(q) = \frac{\text{tr}(A_S e^{iq})}{\text{tr}(A_S)} = \int \frac{d\mathcal{D}}{Z} p_S(\mathcal{D}) e^{iq}; \quad (5.51)$$

although it does not have a direct interpretation as a probability, like it happens for the entropy.

After having set up the framework for our calculation, we are already in position to make a first fundamental observation, without doing any calculation. Namely, the fluctuations of the  $U(1)$  charge are divergent in the limit  $L \rightarrow 1$ , as variance grows as  $\log L$  [51, 180, 182]; more precisely, the way this divergence appears is the same for the ground-state and the low-lying states, while the differences are seen in the  $\mathcal{O}(1)$  contribution. Hence,  $p_S(q)$  at the leading order in  $L$  is always a Gaussian shaped probability with a variance growing like  $\log L$  that does not depend on the choice of the states. In particular, in the limit of  $L \rightarrow 1$  with  $q; \ell = L$  fixed, one can show

$$\frac{p_S(q)}{p_n^1(q)} \xrightarrow{L \rightarrow 1} 1; \quad (5.52)$$

Consequently, for the states considered above it always holds

$$S_n(k)(q) \xrightarrow{L \rightarrow 1} S_n(k); \quad (5.53)$$

and similarly, one can show that

$$\frac{D_1(\dots)(q)}{D_1(\dots)} \neq 1: \tag{5.54}$$

The Eqs. above shows that, in the limit we are considering, there is no explicit dependence on the charge  $q$ . This property has been dubbed *equipartition* for the entanglement resolution of a single state [50], and we showed that it holds also for measures of distinguishability (relative entropies and distance).

### 5.3 Analytical predictions for the compact boson and the Dirac fermions

In this section, we provide some explicit expressions for the universal functions of the correlation functions necessary for relative entropies and subsystems distances, generically given by Eq. (5.47), and we consider the low-lying states of the compact boson. In some cases, especially when the calculation becomes too involved, we are able to analyze small subsystem sizes via the OPE of composite twist fields.

The CFT of the compact boson (or Luttinger liquid) is described by the Euclidean action [97]

$$S[\phi] = \frac{1}{8K} \int d^2x (\partial_\mu \phi)^2; \tag{5.55}$$

with the additional requirement that the bosonic field is compact

$$\phi \sim \phi + 2\pi; \tag{5.56}$$

This CFT has central charge  $c = 1$ . The left and right modes of the fields are decoupled, so one can write in complex coordinates

$$\phi(z; \bar{z}) = \phi(z) + \bar{\phi}(\bar{z}); \tag{5.57}$$

This theory admits a topological  $U(1)$  symmetry generated by the following vertex operator

$$V_\alpha(z; \bar{z}) = e^{i\alpha(\phi(z) + \bar{\phi}(\bar{z}))}; \tag{5.58}$$

that we aim to investigate through symmetry-resolution. The primaries of this CFT and their conformal weights  $(h; \bar{h})$  are respectively

$$(i\alpha)(z) (1; 0); \quad (i\alpha)(z) (0; 1); \quad V_\alpha(z; \bar{z}) = e^{i\alpha(\phi(z) + \bar{\phi}(\bar{z}))} \left( \frac{K}{2} \alpha^2; \frac{K}{2} \alpha^2 \right); \tag{5.59}$$

Not all the values of  $(\alpha; \bar{\alpha})$  give rise to physical states, but the set of the allowed values is quantised (see [97]); however, this discussion is not important for our purposes. We also choose to deal only with the holomorphic part of the vertex operator ( $\bar{\alpha} = 0$ ), keeping  $\alpha$  as a free parameter.

In what follows, we will set  $\alpha = K = 1$ . This value of  $K$  is related to a free Dirac fermion via bosonisation, corresponding to a lattice Fermi gas which we will use to numerically test the analytic predictions obtained in the following. In that case, the symmetry is the global  $U(1)$  charge given by the number of particles minus the number of antiparticles. The explicit correspondence between microscopic low energy excitations of the XX chain and the primary

operators of the compact boson, via bosonisation techniques, has been discussed in the work by Alcaraz et al. [132]. We mention that although the Dirac fermions and the compact boson are related, the correspondence is non-local and their entanglement is different in general (see [170] for the case of two intervals): however, this issue does not play a role in the following discussion, as we focus on a single-interval geometry only.

Let us briefly recall the OPE among the primaries [97] of the compact boson, which can be recovered by their 3-point functions, see Appendix 5.A. The following fusion rules are present

$$[V] [V] = [1] + [i@]; \quad [i@] [i@] = [1]; \quad (5.60)$$

The only nontrivial (the others are 1) OPE coefficient is

$$C_{VV}^{i@} = 1; \quad (5.61)$$

We will also make use of the OPE coefficient associated to the generation of the stress-energy tensor  $T = \frac{1}{2}(i@)^2$ , which is fixed by the Virasoro algebra only (see [97]), as

$$C_{i@i@}^T = 2; \quad C_{VV}^T = -2; \quad (5.62)$$

Finally, going to the replica theory, we also need the OPE of the charged twist fields. We will focus only on the fusion channels<sup>2</sup>

$$T_n; \quad (T_n; )^y = 1; i@; T; \quad (5.63)$$

discarding explicitly the generation of the vertex operators. For instance, while  $i@$  are generated in the OPE, their expectation value is zero for the states we consider (by neutrality condition), and thus they do not contribute to the quantity we are interested in. In the forthcoming subsections, we will characterise  $f_S^i(\cdot)$  for different states, giving the exact results when possible or the leading order, obtained by OPE expansion, for  $\epsilon = \frac{1}{n} \rightarrow 0$  in the other cases.

### 5.3.1 Universal function for the pair of states $\psi = V_1$ and $\phi = V_2$

Let us start from those excited states both associated vertex operators with weight  $h_1$  and  $h_2$ , i.e.  $\psi = V_1$  and  $\phi = V_2$ . We first consider the universal function  $f_S^{V_1; V_2}(\cdot)$  in Eq. (5.45) for the partition  $S = (m_1; m_2)$ , given as

$$f_S^{V_1; V_2}(\cdot) = \frac{\prod_{k=1}^{m_1} V_1(w_k) V_1(w_k^+) \prod_{k=m_1+1}^{m_1+m_2} V_2(w_k) V_2(w_k^+)}{h_{V_2}(\cdot) V_2(\cdot) i_{cyl} \prod_{k=1}^{m_1} V_1(w_k) V_1(w_k^+) \prod_{k=m_1+1}^{m_1+m_2} V_2(w_k) V_2(w_k^+) i_{cyl}} =$$

$$\frac{\prod_{k=1}^{m_1} h_{V_2}(\cdot) V_1(w_k) i_{cyl} h_{V_2}(\cdot) V_1(w_k) i_{cyl} \prod_{k=1}^{m_1} h_{V_2}(\cdot) V_1(w_k^+) i_{cyl} h_{V_2}(\cdot) V_1(w_k^+) i_{cyl} \prod_{k=m_1+1}^{m_1+m_2} h_{V_2}(\cdot) V_2(w_k) i_{cyl} h_{V_2}(\cdot) V_2(w_k) i_{cyl}}{h_{V_2}(\cdot) V_2(w_k^+) i_{cyl} h_{V_2}(\cdot) V_2(w_k^+) i_{cyl}}; \quad (5.64)$$

<sup>2</sup>To be precise, we are considering the generation of the following operators in the orbifold theory:  $1, \dots, 1, i@, \dots, 1, 1, \dots, T, \dots, 1$ , where  $i@$  and  $T$  are inserted in any of the  $n$  replicas.

Here we used the correlation function between vertex operators on the cylinder

$$h \prod_j V_j(w_j) i_{cyl} = \prod_{i < j} \frac{L}{L} \sin \frac{(w_i - w_j)}{L} i^j; \quad \text{if } \sum_j X_j = 0; \quad (5.65)$$

while it vanishes if  $\sum_j X_j \neq 0$ : the requirement  $\sum_j X_j = 0$  is the neutrality condition. All the correlation functions appearing in the first line of Eq. (5.64) satisfy the neutrality condition, and so the previous formula can be safely applied. With a slight abuse of notation, we identify (for notational convenience) the putative two-point correlators in (the rhs of) Eq. (5.64) as

$$hV_i(w_i)V_j(w_j)i_{cyl} = \frac{L}{L} \sin \frac{(w_i - w_j)}{L} i^j; \quad (5.66)$$

Eq. (5.64) has to be regularised due to the insertion of the vertex operators at infinity. One way to do so is through their insertion at  $i$  and, only at the end, take the limit  $|i| \rightarrow \infty$ . Doing so, with calculations similar to those in Ref. [1], one straightforwardly gets

$$hV_{=2}(i_1)V(w_k)i_{cyl} hV_{=2}(i_1)V(w_k)i_{cyl} = e^{i \frac{x}{n}}; \quad (5.67)$$

Taking the product over the different  $k$ 's we finally obtain the extremely simple form  $f_S^{V_1;V_2}(x) = e^{\frac{i x}{n} [m_1 + m_2]}$ . Clearly, because of the simple factorisation property of the correlation functions, if we chose a different partition  $S$ , i.e. a different order of insertion of  $V_1; V_2$  in the replica case, we would have got the same result, i.e.

$$f_S^{V_1;V_2}(x) = e^{\frac{i x}{n} [m_1 + m_2]}; \quad \forall S; \quad (5.68)$$

As a byproduct, we compare the result (5.68) with the OPE expansion valid in the small  $x$  limit, that is expected to give

$$f_S^{V_1;V_2}(x) \sim 1 + \frac{i x}{n} [m_1 + m_2] + O(x^2); \quad (5.69)$$

To do so, we first express  $f_S^{V_1;V_2}(x)$  as an expectation value of charged twist fields as

$$f_S^{V_1;V_2}(x) = \frac{hV_{1;V_2}; jT_n(0)\bar{T}_n(\infty)jV_{1;V_2}; i_1; i_2; \dots; i_n; 0jT_n(0)\bar{T}_n(\infty)j0; \dots; 0i}{hV_{1;V_2}; jT_n(0)\bar{T}_n(\infty)jV_{1;V_2}; i_1; i_2; \dots; i_n; 0jT_n(0)\bar{T}_n(\infty)j0; \dots; 0i}; \quad (5.70)$$

Restricting our analysis to order  $O(x)$  (non-vanishing) contributions in the OPE, we can approximate

$$T_n(0)\bar{T}_n(\infty) \sim hT_n(0)\bar{T}_n(\infty)i_C(1 + o(x)); \quad (5.71)$$

$$T_n(0)\bar{T}_n(\infty) \sim hT_n(0)\bar{T}_n(\infty)i_C \left( 1 + \frac{i}{n} C_{V=2}^{i@} \prod_j (i@)^j(0) + o(x) \right); \quad (5.72)$$

The expectation value of  $\prod_j (i@)^j(0)$  is just the sum of the contributions of each single replica, namely

$$h0; \dots; 0j \prod_j (i@)^j(0) j0; \dots; 0i = 0; \quad (5.73)$$

$$hV_{1;V_2}; j \prod_j (i@)^j(0) jV_{1;V_2}; i = \frac{i^2}{L} (m_1 + m_2); \quad (5.74)$$

Figure 5.2: Excess of the average charge  $h_{S^{1;V}}^{1;V} - h_{S^{(1;1)}}^{1;V}$  as a function of  $x = \ell/L$  for different values of  $(n = 2; 1; 1; 2)$ . The universal CFT results, which are linear functions of  $x$ , cf. Eq. (5.76) are tested against exact numerical result for the XX chain at half-filling ( $L = 200$ ).

Putting all the pieces together

$$\frac{h_{S^{1;V}}^{1;V} - h_{S^{(1;1)}}^{1;V}}{h_{S^{1;V}}^{1;V} - h_{S^{(1;1)}}^{1;V}} = \frac{h_{S^{1;V}}^{1;V} - h_{S^{(1;1)}}^{1;V}}{h_{S^{1;V}}^{1;V} - h_{S^{(1;1)}}^{1;V}} = 1 + \frac{x}{n} (m_{1;1} + m_{2;2}) ; \quad (5.75)$$

that is precisely the result (5.69) we expected.

In Figs. 5.2 and 5.3 we test the CFT prediction (5.68) against numerics for the XX chain (obtained with the methods of Appendix 5.B). We focus on the excess of average charge

$$h_{S^{1;V}}^{1;V} - h_{S^{(1;1)}}^{1;V} = \frac{1}{L} \frac{d}{dx} f_{S^{1;V}}^{1;V}(x) \Big|_{x=0} = \frac{m_{1;1} + m_{2;2}}{n} x ; \quad (5.76)$$

and plot it as a function of  $x = \ell/L$ . As shown in Fig. 5.2, for  $n = 2$  and  $S = (1; 1)$  the agreement with numerical data (system size  $L = 200$ ) is remarkable for different vertex states and no significant corrections are visible for this relatively small system size. In Fig. 5.3 we consider instead  $n = 4$  considering the partitions  $S = (2; 2)$  and  $S = (1; 1; 1; 1)$ . We emphasise that now there are evident deviations of the numerics from the CFT predictions with the numerical data oscillating around the analytical value, with an amplitude of going to zero as the system size increases. This behavior is expected from the exact analysis of the symmetry-resolved Renyi entropies of the XX chain performed in [183], where the deviations from CFT are more severe as the number of replicas is increased (and it is a consequence of the presence of well known unusual corrections to the scaling [184]).

### 5.3.2 Universal function for the pair of states $|i\rangle$ and $|1\rangle$

Here, we compare the excitation associated with  $|i\rangle$  with the ground state, i.e.  $|1\rangle$ . In Ref. [1], we analyzed the symmetry-resolved entropy of  $|i\rangle$ , and we were able to express  $S_n^{i@}(x)$  as a characteristic polynomial of a certain matrix. The argument of [1] was based on the fact

Figure 5.3: Excess of average charge  $f_S^{i@;1}(\lambda)$  for the partitions  $S = (2; 2)$  and  $S = (1; 1; 1; 1)$  (left/right panel respectively) as a function of  $x = \lambda/L$ . The CFT predictions are tested against numerical data for the XX chain for different system sizes ( $L = 100; 200; 400; 800$ ). The order of insertion of the operator is different in the two cases, indeed  $V_1$  is present in the first and second replica for  $S = (2; 2)$  while for  $S = (1; 1; 1; 1)$  it is inserted in the second and fourth replica; nevertheless, the analytical prediction is the same which is a special feature of the vertex states.

that

$$f_S^{i@;1}(\lambda) = \frac{\sum_{k=1}^n \langle V_{=2}(i_1) V_{=2}(i_1) \rangle_{\text{cyl}} (i@)(w_k) (i@)(w_k^+)}{hV_{=2}(i_1) V_{=2}(i_1) \rangle_{\text{cyl}}} \quad (5.77)$$

has a certain diagrammatic expansion (see the Appendix 5.A) which can be recast in a clever way. For instance, the order  $O(0)$  is given by the contractions of the derivative operators among themselves, which can be expressed as a determinant using Wick theorem. At order  $O(2)$  two derivative operators are contracted with  $V_{=2}$ , while the remaining  $2(n-1)$  ones are contracted among themselves, and so on.

The same argument can be applied to  $f_S^{i@;1}$ , that is the quantity we are interested here. The only difference is the explicit form of the resulting matrix for the characteristic polynomial. For instance, for any partition  $S$  where  $i@$  appears  $m_{i@}$  times in the product  $A_S$ , we construct an antisymmetric matrix  $M$  of dimension  $2m_{i@} \times 2m_{i@}$  with elements

$$M_{ij} = \begin{cases} \frac{1}{2 \sin \frac{w_i - w_j}{2}} & i \neq j; \\ 0 & i = j; \end{cases} \quad (5.78)$$

with  $\{w_i\}$  being the set of points in which  $i@$  is inserted in the cylindrical geometry, cf. Eq. (5.48). In terms of  $M$ ,  $f_S^{i@;1}(\lambda)$  is expressed as follows

$$f_S^{i@;1}(\lambda) = \frac{\det M_{\frac{i}{2}}}{\det(M)}; \quad (5.79)$$

that provides an analytical result for any integer  $n$  and for any partition  $S$ . However, its form becomes more and more cumbersome when many derivative operators are inserted, as the size of matrix  $M$  increases.

As an example, let us see what happens in the simplest case, namely  $f_{(1;n-1)}^{i@;1}(\epsilon)$ , so that the matrix  $M$  is

$$M = \begin{pmatrix} 0 & \frac{1}{2\sin\frac{x}{n}} \\ \frac{1}{2\sin\frac{x}{n}} & 0 \end{pmatrix}; \quad \det M + i\frac{1}{2} = \frac{1}{4\sin^2\frac{x}{n}} - \frac{1}{2}; \quad (5.80)$$

and we get

$$f_{(1;n-1)}^{i@;1}(\epsilon) = 1 - \frac{2}{n} \sin^2 \frac{x}{n}; \quad (5.81)$$

As the number of replicas  $n$  increases, it is really unlikely to get a simple close formula that can be eventually analytically continued in  $n$ . A case that has been handled explicitly (see Ref. [1]) is  $S = (n; 0)$ , when  $f_S^{i@;1} = f_n^{i@}(\epsilon)$  that is

$$f_n^{i@}(\epsilon) = \prod_{p=1}^n \left( 1 - \frac{1}{(\frac{n}{\sin(x)})^{n-1+2p}} \right) = \frac{(1 + n + \frac{1}{2}(\frac{n}{\sin(x)})^{n-1} + \frac{1}{2})!}{(1 + \frac{1}{2}(\frac{n}{\sin(x)})^{n-1} + \frac{1}{2})!} \frac{(1 + n + \frac{1}{2}(\frac{n}{\sin(x)})^{n-1} + \frac{1}{2})!}{(1 + \frac{1}{2}(\frac{n}{\sin(x)})^{n-1} + \frac{1}{2})!} : \quad (5.82)$$

We now consider the small  $\epsilon$  behaviour of  $f_S^{i@;1}(\epsilon)$  for a general partition  $S$ , which can be obtained via OPE of charged twist fields.

Let us start with the partition  $S = (m_{i@}; n - m_{i@})$ . The function  $f_S^{i@;1}$  is written in terms of twist fields as

$$f_S^{i@;1}(\epsilon) = \frac{\langle \psi_{i@}; \dots; 0; j T_n(0) \bar{\psi}_n(\epsilon) \rangle_{j_{i@}; \dots; 0; i \psi_0; \dots; 0; j T_n(0) \bar{\psi}_n(\epsilon) \rangle_{j_0; \dots; 0; i}}{\langle \psi_{i@}; \dots; 0; j T_n(0) \bar{\psi}_n(\epsilon) \rangle_{j_{i@}; \dots; 0; i \psi_0; \dots; 0; j T_n(0) \bar{\psi}_n(\epsilon) \rangle_{j_0; \dots; 0; i}}; \quad (5.83)$$

where  $j_{i@}; \dots; 0; \dots; i$  stands for the state where  $i@$  appears  $m_{i@}$  times in the first replicas. Since the terms of order  $O(\epsilon^2)$  in the OPE come from the expectation value of the stress energy-tensor, we keep

$$T_n(0) \bar{\psi}_n(\epsilon) = h T_n(0) \bar{\psi}_n(\epsilon) + \frac{2h_{T_n}}{n} \sum_j T^j(0) + O(\epsilon^2) A; \quad (5.84)$$

where we used that the central charge of this model is  $c = 1$ . Putting the pieces together, we get

$$f_S^{i@;1}(\epsilon) \sim 1 + \frac{2h_V}{n^2} \sum_j h_{i@}; \dots; 0; j T^j(0) \langle j_{i@}; \dots; 0; i \psi_0; \dots; 0; j T^j(0) \rangle_{j_0; \dots; 0; i}; \quad (5.85)$$

Using the dimension of the  $U(1)$  twist fields

$$h_V = h_{V=2} = \frac{1}{2} \frac{1}{2} = \frac{1}{4}; \quad (5.86)$$

and (see e.g. [167])

$$\sum_j \langle h_{i@} ; ; 0; \rangle_j T^j(0) \langle j_{i@} ; ; 0; \rangle_i h_{0; \dots; 0} T^j(0) \langle j_{0; \dots; 0} \rangle = \frac{4}{L^2} m_{i@} ; \quad (5.87)$$

one finally obtains the desired result

$$f_S^{i@;1}(\cdot) \approx 1 - \frac{m_{i@}}{n^2} x^2 \quad (5.88)$$

As a consistency check, for  $m_{i@} = 1$ , Eq. (5.82) reduces to

$$f_n^{i@}(\cdot) \approx 1 - \frac{x^2}{n} \quad (5.89)$$

This simple result has an interesting physical meaning: in the small  $x$  regime, the contributions coming from each replica are decoupled (at order  $O(x^2)$ ), that is a consequence of the additivity of the stress-energy tensor. It also means that, while the partition  $S = (m_{i@}; n - m_{i@})$  was chosen for clarity, the same result is recovered for other partitions with  $m_{i@}$  insertion of the derivative operator (at the leading order  $O(x^2)$ ).

We now test how the CFT results in this subsection match with the numerical data for the XX chain. We start from  $f_{(1;n-1)}^{i@;1}(\cdot)$  in Eq. (5.81). In Fig. 5.4 we plot the CFT result of excess of variance

$$h \langle \sigma_{(1;1)}^{i@;1} \rangle - h \langle \sigma_{(1;2)}^{i@;1} \rangle = \frac{1}{(i)^2} \frac{d^2}{dx^2} \log f_{(1;1)}^{i@;1}(\cdot) \Big|_{x=0} = \frac{2}{L} \sin^2 \frac{x}{2}; \quad (5.90)$$

as a function of  $x = \ell/L$  against the numerics for different sizes ( $L = 100; 200; 400; 800$ ). The  $O(x^2)$  approximation is indistinguishable from the full result up to  $x \approx 0.3$ . As expected, the numerical data approach the prediction when  $x$  is kept fixed and  $L$  gets larger. The finite-size corrections are small for  $x$  close to 0, but they become rather large in the opposite regime  $x \rightarrow 1$ .

In Fig. 5.5 we plot  $f_{(1;n-1)}^{i@;1}(\cdot)$  for  $n = 2; 3$  (left/right panel respectively) as functions of fixed  $x$  and compare it with numerical data. We consider system sizes large enough so that the finite size-corrections of the excess of variance are negligible; in particular, as  $n$  increases a larger  $L$  is required to satisfy the latter requirement (as expected from the ground state results [183]). The numerical data give a function  $f_{(1;n-1)}^{i@;1}(\cdot)$  which is always smooth and periodic under  $x \rightarrow 1-x$ . Although we expect a singularity at  $x = 1/2$  from the analytical predictions of  $f_{(1;n-1)}^{i@;1}(\cdot)$ , the convergence of the numerics to this singularity is slow. This is the reason why in the neighborhood of  $x = 1/2$  numerics and CFT do not yet match well and much larger system sizes are required to reproduce correctly the singularity. A full and detailed explanation of these phenomena is given in Ref. [185]. We just notice that as  $x$  gets larger, the phenomenon is amplified, as shown in Fig. 5.4.

## 5.4 Symmetry resolution

In this section, we link the universal results that can be obtained by CFT to the symmetry resolved measures of indistinguishability we have introduced (relative entropies and distances). In principle, one just needs to put together many ingredients that have been characterized carefully in the previous section, a task that is technically cumbersome. While our original paper extensively analyzed the low-energy states of the compact boson, our current focus is primarily on the

Figure 5.4: Excess of variance associated to the partition  $S = (1; 1)$  of the operators  $(; ) = (i@ ; 1)$ . The universal CFT results are compared to the XX chain at half-filling. The numerical data for different sizes ( $L = 100; 200; 400; 800$ ) are compared with both the full CFT result (solid line) and the small  $x$  expansion at order  $O(x^2)$  (dashed line).

overall structure of the results in the thermodynamic limit (with large system size, denoted as  $L$ , and fixed  $\ell=L$ ), taking into account the most prominent corrections. We commence by examining the symmetry resolved relative entropy, and subsequently provide insights into certain aspects of the distances.

Given  $;$  the two RDM associated to the excited states  $;$ , we express their symmetry resolved relative entropy as [3]

$$S_n(k)(q) = S_n(k) + \frac{1}{1-n} \log \frac{p_{(1;n-1)}(q)}{p_n(q)} + \log \frac{p_1(q)}{p_1(q)} \quad (5.91)$$

As we have discussed already, in the thermodynamic limit, the ratio of probabilities tends to 1 (cf. Eq. (3.84)) leading relative entropy equipartition (5.53), i.e.  $S_n(k)(q) \sim S_n(k)$ . Starting from Eq. (5.91), we can systematically characterise the corrections to this asymptotic behaviour and identify the terms breaking the equipartition. The leading and physically most important corrections to equipartition comes from the orders  $O( )$  and  $O( ^2)$  of  $f_{(1;n-1)}( )$ . At this order, the generalised probabilities appearing in Eq. (5.91) are Gaussian<sup>3</sup>, but with different values of average charge and variance compared to the vacuum. We now compute the probability distributions appearing in Eq. (5.91) via Fourier transform of the corresponding charged moments. In particular, we express  $p_S^1( ) = p_n^1( ) f_S^1( )$ , for the partitions  $S = (1; n-1)$  of interest, and  $p^1( ) = p_n^1( ) f^1( )$ , so that the ground state contribution  $p_n^1( )$  is explicitly factorized out. At the leading order, we write  $p_n^1(q)$  as

$$p_n^1( ) \sim \exp \left( -\frac{2}{2} h q^2 i_n^1 \right); \quad p_n^1(q) \sim p \frac{1}{2 h q^2 i_n^1} \exp \left( -\frac{q^2}{2h q^2 i_n^1} \right); \quad (5.92)$$

where the ground state average charge has been set to  $Q_n^1 = 1$ . We recall that the (generalized) variances of the ground state diverge logarithmically in the system size, and from CFT [1]

<sup>3</sup>This leading Gaussian behaviour is a consequence of the  $\ell$ -dependence of the scaling dimension of the modified twist fields, which leads to a diverging variance in the continuum limit. Other cumulants are present, but they do not affect the leading behaviour

Figure 5.5: The universal functions  $f_{(1;1)}^{i@;1}(\cdot)$  and  $f_{(1;2)}^{i@;1}(\cdot)$  (left/right panels respectively) as functions of  $\ln L$  for different values of  $x$  ( $x = 1=10; 1=4; 1=2$ ). The agreement with numerical data for the XX chain at half-filling, is good for small  $L$  but it worsens as  $L$  gets closer to  $\infty$ , as discussed in the text.

one easily gets

$$h \ln q^2 i_n^1 = \frac{1}{2n} \log \frac{L}{L} \sin \frac{\pi}{L} + \ln n + o(1); \tag{5.93}$$

where the additive constant  $\ln n$  is not universal (but it is known [183] in the XX chain, used for the numerics). Also  $p_S^i(q)$  is Gaussian, and we write

$$p_S^i(\cdot) \sim \exp \left( i h q i_S^i - \frac{2}{2} h \ln q^2 i_S^i \right); \quad p_S^i(q) \sim \exp \left( \frac{1}{2 h \ln q^2 i_S^i} \exp \left( \frac{(q - h q i_S^i)^2}{2 h \ln q^2 i_S^i} \right) \right); \tag{5.94}$$

The average charge and variance of these distributions are read directly from the expansion of the universal functions  $f_S^i(\cdot)$

$$\log f_S^i(\cdot) = i a_S^i - \frac{2}{2} b_S^i + O(L^{-4}); \tag{5.95}$$

and so

$$h q i_S^i = a_S^i; \quad h \ln q^2 i_S^i = h \ln q^2 i_n^1 + b_S^i; \tag{5.96}$$

Obviously, the very same formulas remain valid if there is the insertion of a single operator in  $p_n(q)$  (which indeed correspond to  $S = (n; 0)$ ). Crucially, while the explicit values of these means and variances shifts ( $a_S^i$  and  $b_S^i$ ) clearly depend on the states and the ratio  $x = \frac{1}{L}$ , we know that they are universal (they are finite in the thermodynamic limit we are considering). This means that the dominant behavior is basically ruled by the ground state fluctuations. Thus, we express the symmetry resolved entropy as a formal expansion in the inverse of the ground state

variances and, after long but straightforward algebra, we eventually get

$$S_n(\mathcal{K})(q) = S_n(\mathcal{K}_0) + \frac{1}{2(1-n)h} \frac{1}{q^2 i_n^1} (q a_{(1;n-1)})^2 + \frac{1}{h} \frac{b_{(1;n-1)}}{q^2 i_n^1} A + (q a_n)^2 + \frac{1}{h} \frac{b_n}{q^2 i_n^1} A + \frac{1}{2h} \frac{1}{q^2 i_1^1} (q a_1)^2 + \frac{1}{h} \frac{b_1}{q^2 i_1^1} (q a_1)^2 + \dots \quad (5.97)$$

This shows that quite generally equipartition is broken at order  $(\log L)^{-1}$  (unless some fine-tuned cancellations take place), as the relative entropy  $S_n(\mathcal{K})$  is finite in the thermodynamic limit [159].

For the sake of completeness, we briefly review a result for the short expansion of the standard relative entropies [159] that is

$$S_1(\mathcal{K}) / (h_i - h_{i'})^2 \sim c + o\left(\frac{1}{L}\right)^2; \quad (5.98)$$

where  $c$  is the lightest quasi-primary satisfying  $h_i - h_{i'} \neq 0$ . The prefactor is a universal dimensionless number, that has been worked out explicitly for the case in which  $\mathcal{K}$  is a primary operator or the stress-energy tensor [159]. The expansion (5.98) shows explicitly universal features, as  $h_i - h_{i'} = L^{-1}$  (from scale invariance) and the relative entropy depends on  $L$  only. Furthermore, it is evident that the most significant observable  $\mathcal{K}$  effectively captures the distinction between the two states,  $\rho$  and  $\rho'$ , when considering a small subsystem size, a property that is ultimately related to the OPE expansion (of twist fields).

We now investigate the distances and their symmetry resolution. To do so, we have to characterise the following quantity

$$\text{tr}(\rho^{\otimes n_e} \rho'^{\otimes n_e}); \quad (5.99)$$

with  $n_e$  being an even integer and eventually analytically continue the result to any value of  $n_e$  [167, 186], in particular  $n_e = 1$  that is the most interesting value. In quantum field theory, it is custom to normalise the distances via the moments of the RDM of vacuum. In particular, it is convenient to define

$$D_n(\rho; \rho') = \frac{1}{2} \frac{\text{tr}(\rho^{\otimes n} \rho'^{\otimes n})}{\text{tr}(\rho^{\otimes n})}; \quad (5.100)$$

as it is universal in the thermodynamic limit. As discussed in Ref. [167] it might be hard to characterise  $\text{tr}(\rho^{\otimes n} \rho'^{\otimes n})$  analytically. However, in the small  $x = L^{-1}$  one gets [167] a simple expansion coming from the OPE

$$\frac{\text{tr}(\rho^{\otimes n} \rho'^{\otimes n})}{\text{tr}(\rho^{\otimes n})} = \sum_{i_1, \dots, i_n} b_{i_1, \dots, i_n} x^{1 + \sum_{j=1}^n (h_{i_j} - h_{i_j'})} \dots (h_{i_n} - h_{i_n'}); \quad (5.101)$$

In the presence of the flux, those techniques can be extended and shows the universality of the ratio  $\frac{\text{tr}(\rho^{\otimes n} e^{iQ})}{\text{tr}(\rho^{\otimes n} e^{iQ'})}$  in the thermodynamic limit. However, when the Fourier transform is taken and the symmetry resolution is performed, the 'universality' is somehow lost (as it happens for the relative entropies) and one needs to be careful.

In analogy with [167, 186], we first define

$$D_n^0(\rho; \sigma)(q) = \frac{1}{2} \frac{\text{tr}(\rho^q \sigma^{1-q})}{\text{tr}(\rho \sigma)}; \tag{5.102}$$

which differs from  $D_n^0(\rho; \sigma)(q)$  for an overall  $q$ -independent constant.  $D_n^0(\rho; \sigma)(q)$  satisfies the following sum-rule

$$\sum_q D_n^0(\rho; \sigma)(q) = D_n(\rho; \sigma) \tag{5.103}$$

analogous to Eq. (5.14). In the limit  $n \rightarrow 1$ , since the RDM is normalised as  $\text{tr}(\rho) = 1$ ,  $D_n^0(\rho; \sigma)(q)$  and  $D_n^0(\rho; \sigma)(q)$  become equal, but for  $n \neq 1$  this is not the case. The sum rule above has a simple consequence, that might be disappointing at first sight. For instance, since  $D_n(\rho; \sigma)$  is finite while the variance of  $q$  diverges in the thermodynamic limit, one has that  $D_n^0(\rho; \sigma)(q)$  is expected to vanish for any given  $q$ . In particular, in [3] we have showed that

$$D_n^0(\rho; \sigma)(q) \sim \frac{1}{2} \frac{1}{h} \frac{1}{q^{2i_n^1}} \exp\left(-\frac{q^2}{2h} \frac{1}{q^{2i_n^1}}\right) D_n(\rho; \sigma) + \frac{c_n}{2h} \frac{1}{q^{2i_n^1}} \left(1 + \frac{q^2}{h} \frac{1}{q^{2i_n^1}}\right); \tag{5.104}$$

with  $c_n$  being a universal number (related to the CFT predictions of the main text). This equation shows that, at leading order, the symmetry resolved distance  $D_n^0(\rho; \sigma)(q)$  is just given by the total distance  $D_n(\rho; \sigma)$  weighted with the (ground state) probability distribution  $p_n^1(q)$ . Beyond the leading order, one can investigate systematically the corrections, expressing  $D_n^0(\rho; \sigma)(q) = p_n^1(q)$  as a formal power series of  $\frac{1}{h} \frac{1}{q^{2i_n^1}}$   $1 = \log L$ .

## 5.5 Concluding remarks

We extended the measures of indistinguishability, such as the relative entropies and the Schatten distances, by employing the concept of symmetry resolution. Specifically, we introduced a natural definition using "projected" density matrices, inspired by the symmetry resolution of entanglement entropies explored in previous literature. Additionally, we established a formalism to systematically study the low-energy states of CFTs. By employing this framework, we derived analytical predictions for the universal ratio of charged moments in compact systems, which we validated through numerical testing in the XX chain.

It is necessary to include some general remarks, particularly in relation to Chapter 4. We demonstrated that various aspects of the low-lying states of CFTs are crucial for calculating entanglement measures. For instance, determining the explicit value of a multi-point correlation function is necessary for providing analytical predictions of the universal ratio of charged moments. This quantity heavily relies on the specific theory and states under consideration. In principle, it is also possible to analyze descendant states corresponding to higher energy excitations. Although the overall framework remains intact, dealing with descendant states becomes technically challenging due to the non-trivial transformation law of descendant [97]. Nonetheless, the OPE expansion of twist fields suggests that the energy of the states influences the behavior in small subsystem sizes.

In contrast, the findings presented in Chapter 4 emphasize the simplicity and generality of certain entanglement measures for a broad class of quasi-particle states. These measures do not explicitly depend on the energy of excitations or other specific state details. It remains unclear how the results from this chapter can be reconciled with those of Chapter 4. Nevertheless, it is

important to note that the CFT approach developed here focuses on low-energy states (with fixed EL in the thermodynamic limit) of CFTs, while the predictions from Chapter 4 are expected to be applicable to massless theories for excitations at a given energy  $E$  (fixed). In the future, we plan to revisit the problem and explore the possibility that a pure CFT approach, utilizing correlation functions of heavy states, could potentially yield results similar to those presented in Chapter 4.

### 5.A Correlation functions of primaries for the massless compact boson

In this appendix, following Ref. [1], we give a graphical representation of the correlation function

$$\langle V_{-1}(\tau_1) \dots V_k(\tau_k) (i\partial)(z_1) \dots (i\partial)(z_n) \rangle_C \tag{5.105}$$

evaluated in the ground state of a planar geometry. In the following we keep the Luttinger parameter  $K$  generic, but we do not superimpose explicitly the quantization conditions for the vertex operators, keeping their charge generic.

The starting point is the correlation function between chiral vertex operators

$$\langle V_{-1}(\tau_1) \dots V_k(\tau_k) \rangle_C = \prod_{i < j} (\tau_i - \tau_j)^{K^{-1} q_i q_j}; \tag{5.106}$$

valid for  $\sum_j q_j = 0$ , otherwise it vanishes. Hereafter, we suppose that the neutrality condition  $\sum_j q_j = 0$  is always satisfied. The derivative operator  $i\partial$  can be represented as follows

$$(i\partial)(z) = \lim_{\epsilon \rightarrow 0} \frac{1}{\epsilon} (\partial V)(z); \tag{5.107}$$

allowing us to write (5.105) as a number of derivatives of (5.106). The full expression that arises is quite involved (see [1] for some details), so we introduced diagrammatic rules to deal with it.

Diagrammatic rules (for the planar geometry  $C$ ):

- ^ The full correlation function is made by different terms containing different contractions.
- ^ The contraction between  $(i\partial)(z)$  and  $V(\tau)$  gives a factor  $\frac{K}{z}$ .
- ^ The contraction between  $V_i(\tau_i)$  and  $V_j(\tau_j)$  gives a factor  $(\tau_i - \tau_j)^{K^{-1} q_i q_j}$ .
- ^ The contraction between  $(i\partial)(z_i)$  and  $(i\partial)(z_j)$  gives a factor  $\frac{K}{(z_i - z_j)^2}$ .
- ^ Every  $(i\partial)(z_i)$  is contracted to just another operator.
- ^ Every  $V(\tau_j)$  is contracted to any other operator, keeping the previous constraint.

Fig. 5.6 reports all possible contractions for  $\langle V_{-1}(\tau_1) V_2(\tau_2) (i\partial)(z_1) (i\partial)(z_2) \rangle_C$ .

In the case of a cylindrical geometry of circumference  $L$ , it is enough to make the following replacement in Eq.(5.106)

$$(\tau_i - \tau_j)^{K^{-1} q_i q_j} \rightarrow \frac{L}{\sin \frac{(\tau_i - \tau_j)}{L}}; \tag{5.108}$$

Also, the results for  $K \neq 1$  can be obtained starting from  $K = 1$  and replacing

$$(\tau_i - \tau_j)^{K^{-1} q_i q_j} \rightarrow (\tau_i - \tau_j)^{q_i q_j}; \tag{5.109}$$

a simple fact that follows directly from Eq. (5.106).

Figure 5.6: This is a graphical representation for  $V_1(z_1)V_2(z_2)(i@)(z_1)(i@)(z_2)$ .

### 5.B Numerical methods for the XX chain

We consider the tight-binding 1D chain of free fermions described by the hamiltonian

$$H = \sum_j c_j^\dagger c_{j+1} + c_{j+1}^\dagger c_j - 2h \sum_j c_j^\dagger c_j \quad (5.110)$$

where  $c_j^\dagger; c_j$  are the creation/annihilation operators of spinless fermions at the site  $j$ . One can study either the Ramond(R) or the Neveu-Schwarz sectors, which correspond to periodic or antiperiodic boundary conditions respectively. By Jordan-Wigner transformation, this fermion model is mapped to the XX spin-chain.

The correlation matrix of a given state is defined as

$$C_{ij} = \text{tr}(c_i^\dagger c_j) \quad (5.111)$$

The restriction of  $C$  to a subsystem  $A$  is denoted by  $C_A$ , that is a  $|A| \times |A|$  matrix with  $|A|$  the number of sites in  $A$ . A quadratic hamiltonian like (5.110) admits a basis of gaussian eigenstates, whose RDM is also gaussian, i.e.

$$\rho_A = \text{tr}_B(\rho) / \exp\left(\sum_{ij} c_i^\dagger c_j\right) \quad (5.112)$$

and  $\rho$  is a  $|L| \times |L|$  matrix. By Wick theorem,  $\rho_A$  and  $C_A$  are related as [142, 187]

$$C_A = \frac{1}{e + 1} \quad (5.113)$$

The proportionality constant in (5.112) ensures that  $\text{tr}(\rho_A) = 1$  and it is given by  $\det(C_A)$ .

Given two gaussian states  $\rho_1; \rho_2$  also their product  $\rho = \rho_1 \rho_2$  is gaussian. In particular, the correlation matrix for the product is [188, 189]

$$C = C_1 \oplus C_2 - C_2 \frac{1}{C_1 C_2 + 2C_1 C_2} C_1 \quad (5.114)$$

We now focus on the  $U(1)$  symmetry associated to the number of lattice fermions, that is generated by  $Q = \sum_j c_j^\dagger c_j$ . Its full-counting statistics in a given state is

$$p(\lambda) = \text{tr}(e^{i\lambda Q}) \quad (5.115)$$

and for a gaussian state it can be expressed as a function of [51, 180, 182]

$$p(\lambda) = \det(Ce^{i\lambda} + (1 - C)) \quad (5.116)$$

Consequently, the average number of particles  $\langle Q_i \rangle$  and its variance  $\langle Q_i^2 \rangle$  are

$$\langle Q_i \rangle = \frac{1}{i} \frac{d}{d\epsilon} \log p(\epsilon) \Big|_{\epsilon=0} = \text{tr}(C); \quad (5.117)$$

$$\langle Q_i^2 \rangle = \frac{1}{(i)^2} \frac{d^2}{d\epsilon^2} \log p(\epsilon) \Big|_{\epsilon=0} = \text{tr}(C) + \text{tr}(C^2); \quad (5.118)$$

The formula expressed above are sufficient to compute efficiently the charged moments considered in the main text.

Part II

**Interfaces**



## Chapter 6

# Renyi entropy and negativity for free theories at conformal interfaces and junctions

We are examining the ground state of a quantum system composed of  $M$  wires connected through a junction, with the objective of understanding the entanglement between these wires. Our focus is on critical systems governed by conformal field theories (CFTs) featuring interface defects. We present analytical predictions specifically for massless free theories involving fermions and bosons. Our main goal is to establish a systematic approach for calculating the Renyi entropies for any division between the wires, as well as the entanglement negativity between two sets of wires that are not complementary. We have discovered that these measures of entanglement exhibit logarithmic growth with respect to the size of the wires, which extends the findings of Sakai and Satoh for a bosonic system consisting of two wires[55]. Crucially, the logarithmic prefactor is universal and depends on the scattering matrix that describes the defect: it is determined by the eigenvalues of a specific projection of the scattering matrix, which varies between bosons and fermions. This chapter is based on Refs. [8, 9]

### 6.1 CFT approach

In this section, we present a CFT approach to characterize the junction, that is employed in the evaluation of the entanglement measures. The method, which closely follows Refs. [55, 190, 191], does not require any explicit assumption of the underlying CFT. However, the explicit construction and the predictions for the entropy and the negativity will be given for complex free (Dirac) fermions and bosons only.

Let us consider  $M$  wires of length  $L$ , each of them described by a CFT denoted by

$$\text{CFT}_j; \quad j = 1; \dots; M: \tag{6.1}$$

These wires are coupled together at a single spatial point, and boundary conditions, encoding the details of the junction, have to be specified at that point. In Euclidean space-time, the junction geometry above is pictorially represented by a booklet (with each page corresponding to one CFT) bound along the imaginary axis at  $x = 0$ , see the left panel of Fig. 6.2.

Figure 6.1: The conformal junction:  $M$  wires are joined together at  $x = 0$  by a conformally invariant scattering matrix  $S$ . We consider a tripartition in three sets  $A; B; C$  with  $M_A; M_B; M_C$  wires each. The entanglement between  $A$  and  $B$  is given by the negativity. A bipartite configuration is simply obtained by letting  $M_C = 0$ .

For later convenience, we are going to work in the folded picture in which the system is represented as a single CFT

$$\text{M-CFT} = \text{CFT}_1 \times \dots \times \text{CFT}_M; \quad (6.2)$$

i.e. the world-sheet is a single infinite strip of width  $L$  where  $M$  copies of the CFT live. See the middle panel of Fig. 6.2 for a pictorial representation.

The joining between the distinct wires is specified by the boundary conditions along the lines

$$\text{Re}(w) = 0; \quad \text{Re}(w) = L; \quad (6.3)$$

that correspond to boundary states (see Ref. [97] for details about the correspondence) of M-CFT.

We require that the boundary condition at  $\text{Re}(w) = L$  decouples the replicas, and can be thus described by a boundary state  $|jB_i\rangle$  factorised as

$$|jB_i\rangle = |jB_{1i}\rangle \otimes \dots \otimes |jB_{Mi}\rangle; \quad (6.4)$$

with  $|jB_{ji}\rangle$  being a boundary state of  $\text{CFT}_j$ .

Instead, the boundary conditions at  $\text{Re}(w) = 0$ , describing the defect/junction, in general couple explicitly distinct wires. We denote by  $|jS_i\rangle$  the associated boundary state in M-CFT.

In the remainder of the manuscript, the precise details of the boundary state  $|jB_i\rangle$  appearing at  $\text{Re}(w) = L$  would not matter, and so we do not specify more about it. The physical motivation is that, as long as it decouples the wires, we do not expect that its features affect (at least at

Figure 6.2: The folding procedure. The junction in Euclidean spacetime is the booklet with the CFTs bound in  $x = 0$  (left panel). The folding consists in merging together the  $M$  CFTs in a worldsheet being a single infinite strip with an appropriate boundary state  $|j_S\rangle$  at  $x = 0$  (middle panel). To compute the entanglement, we cut the system for  $|j| < \epsilon$  and  $|j| > L - \epsilon$  (dashed lines) and map the  $M$ -CFT onto a rectangle of size  $\log \frac{L}{\epsilon}$  (right) with  $\text{Re}(z) \in [\log \epsilon; \log L]$  and  $\text{Im}(z) \in [-\frac{\pi}{2}; \frac{\pi}{2}]$ .

leading order) the correlation properties among distinct wires. In contrast, this is not the case for the boundary state  $|j_S\rangle$ , and for this reason we have to be careful about its characterisation, as the features  $|j_S\rangle$  rule the leading behavior of the entanglement measures.

We now describe a convenient conformal map, that eventually will be employed to express the entanglement measures as thermal partition functions (with proper boundary conditions along the thermal direction). We first regulate the theory through an ultraviolet and infrared cut-off, that is a standard procedure to extract the leading divergence of the entropy [59, 192, 195]: we 'cut' the space-time for  $|j| < \epsilon$  and  $|j| > L - \epsilon$  (see Fig. 6.2, middle panel), keeping only  $\epsilon < |j| < L - \epsilon$ . In principle, this procedure gives a different boundary field theory, and, to make the theory well-defined, boundary conditions should be specified at  $|j| = \epsilon; L - \epsilon$  (see [195]). However, these issues do not affect the leading behavior of the entanglement measures, and we do not discuss them further.

The cut strip can then be mapped into a rectangle by the conformal transformation

$$z = \log w; \quad (6.5)$$

The semicircles  $|j| = \epsilon$  and  $|j| = L - \epsilon$  are mapped respectively onto the segments

$$z \in [\log \epsilon + i\frac{\pi}{2}; \log \epsilon + i\frac{\pi}{2}]; \quad z \in [\log L - i\frac{\pi}{2}; \log L - i\frac{\pi}{2}]; \quad (6.6)$$

The line at  $\text{Re}(w) = 0$ , describing the defect, is mapped onto the two lines  $\text{Im}(z) = \pm \frac{\pi}{2}$ . The resulting geometry is thus another strip of spatial length  $\log \frac{L}{\epsilon}$  and inverse temperature  $\beta = \frac{2\pi}{\log \frac{L}{\epsilon}}$ , as shown in the right panel of Fig. 6.2.

The partition function can be written as

$$Z = \langle \text{tr} S_j \exp(-H) |j_S\rangle; \quad (6.7)$$

where  $\beta$  is the height of the rectangle (see Fig. 6.2), while the hamiltonian is (up to the Casimir energy which does not play any role in our discussion)

$$H = \frac{2}{\log \frac{L}{\epsilon}} (L_0 + \bar{L}_0); \quad (6.8)$$

with  $L_0; \bar{L}_0$  being generators of the Virasoro algebra of  $\text{CFT} \equiv \text{CFT}_M$ . In the limit  $L \rightarrow \infty$ , one expects [190] that the free-energy, i.e. the logarithm of the partition function  $Z$ , is extensive

$$\log Z / \log \frac{L}{\pi}; \tag{6.9}$$

with a prefactor carrying information about the boundary conditions in the time-like direction ( $\text{Im}(z) = \tau = 2$ ).

So far, everything is general and no assumption on the bulk theory or the boundary state  $|j\rangle_{\text{Si}}$  has been made yet. Small variations of the method presented so far allow to compute the entanglement measures we are interested in, that requires the replica trick and the insertion of an additional branch-cut [46, 60]. While the general picture applies for both boson and fermions, some technical differences are present, and we prefer to analyse them separately. We do it in the following sections, giving predictions for the Renyi entropies and the Renyi negativity.

## 6.2 Free Fermions

### 6.2.1 Boundary states

Here, we first review the construction of boundary states for a theory of many species of massless Majorana fermions [190, 196], and then we discuss the straightforward generalisation to Dirac fermions, obtained through a doubling of the degrees of freedom [97].

We consider the CFT given by  $M$  copies of the Majorana free fermionic theory. This CFT has central charge  $c = M=2$ , and it is described in terms of the left/right chiral fermionic fields denoted by

$$\psi_j; \quad \bar{\psi}_j; \quad j = 1; \dots; M; \tag{6.10}$$

We focus on the Neveu-Schwarz (NS) sector [97], and we decompose the fermionic fields in their Laurent modes<sup>1</sup>

$$\psi_j(z) = \sum_{k \in \mathbb{Z} + 1/2} \frac{\psi_k^j}{z^{k+1/2}}; \quad \bar{\psi}_j(z) = \sum_{k \in \mathbb{Z} + 1/2} \frac{\bar{\psi}_k^j}{z^{k+1/2}}; \tag{6.11}$$

Within this convention, the creation/annihilation operators of a fermion of the  $j$ -th species in the mode  $k$  ( $k > 0$ ) are  $\psi_k^j$ . The number  $k$  is (proportional to) the momentum of the particle. More precisely, one can show that the commutation relations between the fermionic fields and the Virasoro operators  $L_0; \bar{L}_0$  are

$$[L_0; \psi_k^j] = k \psi_k^j; \quad [\bar{L}_0; \bar{\psi}_k^j] = k \bar{\psi}_k^j; \tag{6.12}$$

A family of boundary states, each one associated with a (boundary) scattering matrix  $S$  and labeled by  $|j\rangle_{\text{Si}}$ , is characterized by the following consistency condition

$$\psi_k^j + i S_{jj} \psi_k^0 |j\rangle_{\text{Si}} = 0; \tag{6.13}$$

where, hereafter, repeated indices are summed over. As shown in [197, 198], the  $M \times M$  matrix  $S$  has to be orthogonal in order to represent a physical boundary state<sup>2</sup>, namely

$$S^2 = O(M); \tag{6.14}$$

<sup>1</sup>In the Ramond sector,  $k$  would be integer and the discussion would be slightly more involved due to the presence of a zero mode  $\psi_k = 0$ .

<sup>2</sup>This requirement comes from the absence of flows of energy/momentum across the boundary (see Ref. [97] for details).

In particular, any possible momentum-dependence of the scattering matrix is ruled out by scale invariance. The solution for  $|jSi\rangle$  of Eq. (6.13) is simply

$$|jSi\rangle = \prod_{k=2N-1}^Y \exp(iS_{jj} \int_0^j \psi_k^\dagger \psi_k) |j0i\rangle; \tag{6.15}$$

with  $|j0i\rangle$  being the vacuum of the theory. Thus, we interpret  $|jSi\rangle$  as a coherent state constructed as linear combination of many multiparticle-excitations above the vacuum.

Notice that the different values of  $k$  are decoupled, a fact that will simplify the forthcoming computations. Nevertheless, in general, different species of particles, expressed by the index  $j$ , are coupled, due to the possible occurrence of non-diagonal terms in the matrix  $S$ . Those terms represent physically the amplitudes of transmission between different wires and cause the entanglement among them.

We now consider a theory of  $M$  free Dirac fermions (having central charge  $c = M$ ), for which the associated fields are

$$\psi_j; \quad \psi_j^\dagger; \quad \bar{\psi}_j; \quad \bar{\psi}_j^\dagger; \quad j = 1; \dots; M; \tag{6.16}$$

where  $\psi$  and  $\psi^\dagger$  represent the particles/antiparticles respectively. This theory is equivalent to a theory with  $2M$  Majorana fermions, and so the previous derivation is valid also in this case. The number of degrees of freedom is doubled and one should take an orthogonal real  $2M \times 2M$  scattering matrix  $S \in O(2M)$ . However, we are interested in boundary conditions which preserve the global  $U(1)$  symmetry

$$\psi_j^\dagger = e^{i\theta} \psi_j; \quad \bar{\psi}_j = e^{-i\theta} \bar{\psi}_j; \tag{6.17}$$

that is ultimately related to the conservation of the number of particles in the corresponding microscopic realization of the theory. This means that  $S$  has to satisfy some additional requirements. In particular,  $U(1)$  symmetry implies that a left/right-moving particle can be produced from the vacuum (through the boundary state) together with its right/left antiparticle only. In the end, with a slight abuse of notation, we parametrize the  $U(1)$  symmetric boundary states via complex unitary  $M \times M$  matrix

$$S \in U(M); \tag{6.18}$$

that constrains the corresponding boundary state  $|jSi\rangle$  as

$$\psi_k^j + iS_{jj} \int_0^j \bar{\psi}_k^\dagger \psi_k = 0; \quad \bar{\psi}_k^j + i\bar{S}_{jj} \int_0^j \psi_k^\dagger \psi_k = 0; \tag{6.19}$$

with  $\bar{S}$  being the matrix complex conjugated to  $S$ . The solution of such constraint is

$$|jSi\rangle = \prod_{k=2N-1}^Y \exp(iS_{jj} \int_0^j \psi_k^\dagger \bar{\psi}_k^\dagger + (\dots) \psi_k) |j0i\rangle; \tag{6.20}$$

and it shows the explicit absence of pair-production amplitudes of two particles with the same charge.

### 6.2.2 Renyi entropies

We describe how to compute the  $n$ -th Renyi entropy of a subset made up of  $M_A$  wires via the replica trick. In the path integral approach [46, 60], the (ground state) Renyi entropy of

integer order  $n$  can be obtained as a path-integral over an  $n$ -sheeted Riemann surface  $R_n$ , with a branch-cut along the subsystem  $A$  connecting the  $i$ -th and the  $(i + 1)$ -th sheet [60]. More precisely, the moments of the reduced density matrices can be then written in terms of a ratio of partition functions as

$$\text{Tr}(\rho_A^n) = \frac{Z_n}{Z_1^n}; \tag{6.21}$$

where  $Z_n$  is the partition function of  $R_n$ , while  $Z_1^n$  is just the partition function of a single replica raised to the  $n$ -th power. For free Dirac fermion, the partition function  $Z_n$  can be further factorised using the replica diagonalisation as, e.g., shown in [76]. Within this method, the replicated partition function  $Z_n$  is expressed as the product of  $n$  single-replica  $U(1)$  charged partition functions  $Z_1(\alpha)$ , where a flux  $e^{i\alpha}$  is inserted along the branch-cut. In this way  $Z_n$  can be rewritten as

$$Z_n = \prod_{p=1}^{n-1} Z_1(\alpha_p) = \frac{2\pi}{n}; \tag{6.22}$$

The partition function  $Z_1(\alpha)$  is, up to an irrelevant normalization factor (that vanishes in the ratio (6.21)), the ground-state expectation value of the  $U(1)$  generator restricted to  $A$ , denoted by  $Q_A$ , say

$$Z_1(\alpha) = \langle \psi | e^{iQ_A} | \psi \rangle; \tag{6.23}$$

In Ref. [76] the factorisation above is derived by writing  $Z_n$  as a fermionic Gaussian integral, therefore it strongly relies on the 'Gaussian properties' of the ground-state. The same considerations can be applied in our case of interest, that is the conformal junction, as the boundary condition we are considering leads to a ground state that is Gaussian. Technically, the latter property is related to the explicit expression of the boundary state  $| \psi \rangle$  in Eq. (6.20), that is Gaussian too (and it obtained as an exponential of a bilinear of fermion applied to the vacuum).

We employ these ideas to compute the charged partition  $Z_1(\alpha)$  in the junction geometry. In particular, after the conformal transformation  $z = \log w$ , we identify the expectation value of the symmetry operator over the finite-size geometry as a charged thermal partition function as follows

$$Z_1(\alpha) = \langle \psi | e^{iQ_A} q^{L_0 + \bar{L}_0} | \psi \rangle; \tag{6.24}$$

Here, the modular parameter  $q$  is defined as

$$q = \exp\left(-\frac{2\pi^2}{\log(L)}\right); \tag{6.25}$$

We are interested in the subsystem  $A$  given by the first  $M_A$  species of fermions, corresponding to the first  $M_A$  wires, while the complement  $B$  is made by the remaining  $M_B = M - M_A$  species. Therefore, it is convenient to split the set of indices  $j = 1, \dots, M_A + M_B$ , associated to all the species, in the following two subsets

$$a = 1, \dots, M_A; \quad b = 1, \dots, M_B \tag{6.26}$$

to shorthand the species of  $A$  and  $B$  respectively. In this way, the charge operator  $Q_A$  is just

$$Q_A = \sum_{k=1}^{M_A} \psi_k^\dagger \psi_k + \sum_{k=1}^{M_B} \psi_k^\dagger \psi_k \quad (\text{!}); \tag{6.27}$$

where the summation over the index  $\alpha$  is understood. Similarly, it is convenient to decompose  $S$  in a block form as

$$S = \begin{pmatrix} S_{AA} & S_{AB} \\ S_{BA} & S_{BB} \end{pmatrix}; \quad (6.28)$$

with  $S_{AA}$  being a  $M_A \times M_A$  matrix,  $S_{AB}$  a  $M_A \times M_B$  matrix, and so on.

Our goal then becomes the computation of

$$Z_1(\eta) = \prod_{k=1}^N \int \prod_{j=0}^{\infty} \exp \left[ i(S^Y)_{jj} \eta^{-j} \eta^{j^0} + (S^Y)_{jk} \eta^{L_0+L_0} e^{iQ_A} \exp \left[ iS_{jj} \eta^j \eta^{-j^0} + (S^Y)_{jk} \eta^{j^0} \right] \right]; \quad (6.29)$$

in the limit  $q \rightarrow 1$ , corresponding to  $\frac{1}{q} \rightarrow 1$ . We consider the contribution to the partition function (6.29) coming from the single Laurent mode, which requires the evaluation of

$$\int \prod_{j=0}^{\infty} \exp \left[ i(S^Y)_{jj} \eta^{-j} \eta^{j^0} + (S^Y)_{jk} \eta^{L_0+L_0} e^{iQ_A} \exp \left[ iS_{jj} \eta^j \eta^{-j^0} + (S^Y)_{jk} \eta^{j^0} \right] \right]; \quad (6.30)$$

The commutation relations among  $q^{L_0+L_0} e^{iQ_A}$  and the fermionic fields are

$$\begin{aligned} q^{L_0+L_0} e^{iQ_A} \psi_k^a &= e^{-i} q^k \psi_k^a q^{L_0+L_0} e^{iQ_A}; \\ q^{L_0+L_0} e^{iQ_A} \psi_k^b &= q^k \psi_k^b q^{L_0+L_0} e^{iQ_A}; \\ q^{L_0+L_0} e^{iQ_A} \psi_k^a &= e^i q^k \psi_k^a q^{L_0+L_0} e^{iQ_A}; \\ q^{L_0+L_0} e^{iQ_A} \psi_k^b &= q^k \psi_k^b q^{L_0+L_0} e^{iQ_A}; \end{aligned} \quad (6.31)$$

and they can be easily derived from the momentum/charge of the Laurent modes. Using the neutrality of the vacuum and its vanishing energy, namely  $q^{L_0+L_0} e^{iQ_A} |j\rangle = |j\rangle$ , together with the commutation relations (6.31), we get

$$\begin{aligned} & \int \prod_{j=0}^{\infty} \exp \left[ i(S^Y)_{jj} \eta^{-j} \eta^{j^0} + (S^Y)_{jk} \eta^{L_0+L_0} e^{iQ_A} \exp \left[ iS_{jj} \eta^j \eta^{-j^0} + (S^Y)_{jk} \eta^{j^0} \right] \right] |j\rangle = \\ & \int \prod_{j=0}^{\infty} \exp \left[ i(S^Y)_{jj} \eta^{-j} \eta^{j^0} + (S^Y)_{jk} \eta^{L_0+L_0} e^{iQ_A} \exp \left[ iS_{jj} \eta^j \eta^{-j^0} + (S^Y)_{jk} \eta^{j^0} \right] \right] |j\rangle = \\ & \exp \left[ iq^{2k} S_{aa^0} \psi_k^a \psi_k^{-a^0} + iq^{2k} S_{bb^0} \psi_k^b \psi_k^{-b^0} + ie^{-i} q^{2k} S_{ab^0} \psi_k^a \psi_k^{-b^0} + ie^i q^{2k} S_{ba^0} \psi_k^b \psi_k^{-a^0} \right] |j\rangle; \end{aligned} \quad (6.32)$$

The last expression can be evaluated (see Eq. 6.A in the Appendix), and we get

$$\int \prod_{j=0}^{\infty} \exp \left[ i(S^Y)_{jj} \eta^{-j} \eta^{j^0} + (S^Y)_{jk} \eta^{L_0+L_0} e^{iQ_A} \exp \left[ iS_{jj} \eta^j \eta^{-j^0} + (S^Y)_{jk} \eta^{j^0} \right] \right] |j\rangle = \det \begin{pmatrix} 1 & 0 \\ 0 & 1 \end{pmatrix} + q^{2k} \begin{pmatrix} S_{AA}^Y & S_{BA}^Y \\ S_{AB}^Y & S_{BB}^Y \end{pmatrix} e^i \begin{pmatrix} S_{AA} \\ S_{BA} \end{pmatrix} e^{-i} \begin{pmatrix} S_{AB} \\ S_{BB} \end{pmatrix}; \quad (6.33)$$

Using the unitarity of  $S$ ,  $SS^Y = S^Y S = 1$ , one can show that (see Appendix 6.B),

$$\det \begin{pmatrix} 1 & 0 \\ 0 & 1 \end{pmatrix} + q^{2k} \begin{pmatrix} S_{AA}^Y & S_{BA}^Y \\ S_{AB}^Y & S_{BB}^Y \end{pmatrix} e^i \begin{pmatrix} S_{AA} \\ S_{BA} \end{pmatrix} e^{-i} \begin{pmatrix} S_{AB} \\ S_{BB} \end{pmatrix} = \det \left[ 1 + 2(S_{AA}^Y S_{AA} + (S_{AA}^Y S_{AA}) \cos \eta) q^{2k} + q^{4k} \right]; \quad (6.34)$$

where the proportionality constant is an unimportant  $q$ -independent prefactor (see the appendix). Putting all the pieces together and taking into account the contribution coming from exchanging  $S_{AA}^y$ , we find the analytic expression of the  $U(1)$  charged partition function in Eq. (6.29)

$$Z_1(q) = \prod_{k=2N-1}^Y \det \left( 1 + 2(S_{AA}^y S_{AA} + (1 - S_{AA}^y S_{AA}) \cos \theta) q^{2k} + q^{4k} \right)^2; \quad (6.35)$$

According to Eq. (6.22), the  $n$ -sheeted partition function  $Z_n$  can be written formally as

$$Z_n = \prod_{p=\frac{n-1}{2}}^{\frac{n-1}{2}} Z_1(\theta = 2p\pi) = \prod_{p=\frac{n-1}{2}}^{\frac{n-1}{2}} \prod_{k=2N-1}^Y \det \left( 1 + 2(S_{AA}^y S_{AA} + (1 - S_{AA}^y S_{AA}) \cos(2p\pi)) q^{2k} + q^{4k} \right)^2; \quad (6.36)$$

which is the main result of this section, and we discuss it below.

From Eq. (6.36) it is clear that in the presence of several wires belonging to  $\mathcal{A}$ ,  $M_A = 1$ , there are  $M_A$  factorised contributions depending on the eigenvalues of  $1 - S_{AA}^y S_{AA}$  and coming from the presence of the determinant of a  $M_A \times M_A$  matrix. In other words, if we define

$$Z_{n;T_a} = \prod_{p=\frac{n-1}{2}}^{\frac{n-1}{2}} \prod_{k=2N-1}^Y \left( 1 + 2((1 - T_a) + T_a \cos(2p\pi)) q^{2k} + q^{4k} \right)^2; \quad (6.37)$$

as the contribution coming from the generic eigenvalue  $T_a \in \text{Spec}(1 - S_{AA}^y S_{AA})$ , one has

$$Z_n = \prod_{a=1}^{M_A} Z_{n;T_a}; \quad (6.38)$$

$T_a$  can be somehow interpreted as 'generalized effective' transmission probability<sup>3</sup>. Plugging this relation in the definition of the Renyi entropy, one gets

$$S_n(A) = \frac{1}{n} \sum_{a=1}^{M_A} S_{n;T_a}; \quad (6.39)$$

with

$$S_{n;T_a} = \frac{1}{n} \log \frac{Z_{n;T_a}}{Z_{1;T_a}^n} \quad (6.40)$$

being the Renyi entropy associated to each  $T_a$ . For the sake of completeness, we provide the explicit result for the partition functions and for the entanglement entropies in the relevant limit  $\frac{L}{\epsilon} \gg 1$ . Since the total entropy is just given by the sum of  $M_A$  independent contributions with

<sup>3</sup>For  $M = 2$  and  $M_A = 1$ , the only eigenvalue  $T_a$  is precisely the transmission probability across the interface. In the other cases, the analogy is only handwaving (and this is the reason of the sloppy term 'generalized effective') as the relation between the entries of  $S_A$  and its eigenvalues is not simple.

effective transmission,  $T_a$  it is sufficient to write only one term (for a given value of  $T_A$ ). For convenience, we also define a parameter  $^0$ , being a function of  $T_a$  and the effective transmission  $T_a$ , satisfying

$$2 \cos ^0 = 2(1 - T_a + T_a \cos \theta): \quad (6.41)$$

The infinite product appearing in Eq. (6.35) which gives the U(1) partition function is explicitly evaluated in Appendix 6.C, obtaining

$$\frac{Z_1(\theta)}{Z_1(0)} = \frac{3 \frac{0}{2}; q}{3(0; q)}: \quad (6.42)$$

In the limit  $q \rightarrow 1$ , the leading term of the partition function gives

$$\log \frac{Z_1(\theta)}{Z_1(0)} \sim \frac{1}{\log q} \left[ \text{Li}_2(e^{i^0}) + \text{Li}_2(e^{-i^0}) - 2\text{Li}_2(1) \right] = \frac{0}{2} \log \frac{L}{\pi}; \quad (6.43)$$

with  $^0$  given by (6.41). Summing over then values of the flux  $\theta$ , one gets straightforwardly the n-th Rényi entropy plugging Eq. (6.43) into Eq. (6.22). After some long but simple algebra, the final result is

$$S_{n; T_a} = \frac{0}{2(n-1)} \sum_{p=1}^{n-1} \arcsin^2 \left( \frac{p}{T_a} \cos \frac{(2p-1)\theta}{2n} \right) \log \frac{L}{\pi}; \quad (6.44)$$

which matches the one in Ref. [199]. We stress that the major advance in this section, compared to the existing literature [196, 199] has been to understand how the elements  $S_{AA}$  combine (via the eigenvalues of  $(1 - S_{AA}^y S_{AA})$ ) to give the entanglement entropy of more than one wire, while previous studies focused on a single one. For instance, Ref. [196] proposed a conjecture for the value of the entropy of many wires, that has been ruled out in our work<sup>4</sup>.

### 6.2.3 Rényi negativities

In this section, we apply the CFT formalism to the calculation of the negativity between two subsets of wires of a conformal junction. In particular, we consider here the partial time-reversal negativity (often just called fermionic negativity), which is a more suitable entanglement measure for fermionic systems (see [119, 120, 200, 206]). We provide a general set up for any number of wires, giving explicit results only for  $M = 3$  wires. We proceed via the evaluation of the Rényi negativity for even  $n = n_e$ , and then we will perform the replica limit  $n_e \rightarrow 1$ .

We consider the conformal junction of Fig. 6.1 with the subsystems A, B, and C formed by three sets of wires. We are interested in the fermionic negativity between A and B, which requires specify a notion of partial time-reversal transformation of the reduced density matrix [119] that slightly differ wrt the one usually employed for bosons or spin-system: in this section we will always refer to these 'fermionic' definitions.

<sup>4</sup>In their concluding remarks, Ref.[196] proposed an extension of their research, suggesting that the outcomes when multiple wires are present can be derived by considering the single wire case and identifying a total transmission probability  $T$ . This probability is obtained by summing the squared entries of  $S_{AA}$ . However, upon closer examination, this conjecture is found to be inconsistent with our findings, at least in the general case.

The replica approach to the negativity [207, 208] starts from the computation of the moments of the partial transpose reduced density matrix that can be written in terms of a ratio of partition functions as

$$\text{Tr}(\rho_{AB}^T)^n = \frac{Z_n}{Z_1^n} \tag{6.45}$$

Here  $Z_n$  is a partition function in a  $n$ -sheeted Riemann surface built in such a way to implement the partial time reversal transposition in the subsystem  $B$  (see Refs. [207, 208] for more details on the partial transpose and [119, 120] for the fermion case). The negativity is finally obtained as [207, 208]

$$E = \lim_{n_e \rightarrow 1} \frac{1}{n_e!} \text{Tr}(\rho_{AB}^T)^{n_e}; \tag{6.46}$$

i.e. by taking the analytic continuation from the even sequence of replicas  $n = n_e$ . For free fermions,  $Z_n$  can be further factorised, using the replica diagonalisation, due to the Gaussian properties of the transposed RDM  $\rho_{AB}^T$ . In this way, it becomes the product of  $n$  single-replica  $U(1)$  charged partition functions, similarly to what has been done for the Renyi entropy in the previous section.

Let us focus on even  $n = n_e$ , which is the only necessary object to compute the negativity. The needed charged partition  $Z_1(\theta)$  has twisting phases equal to  $\theta e^{i\phi}$  in  $A$  and  $e^{i(\phi - \theta)}$  in  $B$ , i.e. it reads [119, 202]

$$Z_1(\theta) = \langle \text{Tr} [ e^{iQ_A} e^{i(\phi - \theta)Q_B} \rho ] \rangle; \tag{6.47}$$

The operator  $e^{iQ_A}$  implements a flux  $e^{i\phi}$  over  $A$ , while  $e^{i(\phi - \theta)Q_B}$  inverts the flux ( $-\theta$ ) and it introduces an additional phase  $-\theta$  along  $B$ , which is the combined net effect of the partial transpose operation on fermionic systems. The final result of this approach is that the  $n_e$ -th Renyi negativity can be computed as

$$E_{n_e} = \frac{1}{n_e} \log \text{Tr} [\rho_{AB}^T]^{n_e} = \log \text{Tr} (\rho_{AB}^T)^{n_e} = \frac{n_e - 1}{2} \log \frac{Z_1(\theta = 2\pi/n_e)}{Z_1(0)}. \tag{6.48}$$

So far the discussion is general, and it refers to any free fermionic system with  $U(1)$  symmetry. We now express the  $U(1)$  charged partition function in the junction geometry and, in analogy with the previous section, we get

$$Z_1(\theta) = \langle \text{Tr} [ q^{L_0 + L_0} e^{iQ_A} e^{i(\phi - \theta)Q_B} \rho ] \rangle = \sum_{\mathbf{y}} \langle \text{Tr} [ \exp(i(S^y)_{jj_0}^{-j} y_k^{j_0} + (\theta - \phi) y) q^{L_0 + L_0} e^{iQ_A} e^{i(\phi - \theta)Q_B} \exp(iS_{jj_0} y_k^j - j_0^0) + (\theta - \phi) y] \rho ] \rangle; \tag{6.49}$$

To proceed for the calculation we restrict to the following specific situation:

- $M_A; M_B; M_C = 1$ , so that the total number of wires is  $M = 3$ .
- $S$  is not only unitary but also Hermitian, which means that  $S^2 = 1$  and its eigenvalues can be just  $\pm 1$ . For some physical systems (including the Schrodinger junction [199]), the hermiticity of the  $S$  matrix is a necessary condition for physical consistency. Hence, this is not at all a very restrictive assumption.

With these working assumptions, it is possible to obtain nice analytic results in a rather compact form. It is clear from Eq. (6.49) that the key object to be evaluated is

$$\langle 0 | \exp \left( i \sum_{j,k} S_{jj} \psi_k^{\dagger} \psi_k \right) q^{L_0 + \bar{L}_0} e^{i Q_A} e^{i Q_B} \exp \left( i \sum_{j,k} S_{jj} \psi_k^{\dagger} \psi_k \right) | 0 \rangle = \det \begin{pmatrix} 1 + q^{2k} S_{AA} & e^{i2} S_{AB} & e^{i} S_{AC} \\ e^{i2} S_{BA} & S_{BB} & e^{i} S_{BC} \\ e^{i} S_{CA} & e^{i} S_{CB} & S_{CC} \end{pmatrix}; \quad (6.50)$$

where we used the commutation relations between  $q^{L_0 + \bar{L}_0} e^{i Q_A} e^{i Q_B}$  and the fields (see Eq. (6.31)), and the formulas in Appendix 6.A, which provides the vacuum expectation value. The determinant of the  $3 \times 3$  matrix appearing in (6.50) can be evaluated directly, and the working assumption  $S^y = S$  simplifies its expression, as we see below. We first define the matrix  $O$  as

$$O = S \begin{pmatrix} S_{AA} & e^{i2} S_{AB} & e^{i} S_{AC} \\ e^{i2} S_{BA} & S_{BB} & e^{i} S_{BC} \\ e^{i} S_{CA} & e^{i} S_{CB} & S_{CC} \end{pmatrix}; \quad (6.51)$$

and we verify the following properties:

- $O$  is unitary ( $OO^y = 1$ ) and its eigenvalues are phases;
- $\det(O) = 1$  and the product of the eigenvalues is 1;
- $O = SO^yS$  and the spectrum of  $O$  is thus invariant under complex conjugation, a feature that relies on our hermiticity assumption  $S = S^y$ .

These properties imply that the spectrum of  $O$  has to take this form

$$\text{Spec}(O) = \{1; e^{i\alpha^0}; e^{-i\alpha^0}\}; \quad (6.52)$$

with  $\alpha^0$  a real parameter. After straightforward linear algebra, we can finally rewrite the determinant in Eq. (6.50) as

$$\det(1 + q^{2k}O) = (1 + q^{2k})(1 + 2 \cos \alpha^0 q^{2k} + q^{4k}); \quad (6.53)$$

and the explicit expression of  $\alpha^0$  as a function of the  $S$  matrix is

$$2 \cos \alpha^0 = 1 + S_{AA}^2 + S_{BB}^2 + S_{CC}^2 + (1 - S_{CC}^2 + S_{BB}^2 + S_{AA}^2) \cos(2\theta) + 2(S_{BB}^2 - S_{AA}^2) \cos \theta; \quad (6.54)$$

It is worth notice that  $\alpha^0$  depends on the matrix  $S$  only through its diagonal entries.

Putting all the pieces together, we express the partition function  $Z_1(\beta)$  as

$$Z_1(\beta) = \prod_{k=2N-1}^Y (1 + q^{2k})^2 (1 + 2 \cos \alpha^0 q^{2k} + q^{4k})^2; \quad (6.55)$$

We find the same formal structure of the partition function which appeared for the Renyi entropies in Eq. (6.35), up to the replacement  $0! \rightarrow \alpha^0$ . Analogously to Eq. (6.43), for  $L = 1$ , we have

$$\log \frac{Z_1(\beta)}{Z_1(0)}, \quad \frac{\alpha^0}{2} \log \frac{L}{\beta}; \quad (6.56)$$

with  $\lambda^0$  given by Eq. (6.54), which is the main result of this section. Indeed, by plugging this result into Eq. (6.48), we obtain the Renyi negativities

$$E_{n_e} = \frac{1}{4} \frac{(n_e - 1)^2}{2} \arccos^2 S_{CC}^2 + (1 - S_{CC}^2 + S_{BB}^2 + S_{AA}^2) \cos(2p = n_e)^2 + (S_{BB}^2 - S_{AA}^2) \cos(2p = n_e) \log \frac{L}{\pi} ; \quad (6.57)$$

We provide few simple consistency checks in some limits. If the wire  $C$  is decoupled from the other two, then  $S_{CC}^2 = 1$  and the transmission probability between A and B is  $1 - S_{AA}^2 = 1 - S_{BB}^2$ . In that case

$$2 \cos \lambda^0 = 2 S_{AA}^2 - 2(1 - S_{AA}^2) \cos(2) ; \quad (6.58)$$

This value of  $\lambda^0$  is the same one would obtain for  $\lambda^0$  in the  $U(1)$  partition function of A and B in the presence of a flux  $e^{i2}$  inserted along A. The reason is that in this limit the system becomes invariant under the  $U(1)$  symmetry generated by  $Q_A + Q_B$  and, thanks to

$$e^{iQ_A} e^{i(Q_B)} = e^{i(Q_B + Q_A)} e^{i(2)Q_A} ; \quad (6.59)$$

one recognises an equivalence with the insertion  $e^{i(2)Q_A}$ .

Finally, we consider  $n_e = 2$  because it corresponds to the evaluation of the 2-Renyi negativity (indeed, from Eq. (6.48),  $E_2 = \log \hat{Z}_1(\lambda = 2) \hat{Z}_1(\lambda = 2) = \hat{Z}_1^2(0) = 2 \log \hat{Z}_1(\lambda = 2) = \hat{Z}_1(0)$ ). In this case,

$$2 \cos \lambda^0 = 2 S_{CC}^2 ; \quad (6.60)$$

and there is no explicit dependence on  $S_{AA}^2 ; S_{BB}^2$ . Now this parameter is the same  $\lambda^0$  one would get in the presence of a flux  $e^{i2}$  along C only. In this way, we reproduced the general identity [207]

$$\text{Tr} \left( \frac{T_B}{AB} \right)^2 = \text{Tr} \left( \frac{T_A}{AB} \right)^2 ; \quad (6.61)$$

which is the well known relation between the 2-Renyi negativity and the 2-Renyi entropy.

We conclude this section with the analytic continuation  $n_e \rightarrow 1$ , that provides the negativity  $E$ . The idea is simple, and it relies mostly on an integral representation of the charged partition function  $\hat{Z}_1(\lambda)$ . In particular, the strategy is:

- Using the identities of Appendix 6.C, the  $U(1)$  partition function  $\hat{Z}_1(\lambda)$  in Eq. (6.56) can be expressed through an integral representation in the limit  $q \rightarrow 1$

$$\log \frac{\hat{Z}_1(\lambda)}{\hat{Z}_1(0)} = \sum_{k=2N-1}^{\infty} 2 \log[(1 + q^{2k})^{-2} (1 + 2 \cos \lambda q^{2k} + q^{4k})] , \quad \frac{1}{\log q} \int_0^1 \frac{dt}{t} [\log(1 + 2 \cos \lambda t + t^2) - 2 \log(1 + t^2)] ; \quad (6.62)$$

- The sum over the value of fluxes (6.57) can now be performed inside the integral. Through some simple trigonometric identities, this leads to an analytic continuation of the integrand.
- The result is an integral, which represents our analytic continuation, and it is eventually evaluated numerically.

The final expression we get (see [8] for the details) is

$$E = \frac{\log(L)}{2} \int_0^1 \frac{dt}{t} \log \frac{((x_1 + \frac{c}{x_1})^{1/2} + (x_1 + \frac{c}{x_1})^{1/2})((x_2 + \frac{1}{x_2})^{1/2} + (x_2 + \frac{1}{x_2})^{1/2})}{(1+t)}, \quad (6.63)$$

where the variables  $a; b; c; x_1; x_2$ , which depend on  $t$  as well, are defined as

$$a = 1 + 2 S_{CC}^2 t + t^2; \quad b = 2(S_{BB}^2 - S_{AA}^2)t; \quad c = 2(S_{AA}^2 + S_{BB}^2 - S_{CC}^2 - 1)t; \quad (6.64)$$

$$x_1 = \frac{b + \sqrt{b^2 - 4ac}}{2}; \quad x_2 = \frac{b - \sqrt{b^2 - 4ac}}{2c}. \quad (6.65)$$

We finally mention that, in the remarkable limit  $S_{CC}^2 = 1$ , where the third wire is decoupled from the other two,  $E$  gives the 1/2-Renyi entropy (as  $\rho_{AB}$  is now a pure state, see Ref. [209]). In this case, we obtain

$$E = \frac{1}{2} \int_0^1 \frac{dt}{t} \log \left( 1 + \frac{2 \sqrt{1 - S_{AA}^2}}{1+t} \right) = \frac{1}{2} \arcsin \frac{\sqrt{1 - S_{AA}^2}}{1} = \arcsin \frac{\sqrt{1 - S_{AA}^2}}{1}; \quad (6.66)$$

a result that has been obtained already in Ref. [199].

## 6.3 Free Bosons

We consider the junction CFT of complex free boson, and we characterize the entanglement among the wires. As we will see, the salient features are shared with the Dirac fermions (considered in Sec. 6.2). Specifically, we examine a specific set of boundary conditions that rely on a single-particle scattering matrix, denoted as  $S$ . The entanglement of the ground state is ultimately expressed through functions of the matrix elements of  $S$ . We should note that the bosonic system discussed in this section is unrelated, in terms of bosonization, to the fermionic system of Sec. 6.2. As we demonstrate, the quantitative predictions for the Renyi entropies and negativities differ explicitly between the two systems.

### 6.3.1 Boundary states

In this section, we review the characterisation of the boundary states of a multispecies free complex boson, following [190, 196]. We emphasise that a complex bosonic system can be expressed as two copies of a real bosonic one, thus one can generalise the results available for real bosons via a doubling of the degrees of freedom. In particular, a theory made of  $M$  complex bosonic species has a total central charge

$$c = 2M; \quad (6.67)$$

since each real bosonic species carries a central charge  $c = 1$  [97]. We denote the left/right components of the  $j$ -th species of the field as

$$\phi_j^{\pm}(z); \quad j = 1; \dots; M; \quad (6.68)$$

and, similarly, for the antiparticle field  $\psi$  we use the following symbols

$$(\psi)^j(z); (\bar{\psi})^j(z); \quad j = 1; \dots; M; \quad (6.69)$$

Expanding the fields in their Laurent modes via radial quantisation [97], it is possible to extract the creation/annihilation operator. In fact, to each mode, parametrised by a natural number  $k \in \mathbb{N}$ ; we can associate an operator  $\alpha_k^j$ , which creates a left-moving particle of the  $j$ -th species, and an annihilation operator  $\beta_k^j$  that destroys it. For the sake of convenience, we normalise the Fourier modes so that their commutation relations are<sup>5</sup>

$$[\alpha_k^j; \beta_{k^0}^j] = \delta_{j,j^0} \delta_{k,k^0}; \quad k, k^0 > 0; \quad j, j^0 = 1; \dots; M; \quad (6.70)$$

The same construction applies for the right modes, and similarly to the left/right modes of the antiparticle field  $\bar{\psi}$ .

Particular emphasis needs to be placed on the zero-mode, that is  $k = 0$ . The zero-modes of the fields commute among each other

$$[\alpha_0^j; \beta_0^j] = 0; \quad j, j^0 = 1; \dots; M \quad (6.71)$$

as explained in [97], and with the other modes, thus they can be regarded as constants of motion. For the sake of simplicity, we will assume that

$$\alpha_0^j \beta_0^j = \beta_0^j \alpha_0^j = (\psi)_0^j \beta_0^j = (\bar{\psi})_0^j \alpha_0^j = 0; \quad (6.72)$$

which amounts to neglect the presence of the zero modes. This technical assumption does not spoil the leading behaviour of the entanglement measures we are interested in, and simplifies the calculations (see [190, 196] for further details about the zero modes contributions).

Let us proceed with the explicit construction of the boundary states, and we require that the global  $U(1)$  symmetry

$$j \rightarrow e^{i\theta} j; \quad (\psi)^j \rightarrow e^{-i\theta} (\psi)^j; \quad (6.73)$$

corresponding to the imbalance of particles and antiparticles (that is a symmetry in the bulk), is preserved. In analogy with the fermions, the set of Gaussian boundary conditions, compatible with the  $U(1)$  symmetry above, is parametrised by a unitary matrix  $S$  such that

$$S \in U(M); \quad (6.74)$$

and the associated boundary states  $|S\rangle$  satisfy

$$(\alpha_k^j - S_{ij} \beta_k^j) |S\rangle = (\beta_k^j - S_{ij} \alpha_k^j) |S\rangle = 0; \quad (6.75)$$

Here  $S$  is the matrix complex conjugated to  $S$  and the sum over  $j$  is implicit. A solution to the previous relation is provided by

$$|S\rangle = \prod_{k>0} \exp \left[ S_{jj^0} \alpha_k^j \beta_{k^0}^{j^0} + (\delta_{jj^0} - S_{jj^0}) \alpha_k^j \alpha_{k^0}^{j^0} \right]; \quad (6.76)$$

<sup>5</sup>This is rather common in the condensed matter community, but it slightly differs from the 'stringy' convention adopted [97].

### 6.3.2 Rényi entropies

We now consider a subset  $A$  of  $M_A = M$  wires, and we describe how to compute the Rényi entropies using the replica trick. As usual, the key objects are the moments of the reduced density matrix  $\rho_A$ , expressed by [46, 60]

$$\text{Tr}(\rho_A^n) = \frac{Z_n}{Z_1^n}; \tag{6.77}$$

with  $Z_n$  being a partition of the  $n$ -replicated theory with branch-cuts along  $A$  and  $Z_1$  the partition function of the single replica theory. To proceed with the calculations, we employ a relation between  $Z_n$  and a  $U(1)$ -charged single-replica partition function  $Z_1(\beta, \nu)$ , that is a property of free bosons. In particular, as shown in [143], we make use of the following factorisation

$$Z_n = \sum_{p=0}^{n-1} Z_1(\beta, \nu + \frac{2\pi p}{n}) \tag{6.78}$$

This is completely analogous to the replica diagonalisation considered for free fermions in Eq. (6.22): the only difference is given by the values of the flux we have to pick to reconstruct  $Z_n$ .

In our specific case, where  $A$  is given by a set of  $M_A$  wires, we express the charged partition function as

$$Z_1(\beta, \nu) = \langle \text{Tr} S_j e^{i Q_A} q^{L_0 + \bar{L}_0} \rangle_S; \tag{6.79}$$

in analogy with the fermions, where the modular parameter  $q$  is

$$q = \exp\left(\frac{2\pi^2}{\log(L)}\right); \tag{6.80}$$

We now proceed with the computation of  $Z_1(\beta, \nu)$  given by

$$Z_1(\beta, \nu) = \sum_{k>0} \langle \text{Tr} S_j \exp\left(-\beta \sum_{j=0}^{n-1} \left( \sum_k y_k^{j_0} + \left( \sum_k y_k \right) q^{L_0 + \bar{L}_0} e^{i Q_A} \right) \right) \exp\left(-\sum_{j=0}^{n-1} \left( \sum_k y_k^{-j_0} + \left( \sum_k y_k \right) \right) \right) \rangle_S; \tag{6.81}$$

Here  $L_0$  and  $\bar{L}_0$  act on the creation operators of  $\phi$  (or equivalently  $\psi$ ) as

$$[L_0, \phi_k^j] = k \phi_k^j; \quad [\bar{L}_0, \psi_k^j] = k \psi_k^j; \tag{6.82}$$

Then, we split the set of indices  $j = 1, \dots, M_A + M_B$ , associated to all the species, in the following two sets

$$a = 1, \dots, M_A; \quad b = 1, \dots, M_B \tag{6.83}$$

to shorthand the species of  $A$  and  $B$  respectively. This allows us to write explicitly the  $U(1)$  charge  $Q_A$ , representing the imbalance between particles and antiparticles in  $A$ , as

$$Q_A = \sum_{k>0} \left( \sum_a a_k \phi_k^a + \sum_b a_k \psi_k^b \right); \tag{6.84}$$

where the sum over  $a$  is implicit. As a consequence, it is possible to derive straightforwardly

$$\begin{aligned} q^{L_0+L_0} e^{iQ_A} y^a_k &= e^{-i} q^k y^a_k q^{L_0+L_0} e^{iQ_A}; \\ q^{L_0+L_0} e^{iQ_A} y^b_k &= q^k y^b_k q^{L_0+L_0} e^{iQ_A}; \\ q^{L_0+L_0} e^{iQ_A} a_k &= e^i q^k a_k q^{L_0+L_0} e^{iQ_A}; \\ q^{L_0+L_0} e^{iQ_A} b_k &= q^k b_k q^{L_0+L_0} e^{iQ_A}; \end{aligned} \tag{6.85}$$

We now focus on the contribution of a single bosonic mode of field  $\phi$ , namely we evaluate

$$\begin{aligned} \langle 0 | \exp(S^y)_{jj_0} \prod_k y_k^{-j} y_k^{j_0} q^{L_0+L_0} e^{iQ_A} \exp(S_{jj_0}) \prod_k y_k^j y_k^{-j_0} | 0 \rangle &= \\ \langle 0 | \exp(S^y)_{jj_0} \prod_k y_k^{-j} y_k^{j_0} & \\ \exp(q^{2k} S_{aa^0} y^a_k y^{-a^0}_k + q^{2k} S_{bb^0} y^b_k y^{-b^0}_k + e^{-i} q^{2k} S_{ab^0} y^a_k y^{-b^0}_k + e^i q^{2k} S_{ba^0} y^b_k y^{-a^0}_k) & | 0 \rangle; \end{aligned} \tag{6.86}$$

where the property  $q^{L_0+L_0} e^{iQ_A} | 0 \rangle = | 0 \rangle$  has been used. To further represent the expression above, we decompose  $S$  in a block form

$$S = \begin{pmatrix} S_{AA} & S_{AB} \\ S_{BA} & S_{BB} \end{pmatrix}; \tag{6.87}$$

and (see Appendix 6.A) we compute

$$\begin{aligned} \langle 0 | \exp(S^y)_{jj_0} \prod_k y_k^{-j} y_k^{j_0} q^{L_0+L_0} e^{iQ_A} \exp(S_{jj_0}) \prod_k y_k^j y_k^{-j_0} | 0 \rangle &= \\ \det^{-1} \begin{pmatrix} 1 & 0 \\ 0 & 1 \end{pmatrix} q^{2k} \begin{pmatrix} S_{AA}^y & S_{BA}^y \\ S_{AB}^y & S_{BB}^y \end{pmatrix} e^{-i} \begin{pmatrix} S_{AA} & S_{AB} \\ S_{BA} & S_{BB} \end{pmatrix} & : \end{aligned} \tag{6.88}$$

Thanks to the unitarity of  $S$ , one can show (see Appendix 6.B and Ref. [8] for similar calculations)

$$\begin{aligned} \det^{-1} \begin{pmatrix} 1 & 0 \\ 0 & 1 \end{pmatrix} q^{2k} \begin{pmatrix} S_{AA}^y & S_{BA}^y \\ S_{AB}^y & S_{BB}^y \end{pmatrix} e^{-i} \begin{pmatrix} S_{AA} & S_{AB} \\ S_{BA} & S_{BB} \end{pmatrix} & / \\ \det^{-1} \begin{pmatrix} 1 & 2(S_{AA}^y S_{AA} + (1 - S_{AA}^y S_{AA}) \cos \theta) \\ 1 & 2(S_{AA}^y S_{AA} + (1 - S_{AA}^y S_{AA}) \cos \theta) \end{pmatrix} q^{2k} + q^{4k} & ; \end{aligned} \tag{6.89}$$

up to an irrelevant  $\theta$ -independent proportionality constant. Combining the contributions coming from all the modes  $k$  of  $\phi$  and  $\psi$ , one arrives at the following closed expression for the charged partition function

$$Z_1(\theta) / \prod_{k>0} \det^{-2} \begin{pmatrix} 1 & 2(S_{AA}^y S_{AA} + (1 - S_{AA}^y S_{AA}) \cos \theta) \\ 1 & 2(S_{AA}^y S_{AA} + (1 - S_{AA}^y S_{AA}) \cos \theta) \end{pmatrix} q^{2k} + q^{4k} : \tag{6.90}$$

Summing over then values of the  $U(1)$  flux, we can finally write the  $n$ -sheeted partition function  $Z_n$  as

$$\begin{aligned} Z_n &= \sum_{p=0}^{n-1} Z_1(\theta = 2\pi p/n) / \\ & \sum_{p=0}^{n-1} \prod_{k>0} \det^{-2} \begin{pmatrix} 1 & 2(S_{AA}^y S_{AA} + (1 - S_{AA}^y S_{AA}) \cos(2\pi p/n)) \\ 1 & 2(S_{AA}^y S_{AA} + (1 - S_{AA}^y S_{AA}) \cos(2\pi p/n)) \end{pmatrix} q^{2k} + q^{4k} : \end{aligned} \tag{6.91}$$

As shown for fermions in Sec. 6.2, one easily realises that, whenever  $M_A = 1$ , the bosonic partition function  $Z_n$  can be written as a product of  $M_A$  factorised contributions corresponding to the eigenvalues of the  $M_A \times M_A$  matrix  $1 - S_{AA}^y S_{AA}$ .

Indeed, for each eigenvalue  $T_a \in \text{Spec}(1 - S_{AA}^y S_{AA})$  we introduce the following quantity

$$Z_{n;T_a} = \prod_{p=0}^{n-1} \det^{2-p} \left( (1 - T_a) + T_a \cos\left(\frac{2p\pi}{n}\right) \right) q^{2k} + q^{4k}; \quad (6.92)$$

so that  $Z_n$  can be written as

$$Z_n = \prod_{a=1}^{M_A} Z_{n;T_a}; \quad (6.93)$$

Plugging this relation into the definition of the Renyi entropy, we obtain

$$S_n(A) = \sum_{a=1}^{M_A} S_{n;T_a}; \quad S_{n;T_a} = \frac{1}{n} \log \frac{Z_{n;T_a}}{Z_{1;T_a}^n}; \quad (6.94)$$

where  $S_{n;T_a}$  is the contribution coming from the eigenvalue  $T_a$ .

We proceed further to get the leading term in the limit  $q \rightarrow 1$ , corresponding to  $L \rightarrow \infty$ . For future convenience, we define a parameter  $\theta$ , depending on  $T_a$ , as follows

$$\cos \theta = \frac{1 - T_a}{2(1 + T_a)}; \quad (6.95)$$

a relation which appeared already for fermions in Eq. (6.41). Using the results of the Appendix 6.C, we first express the product in Eq. (6.90) as a Theta function and we recast it as an interval (see [9] for details), and we finally obtain

$$\log \frac{Z_{1;T_a}(L)}{Z_{1;T_a}(0)} = \frac{\theta}{2} - \frac{\theta^2}{2} \log \frac{L}{\pi}; \quad L \in [0; 2\pi]; \quad (6.96)$$

valid in the limit  $L \rightarrow \infty$  which is the main result of this section. Making explicit the  $T_a$  dependence as

$$\theta = 2 \arcsin \sqrt{\frac{1 - T_a}{2}}; \quad (6.97)$$

we write down its corresponding contribution to the Renyi entropy as

$$S_{n;T_a} = \log \frac{L}{\pi} - \frac{1}{n} \sum_{p=0}^{n-1} \left[ 1 - \arcsin \sqrt{\frac{1 - T_a}{2}} \sin \frac{p\pi}{n} \right] - \frac{1}{n} \arcsin \sqrt{\frac{1 - T_a}{2}} \sin \frac{p\pi}{n} \frac{2^{\#}}{n}; \quad (6.98)$$

As a sanity check, we specialise this prediction to the case  $M = 2$ ,  $M_A = 1$ , and

$$S = \begin{pmatrix} 0 & 1 \\ 1 & 0 \end{pmatrix}; \quad (6.99)$$

which describes a completely transmissive interface between two wires. Here  $S_{AA} = 0$  is just a number and the only eigenvalue of  $1 - S_{AA}^y S_{AA}$  is thus

$$T_a = 1; \quad (6.100)$$

Inserting this value of  $T_a$  in (6.95) one finds  $\lim_{n \rightarrow 1} S_n(A) = \frac{1}{6} \log \frac{L}{\pi}$ . Putting all the pieces together we get

$$S_n(A) = \frac{1}{1-n} \sum_{p=0}^{n-1} \log \frac{Z_{1;T_a}(\frac{2\pi p}{n})}{Z_{1;T_a}(0)} + \log \frac{L}{\pi} \frac{1}{1-n} \sum_{p=0}^{n-1} \frac{p}{n} \frac{p}{n} = \frac{1}{6} \left( 1 + \frac{1}{n} \right) \log \frac{L}{\pi}; \quad (6.101)$$

For  $n \rightarrow 1$ , this is compatible with the general prediction available for a boundary CFT of central charge  $c = 2$  (i.e. the complex boson)

$$S_1(A) = \frac{1}{3} \log \frac{L}{\pi}; \quad (6.102)$$

Similarly, for a partially transmissive interface with scattering matrix

$$S = \begin{pmatrix} p & 1-T \\ 1-T & p \end{pmatrix}; \quad (6.103)$$

the only eigenvalue of  $1 - S_{AA}^y S_{AA}$  is precisely

$$T_a = T; \quad (6.104)$$

with  $T$  the parameter entering in the definition of the scattering matrix  $S$ . In this case, the Renyi entropy takes the following form

$$S_n(A) = \log \frac{L}{\pi} \frac{1}{1-n} \sum_{p=0}^{n-1} \left[ 1 - \arcsin \left( \frac{p}{T} \sin \frac{p}{n} \right) \right]^{2\frac{1}{n}}; \quad (6.105)$$

which gives back (6.101) once specialised to  $T = 1$ .

We mention that the result (6.105) already appeared in the literature [55] for the real boson (i.e. the prefactor of the logarithmic term is half of the one appearing in Eq. (6.105)), together with its analytical continuation for  $n \rightarrow 1$  which is not reported here.

### 6.3.3 Renyi negativities

The replica approach for the computation of the negativity [207, 208, 210], which eventually boils down to the characterization of single-replica charged partition functions, is closely related to the method described for fermions in Sec. 6.2. There is however an important conceptual difference, and, while here we consider the standard (bosonic) negativity, in Sec. 6.2 we employed its fermionic counterpart. This difference gives rise to a different expression of the charged partition function, and the key quantity we aim to compute is

$$\hat{Z}_1(\rho) = \langle e^{iQ_A} e^{-iQ_B} \rangle; \quad (6.106)$$

where the expectation value  $\langle \cdot \rangle$  refers to the ground-state of the junction. As we see, the discrepancy is the absence of the additional flux  $\pm 1$  over  $B$  that is present for fermions (see Eq. (6.47)). From  $\hat{Z}_1(\rho)$  one recovers the Renyi negativity  $E_n$  via replica diagonalization (see Ref. [9] for further details) as

$$E_n = \sum_{p=0}^{n-1} \log \frac{\hat{Z}_1(\frac{2\pi p}{n})}{\hat{Z}_1(0)}; \quad (6.107)$$

In our case, we focus on  $A$  being a set of wires and, after the conformal transformation (6.5) we express

$$\hat{Z}_1(\lambda) = \prod_{k>0} \int d\phi_k \exp \left( -\sum_{j=0}^{\infty} \left( S_{jj}^{-j} \phi_k^{j+1} + (\lambda - \mu) \phi_k^{j+1} \right) \right) \exp \left( \sum_{j=0}^{\infty} \left( S_{jj}^{-j} \phi_k^{j+1} + (\lambda - \mu) \phi_k^{j+1} \right) \right); \quad (6.108)$$

that we evaluate explicitly below. We evaluate the building block entering in our formula as

$$\int d\phi_k \exp \left( -\sum_{j=0}^{\infty} \left( S_{jj}^{-j} \phi_k^{j+1} + (\lambda - \mu) \phi_k^{j+1} \right) \right) \exp \left( \sum_{j=0}^{\infty} \left( S_{jj}^{-j} \phi_k^{j+1} + (\lambda - \mu) \phi_k^{j+1} \right) \right) = \frac{1}{\det \left( \begin{matrix} S_{AA} & e^{i2} S_{AB} & e^{i1} S_{AC} \\ e^{i2} S_{BA} & S_{BB} & e^{i1} S_{BC} \\ e^{i1} S_{CA} & e^{i1} S_{CB} & S_{CC} \end{matrix} \right)}; \quad (6.109)$$

a relation which can be shown through the formula (6.175), as done for the Rényi entropies.

So far, we did not specify explicitly the number of wires belonging to the bipartitions. To provide some compact analytical results, from now on we restrict to the following specific situations considered already for fermions

- $M_A = M_B = M_C = 1$ , so that the total number of wires is  $M = 3$  and we compute the negativity between two of them;
- $S$  is not only unitary but also Hermitian, which implies  $S^2 = 1$  and its eigenvalues can be just  $\pm 1$ .

After some algebraic manipulations, using the unitarity of  $S$  and taking the product over the Fourier modes, one can show that (see [8] for similar computations)

$$\hat{Z}_1(\lambda) / \prod_{k>0} (1 - 2 \cos \lambda q^{2k} + q^{4k})^{-2}; \quad (6.110)$$

up to an irrelevant  $\lambda$ -independent prefactor, with  $\lambda^0$  being a function of the  $S$ -matrix and the flux defined by

$$2 \cos \lambda^0 = 1 + S_{AA}^2 + S_{BB}^2 + S_{CC}^2 + (1 + S_{CC}^2 - S_{BB}^2 - S_{AA}^2) \cos(2\lambda) + 2(1 - S_{CC}^2) \cos \lambda; \quad (6.111)$$

We stress that the expression above for  $\lambda^0$ , valid for bosons, differs explicitly from the result of free fermions in Ref. [8], as a consequence of the different flux insertion in the corresponding charged partition functions.

The same formal structure of  $Z_1(\lambda)$ , appearing for the calculation of the Rényi entropy, is found for  $\hat{Z}_1(\lambda)$  (see Eq. (6.96)) up to the replacement  $\lambda^0 \rightarrow \lambda^0$ , and we get

$$\log \frac{\hat{Z}_1(\lambda)}{\hat{Z}_1(0)} = \frac{\lambda^0}{2} - \frac{\lambda^0}{2} \sum_{n=1}^{\infty} \log \frac{L}{n}; \quad 2 [0; 2]; \quad (6.112)$$

which already provides a prediction of the Rényi negativity  $E_n$

$$E_{n_e} = \sum_{p=0}^{n-1} \log \frac{\hat{Z}_1(2p=n)}{\hat{Z}_1(0)}; \quad (6.113)$$

for integer values of  $n$ . By plugging the results (6.111) for  $\lambda^0$  into Eq. (6.113), we finally obtain

$$E_n = \sum_{p=0}^{n-1} \frac{1}{4} \arccos^2 \left( 1 + S_{BB}^2 + S_{AA}^2 + (1 + S_{CC}^2 - S_{BB}^2 - S_{AA}^2) \cos(2p\pi/n) \right)^2 \\ + (1 - S_{CC}^2) \cos(2p\pi/n) \frac{1}{2} \arccos \left( 1 + S_{BB}^2 + S_{AA}^2 + (1 + S_{CC}^2 - S_{BB}^2 - S_{AA}^2) \cos(2p\pi/n) \right)^2 + (1 - S_{CC}^2) \cos(2p\pi/n) \log \frac{L}{\pi} \quad (6.114)$$

which is the main result of this subsection.

To conclude this part, we give some checks for the charged partition function  $Z_1(\lambda)$  in specific simple cases. For instance, let us assume that the third wire is decoupled from A and B, which implies

$$S_{CC}^2 = 1: \quad (6.115)$$

In this case A and B are coupled via a transmission probability

$$1 - S_{AA}^2 = 1 - S_{BB}^2; \quad (6.116)$$

and  $\lambda^0$  is given by

$$2 \cos \lambda^0 = 2 S_{AA}^2 + 2(1 - S_{AA}^2) \cos(2\lambda): \quad (6.117)$$

One recognises that this is the same value one would obtain for the parameter  $\theta$  in Eq. (6.95), once a flux  $e^{i2}$  is inserted along A in the U(1) partition function  $Z_1(\lambda)$  involving A and B only. Indeed, in this specific limit the theory becomes invariant under the symmetry generated by  $Q_A + Q_B$ , being C decoupled, and since

$$e^{iQ_A - iQ_B} = e^{i2Q_A - i(Q_A + Q_B)}; \quad (6.118)$$

the equivalence with the insertion of  $e^{i2Q_A}$  is manifest.

We now consider  $\lambda = \pi$ , whose value is related to the 2-nd Renyi negativity, and from (6.113) one gets

$$E_2 = \log Z_1(\pi): \quad (6.119)$$

In this case

$$2 \cos \lambda^0 = 2 S_{CC}^2 - 2(1 - S_{CC}^2); \quad (6.120)$$

which is the same value we would get for a charged partition function with the insertion of  $e^{iQ_C}$  only. This is expected since it follows from the more general identity

$$\text{Tr} \left( \left( \begin{smallmatrix} T_B \\ AB \end{smallmatrix} \right)^2 \right) = \text{Tr} \left( \left( \begin{smallmatrix} T_C \\ AB \end{smallmatrix} \right)^2 \right) = \text{Tr} \left( \left( \begin{smallmatrix} T_C \\ C \end{smallmatrix} \right)^2 \right); \quad (6.121)$$

which relates the 2-Renyi negativity to the 2-Renyi entropy.

Finally, we provide an expression for the logarithmic negativity by applying the replica limit  $n_e \rightarrow 1$  from the expression we got. To this goal, we use the same strategy employed for fermions in Sec. 6.2, and we summarize below the main finding (the details are found in [9]), that is

$$E = \frac{\log(L=\infty)}{2} \lim_{t \rightarrow 0} \frac{Z_1(t)}{t} \\ = \frac{\log \left( (x_1 - \frac{p}{x_1^2 - c^2})^{1=2} (x_1 + \frac{p}{x_1^2 - c^2})^{1=2} ((x_2 - \frac{p}{x_2^2 - 1})^{1=2} (x_2 + \frac{p}{x_2^2 - 1})^{1=2}) \right)}{2(1-t)}; \quad (6.122)$$

with  $a; b; c; x_1; x_2$  being

$$a = 1 + 2(1 - S_{AA}^2 - S_{BB}^2)t + t^2; \quad b = 2(S_{CC}^2 - 1)t; \quad c = 2(S_{AA}^2 + S_{BB}^2 - S_{CC}^2 - 1)t; \quad (6.123)$$

$$x_1 = \frac{b + \sqrt{b^2 - 4ac}}{2}; \quad x_2 = \frac{b - \sqrt{b^2 - 4ac}}{2c}. \quad (6.124)$$

## 6.4 Numerics for the fermions: Schroedinger junction

In this section, we describe a fermion gas on a star graph modelling a junction made up of  $M$  wires of length  $L$ , joined together through a single defect. This is employed as a microscopic model to test the CFT predictions numerically.

We consider a star graph like the one in Fig. 6.1, with  $M$  wires joined together at the vertex via a defect described by a scattering matrix. We take the laplacian on such graph, and we construct a Fermi sea with the first  $MN$  levels being occupied, following the procedure of Refs. [199, 211, 212]. The resulting many-body state hosts non-trivial quantum correlation, whose universal properties are described by the CFT of Dirac fermions (with a defect) in the limit  $N \rightarrow \infty$ , that we aim to characterize below.

We parametrize each point of the junction with a pair

$$(x; j); \quad x \in [0; L]; \quad j = 1; \dots; M; \quad (6.125)$$

where  $j$  is the index identifying the wire and  $x$  the spatial coordinate along the wire. The bulk hamiltonian of the Fermi gas is

$$H = \sum_{j=1}^M \int_0^L dx \frac{1}{2} \psi_j^\dagger(x) (-\partial_x^2) \psi_j(x); \quad (6.126)$$

with  $\psi_j; \psi_j^\dagger$  being the fermionic fields associated to the  $j$ -th wire (also called Schroedinger field, from which the name Schroedinger junction). To make this problem well-defined, it is essential to provide explicit boundary conditions<sup>6</sup> at  $x = 0$  and  $x = L$ , and this is where the defect appears. We consider a scale-invariant, say momentum independent, scattering matrix  $S_{jj'}$  at  $x = 0$

$$S_{jj'}; \quad j, j' = 1; \dots; M; \quad (6.127)$$

which has to be hermitian and unitary [199, 213]

$$S = S^\dagger; \quad S S^\dagger = 1; \quad (6.128)$$

$S$  describes the mixing among the wires, and, in terms of the fermionic fields, it expresses the boundary conditions

$$(1 - S) \psi(0) - i(1 + S) \psi^\dagger(0) = 0; \quad (6.129)$$

where  $\psi = \sum_{j=1}^M \psi_j$ , is an arbitrary real parameter with the dimension of mass. We also require the boundary conditions at  $x = L$  to be of the Dirichlet type, namely

$$\psi_j(L) = 0; \quad (6.130)$$

<sup>6</sup>More precisely, to make  $H$  self-adjoint, it is necessary to specify the boundary terms. Many choices are possible, and each boundary condition corresponds to a possible self-adjoint extension of the Laplace operator.

In order to simplify the treatment, it is possible to diagonalise  $S$  via a unitary transformation  $U$  and its eigenvalues are just  $\pm 1$ . In this way, a set of unphysical fields  $\psi_j(x)$  is introduced

$$\psi_i(x) = \sum_{j=1}^M U_{ij} \psi'_j(x); \quad (6.131)$$

whose boundary conditions at the defect are just Neumann/Dirichlet  $\psi'_j(0) = 0; \psi'_j(0) = 0$  depending on the corresponding eigenvalue  $\pm 1$  respectively); moreover, at  $x = L$  they satisfy  $\psi'_j(L) = 0$ . Hence, the unphysical fields  $\psi'_j(x)$  have either Neumann or Dirichlet bc (boundary conditions) at  $x = 0$  and Dirichlet bc's at  $x = L$ , so that it is natural to use the shorthand notation

$$ND \text{ Neumann-Dirichlet}; \quad DD \text{ Dirichlet-Dirichlet}; \quad (6.132)$$

to refer to the two possibilities. For these two possible boundary conditions, the single-particle wavefunctions are

$$\begin{aligned} \psi_n^{DD}(x) &= \sqrt{\frac{2}{L}} \sin \frac{n x}{L}; \quad n = 1; \dots \\ \psi_n^{ND}(x) &= \sqrt{\frac{2}{L}} \cos \frac{(n-1/2) x}{L}; \quad n = 1; \dots \end{aligned} \quad (6.133)$$

with  $x \in [0; L]$ . We now consider the ground state with  $N$  particles for each unphysical field  $\psi_j$ , so that the correlation function is

$$\langle \psi_j(x) \psi_j(x^0) \rangle = \delta_{jj^0} \begin{cases} C_{DD}(x; x^0); & DD \text{ bc's} \\ C_{ND}(x; x^0); & ND \text{ bc's;} \end{cases} \quad (6.134)$$

with

$$\begin{aligned} C_{DD}(x; x^0) &= \sum_{n=1}^N \psi_n^{DD}(x) \overline{\psi_n^{DD}(x^0)} = \frac{\sin \frac{N+1/2}{L} (x-x^0)}{2L \sin \frac{(x-x^0)}{2L}} \delta(x^0 < x) \\ C_{ND}(x; x^0) &= \sum_{n=1}^N \psi_n^{ND}(x) \overline{\psi_n^{ND}(x^0)} = \frac{\sin \frac{N}{L} (x-x^0)}{2L \sin \frac{(x-x^0)}{2L}} + \delta(x^0 < x) \end{aligned} \quad (6.135)$$

Going back to the physical fields  $\psi_j$ , linear algebra straightforwardly gives

$$C_{jj^0}(x; x^0) = \delta_{jj^0} \langle \psi_j(x) \psi_j(x^0) \rangle = \frac{1+S}{2} \delta_{jj^0} C_{ND}(x; x^0) + \frac{1-S}{2} \delta_{jj^0} C_{DD}(x; x^0); \quad (6.136)$$

Here, the matrices  $\frac{1 \pm S}{2}$  are the projectors over the eigenspaces  $\pm 1$  respectively.

The correlation functions (6.136) are continuous kernel of the spatial variables. While it is possible to work directly with such kernels (as done, e.g., in Refs. [214, 215]), it is more convenient to work with a finite-dimensional representation of such correlation. Hereafter, we set  $L = 1$  without loss of generality.

We start noticing that  $C_{jj^0}(x; x^0)$  can be thought as an operator acting on the Hilbert space  $C^M \otimes L^2([0; 1])$ , with  $C^M$  representing the space of the wires and  $L^2([0; 1])$  being the one of wave-functions on  $[0; 1]$ . Although  $L^2([0; 1])$  is an infinite-dimensional Hilbert space, both  $C_{ND}$

and  $C_{DD}$  are projectors acting non-trivially only in a finite-dimension subspace  $H_0$ . We can choose the following basis for  $H_0$

$$e_n = \begin{pmatrix} C_{DD}^{DD}(n; x); & 1 & n & N \\ C_{DD}^{ND}(n & N; x); & 1 + N & n & 2N; \end{pmatrix} \quad (6.137)$$

which is not orthonormal. Careful is needed to represent the projectors  $C_{ND}; C_{DD}$  onto the non-orthogonal basis above, that amounts to consider the dual basis  $e_n^*$  and to compute the matrix elements among the two basis. We only report the final results, while the details can be found in [8]. The projectors  $C_{ND}; C_{DD}$  are represented by the following  $2N \times 2N$  block matrix

$$C_{DD} = \begin{pmatrix} 1 & Q \\ 0 & 0 \end{pmatrix}; \quad C_{ND} = \begin{pmatrix} 0 & 0 \\ Q^y & 1 \end{pmatrix}; \quad (6.138)$$

with  $Q$  being a  $N \times N$  matrix

$$Q_{n;n^0} = \frac{2n}{(n^2 - (n^0 - 1)^2)}; \quad n; n^0 = 1; \dots; N; \quad (6.139)$$

Finally, we represent the correlation kernel  $C_{jj^0}(x; x^0)$  in Eq. (6.136) as a  $(2MN; 2MN)$  matrix acting on

$$C^M \otimes H_0; \quad C^M \otimes C^{2N}; \quad (6.140)$$

as follows

$$C = \frac{1}{2} \begin{pmatrix} S & 1 \\ 0 & 0 \end{pmatrix} + \frac{1+S}{2} \begin{pmatrix} 1 & Q \\ 0 & 0 \end{pmatrix} + \begin{pmatrix} 0 & 0 \\ Q^y & 1 \end{pmatrix}; \quad (6.141)$$

In this way, we first make explicitly that the non-vanishing spectrum of  $C$  is finite: this is not surprising as, since  $MN$  particles are present in the systems, we already know that  $C$  has to have only  $+1$  as non-trivial eigenvalue with multiplicity  $MN$  (simple algebra shows also that it is the case for the matrix in Eq. (6.141)). Furthermore, we discover that the projection of the kernel onto a subset of the wire exhibits a finite non-zero spectrum too. This characteristic is of utmost importance as it enables efficient numerical computation of entanglement among wires, as shown in the next sections.

#### 6.4.1 The Renyi entropy between two arbitrary sets of wires

A useful auxiliary quantity for the computation of the entanglement entropy and negativity is the matrix  $\Sigma = 1 - 2C$  (sometimes referred to as covariance matrix) of dimension  $2MN$ . We construct its restriction to an arbitrary set of  $M_A$  wire, and we denote it by  $\Sigma_{AA}$ , that is a  $(2M_A N; 2M_A N)$  matrix. This amounts to construct a linear map

$$\text{End}(C^M \otimes C^{2N}) \rightarrow \text{End}(C^{M_A} \otimes C^{2N}); \quad (6.142)$$

that is obtained by projecting the  $S$  matrix over  $A$ , and gives  $\Sigma_{AA}$ . Using that  $C_{ND}; C_{DD}$  are projectors (they square to themselves), it is not difficult to show that

$$\Sigma_{AA}^2 = (1 - S_{AA}^2) (C_{ND} \otimes C_{DD})^2; \quad (6.143)$$

with  $S_{AA}$  being a  $M_A \times M_A$  matrix. In the end, the entanglement contribution from the defect is eventually encoded in the projected  $S$ -matrix  $S_{AA}$ , that satisfies  $S_{AA}^2 = 1$  (and  $S_{AA} = S_{AA}^y$ ), but in general is not unitary, as the inequality is not always saturated.

Figure 6.3: The Renyi entropies  $S_n(A)$  in a four-wire junction where  $A$  is made up of two wires. We choose different values of  $s$ ;  $n$  and we plot it as a function of the number of particles  $N$ . The lines show the curve  $C_n(s) \log N + b_0 + b_1 N^{-1/n}$  where the coefficients  $b_i$  are fitted using the data for  $N \leq 80$ . The coefficients  $C_n(s)$  are obtained by summing over the single-wire results, as explained in Eq. (6.44)

Once the covariance matrix  $\chi_{AA}$  is known, the entanglement Renyi entropy between  $A$  and the complement is [187]

$$S_n(A) = \frac{1}{1-n} \text{Tr} \log \left( \frac{1 + \chi_{AA}}{2} \right)^n + \frac{1}{2} \chi_{AA}^{-n} = \sum_{T_a} S_{n;T_a}; \quad (6.144)$$

and it is easy to show that

$$S_n(A) = \sum_{T_a} S_{n;T_a}; \quad (6.145)$$

where the  $T_a$ 's are the eigenvalues of  $1 - S_{AA}^2$ , and  $S_{n;T_a}$  is the Renyi entropy of a single wire with transmission probability  $T_a$ . This analytic results for the microscopic model perfectly match Eq. (6.44) in CFT.

To conclude this subsection, we present a numerical test, obtained from the exact diagonalization of the matrix  $\chi_A$ , for the validity of the CFT result. In particular, we check that the prefactor of logarithmic scaling in the limit  $N \rightarrow 1$  is compatible with the analytical predictions. We mention that the case of  $A$  consisting of a single wire has been discussed and tested in Ref. [199], and here we focus on a four-wire junction with the subsystem  $A$  consisting of two wires. The  $S$  matrix is chosen of the form

$$S = U \begin{pmatrix} 0 & p \frac{1-s^2}{1+s^2} & 0 & 1 \\ s & p \frac{s}{1+s^2} & 0 & 0 \\ 0 & 0 & 1 & 0 \\ 0 & 0 & 0 & 1 \end{pmatrix} U^{-1}; \quad U = \begin{pmatrix} 0 & 1 & 0 & 0 \\ 0 & \cos & \cos \sin & \sin^2 \\ 0 & \sin & \cos^2 & \cos \sin \\ 0 & 0 & \sin & \cos \end{pmatrix} \begin{pmatrix} 1 \\ 0 \\ 0 \\ 1 \end{pmatrix} \quad (6.146)$$

The numerical results are reported in Fig. 6.3 finding a perfect agreement with CFT.

### 6.4.2 Entanglement negativity

We now consider a tripartition  $A [ B [ C$ , where  $A$  ( $B$ ) contains  $M_A$  ( $M_B$ ) wires, and we study the entanglement negativity between  $A$  and  $B$ . This amounts to project the scattering-matrix  $S$  over a subset of rows/columns belonging to  $A [ B$ . In particular, we denote

$$(C_{A[B})_{jj^0}(x; x^0) = \langle \psi_j(x) | \psi_{j^0}(x^0) \rangle; \quad j, j^0 = 1, \dots, M_A + M_B; \quad (6.147)$$

as the correlation function of  $A [ B$ , and

$$(S_{A[B})_{jj^0} = S_{j^0 j}; \quad j, j^0 = 1, \dots, M_A + M_B; \quad (6.148)$$

as the restriction of the scattering matrix;  $S_{A[B}$  is not unitary in general, and it satisfies the following relations

$$(S_{A[B})^y = (S_{A[B}); \quad 0 \leq y \leq 1; \quad (6.149)$$

Using the matrix representation of the correlation function  $C$  in Eq. (6.141) and restricting it to  $A [ B$ , we obtain a  $(2N(M_A + M_B); 2N(M_A + M_B))$  matrix  $C_{A[B}$ . The covariance matrix  $A_{A[B}$  has the natural block form

$$A_{A[B} = \begin{pmatrix} A_{AA} & A_{AB} \\ A_{BA} & A_{BB} \end{pmatrix}; \quad (6.150)$$

from which we construct the matrix [119, 203]

$$A_{A[B} = \frac{2}{1 + \frac{2}{A_{A[B}}} \begin{pmatrix} A_{AA} & 0 \\ 0 & A_{BB} \end{pmatrix}; \quad (6.151)$$

The latter matrix  $A_{A[B}$  is the crucial object to write the Renyi negativities  $E_{n_e}$  which indeed are [119]

$$E_{n_e} = -\log \text{Tr} (j_{A[B}^{n_e}) = \text{Tr} \log \left[ \frac{1 + \frac{A_{A[B}}{2}}{1 + \frac{A_{A[B}}{2}}^{n_e=2}} + \frac{1 - \frac{A_{A[B}}{2}}{1 + \frac{A_{A[B}}{2}}^{n_e=2}}}{2} \right] + \frac{n_e}{2} \text{Tr} \log \left[ \frac{1 + \frac{A_{A[B}}{2}}{1 + \frac{A_{A[B}}{2}}^{n_e=2}} + \frac{1 - \frac{A_{A[B}}{2}}{1 + \frac{A_{A[B}}{2}}^{n_e=2}}}{2} \right]; \quad (6.152)$$

The above equation is valid for arbitrary real  $n_e$  (i.e. also for a non-even integer) and so the negativity  $E$  is obtained just by taking  $n_e = 1$ .

Eq. (6.152) gives the Renyi negativities in terms of the correlation matrices that, once numerically evaluated, provides a test of the CFT results for the coefficient of the logarithm obtained in Section 6.2. For the numerical evaluation, we focus on a three-wire junction and on the two-parameter family of scattering matrices given by

$$S = U @ \begin{pmatrix} 0 & p \frac{1-s^2}{1+s^2} & 0 & 1 \\ s & p \frac{s}{1+s^2} & 0 & A U^{-1}; \\ 0 & 0 & 1 & 0 \end{pmatrix}; \quad U = @ \begin{pmatrix} 0 & 1 & 0 & 0 \\ 0 & \cos A & \sin A & 1 \\ 0 & \sin A & \cos A & 0 \end{pmatrix}; \quad (6.153)$$

We select as subsystems  $A$  and  $B$  the first two wires and compute numerically the Renyi negativity for several values of  $s$ ;  $p$ ; and  $N$ . In Fig. 6.4 we reported the coefficient of the

Figure 6.4: The coefficient of the logarithmic term of the negativity between two wires (A and B) as a function of  $\theta$ , with fixed  $s = 0.75$ . The solid line corresponds to Eq. (6.122) while the points have been obtained through a fit of the numerics with the form  $a \log N + b_0 + b_1 N^{-1}$ .

logarithm obtained as follows. We fixed  $s = 0.75$  and we selected some values of  $\theta$  for each value of  $(s; \theta)$ , we calculated numerically the negativity, for several values of  $N$  up to 200. We fitted the obtained numerical results with  $a \log N + b_0 + b_1 N^{-1}$ . Fig. 6.4 finally reports the best fit of  $a$  as a function of  $\theta$  and compares it to the corresponding analytic result, finding perfect agreement.

## 6.5 Numerics for the bosons: harmonic chain

In this section, we describe a lattice realisation of a junction made of  $M$  wires hosting bosonic degrees of freedom, employing standard techniques for Gaussian states [187]. These exact computations are then tested for the CFT predictions of the previous sections.

We start with a formulation of the problem in the continuous, that is analogous to the Schroedinger junction for the fermions. For instance, we consider a one-dimensional complex massless boson on the line  $[0, L]$  with Hamiltonian:

$$H = \sum_{j=1}^M \int_0^L dx \left( \frac{1}{2} \dot{\phi}_j(x)^2 + \frac{1}{2} \phi_j(x)^2 \right); \quad (6.154)$$

with  $\phi_j(x)$ ;  $\dot{\phi}_j(x)$  being the conjugated momentum associated to the bosonic fields  $\phi_j(x)$ ;  $\dot{\phi}_j(x)$  respectively. The boundary conditions at  $x = 0$  are described by a scattering matrix  $S$ , while at  $x = L$  we pick Dirichlet boundary conditions. This is completely equivalent to the Schroedinger junction, and we do not repeat all the details here.

For the sake of convenience, we decide to discretize the system, taking  $a = N^{-1}$ , where  $a$  is the lattice spacing (from now on, we set  $a = 1$ ) and  $N$  is integer, and discretizing the Laplace operator. The main reason behind this choice is that, strictly speaking, the entanglement entropy of the bosonic system is infinite in the continuous, and it diverges logarithmically in the number of sites when regularized on a lattice.

The ground-state correlation functions can be computed [9], and eventually one gets

$$\begin{aligned} X_{jj^0}(x; x^0) &= \langle \psi_j(x) \psi_{j^0}(x^0) \rangle = \frac{1+S}{2} X_{ND}(x; x^0) + \frac{1-S}{2} X_{DD}(x; x^0); \\ P_{jj^0}(x; x^0) &= \langle \psi_j(x) \psi_{j^0}(x^0) \rangle = \frac{1+S}{2} P_{ND}(x; x^0) + \frac{1-S}{2} P_{DD}(x; x^0); \end{aligned} \tag{6.155}$$

with  $x, x^0 = 1; \dots; N$ . Here, the kernels  $X_{ND=DD}; P_{ND=DD}$  are just

$$\begin{aligned} X_{DD=ND}(x; x^0) &= \frac{X^N}{2^N} \frac{DD=ND(x) DD=ND(x^0)}{k}; \\ P_{DD=ND}(x; x^0) &= \frac{X^N}{2^N} \frac{DD=ND(x) DD=ND(x^0)}{k}; \end{aligned} \tag{6.156}$$

where the single-particle eigenfunctions/eigenvalues read as (see [53, 208])

- Dirichlet-Dirichlet:  $\psi_k^{DD}(x) = \frac{1}{\sqrt{2}} \sin \frac{kx}{N+1}; \lambda_k^{DD} = 2 \sin \frac{k}{2N+2}$ ,
- Neumann-Dirichlet:  $\psi_k^{ND}(x) = \frac{1}{\sqrt{2}} \cos \frac{(k-1/2)x}{N+1/2}; \lambda_k^{ND} = 2 \sin \frac{(k-1/2)}{2N+1}$ .

In this way, the correlation functions appearing in Eq. (6.155) are just  $MN \times MN$  matrices, that can be directly employed to compute the entanglement measures as we explain in the next sections.

### 6.5.1 Renyi entropy

Let us now consider the Renyi entropy between the first  $M_A$  wires and the remaining  $M - M_A$  ones. It is convenient to introduce the matrices  $X_A$  and  $P_A$  of dimension  $(M_A N; M_A N)$  obtained from  $X; P$  in Eq. (6.155) by restricting  $j; j^0 = 1; \dots; M_A$ .

In terms of these matrices, the Renyi entropy of  $A$  is given by [143]

$$S_n(A) = \frac{2}{1-n} \text{Tr} \log \left( \frac{1}{2} X_A P_A + \frac{1}{2} \right)^n \left( \frac{1}{2} X_A P_A - \frac{1}{2} \right)^n; \tag{6.157}$$

We mention that the prefactor 2 is absent for real bosons, and it comes from the fact we are considering complex bosons (say, the degrees of freedom are doubled).

Recalling that  $S_{AA}$  is the projected S-matrix in the subsystem  $S$ , it is relevant to observe that

$$X_A P_A = \frac{1}{4} + \frac{1}{4} S_{AA}^2 (X_{DD} \ X_{ND})(P_{ND} \ P_{DD}); \tag{6.158}$$

which is a straightforward consequence of  $X_{ND} P_{ND} = X_{DD} P_{DD} = \frac{1}{4}$ . One can show that this property implies

$$S_n(A) = \sum_{T_a} S_{n; T_a}; \tag{6.159}$$

where  $T_a$  is an eigenvalue of  $1 - S_{AA}^2$ . Therefore, the total Renyi entropy can be decomposed as a sum of single-wire contributions, in agreement with the CFT result in Eq. (6.94).

Figure 6.5: The Renyi entropies  $S_n(A)$  of the bosonic junction for  $M = 4$   $M_A = 2$ . We choose different values of  $s$ ;  $\theta$  and we plot it as a function of the number of sites  $N$ . The lines show the curve  $C_n(s; \theta) \log N + b_0 + b_1 N^{-1-n}$  where the coefficients  $b_i$  are fitted using the data for  $N = 100$ .

We can use the machinery developed in this section to test the validity of the CFT result for the logarithmic scaling of the Renyi entropy. We consider the case  $M_A = M_B = 2$  and the  $S$  matrix is chosen of the form (we observe that the same choice has been done for the fermionic junctions in [8])

$$S = U \begin{pmatrix} 0 & p \frac{1-s^2}{s} & 0 & 1 \\ p \frac{s}{1-s^2} & 0 & 0 & 0 \\ 0 & 0 & 1 & 0 \\ 0 & 0 & 0 & 1 \end{pmatrix} U^{-1}; \quad U = \begin{pmatrix} 0 & 1 & 0 & 0 \\ 0 & \cos \theta & \cos \theta \sin \theta & \sin^2 \theta \\ 0 & \sin \theta & \cos^2 \theta & \cos \theta \sin \theta \\ 0 & 0 & \sin \theta & \cos \theta \end{pmatrix} \begin{pmatrix} 0 \\ 1 \\ 0 \\ 1 \end{pmatrix}. \quad (6.160)$$

The numerical results are reported in Fig. 6.5 finding a perfect agreement with the CFT result.

### 6.5.2 Entanglement negativity

We now consider a tripartition  $A [ B [ C$ , where  $A$  ( $B$ ) contains  $M_A$  ( $M_B$ ) wires, and we study the entanglement negativity between  $A$  and  $B$ . To achieve this goal, we have to consider the  $(M_A + M_B)N \times (M_A + M_B)N$  correlation matrices  $X_{A|B}; P_{A|B}$ . As explained in [208] one needs to construct the correlation matrices associated to the partial transposed reduced density matrix (see Ref. [208] for details). We recall that the partial transpose operation  $\text{tr}_A$  has the net effect of changing the sign of the momenta corresponding to the transposed subsystem. In other words, given the block decomposition

$$P_{A|B} = \begin{pmatrix} P_{AA} & P_{AB} \\ P_{BA} & P_{BB} \end{pmatrix} \quad (6.161)$$

the partial transposition along  $A$  produces the correlation matrix

$$P_{A|B} = \begin{pmatrix} P_{AA} & P_{AB} \\ P_{BA} & P_{BB} \end{pmatrix}; \quad (6.162)$$

Figure 6.6: The Renyi negativities  $E_n$  in the three-wire junction for different values of  $s$ ;  $\theta$  and as a function of number of particles  $N$ . The lines show the curve  $C_n(s; \theta) \log N + b_0 + b_1 N^{-1}$  where the coefficients  $b_i$  are fitted using the data for  $N \leq 80$ .

while  $X_{A|B}$  is kept untouched. Eventually, one expresses the  $n$ -th Renyi negativity between  $A$  and  $B$  as

$$E_n = -2 \text{Tr} \log \frac{\text{Tr} X_A P_A + 1}{2}^n - \frac{1}{n} \log \frac{\text{Tr} X_A P_A}{2}^n : \quad (6.163)$$

The replica limit is obtained by taking  $n \rightarrow 1$ , and it gives

$$E = -2 \text{Tr} \log \frac{\text{Tr} X_A P_A + 1}{2} - \log \frac{\text{Tr} X_A P_A}{2} : \quad (6.164)$$

Eq. (6.163) gives the Renyi negativities in terms of the correlation matrices that, once numerically evaluated, provides a test of the CFT results for the coefficient of the logarithmic growth. We test a three-wire junction with a two-parameter family of scattering matrices given by

$$S = U @ \begin{pmatrix} 0 & p \frac{1-s^2}{s} & 0 \\ p \frac{s}{1-s^2} & 0 & 0 \\ 0 & 0 & 1 \end{pmatrix} U^{-1}; \quad U = @ \begin{pmatrix} 0 & 1 & 0 \\ 0 & \cos \theta & \sin \theta \\ 0 & \sin \theta & \cos \theta \end{pmatrix} : \quad (6.165)$$

Here  $A$  and  $B$  are the first two wires, and we compute numerically the Renyi negativity for several values of  $s$ ;  $\theta$ ; and  $N$ . In Fig. 6.6 we benchmark the  $N$  dependence of the Renyi negativity and, in particular, the prefactor of the logarithmic term in Eq. (6.122) for different values of  $n$  (right panel) and for the replica limit  $n \rightarrow 1$  (left panel). In Fig. 6.7 we test the coefficient of the logarithm obtained fixing  $s = 0.75$  and varying  $\theta$ ; for each pair  $(s; \theta)$ , we calculate numerically the negativity, for several values of  $N$  up to 300. We use as fitting formula for the numerical results  $a \log N + b_0 + b_1 N^{-1}$ . Fig. 6.7 finally reports the best fit of  $a$  as a function of  $\theta$ , finding good agreement with the analytic continuation done in Eq. (6.122). The minor discrepancy close to  $\theta = 0.2$  (and to the symmetric point) is due to finite size corrections that for small, but non-vanishing,  $s$  are more relevant.

## 6.6 Concluding remarks

We have demonstrated that certain measures of entanglement (such as entropies and negativity) between wires in a critical junction exhibit a universal logarithmic divergence. The prefactor of

Figure 6.7: The coefficient of the logarithmic term of the negativity between two wires (A and B) as a function of  $\ell$ , with fixed  $s = 0.75$ . The solid line corresponds to Eq. (6.122) while the points have been obtained through a fit of the numerics with the form  $a \log N + b_0 + b_1 N^{-1}$ .

this divergence is predicted by CFT and can be computed for free theories. It is related to the eigenvalues of the projections of the scattering matrix that describes the defect.

While our method can be extended to other theories and measures of entanglement, it does have some notable limitations that we explicitly point out.

- ^ The UV/IR cutoff procedure, based on the work of [55], appears somewhat arbitrary. While it effectively captures the logarithmic divergences we focused on, it may not be suitable for characterizing universal finite effects, such as the Alicki-Ludwig g-function.
- ^ It is unlikely that the same method can be employed to analyze low-energy excitations or different regions, such as an interval within a single wire.

In a recent study [10], which addresses global quenches with a defect, we proposed an alternative approach that potentially resolves the aforementioned issues. Specifically, we highlighted the possibility of describing Rényi entropies using twist fields for junction geometries. The key aspect is that these fields possess a non-trivial boundary scaling dimension at the defect point, which strongly depends on the boundary scattering properties. We believe that utilizing a twist field approach could offer greater clarity on various aspects of entanglement compared to the method presented in this chapter. We intend to revisit this problem in future research.

## 6.A Expectation values of Gaussian operators

### 6.A.1 Fermionic case

We want to prove the following identity for the expectation value of Gaussian operators

$$\langle 0 | \exp \left[ \sum_{j,k} O_{jj}^0 \psi_k^j \psi_k^{j0} \right] \exp \left[ \sum_{j,k} O_{jj}^0 \psi_k^j \psi_k^{j0} \right] | 0 \rangle = \det \left[ 1 + O^0 \right] : \quad (6.166)$$

Here  $\psi_k^j$  is the creation/annihilation operator of a Majorana fermion in the  $k$ -th left mode of the  $j$ -th species (among the  $M$  ones), while  $\psi_k^{j0}$  is the corresponding right mover.  $O_{jj}^0$  and  $O_{jj}^0$  are  $M \times M$  matrices and the sum over  $j; j^0$  is implicit.

Before proving Eq. (6.166) in the most general case, we highlight simple cases in which it holds. Let us suppose there is just one species of fermions, so that we can suppress the indices and the matrices  $O$  and  $O^0$  become numbers. Using that the annihilation operators annihilate the vacuum, that the fermionic operators square to zero, and applying Wick theorem, one gets

$$\langle 0 | \exp O \exp O^0 | 0 \rangle = \langle 0 | (1 + O)(1 + O^0) | 0 \rangle = \langle 0 | 1 + O + O^0 + OO^0 | 0 \rangle = 1 + OO^0: \quad (6.167)$$

Similarly, when  $O$  and  $O^0$  commute, one can diagonalise them simultaneously and apply the previous consideration to show Eq. (6.166).

We provide a general proof of Eq. (6.166) using Gaussian integrals over Grassmann variables (whose basic properties can be found on [216]). We start by representing the Gaussian operators as integrals over Grassmann variables. In particular, for each  $j$ -th Dirac fermion field we associate a pair of Grassmann variables  $\psi_j, \psi_j^0$ , and we express the Gaussian operator  $\exp O_{jj^0} \psi_j \psi_j^0$  as follows

$$\exp O_{jj^0} \psi_j \psi_j^0 = \int d\psi_j d\psi_j^0 \exp (\psi_j + \psi_j^0 O_{jj^0} \psi_j^0 + \psi_j \psi_j^0); \quad (6.168)$$

where the sums over  $j$  and  $j^0$  are implicit. Similarly, we introduce a pair of Grassmann variables  $\psi_j, \psi_j^0$  to each species and we express  $\exp O_{jj^0}^0 \psi_j \psi_j^0$  as

$$\exp O_{jj^0}^0 \psi_j \psi_j^0 = \int d\psi_j d\psi_j^0 \exp (\psi_j + \psi_j^0 O_{jj^0}^0 \psi_j^0 + \psi_j \psi_j^0); \quad (6.169)$$

Using the previous relations, we write the product of the two Gaussian operators as follows

$$\begin{aligned} \langle 0 | \exp O_{jj^0}^0 \psi_j \psi_j^0 \exp O_{jj^0} \psi_j \psi_j^0 | 0 \rangle &= \int d\psi_j d\psi_j^0 d\psi_j d\psi_j^0 \exp (\psi_j + \psi_j^0 O_{jj^0}^0 \psi_j^0 + \psi_j \psi_j^0) \\ &\quad \exp (\psi_j + \psi_j^0 O_{jj^0} \psi_j^0 + \psi_j \psi_j^0) \\ \langle 0 | \exp \psi_j \psi_j^0 \exp \psi_j \psi_j^0 | 0 \rangle \langle 0 | \exp \psi_j^0 O_{jj^0}^0 \psi_j^0 \exp \psi_j O_{jj^0} \psi_j^0 | 0 \rangle &= \\ \int d\psi_j d\psi_j^0 d\psi_j d\psi_j^0 \exp (\psi_j + \psi_j^0 O_{jj^0}^0 \psi_j^0 + \psi_j \psi_j^0) & \quad \exp (\psi_j + \psi_j^0 O_{jj^0} \psi_j^0 + \psi_j \psi_j^0): \end{aligned} \quad (6.170)$$

The last step is the evaluation of the Gaussian integral over the  $4M$  Grassmann variables  $\psi_j, \psi_j^0, \psi_j, \psi_j^0$ . We introduce a  $4M$ -dimensional vector of Grassmann variables as follows

$$\Psi = \begin{pmatrix} \psi_j \\ \psi_j^0 \\ \psi_j \\ \psi_j^0 \end{pmatrix}; \quad (6.171)$$

and the Gaussian integral in (6.170) as

$$\langle 0 | \exp O_{jj^0}^0 \psi_j \psi_j^0 \exp O_{jj^0} \psi_j \psi_j^0 | 0 \rangle = \int d\Psi \exp \frac{1}{2} \Psi^T \Theta \Psi; \quad (6.172)$$

with  $\Theta$  being the following  $4M \times 4M$  matrix

$$\Theta = \begin{pmatrix} 0 & 0 & 0 & 1 \\ \begin{matrix} B \\ C \end{matrix} & 0 & 0 & 1 \\ \begin{matrix} A \\ 0 \end{matrix} & 1 & 1 & 0 \\ (OO^0)^T & 1 & 0 & 0 \end{pmatrix}; \quad (6.173)$$

The integral over  $\mathcal{O}$  in Eq. (6.172) gives the Pfaffian of the matrix  $\mathcal{G}$  [216], which we write as

$$\text{Pf } \mathcal{G} = \det^{1/2} \mathcal{G} = \det \begin{pmatrix} 1 & \mathcal{O} \mathcal{O}^0 \\ & 1 \end{pmatrix} = \det(1 + \mathcal{O} \mathcal{O}^0); \quad (6.174)$$

This completes the proof of Eq. (6.166), which is the main result of this section.

### 6.A.2 Bosonic case

Here we prove a useful identity valid for the vacuum expectation value of Gaussian operators

$$\langle 0 | \exp \left( \sum_{j,k} O_{jj}^0 a_j^\dagger a_k^\dagger \right) \exp \left( \sum_{j,k} O_{jj} a_j a_k \right) | 0 \rangle = \det \left( 1 - \mathcal{O} \mathcal{O}^0 \right)^{-1}; \quad (6.175)$$

We denote by  $a_k^\dagger$  the creation/annihilation operators associated to the  $k$ -th left mode of the  $j$ -th bosonic specie, and similarly we use the symbol  $a_k$  for the right modes. We consider  $\mathcal{O}$  and  $\mathcal{O}^0$  as two generic  $M \times M$  matrices, keeping implicit the sum over the indices  $j, k$  in Eq. (6.175). We assume further that  $\mathcal{O} \neq 0$ , so that the zero-mode of the boson does not appear here, and we use the following convention for the normalisation of the modes

$$[a_k, a_{k'}^\dagger] = [a_k, a_{k'}] = \delta_{kk'}; \quad k, k' > 0; \quad (6.176)$$

It is possible to highlight a simple case where (6.175) holds. For instance, we take a single bosonic specie ( $M = 1$ ), we suppress the index  $j$ , and then  $\mathcal{O}^0$  and  $\mathcal{O}$  are just numbers. Expanding the exponential as a power series in (6.175) we get

$$\langle 0 | \exp \left( \sum_k \mathcal{O}^0 a_k^\dagger a_k^\dagger \right) \exp \left( \sum_k \mathcal{O} a_k a_k \right) | 0 \rangle = \langle 0 | \sum_{n=0}^{\infty} \sum_{m=0}^{\infty} \frac{(\mathcal{O}^0)^n (\mathcal{O})^m}{n! m!} (\mathcal{O}^0)^n (\mathcal{O})^m (\mathcal{O}^0)^m (\mathcal{O})^n | 0 \rangle; \quad (6.177)$$

Via Wick theorem, one easily shows that

$$\langle 0 | (\mathcal{O}^0)^n (\mathcal{O})^m | 0 \rangle = \langle 0 | (\mathcal{O})^n (\mathcal{O}^0)^m | 0 \rangle = m! \delta_{m,n}; \quad (6.178)$$

Inserting this relation back into (6.177) one gets

$$\langle 0 | \exp \left( \sum_k \mathcal{O}^0 a_k^\dagger a_k^\dagger \right) \exp \left( \sum_k \mathcal{O} a_k a_k \right) | 0 \rangle = \sum_{n=0}^{\infty} (\mathcal{O} \mathcal{O}^0)^n = \frac{1}{1 - \mathcal{O} \mathcal{O}^0}; \quad (6.179)$$

which is compatible with the general case in Eq. (6.175). Clearly for  $M = 1$ , whenever the matrices  $\mathcal{O}$  and  $\mathcal{O}^0$  commute, one can diagonalise them simultaneously and apply the previous argument to show the validity of (6.175).

A general proof of (6.175) is given through Gaussian integrals over complex variables. We start from the basic property [216]

$$\int \frac{dz dz^*}{2\pi} \exp(-z z^*) = 1; \quad (6.180)$$

which is the building block of the foregoing relations. For each  $j$  we introduce a complex variable  $z_j$ , and we express the operator  $\exp \left( \sum_{j,k} O_{jj}^0 a_j^\dagger a_k^\dagger \right)$  as follows

$$\exp \left( \sum_{j,k} O_{jj}^0 a_j^\dagger a_k^\dagger \right) = \int \prod dz_j dz_j^* \exp \left( \sum_j z_j z_j^* + \sum_{j,k} O_{jj}^0 z_j^* z_k + \sum_{j,k} a_j^\dagger z_k \right); \quad (6.181)$$

with  $dzdz$  being a short-hand notation for the normalised measure

$$dzdz = \frac{dz_1 dz_1 \dots dz_M dz_M}{M}; \tag{6.182}$$

and the sum over  $j; j^0$  is implicit. Similarly, we represent

$$\exp \left( \sum_{j,k} O_{jj^0}^0 \alpha_j \alpha_k^0 \right) = \int dw dw \exp \left( w_j w_j + \sum_k O_{jj^0}^0 w_j \alpha_k^0 + w_j \alpha_k \right); \tag{6.183}$$

after the introduction of a set of complex variables  $w_j, \alpha_{j^0}^0, \dots, \alpha_M$ . We now use (6.181) and (6.183) and we write

$$\begin{aligned} \langle h \rangle &= \int dz dz dw dw \exp \left( \sum_j z_j z_j + w_j w_j \right) \exp \left( \sum_{j,k} O_{jj^0}^0 \alpha_j \alpha_k^0 \right) \exp \left( \sum_{j,k} O_{jj^0} \alpha_j \alpha_k^0 \right) \langle j | O_i | j^0 \rangle \\ &= \int dz dz dw dw \exp \left( \sum_j z_j z_j + w_j w_j + \sum_j (O_{jj^0}^0) w_j \alpha_j^0 \right) \exp \left( \sum_{j,k} O_{jj^0} \alpha_j \alpha_k^0 \right) \langle j | O_i | j^0 \rangle \end{aligned} \tag{6.184}$$

where the basic properties of bosonic coherent states have been used (see [216]). As a final step, we perform the evaluation of the integral through the introduction of a  $4M$ -dimensional vector of complex variables as follows

$$\int dz dz dw dw \exp \left( \sum_j z_j z_j + w_j w_j + \sum_j (O_{jj^0}^0) w_j \alpha_j^0 \right) \exp \left( \sum_{j,k} O_{jj^0} \alpha_j \alpha_k^0 \right) \langle j | O_i | j^0 \rangle = \int dZ dZ \exp \left( \frac{1}{2} Z^T \mathcal{O} Z \right); \tag{6.185}$$

In this way, we express (6.184) concisely as

$$\langle h \rangle = \int dZ dZ \exp \left( \frac{1}{2} Z^T \mathcal{O} Z \right) \langle j | O_i | j^0 \rangle; \tag{6.186}$$

where  $\mathcal{O}$  is the  $4M \times 4M$  symmetric matrix given by

$$\mathcal{O} = \begin{pmatrix} 0 & 0 & 0 & 1 & (O_{jj^0}^0)^T \\ B & 0 & 0 & 1 & C \\ @ & 1 & 1 & 0 & A \\ (O_{jj^0})^T & 1 & 0 & 0 & 0 \end{pmatrix}; \tag{6.187}$$

One can perform the Gaussian integral over  $Z$ , which gives  $\det \mathcal{O}^{-1/2}$ , and we express the final result as follows

$$\langle h \rangle = \det^{-1/2} \mathcal{O} = \det^{-1/2} \begin{pmatrix} 1 & 1 & (O_{jj^0}^0)^T \\ 1 & 1 & 0 \\ 1 & 0 & 0 \end{pmatrix} = \det^{-1/2} (1 - O_{jj^0}^0); \tag{6.188}$$

In this way, we complete the proof of Eq. (6.175) in the most general case, which is the main result of this section.

## 6.B A useful determinant

In this section we show that for a complex unitary  $M \times M$  matrix  $S$  having the block structure (6.28) the following relation holds

$$\det \begin{pmatrix} 1 & 0 \\ 0 & 1 \end{pmatrix} + q^{2k} \begin{pmatrix} S_{AA}^y & S_{BA}^y \\ S_{AB}^y & S_{BB}^y \end{pmatrix} = \det \begin{pmatrix} 1 + 2(S_{AA}^y S_{AA} + (1 - S_{AA}^y S_{AA}) \cos \theta) & 0 \\ 0 & 1 + 2(S_{BB}^y S_{BB} + (1 - S_{BB}^y S_{BB}) \cos \theta) \end{pmatrix} q^{2k} + q^{4k} (1 + q^{2k})^{M - 2M_A} \quad (6.189)$$

Before proceeding with the proof, we notice that the  $\theta$  dependence in the rhs above is related only to the non-zero eigenvalues of  $1 - S_{AA}^y S_{AA}$ . Despite the explicit dependence of  $1 - S_{AA}^y S_{AA}$  on  $A$ , this fact does not lead to any asymmetry between  $A$  and  $B$ . Indeed, the unitarity of  $S$ ,  $SS^y = S^yS = 1$ , implies

$$S_{BB}^y S_{BB}^y + S_{BA}^y S_{BA}^y = 1; \quad S_{AA}^y S_{AA} + S_{BA}^y S_{BA}^y = 1 \quad (6.190)$$

Hence  $1 - S_{BB}^y S_{BB}^y = S_{BA}^y S_{BA}^y$  and  $1 - S_{AA}^y S_{AA} = S_{BA}^y S_{BA}^y$  have the same spectrum, up to zero eigenvalues, which means that (6.189) is symmetric by exchanging  $A$  and  $B$ .

In order to prove Eq. (6.189), we introduce a  $M \times M$  matrix  $O$  as follows

$$O = \begin{pmatrix} S_{AA}^y & S_{BA}^y \\ S_{AB}^y & S_{BB}^y \end{pmatrix}; \quad (6.191)$$

so that Eq. (6.189) requires the evaluation of  $\det(1 + q^{2k}O)$ . Since, as a consequence of the unitarity of  $S$ ,  $O$  is unitary and it has the same spectrum of  $O^y$ , we can write

$$\det(1 + q^{2k}O) = \frac{q}{\det(1 + q^{2k}O) \det(1 + q^{2k}O^y)} = \frac{q}{\det(1 + q^{2k}(O + O^y) + q^{4k})} \quad (6.192)$$

Exploiting the unitarity of  $S$ ,  $O + O^y$  has a block diagonal structure given by

$$O + O^y = \begin{pmatrix} 2S_{AA}^y S_{AA} + 2(1 - S_{AA}^y S_{AA}) \cos \theta & 0 \\ 0 & 2S_{BB}^y S_{BB} + 2(1 - S_{BB}^y S_{BB}) \cos \theta \end{pmatrix} \quad (6.193)$$

Since we have already shown that  $1 - S_{AA}^y S_{AA}$ ;  $1 - S_{BB}^y S_{BB}$  have the same non-zero spectrum, we get

$$\det(1 + q^{2k}O) \propto \det(1 + q^{2k}(2S_{AA}^y S_{AA} + 2(1 - S_{AA}^y S_{AA}) \cos \theta) + q^{4k}) \quad (6.194)$$

The  $\theta$ -independent proportionality constant has to be a power of  $(1 + q^{2k})$ , which comes from the possible presence of zero eigenvalues of  $1 - S_{AA}^y S_{AA}$  (or  $1 - S_{BB}^y S_{BB}$ ). We match this constant by power counting. More precisely, since  $\det(1 + q^{2k}O)$  is a polynomial in  $q^{2k}$  of order  $M$  and

$$\det(1 + q^{2k}(2S_{AA}^y S_{AA} + 2(1 - S_{AA}^y S_{AA}) \cos \theta) + q^{4k}) \quad (6.195)$$

is a polynomial in  $q^{2k}$  of order  $2M_A$ , the right power of  $(1 + q^{2k})$  which matches the proportionality constant has to be  $(1 + q^{2k})^{M - 2M_A}$ . This concludes the proof of Eq. (6.189).

## 6.C Jacobi theta functions

Here we review some properties of the Jacobi Theta functions and the dilogarithm, useful for the evaluation of the partition functions. In particular, we discuss some specific limits of  $\theta_3; \theta_1$  Theta functions, that apply to fermions/bosons respectively.

We consider the following infinite product representation for the Jacobi theta function  $\theta_3(z; q)$  [80]

$$\theta_3(z; q) = \prod_{m=1}^{\infty} (1 - q^{2m}) (1 + 2 \cos(2z) q^{2m-1} + q^{4m-2}) \quad (6.196)$$

We want to evaluate  $\theta_3(z; q) = \theta_3(0; q)$  in the limit  $q \rightarrow 1^-$ . To do so, we first take its logarithm, which turns the infinite product representation into a sum, i.e.

$$\log \frac{\theta_3(z; q)}{\theta_3(0; q)} = \sum_{m=1}^{\infty} [\log(1 + e^{i2z} q^{2m-1}) + \log(1 + e^{-i2z} q^{2m-1}) - 2 \log(1 + q^{2m-1})] \quad (6.197)$$

For  $q \rightarrow 1^-$ ,  $q^m$  goes to zero slowly as  $m$  grows and the sum can be approximated  $\sum$  by an integral

$$\begin{aligned} \log \frac{\theta_3(z; q)}{\theta_3(0; q)} &\approx \int_0^1 dx [\log(1 + e^{i2z} q^{1+2x}) + \log(1 + e^{-i2z} q^{1+2x}) - 2 \log(1 + q^{1+2x})] = \\ &= \frac{1}{2 \log q} \int_0^1 \frac{dt}{t} [\log(1 + e^{i2z} t) + \log(1 + e^{-i2z} t) - 2 \log(1 + t)] = \\ &= \frac{1}{2 \log q} [\text{Li}_2(-e^{i2z}) + \text{Li}_2(-e^{-i2z}) - 2 \text{Li}_2(-1)] = \frac{(2z)^2}{4 \log q} \quad (6.198) \end{aligned}$$

In the previous computation, the integral representation of the dilogarithm function [80]

$$\text{Li}_2(z) = - \int_0^z \frac{dt}{t} \log(1 - tz) \quad (6.199)$$

has been employed, together with the property

$$\text{Li}_2(-e^{i2z}) + \text{Li}_2(-e^{-i2z}) = \frac{2}{6} + \frac{(2z)^2}{2}; \quad (6.200)$$

valid for  $z \in [-\frac{1}{2}; \frac{1}{2}]$ .

Similar properties hold for the Theta function  $\theta_1$ , and we summarize them below. We first express  $\theta_1(z; q)$  as the following infinite product [80]

$$\theta_1(z; q) = 2 \sin(z) q^{1/4} \prod_{m=1}^{\infty} (1 - q^{2m}) (1 - 2 \cos(2z) q^{2m} + q^{4m}) \quad (6.201)$$

In the singular limit  $q \rightarrow 1^-$  we approximate the infinite product as an integral

$$\begin{aligned} \log \frac{\theta_1(z; q)}{\sin(z)} &\approx \int_0^1 dx [\log(1 - e^{i2z} q^{2x}) + \log(1 - e^{-i2z} q^{2x})] + \text{const.} = \\ &= \frac{1}{2 \log q} \int_0^1 \frac{dt}{t} [\log(1 - e^{i2z} t) + \log(1 - e^{-i2z} t)] + \text{const.} = \\ &= \frac{1}{2 \log q} [\text{Li}_2(e^{i2z}) + \text{Li}_2(e^{-i2z})] + \text{const.}; \quad (6.202) \end{aligned}$$

where the irrelevant additive constant does not depend on  $z$ . From the definition in (6.201) it is clear that  $\chi_1(z; q) = \sin(\pi z)$  is periodic under

$$z \rightarrow z + 1; \quad (6.203)$$

and for this reason, we focus only on the region of parameter  $z \in [0; 1]$ . In this case one can show that

$$\log \frac{\chi_1(z; q)}{\sin(\pi z)} = \frac{\chi_2(z - z^2)}{\log q} + \text{const.}; \quad z \in [0; 1]; \quad (6.204)$$

up to an irrelevant  $z$ -independent additive constant.

## Chapter 7

# Entanglement evolution after a global quench across a conformal defect

We study the evolution of entanglement after a global quench in a one-dimensional quantum system with a localized impurity. For systems described by a conformal field theory, the entanglement entropy between the two regions separated by the defect grows linearly in time. Introducing the notion of boundary twist fields, we show how the slope of this growth can be related to the effective central charge that emerges in the study of ground-state entropy in the presence of the defect. On the other hand, we also consider a particular lattice realization of the quench in a free-fermion chain with a conformal defect. Starting from a gapped initial state with a staggered chemical potential, we obtain the slope via a quasiparticle ansatz and observe small universal discrepancies between the field theory and lattice results, which persist in the limit of a vanishing gap. The origin of the discrepancy is traced back to the features of the stationary state that is not thermal, even in a proper continuum limit. This chapter is based on Ref. [10].

### 7.1 CFT results

In this section, we introduce the CFT approach for the global quench in the presence of a defect. We adapt the formalism of Ref. [56] for the dynamics after the global quench, considering the additional inclusion of the defect. The calculation of the entanglement entropy is based on the replica trick, and it provides a field theoretic description of the  $n$ -th Renyi entropy.

In particular, we compute a partition function of a  $n$ -sheeted Riemann surface [46], with a branch-cut starting at the interface and extending along the half-system. This approach requires the expectation value of the twist fields inserted in a bounded geometry, and it gives the dynamics of the Renyi entropy.

We provide a general derivation of the linear growth of the entanglement entropy which does not refer to any specific model, and it is based on conformal symmetry only. Before proceeding with the calculations, it is worth to emphasize the main assumptions behind this approach.

- <sup>^</sup> The post-quench Hamiltonian is described by the same CFT on both sides of the defect, and every excitation propagates at the same speed (set to 1).

- ^ The interface is scale-invariant, thus no dependence on the incoming momenta is present for the scattering properties across the interface (as explained in Ref. [190]).
- ^ The initial state is a regularized boundary state  $|j_0\rangle = \exp(-\frac{1}{4}H)|j_B\rangle$ , which is a short-range entangled state sharing features with a thermal state at inverse temperature [56]. Different choices of the boundary states  $|j_B\rangle$  lead in principle to different initial states: however, the leading term of the entropy does not depend on  $|j_B\rangle$  as we will see.

### 7.1.1 Bulk and boundary twist fields

Here we introduce and discuss the properties of the twist fields in a defect geometry, stressing the distinction between bulk and boundary fields. First, we briefly review the standard definition of these fields in the absence of interfaces and their connection with entanglement entropy [46]. We consider a 1+1D quantum field theory replicated  $n$  times, and a pair of twist fields  $T(x); \bar{T}(x)$ , which introduce a branch-cut along the half-line  $[x; \infty)$ , connecting the  $k$ -th and the  $k-1$ -th replica, respectively. A precise definition can be provided via commutation relations between the twist fields and the local fields. In particular, one requires that [47, 85]

$$T(x)O_k(y) = \begin{cases} O_{k+1}(y)T(x); & x < y \\ O_k(y)T(x); & \text{otherwise;} \end{cases}; \quad \bar{T}(x)O_k(y) = \begin{cases} O_{k-1}(y)\bar{T}(x); & x < y \\ O_k(y)\bar{T}(x); & \text{otherwise;} \end{cases} \quad (7.1)$$

for any local operator  $O_k$  inserted at a point of the  $k$ -th replica (here  $k = 1; \dots; n$  is a replica index and its values are identified up to  $k = k + n$ ). In a CFT, the twist fields are primary fields with scaling dimension given by [46]

$$= \frac{c}{12} \left( n - \frac{1}{n} \right); \quad (7.2)$$

and  $c$  is the central charge of the theory. Their two-point function in the (homogeneous) ground-state is thus fixed by scaling symmetry only [97], and reads

$$\langle T(x_1)\bar{T}(x_2) \rangle = \frac{1}{|x_1 - x_2|^{2\Delta}}; \quad (7.3)$$

The connection between the twist fields and entanglement arises as follows. One considers the ground-state  $|j_0\rangle$  of a CFT, and constructs the reduced density matrix  $\rho_A$  associated to a subsystem  $A$  [48]. For an interval  $A = [0; \ell]$ , one can show that for any integer  $n \geq 1$  [46]

$$\text{Tr}(\rho_A^n) = \int_0^\ell \langle T(0)\bar{T}(x) \rangle dx; \quad (7.4)$$

with  $\ell$  being a UV-cutoff. Putting these informations together, one can eventually express the  $n$ -th Renyi entropy of  $A$  as [46]

$$S_n = \frac{1}{1-n} \log \text{Tr}(\rho_A^n) = \frac{c}{6} \left( 1 + \frac{1}{n} \right) \log \frac{\ell}{\epsilon}; \quad (7.5)$$

which gives the celebrated relation [192]

$$S = S_1 = \frac{c}{3} \log \frac{\ell}{\epsilon} \quad (7.6)$$

for the von Neumann entropy, once the analytical continuation  $n \rightarrow 1$  is taken.

While the result (7.5) is specific to the translational invariant ground-state, the definition (7.1) and the (bulk) scaling dimension (7.2) are general. However, there is an important caveat that arises for a bounded geometry, say an interval  $[0, L]$ . The value of the scaling dimension (7.1) refers only to a twist field  $T(x)$  inserted at a bulk point ( $0 < x < L$ ), as it is well known that boundary effects do not affect bulk dimensions [97]. Nevertheless, this is no longer true if  $x$  is a boundary point ( $x = 0; L$ ). In that case, the dimension of the twist field, which is now a boundary field, takes in general another value, dubbed as boundary scaling dimension. Indeed, if we consider the subsystem  $A = [0; \ell]$ , one finds for  $\ell \ll L$  [63]

$$S_n \sim \frac{1}{1-n} \log T(0) \mathbb{T}(\ell) = \frac{c}{12} \left( 1 + \frac{1}{n} \log \ell + \dots \right) \quad (7.7)$$

a relation which suggests immediately that the dimension of the boundary twist field  $T(0)$  vanishes. This is expected on physical grounds, since the only contribution to the entanglement is given by the correlations localized around the point  $x = \ell$ .

So far we have considered a single theory, with or without boundaries, and we have discussed the entanglement of a single interval. Now, we generalize the construction above for a system made by two CFTs joined together through an interface. The two CFTs are denoted by  $CFT_1$  and  $CFT_2$ , assumed here to be two copies of the same theory, and they extend over the regions  $x \in [0; L]$  and  $[L; 0]$  respectively. An interface is inserted at  $x = 0$ , which is a defect line extended over the Euclidean time, and gives a field theoretical representation of the impurity (see Refs. [55, 191]). We also need to specify the boundary conditions at  $x = L$ . Here, we only assume they do not mix the two theories, so that their precise features are essentially irrelevant for the entanglement between the two halves. We call unfolded picture the geometry described so far. Via the so-called folding procedure, it is possible to describe the same system as the theory  $CFT_1 = CFT_2$  extended over the region  $x \in [0; L]$ , a description which takes the name of folded picture (see Ref. [196] for further details). Comparing the two pictures, every point  $x \in [0; L]$  in the folded geometry corresponds to a pair of points  $x; -x$  (associated to  $CFT_1$  and  $CFT_2$  respectively) in the unfolded one. Moreover, the interface is now described via the boundary condition (BC) at  $x = 0$ , denoted by  $b$ , and similarly the BC at  $x = L$  in the folded picture, denoted by  $b^0$ . Note that the latter is just the product of the BCs at  $x = L$  in the unfolded picture.

The last ingredient we need to establish the correspondence among the two pictures is the characterization of the branch-cuts in the folded geometry. The idea is to introduce a pair of twist fields  $T^j; \mathbb{T}^j$  ( $j = 1; 2$ ) which act nontrivially on the degrees of freedom of  $CFT_1$  or  $CFT_2$  only, and use them as the building blocks for the entanglement measures among the two theories. We propose a definition, which is nothing but a generalization of Eq. (7.1), as follows

$$\begin{aligned} T^j(x) O_{j^0; k}(y) &= \begin{cases} O_{j^0; k+1}(y) T^j(x); & x < y; \quad j = j^0 \\ O_{j^0; k}(y) T^j(x); & \text{otherwise;} \end{cases} \\ \mathbb{T}^j(x) O_{j^0; k}(y) &= \begin{cases} O_{j^0; k-1}(y) \mathbb{T}^j(x); & x < y; \quad j = j^0 \\ O_{j^0; k}(y) \mathbb{T}^j(x); & \text{otherwise;} \end{cases} \end{aligned} \quad (7.8)$$

with  $O_{j; k}(y)$  being local operators of  $(CFT_1 = CFT_2)^n$  with species index  $j = 1; 2$  and replica index  $k = 1; \dots; n$ . As an illustrative example, the insertion of  $T^1(x_1) \mathbb{T}^1(x_2)$  at two points  $0 < x_1 < x_2 < L$  of the folded geometry, corresponds to the insertion of  $T(x_1) \mathbb{T}(x_2)$  in the

unfolded picture, which is a branch-cut along a segment of CFT. Similarly,  $T^2(x_1)\mathcal{T}^2(x_2)$  introduces a branch-cut on  $[x_2; x_1]$  in the unfolded picture. We summarize the construction above in Fig. 7.1 which provides a pictorial representations of the insertion of the branch-cuts in the folded/unfolded pictures.

Figure 7.1: Representation of a system made by two CFTs joined through an interface in the unfolded (left) and folded (right) picture. The interface and the open boundaries are shown by green and blue lines, and are associated to boundary conditions of type  $b$  and  $b^0$ , respectively.

As long as the twist elds  $T^j$  are inserted at bulk points, their (bulk) scaling dimension is simply given by Eq. (7.2). In contrast, the dimension of  $T^j(L)$  is expected to be zero, since the two theories are not coupled at  $x = L$  and one can use the results available for a single theory. Moreover, we argue that the scaling dimension of  $\mathcal{T}^j(0)$  is nontrivial, and strongly depends on the boundary condition  $b$  (and  $n$ ), representing the interface: we denote it by  $b$ . We thus compute the Renyi entropy among the two halves as

$$S_n = \frac{1}{1-n} \log \langle \mathcal{T}^1(0)\mathcal{T}^1(L) \rangle = \frac{b}{n-1} \log \frac{L}{1} + \dots; \quad (7.9)$$

where the last equality follows from scaling arguments only, and subleading terms of order  $\mathcal{O}(1)$  have been neglected. More precisely, if one applies a scale transformation,  $z \rightarrow \frac{L}{1} z$ , then the geometry becomes  $[0; L]$  and the twist elds are inserted at the boundary of this new geometry ( $x = 0; L$ ). An additional scale factor  $b$  appears due to the scaling transformation of the twist elds. Taking for example  $b = 1=L$  for the scaling parameter, one completely loses the  $L$ -dependence of the two-point function which gives directly Eq. (7.9).

Eventually, one concludes that the entropy grows as the logarithm of the size, with an interface dependent prefactor, a result which was firstly obtained for the free boson in [55] and for Ising/free fermions in [191]. In particular, in the limit  $n \rightarrow 1$  one has

$$S = \frac{c_e}{6} \log \frac{L}{1}; \quad (7.10)$$

where  $c_e$  is a parameter dubbed æ effective central charge. Comparing the last expression with our formula (7.9), we establish the equivalence

$$\frac{c_e}{6} = \lim_{n \rightarrow 1} \frac{b}{n-1}; \quad (7.11)$$

It tells us that the origin of the nontrivial scaling of entanglement for systems with conformal defects can be traced back to a nontrivial boundary scaling dimension of the twist eld  $T^j$ .

7.1.2 Global quench

We continue with the study of a global quench for a CFT in the presence of a defect, generalizing the approach of [56] valid without the defect. We mention that a similar method to tackle the problem has been already employed in [217]. Here, we consider instead a novel technique based on the use of the boundary twist fields.

We work in the folded picture, introduced in the previous subsection, and consider the theory  $CFT_1 \cup CFT_2$  extended over the spacial region  $[0, L]$ . We take the initial state

$$|j_0\rangle = \exp\left(-\frac{H}{4}\right) |b^0\rangle; \tag{7.12}$$

with  $|b^0\rangle$  being a boundary state associated to the  $BCb^0$ ,  $H$  the post-quench Hamiltonian and  $\beta$  a parameter representing the inverse temperature of the initial state. Within this choice, the initial state is short-range entangled, having a finite correlation length of order  $\beta$ . Since  $|j_0\rangle$  is not an eigenvector of  $H$ , the unitary dynamics induced by the Hamiltonian is nontrivial. We consider time scales much shorter than the size,  $t \ll L$ , so that finite-size effects are negligible. We express the Rényi entropy between the two halves as

$$S_n(t) = \frac{1}{1-n} \log \langle j_0 | \text{tr} \rho_{0j}^{nH} T^1(0) \mathcal{T}^1(L) e^{-iHt} |j_0\rangle^n \rangle; \tag{7.13}$$

with  $|j_0\rangle^n = |j_0\rangle \otimes \dots \otimes |j_0\rangle$  being a state of the  $n$ -replica theory  $(CFT_1 \cup CFT_2)^n$ . Since  $\mathcal{T}^1(L)$  has dimension 0, we simply drop it from Eq. (7.13), a procedure which is physically motivated by the fact that its insertion should not affect the entanglement among the two halves (see [47] for further details). Taking into account the correct normalization of the state, we finally end up with

$$S_n(t) = \frac{1}{1-n} \log \frac{\langle j_0 | \text{tr} \rho_{0j}^{nH} e^{-H(=4-it)} T^1(0) e^{-H(=4+it)} |j_0\rangle^n \rangle}{\langle j_0 | \text{tr} \rho_{0j}^{nH} e^{-H=2} |j_0\rangle^n \rangle}; \tag{7.14}$$

We now proceed further with the evaluation of the expectation value appearing in Eq. (7.14). We work in the Euclidean theory, described as the bounded geometry (strip)

$$\text{Re}(z) \in [0; +1]; \quad \text{Im}(z) \in [-4; +4]; \tag{7.15}$$

obtained in the limit  $L \rightarrow 1$ . We insert the twist field  $T^1$  at the position  $z = i$  of the strip, with  $t$  being the Wick rotated time

$$t = it; \tag{7.16}$$

To compute  $\langle \text{tr} \rho_{0j}^{nH} T^1(z = i) \rangle$ , we map the strip (7.15) onto the upper half-plane  $\text{Im}(w) \geq 0$  through a sequence of transformations  $z \rightarrow w$  defined by

$$z = \sin \frac{2iz}{\pi}; \quad w = \frac{1+z}{2(1-z)}; \tag{7.17}$$

Via this change of variables, the corners at  $z = i = 4$  are mapped onto the points  $w = 0; 1$  respectively. In this new geometry a change of boundary conditions, from type  $b^0$  to type  $b$ , appears at  $w = 0$  along the real line  $\text{Im}(w) = 0$ . In Fig. 7.2 we represent the insertion of the twist field both in the strip geometry ( $z$  variable) and the upper half-plane ( $w$  variable).

At this point, we observe explicitly that the depicted geometry (upper-half plane) shows a scale-symmetry

$$w \rightarrow w; \quad \beta > 0; \tag{7.18}$$

Figure 7.2: Euclidean boundary geometry describing the global quench in the  $z$  (left) and  $w$  (right) variable. Green/blue colors denote boundary conditions of type  $b=b^0$ , respectively.

Indeed, the boundary conditions  $b^0, b$  are scale-invariant and the point  $w = 0$ , representing the change of BCs, is kept fixed. We use this property to infer the value of the one-point function along the boundary of type  $b$  ( $\text{Im}(w) = 0; w > 0$ ) which is

$$\langle hT^1(w) \rangle_i = \frac{1}{|w|^b}; \tag{7.19}$$

up to a  $w$ -independent proportionality constant not further specified.

We now go back to the original geometry, employing the transformation law of the twist field  $T^1$ , which is a primary operator. We firstly apply  $w \rightarrow z$ , reaching to

$$\langle hT^1(z) \rangle_i = \frac{dw}{dz}{}^b \langle hT^1(w) \rangle_i / \frac{1}{(1-z)^2}{}^b \frac{1}{1+z}{}^b = \frac{1}{1-z^2}{}^b; \tag{7.20}$$

and similarly from the map  $z \rightarrow \tau$  we get

$$\langle hT^1(z) \rangle_i = \frac{d}{dz}{}^b \langle hT^1(\tau) \rangle_i / \frac{4}{\cos(2iz)}{}^b; \tag{7.21}$$

Performing the Wick rotation  $\tau = it$ , for large values  $t \rightarrow \infty$  we obtain

$$\langle hT(z = i) \rangle_i = \frac{8}{3} e^{-2t}{}^b; \tag{7.22}$$

which leads directly to

$$S_n(t) - S_n(0) = \frac{1}{1-n} \log \frac{\langle hT^1(z = i) \rangle_i}{\langle hT^1(z = 0) \rangle_i} = \frac{b}{n-1} 2t; \tag{7.23}$$

the main result of this subsection. One can further take the analytical continuation  $n \rightarrow 1$  from Eq. (7.23) to extract the entanglement entropy, and, using Eq. (7.11), one gets

$$S_1(t) - S_1(0) = \frac{c_e t}{3}; \tag{7.24}$$

We conclude with some remarks regarding the derivation provided above. For instance, even if we did not attempt to calculate explicitly the scaling dimension  $\Delta_b$  of the boundary twist field, we got a precise relation between equilibrium (7.9) and non-equilibrium entropy (7.23) based on conformal invariance only.

Moreover, the same derivation can be applied to the evolution of any boundary (primary) operator, and it is not specific to the twist field. We finally stress again that the linear growth in (7.23) is expected to be valid for  $t \ll L$ , so that the short-time effects, as well as the long-time recurrences, are neglected.

## 7.2 Lattice results

In the following, we consider a lattice realization of the global quench. Our main goal is to derive a formula that relates the entropy growth in the presence of a defect to that in a homogeneous chain. We show that, in contrast to CFT results that predict for the Renyi the appearance of the same proportionality factor both in the global quench and the ground state, this is not true in general for the lattice. Moreover, we provide a quasi-particle description of the protocol above, which matches with CFT only for thermal states at low temperatures. In contrast, we study a family of initial states parametrized by a staggered chemical potential which are not thermal, and therefore they do not reproduce the CFT predictions.

### 7.2.1 Model and setup

We consider a fermionic hopping chain of length  $2L$  with Hamiltonian

$$\hat{H} = \sum_{x;x^0=L+1}^{x^0=L} H_{x;x^0}^0 c_x^\dagger c_{x^0} \quad (7.25)$$

where  $c_x^\dagger, c_x$  are fermionic creation/annihilation operators satisfying anticommutation relations  $\{c_x^\dagger, c_{x^0}\} = \delta_{x;x^0}$ . We consider a conformal defect located in the center of the chain, with the nonzero elements of the hopping matrix given by

$$H_{x;x+1}^0 = H_{x+1;x}^0 = \begin{cases} 1 & x \neq 0 \\ 2 & x = 0 \end{cases} ; \quad H_{0;0}^0 = H_{1;1}^0 = \frac{p}{1 - 2\epsilon} \quad (7.26)$$

The particular form of the coupling at the origin gives rise to scattering properties which do not depend explicitly on the incoming momentum, and  $\epsilon \in [0; 1]$  is precisely the scattering amplitude across the defect.

Throughout this chapter, we use the prime notation to refer to various quantities of the defect problem, whereas the same symbols without prime shall refer to the homogeneous ( $\epsilon = 1$ ) case.

The spectrum of  $H^0$  was studied before in [53] and was shown to have a particularly simple relation to the homogeneous case  $H$ , where the single-particle eigenvalues and eigenvectors are given by

$$k(x) = \frac{r}{2L+1} \sin \frac{kx}{2L+1}; \quad \epsilon_k = \cos \frac{k}{2L+1} \quad (7.27)$$

for  $k = 1; \dots; 2L$ . Indeed, the corresponding quantities for the hamiltonian  $H^0$  are simply related via [53]

$${}^0_k(x) = \begin{pmatrix} k & k(x) \\ k & k(x) \end{pmatrix} \begin{pmatrix} x & 0 \\ x & 1 \end{pmatrix}; \quad \epsilon_k^0 = \epsilon_k \quad (7.28)$$

where the scaling factors read

$$\frac{2}{k} = 1 + (\epsilon_k)^{2p} \frac{1}{1 - \epsilon_k^2}; \quad \frac{2}{k} = 1 - (\epsilon_k)^{2p} \frac{1}{1 - \epsilon_k^2} \quad (7.29)$$

In other words, the eigenvectors of  $H^0$  are only rescaled by a different factor on the left/right-hand side of the defect, while the spectrum remains unchanged.

The simple structure (7.28) of the eigenvectors has important implications on the ground-state entanglement properties between the two halves  $A = [L + 1; 0]$  and  $B = [1; L]$  of the chain. These follow from the fermionic reduced correlation  $C_A^0$  matrix with elements [187]

$$C_{xx^0}^0 = \langle c_x^\dagger c_{x^0} \rangle = \sum_{k=1}^L \frac{\lambda_k}{k} \phi_k(x) \phi_k(x^0); \quad x, x^0 \in A; \quad (7.30)$$

In particular, the entanglement entropy of the reduced density matrix  $\rho_A = \text{Tr}_B \rho$  is obtained as

$$S = - \sum_{l=1}^L s_l \ln s_l; \quad s_l(x) = -x \ln x - (1-x) \ln(1-x) \quad (7.31)$$

where  $s_l^0$  are the eigenvalues of  $C_A^0$ . Using (7.28) for the matrix elements in (7.30), one finds the exact relation for the ground state of the conformal defect

$$C_A^0(1 - C_A^0) = \frac{1}{2} C_A(1 - C_A); \quad (7.32)$$

which yields an analogous relation between the eigenvalues.

The latter relation can then be used to find the scaling of the entanglement entropy which reads

$$S = \left( \frac{c}{3} \right) \ln L; \quad (7.33)$$

where the prefactor of the leading logarithmic term is obtained as [218]

$$s(s) = \frac{1}{2} \left[ h + (1+s) \ln(1+s) + (1-s) \ln(1-s) \right] - \ln s + (1+s) \text{Li}_2(-s) + (1-s) \text{Li}_2(s); \quad (7.34)$$

in terms of the transmission amplitude  $s = \frac{1}{2} \left( 1 + \frac{v}{v_0} \right)$ . One can also extract the scaling of the Rényi entropies of integer index  $n > 1$

$$S_n = - \sum_{l=1}^L s_n(s_l); \quad s_n(x) = \frac{1}{1-n} \ln [x^n + (1-x)^n]; \quad (7.35)$$

The result is completely analogous to (7.33), with the corresponding prefactor given by [53]

$$s_n \left( \frac{c}{3} \right) = \frac{1}{2} \frac{1}{n} \sum_{p=(n-1)/2}^{(nX^1)/2} \frac{h}{1 - \arcsin^2 \sin \frac{p}{n}}; \quad (7.36)$$

where the sum over  $p$  runs over half-integer/integer values for  $n$  even/odd.

We now turn our attention to the quench setup. In order to mimic the global quench scenario of the CFT setting, we choose a gapped initial Hamiltonian  $\hat{H}_0$  and prepare the chain in its ground state. The simplest way to open a gap is to add a staggered chemical potential to the Hamiltonian (7.25) of the conformal defect

$$\hat{H}_0 = \hat{H} + \sum_{x=L+1}^L \mu (1)^x c_x^\dagger c_x; \quad (7.37)$$

The quench then consists of switching off the potential at time  $t = 0$  and time evolve the initial state with  $\hat{H}$ . The size of the gap in  $\hat{H}_0$  is controlled by the mass parameter  $\mu$ , and in the limit

$\mu \rightarrow 1$  one obtains the Néel state, where each odd lattice site is occupied by a particle with the even sites being empty.

## 7.2.2 Quasiparticle picture for the homogeneous case

The entropy growth after a global quench in an integrable translational invariant chain can be understood in terms of a quasiparticle picture [219–221]. Namely, one assumes that the initial state is a coherent superposition of quasiparticle pairs, which are initially short-range correlated, but they spread entanglement due to their ballistic propagation as the system evolves. In particular, a contribution to the entanglement between the subsystems  $A$  and  $B$  is present at time  $t$  if the two particles of the pair belong to  $A; B$  respectively.

In a free-fermion chain, for each mode with momentum  $q$  and group velocity  $v_q$ , the two particles of each pair move at velocity  $\pm v_q$ , therefore they entangle arbitrary distant points. Moreover, according to this picture, the contribution of a given pair is simply the thermodynamic entropy density taken in the steady state of the dynamics, which is uniquely determined by the occupation numbers  $n_q = \langle c_q^\dagger c_q \rangle$ , that are constants of motion.

Putting everything together, in the limit  $L \rightarrow \infty$  of a semi-infinite subsystem one arrives at the expression

$$S_n(t) = t \int_{-\pi/2}^{\pi/2} \frac{dq}{2\pi} |v_q| s_n(n_q); \quad (7.38)$$

where the integral is performed over the first Brillouin zone.

The quasiparticle ansatz (7.38) in the half-chain geometry thus gives a purely linear growth of entanglement,  $S_n(t) = \nu_n(\lambda; 1)t$ , where the second argument of the slope refers to  $\lambda = 1$ . In order to find the slope  $\nu_n(\lambda; 1)$  as a function of the quench parameter  $\lambda$ , one has to evaluate the occupation numbers  $n_q$  characterising the steady state after the quench. These are fixed by the ground state of the staggered chain, and can be found by diagonalizing  $H_0$ , with the result

$$n_q = \frac{1}{2} \left( 1 + \rho \frac{\cos q}{\cos^2 q + \frac{\rho^2}{2}} \right); \quad (7.39)$$

In the limit  $\rho \rightarrow 0$   $n_q$  converges towards the Fermi sea occupation, whereas for the Néel state,  $\rho = 1$ , it becomes completely flat,  $n_q = 1/2$ . It should be clear that, whenever  $\rho$  is kept fixed in the thermodynamic limit, while a possible quantitative agreement with QFT can be possible only if  $\rho \rightarrow 1$ .

With the result (7.39) for the occupation at hand, one can now compare the quasiparticle ansatz (7.38) to the entropy obtained from the lattice calculation. We shall restrict ourselves to the case  $\lambda = 1$ . The correlations at time  $t$  are given by  $C(t) = U^\dagger C(0)U$ , where  $C(0)$  describes the correlations of the staggered ground state, and the propagator is given by  $U = e^{-iHt}$ . For our numerics we choose  $L = 100$ , and consider the short-time regime  $t < L$ , where the presence of the boundaries cannot yet influence the behaviour. The result is shown in Fig. 7.3 for various values of  $\rho$ . On the left, the linear growth with slopes  $\nu_n(\lambda; 1) = \nu_1(\lambda; 1)$  calculated from (7.38) are plotted by red solid lines, showing a very good agreement with the data. Note that we have subtracted the initial value  $S(0)$  of the entropy. On the right of Fig. 7.3 we show the corrections to the quasiparticle ansatz by subtracting the linear piece. Interestingly, the leading correction seems to be logarithmic in time, albeit with a very small prefactor that increases for larger  $\rho$ .

<sup>1</sup>As we will see, even in this limit we have discrepancies with the thermal states of CFT. In particular, we think that the initial state we are considering cannot be considered an irrelevant deformation of a thermal CFT's state (see also Ref. [56] for details about this mechanism).

Figure 7.3: Entropy evolution for a homogeneous chain ( $\nu = 1$ ) with  $L = 100$  after a global quench for various values of  $\beta$ . The red lines show the slopes calculated from (7.38) with the occupation (7.39).

### 7.2.3 Quench with a defect

We now move on to consider the quench with the defect. Motivated by the CFT results, our goal is to establish a relation between the defect and the homogeneous cases, analogous to the one (7.32) found for the ground state.

The first step is to calculate the (single-body) propagator  $U^0 = e^{-iH^0 t}$  with the defect. The matrix elements on the same side of the defect are obtained as

$$U_{xx^0}^0 = \int \frac{dq}{2\pi} e^{-i! q t} e^{i h q(x-x^0)} \int \frac{p}{2\pi} e^{-i q(x+x^0-1)} = U_{xx^0} \int \frac{p}{2\pi} U_{x;1-x^0}; \quad (7.40)$$

where the  $\pm$  sign refers to the case  $x < x^0$  and  $x > x^0$ , respectively. On the other hand, for the off-diagonal terms with  $x < 0$  and  $x^0 > 1$ , as well as  $x > 1$  and  $x^0 < 0$ , one obtains

$$U_{xx^0}^0 = \int \frac{dq}{2\pi} e^{-i! q t} e^{i h q(x-x^0)} = U_{xx^0}; \quad (7.41)$$

It should be noticed that the homogeneous propagator  $U$  is translational invariant, as the Hamiltonian is invariant too, while this is not the case for  $U^0$  as the defect breaks explicitly the invariance above.

For the calculation of the entropy, we need the time-evolved matrix  $C^Q(t) = U^0 C^Q(0) U^0$ , where  $C^Q(0)$  contains the ground-state correlations of the staggered Hamiltonian (7.37) with a defect, and it describes the initial state. In general, this is a rather complicated object of which we do not have a closed-form expression.

To proceed further, let us first note that, due to the purity of the time evolved state, the full correlation matrix satisfies  $C^Q(t)(1 - C^Q(t)) = 0$ . This yields

$$C_A^0(t)(1 - C_A^0(t)) = C_{AB}^0(t)C_{BA}^0(t); \quad (7.42)$$

where  $C_{AB}^0(t)$  is the off-diagonal part of the correlation matrix, and  $C_{BA}^0(t) = C_{AB}^{0y}(t)$ . The relation Eq. (7.42) is extremely useful, as it allows relating the entropies to the spectrum of  $C_{AB}^0(t)$ , a matrix which has some 'nicer' properties compared to  $C_A^0(t)$ . In particular, we found

out that, up to corrections that turned out to be negligible, the following relation between the homogeneous and the defect problem holds

$$C_{AB}^0(t) \approx C_{AB}(t); \quad (7.43)$$

At the physical and heuristic level, we explain (7.43) as follows. We consider a pair of quasiparticles generated at a certain point far from the defect. Particles spread and eventually one of the two hits the defect and goes onto the other half of the chain. This process happens with an amplitude wrt the homogeneous case. Therefore, one expects that the overall contribution due to defect for two-point function  $C_{AB}^0$  is just a factor. This argument does not lead to exact results on finite-size systems, but mostly because corrections are present to the semiclassical dynamics. Still, the consequences of Eq. (7.43) can be tested numerically for large sizes. Hence, we expect that the relation for the eigenvalues

$$\lambda_i^0(t)(1 - \lambda_i^0(t)) \approx \lambda_i(t)(1 - \lambda_i(t)) \quad (7.44)$$

should still hold approximately, even though the corresponding relation between the matrices  $C_A^0(t)$  and  $C_A(t)$  does not hold exactly. The eigenvalue relation is tested in Fig. 7.4 for a chain of size  $L = 100$ , time  $t = 50$  and two different values of  $\beta$ , with full/empty symbols corresponding to the left/right hand side of Eq. (7.44). One can see a very good overlap between the two quantities, with only slight shifts between the symbols, except for the spectral edges where the discrepancy becomes larger.

Figure 7.4: Numerical check of the relation (7.44), with the left/right hand side of the equation shown by the full/empty symbols, for  $L = 100$ ,  $t = 50$  and two different values of  $\beta$ .

Therefore, we introduce  $n_q^0$

$$n_q^0(1 - n_q^0) = \lambda_q^2 n_q(1 - n_q); \quad (7.45)$$

and we interpret them as the 'occupation numbers' for the systems with the defect. While we did not work out the details to make this interpretation rigorous, we think that the 'natural' modes of our system should be superpositions of left/right plane waves and  $n_q^0$  refer to them. Following this analogy, we also propose an ansatz for the growth of Renyi entropy that is

$$S_n(\beta; t) = \int \frac{dq}{2\pi} |v_q| s_n(n_q^0) \quad (7.46)$$

and it gives back the usual quasiparticle prediction for  $\nu = 1$ .

The result (7.46) is compared against the lattice data in Fig. 7.5 for a small and intermediate value of the mass parameter, and various defect strengths. One observes a very good agreement, with the deviations from the quasiparticle result shown on the inset. The subleading term seems to be given by a constant for  $\nu = 0:1$ , whereas for  $\nu = 1$  the corrections are likely to be logarithmic in time, with some superimposed oscillations.

Figure 7.5: Entropy growth after a global quench with mass parameters  $\nu = 0:1$  (left) and  $\nu = 1$  (right), for various defect strengths  $\nu$  and  $L = 100$ . The red lines show the quasiparticle ansatz with slope (7.46), while the insets show the corresponding deviations.

We specialize (7.39) to our initial state, and we get

$$n_q^0 = \frac{1}{2} \int_{-\pi}^{\pi} \frac{s \cos^2 q}{\cos^2 q + \nu^2} dq \quad (7.47)$$

With the expression (7.46) for the slope at hand, one can now compare the result to the CFT prediction. We remind that for CFTs the slope ratio for the global quench at a given  $\nu > 1$  and  $\nu = 1$  should be equal to the ground-state entropy ratio  $n(\nu) = n(1)$ . Indeed, it is reasonable to compare the ratio above with  $n(\nu; \nu) = n(\nu; 1)$ .

Let us first consider the Nèel limit,  $\nu \rightarrow 1^-$ , where the occupation  $n_q^0$  in (7.47) becomes piecewise constant, and the integral (7.46) simply evaluates to

$$n(1; \nu) = \frac{2}{\pi} \int_{-\pi}^{\pi} \frac{1 + \nu \cos^2 q}{2} dq \quad (7.48)$$

Obviously, this result has a rather different analytical behaviour as compared to the ground-state prefactors. Remarkably, however, the ratios turn out to be very close to each other, as shown by the comparison on the left of Fig. 7.6 for  $\nu = 1; 2$ , although the discrepancy increases with  $\nu$ . In fact, in the limit of large mass  $m$ , one does not expect the CFT result to be exact, since one obtains contributions from the entire Brillouin zone and thus the role of the lattice dispersion enters.

In contrast, in the limit  $m \rightarrow 0$  only the modes around the Fermi level  $q = \pm \pi/2$  contribute, and one would expect the CFT description to become exact. Surprisingly, this turns out not

to be the case, as demonstrated on the right of Fig. 7.6. Indeed, in the limit  $\beta \rightarrow 0$ , the slope vanishes linearly with the mass and one can find the closed analytical expression for  $\beta \ll 1$

$$\lim_{\beta \rightarrow 0} \frac{n(\beta; \mu)}{n(\beta; 1)} = \frac{1}{n-1} \sum_{p=(n-1)/2}^{(n-1)/2} \frac{q^{2p}}{1 + 2 \sin^2(p/n)}; \quad (7.49)$$

as shown in appendix 7.A. The ratio  $n(0; \mu) = n(0; 1)$  is thus finite, and the structure of (7.49) shows a close resemblance to that in (7.36), although the expressions in the sum are eventually different. Nevertheless, the mismatch from the ratio  $n(\beta) = n(1)$  turns out to be very small again, and the curves now approach the CFT limits from the other side, as compared to the  $\beta \rightarrow 1$  case.

Figure 7.6: Comparison of the slope ratios (blue) to the CFT prediction (red) in the limits  $\beta \rightarrow 1$  (left) and  $\beta \rightarrow 0$  (right), as a function of  $\mu$ . The solid/dashed lines correspond to  $n = 1$  and  $n = 2$ .

For general  $n$ , the behaviour of the discrepancy  $n(\beta; \mu) - n(\beta; 1) = n(\beta; \mu) - n(\beta; 1)$  between the slope ratios is shown for some fixed values of  $n$ . The deviation remains rather small in the entire regime  $0 < \mu < 1$  as shown. In particular, it decreases for  $\beta \rightarrow 0$  and  $\beta \rightarrow 1$ , while the maximal deviations are observed around  $\mu = 0.5$ , similarly to Fig. 7.6. Interestingly, the curves change sign at around  $\mu = 0.3$ , although they do not intersect at the same  $\beta$  as it might seem. Thus, in general, the lattice quench ratios are governed by a different function of  $\mu$  from the one in CFT, albeit with such a small discrepancy that could not have been found by fitting the data, without the analytical solution of the problem.

The reason of the discrepancy is that, even in the limit  $\beta \rightarrow 0$ , the occupation (7.39) does not correspond to a thermal distribution, which is implicitly assumed in the CFT treatment. In fact, the calculation of the slope can be generalized to this case, since the relation (7.45) holds for arbitrary initial occupations. Choosing a thermal initial state of the homogeneous chain

$$n_q = \frac{1}{e^{\beta \epsilon_q} + 1} \quad (7.50)$$

with  $\epsilon_q = v_F \cos q$ , the details of the dispersion become irrelevant in the low-temperature limit,  $\beta \rightarrow 1$ . As outlined in appendix 7.A, the calculation of the corresponding slope  $n(\beta; \mu)$  can be carried out explicitly by linearizing the dispersion around the Fermi point and yields

$$\lim_{\beta \rightarrow 1} n(\beta; \mu) = 2 n(\mu); \quad (7.51)$$

Figure 7.7: Deviation of the slope ratio from the CFT prediction with  $n = 1$ , plotted in the regime  $0 < t < L$  for various fixed values of  $\nu$ .

Hence, the slope ratios give exactly the expected CFT result in the limit  $t \rightarrow 0$ .

Finally, one should emphasize that the key connection between the ground-state and quench scenarios is the eigenvalue relation (7.44), which is indeed identical for the two cases, even though it is satisfied only approximately (say, up to finite-size effects) for the global quench with the initial state chosen here. The derivation relies on a special property of the initial Hamiltonian that is completely analogous to (7.28), and the relation  $C_{AB}^0 = C_{AB}$  holds exactly for finite  $L$  and arbitrary times.

To conclude this section, we remark that the quench results can also be generalized to other type of defects. While CFT results and some analytical results refer mostly to the conformal defect, whose scattering properties do not depend on the incoming momenta of the particle, we believe this assumption is not important for the applicability of the quasi-particle ansatz. Indeed, let us assume that the defect leaves the system free, and it is a localized perturbation quadratic in the fermions, and it gives rise to a transmission probability  $T(q)$ . In the quasiparticle interpretation, all the formula we discussed so far are expected to be modified by replacing  $\nu \rightarrow T(q)$ , which yields

$$n_q^0 = \frac{1}{2} \left( 1 + \frac{q}{1 - 4T(q)n_q(1 - n_q)} \right) \quad (7.52)$$

#### 7.2.4 Entanglement revivals

For a chain of finite size, the result will be modified for times  $t > L$ , due to particles reflecting from the boundaries of the chain. Such finite-size effects result in a sawtooth-like pattern of the entropy, as shown in Fig. 7.8 for the homogeneous case  $\nu = 1$ . The decay and revival of the entropy was studied for a periodic chain in [222], and the result can easily be generalized to the open chain by finding the proper contributions of the quasiparticle pairs after reflections. Indeed, for a pair with fixed velocity  $\nu_q > 0$ , the emission distance measured from the center of the chain must satisfy  $x < \min(\nu_q t - 2L(n-1); 2L - \nu_q t)$  in order to contribute after  $n$  reflections from

the boundary. Hence, the quasiparticle ansatz reads

$$S_n = \int_{-\frac{Z}{2}}^{\frac{Z}{2}} \frac{dq}{2} s_n(n_q) 2L \min \left\{ \frac{jv_q t}{2L}; 1 \right\} + \int_{-\frac{Z}{2}}^{\frac{Z}{2}} \frac{dq}{2} r_n(n_q) 2L \min \left\{ \frac{jv_q t}{2L}; 1 \right\} ; \quad (7.53)$$

where the curly brackets denote the fractional part. The formula (7.53) is plotted with red solid lines in Fig. 7.8, showing a good agreement with the data, although the discrepancy increases for larger times due to subleading contributions.

Figure 7.8: Entanglement decay and revival in the homogeneous quench for various  $L = 50$ . The red solid lines show the quasiparticle ansatz (7.53).

The case of the defect requires a more careful analysis, by following the quasiparticle trajectories and scattering events for large times. This is shown on the left panel of Fig. 7.9, for a pair emitted at a distance  $x$  from the defect. When reaching the defect, the transmitted part (solid line) of the red particle picks up an amplitude  $s(q)$ , whereas the reflected component (dashed line) receives an amplitude  $r(q)$ . For short times, the dominant contribution to the entanglement is created by the transmitted red and the blue particles. For large enough times, however, the blue particle reaches the defect after a reflection and its transmitted part (solid line) can create entanglement with the reflected part (dashed line) of the red particle, and vice versa. These processes contribute in a time window depicted by the horizontal dotted lines, and both of them carry an amplitude  $s(q)r(q)$ , which we assume to add phase coherently. Finally, when the transmitted and reflected beams join again, they reproduce the original wave with unit amplitude, which is due to the fact that the amplitudes do not carry any phase and satisfy  $s^2(q) + r^2(q) = 1$ .

The slope for the entropy can be found by simply summing up the contributions from the two different processes discussed above. Based on these considerations, we proposed the quasiparticle ansatz

$$S_n = \int_{-\frac{Z}{2}}^{\frac{Z}{2}} \frac{dq}{2} s_n(n_q^0) 2L \min \left\{ \frac{jv_q t}{2L}; 1 \right\} + \int_{-\frac{Z}{2}}^{\frac{Z}{2}} \frac{dq}{2} s_n(n_q^0) L \max \left\{ 0; 1 - 4 \frac{jv_q t}{4L} \right\} ; \quad (7.54)$$

with

$$n_q^0(1 - n_q^0) = 4 \frac{jv_q t}{4L} (1 - \frac{jv_q t}{4L}) n_q(1 - n_q) ; \quad (7.55)$$

Figure 7.9: Left: quasiparticle trajectories with corresponding amplitudes. Right: entropy growth compared to the quasiparticle ansatz (7.54).

The ansatz (7.54) is compared against the lattice data in the bottom right panel of Fig. 7.9, finding a remarkably good agreement. One should stress that the pattern of entanglement is completely different from the one found in Fig. 7.8. Indeed, instead of the decay in the time window  $L < t < 2L$ , one finds a continued growth of entanglement with a slope that can even exceed the one in the initial growth phase  $0 < t < L$ . The decay of the entropy ensues only after  $t > 2L$ , with a quasi-periodic pattern repeating itself after a full period  $t = 4L$ .

A last technical, albeit fundamental, observation is needed. While in the absence of the defect one observes (approximate) revivals with period  $2L$ , whenever  $\nu < 1$  revivals have period  $4L$ . This feature rules out immediately any possible exact validity of  $C_{AB}^0(t) = C_{AB}(t)$ , that was indeed established without caring about finite-size effects (which are crucial here).

### 7.3 Concluding remarks

We examined a global quench protocol that exhibits a complex spread of quantum correlation. The emergence of "long-range correlations" can be attributed to both the pair structure of the initial state and the quantum scattering at the defect point. These effects compete in a non-trivial manner, leading to an entanglement growth prediction that defies a simple semiclassical interpretation.

Initially, we derived our findings in the framework of (CFT), where predictions rely on minimal assumptions such as the initial state's thermality and the defect's scale-invariance. Subsequently, we provided a microscopic explanation of the mechanism in the context of free fermions on a lattice. In addition to quantitative predictions, a common observation in many cases, which appears to be general, is that greater transmissivity of the defect leads to faster entropy growth.

This can be intuitively understood as the entropy growth arising from pairs with opposite velocities spreading across the two sides of the interface.

We would like to highlight some general remarks. While we are confident that the picture we obtained for free fermions in the limit of infinite system size can be rigorously established, possibly within the framework of generalized hydrodynamics (despite the presence of long-range correlations, as discussed in [223]), the assumption of a scale-invariant defect should not play a specific role. However, when multiple scattering events occur, such as in the presence of multiple defects or when considering finite-size effects, the situation becomes qualitatively more intricate. This complexity arises from the delicate interference of distinct semiclassical trajectories, which makes the approach highly sensitive to modifications in local details. Consequently, it remains unclear whether a large-scale approach can provide predictive power when these effects are significant.

Another avenue worth exploring is the investigation of different types of defects, such as those extended in space or even interacting defects. Specifically, it is challenging to distinguish between a smoothly varying extended defect, which is expected to exhibit purely classical behavior with no partial transmission or reflection, and localized defects with a non-trivial scattering matrix. Additionally, it would be valuable to determine if it is possible to predict the entropy growth of free fermions in the presence of an interacting defect by modifying the quasi-particle framework we have presented thus far. We hope to come back to these in future investigations.

## 7.A Calculation of the slope ratio for $\beta \rightarrow 0$

In this appendix we analyze the slope of the Renyi entropy (see Eq. (7.46))

$$n(\beta; \gamma) = \int \frac{dq}{2} \int_{-\pi}^{\pi} \sin qj s_n \frac{1}{2} \left( 1 + \frac{1}{1 + \frac{2}{\cos^2 q + \beta}} \right)^{\gamma} \quad (7.56)$$

in the limit  $\beta \rightarrow 0^+$ , which requires a careful analysis. A preliminary observation is that for  $\beta = 0$  one gets

$$n(0; \gamma) = \int \frac{dq}{2} \int_{-\pi}^{\pi} \sin qj s_n(0) = 0; \quad (7.57)$$

which is a correct conclusion, since in this limit the pre/post-quench Hamiltonians are the same and there is no dynamics. However, here we are mostly interested in the way  $n(\beta; \gamma)$  goes to zero as  $\beta \rightarrow 0$ , to extract eventually the finite limit

$$\lim_{\beta \rightarrow 0} \frac{n(\beta; \gamma)}{n(\beta; 1)}; \quad (7.58)$$

which we denote by  $\frac{n(0; \gamma)}{n(0; 1)}$  with a slight abuse of notation.

To proceed with the evaluation of (7.56), we first notice that the nontrivial contributions to the integral come from the values of the momentum  $q$  close to  $\pm\pi$ , an observation which motivates the change of variable  $q = \pi + \epsilon$ , and we get

$$n(\beta; \gamma) = \int_{-\pi}^{\pi} \frac{dq}{2} \cos q s_n \frac{1}{2} \left( 1 + \frac{1}{1 + \frac{2}{\sin^2 q + \beta}} \right)^{\gamma}; \quad (7.59)$$

At this point, it is natural to introduce the scaling variable

$$z = \frac{\sin \theta}{2}; \tag{7.60}$$

so that we can write the slope as

$$s_n(\theta) = \frac{1}{2} \int_{-1}^1 \frac{dz}{1+z^2} \left[ \frac{1}{2} \left( 1 + \frac{1}{1+z^2} \right)^n \right] \tag{7.61}$$

Up to now, no approximation has been done and Eq. (7.61) is exact for any finite value of  $n$ . Nevertheless, the advantage of this expression comes from the fact that the singular behaviour of the integrand in Eq. (7.56) is not present anymore in Eq. (7.61), which makes the last expression suitable for a numerical evaluation.

From now on, we consider explicitly the limit of small  $\theta$  and we extract only the term of order  $O(\theta^2)$  in Eq. (7.61), obtaining

$$s_n(\theta) \approx \frac{1}{2} \int_{-1}^1 \frac{dz}{1+z^2} \left[ \frac{1}{2} \left( 1 + \frac{1}{1+z^2} \right)^n \right] \tag{7.62}$$

which is the main result of this appendix. While we were not able to perform analytically the integral (7.62) for any real value of  $n$ , and in particular for  $n = 1$  directly related to the entanglement entropy, we provide below a simple closed expression for integer  $n \geq 2$ . The key observation is the following decomposition of the density of Rényi entropy

$$s_n(x) = \frac{1}{n} \log(x^n + (1-x)^n) = \frac{1}{n} \sum_{p=(n-1)/2}^{(n-1)/2} \log e^{i2p\theta} x + (1-x) \tag{7.63}$$

a simple identity which comes from the factorization of the polynomial  $x^n + (1-x)^n$ . We introduce for convenience the function  $f(\theta)$  as

$$f(\theta) = \frac{1}{2} \int_{-1}^1 \frac{dz}{1+z^2} \log \left[ \frac{1}{2} \left( 1 + \frac{1}{1+z^2} \right)^n e^{i2p\theta} + \frac{1}{2} \left( 1 + \frac{1}{1+z^2} \right)^n \right] + \frac{1}{2} \int_{-1}^1 \frac{dz}{1+z^2} \log \left[ \frac{1}{2} \left( 1 + \frac{1}{1+z^2} \right)^n e^{-i2p\theta} + \frac{1}{2} \left( 1 + \frac{1}{1+z^2} \right)^n \right] \tag{7.64}$$

related to  $s_n(\theta)$  by the following relation

$$s_n(\theta) = \frac{1}{n} \sum_{p=(n-1)/2}^{(n-1)/2} f(2p\theta) \tag{7.65}$$

which is a straightforward consequence of Eq. (7.63).

Interestingly, one is able to compute  $f(\theta)$  analytically, as we will show, and then a closed expression for the slope  $s_n(\theta)$  for integer  $n \geq 2$  can be provided. To do so, we first differentiate  $f(\theta)$  over  $\theta$  and we get

$$\frac{d}{d\theta} f(\theta) = \frac{1}{2} \int_{-1}^1 \frac{dz}{1+z^2} \frac{2 \sin(2p\theta)}{2^2 \cos^2(\theta) + 4z^2} = \frac{p}{2} \frac{2 \sin(2p\theta)}{2^2 \cos^2(\theta) + 4}: \tag{7.66}$$

Then, we reintegrate back and obtain

$$f(\beta) = \frac{q}{1 - 2 \sin^2(\beta/2)} - 1; \tag{7.67}$$

where the integration constant has been chosen so that  $f(0) = 0$ , a property which follows from the definition of  $f(\beta)$ . Inserting (7.67) into (7.65) we finally arrive at the expression (7.49) reported in the main text.

We conclude this appendix with the computation of the slopes  $n(\beta; \beta)$  for an initial thermal state, highlighting its discrepancies with  $n(\beta; \beta)$ . The occupation number of such state at temperature  $\beta^{-1}$  is

$$n_q = \frac{1}{e^{-\beta \cos q} + 1}; \tag{7.68}$$

and the quasiparticle ansatz of the slope gives (see Eq. (7.46))

$$n(\beta; \beta) = \frac{1}{2} \int_{-\pi}^{\pi} dq_j \sin q_j s_n \frac{1 - \frac{p}{4} \frac{2n_q(1 - n_q)}{2}}{2}; \tag{7.69}$$

While the latter expression is valid for any  $\beta$ , we are mostly interested in the low-temperature limit ( $\beta \rightarrow 1$ ), whose features are expected to be captured by CFT. After simple algebra, coming from the linearization of the dispersion around the Fermi-point  $q = \pm 2$ , one gets

$$n(\beta; \beta)' \approx \frac{1}{2} \int_{-\pi}^{\pi} dq_j s_n \frac{1 - \frac{p}{4} \frac{2n_q(1 - n_q)}{2}}{2} = \frac{1}{2} \int_{-\pi}^{\pi} dx s_n \frac{1 - \frac{p}{4} \frac{2n_q(1 - n_q)}{2}}{2}; \tag{7.70}$$

a relation valid in the limit of large  $\beta$ . A tedious but straightforward calculation of the integral in Eq. (7.70), analogous to the computation of  $n(\beta; \beta)$ , gives for integer  $n \geq 2$

$$n(\beta; \beta) = \frac{1}{n} \frac{2}{1 - p} \frac{(n-1)^2}{(n-1)^2} \frac{1}{2} \arcsin \left( \sin \frac{p}{n} \right)^2; \tag{7.71}$$

If one compares the latter formula with the logarithmic prefactor in Eq. (7.36), valid for the ground-state entanglement (both in CFT and on the lattice), one realizes that they are proportional. This can be regarded as a non-trivial consistency check of the quasiparticle ansatz with the CFT results in the presence of a defect.

In conclusion the main message is that, even if both the thermal occupation and the one induced by the staggered chemical potential localize around the Fermi points (in the limit  $\beta \rightarrow 1$  and  $\beta \rightarrow 0$  respectively) their scaling behaviour is different. Therefore, also the quasiparticle prediction gives a different result, and this is precisely the origin of the unusual discrepancies with CFT we observed.



# Chapter 8

## Domain wall melting across a defect

In this chapter, based on [12], we study the melting of a domain wall in a free-fermionic chain with a conformal defect and we describe the entanglement evolution. We find that the defect enhances quantum correlations in such a way that even the smallest scatterer leads to a linear growth of the entanglement entropy, contrasting the logarithmic behaviour in the clean system (see Ref. [224]). We propose a modification of the well-established hydrodynamic approach, which takes into account the long-range correlation generated at the defect. In particular, the steady production of correlated pairs at the defect gives rise to correlations among arbitrarily distant points, which is the origin of the linear growth of the entropy. It is important to remark that, while some exact results are already present in the literature for similar specific protocols (see e.g. Refs. [54, 225] for the dynamics, and Refs. [226, 227] for the steady state), it seems that a large-scale general theory to address this class of problems is still missing: our work aims to contribute as a step towards achieving this objective.

Before entering the details of the protocol, it is important to clarify from the beginning some important conceptual differences with the global quench analysed in Chapter 7. For instance, for the global quench we considered a non-equilibrium state, with a certain pair structure that gives rise to large-scale correlations even in the absence of defect: in particular, we found there that the more the defect is transmissive the more the entropy growth is enhanced. Here, we consider instead an initial inhomogeneous state, that is locally at equilibrium, and the only source of long-distance correlation is precisely the defect. As we will see, we show that the maximum entropy growth occurs when the transmission and reflection probabilities are equal.

### 8.1 The protocol and its hydrodynamic limit

We consider a 1D quantum chain of free fermions with  $N$  sites and with nearest-neighbour hopping with a conformal defect [54] located at the center of the system. The Hamiltonian is

$$\hat{H} = \sum_{x;x^0=N+1}^N h_{x;x^0} c_x^\dagger c_{x^0} \quad (8.1)$$

with

$$h_{x;x^0} = \frac{1}{2} (c_{x;x^0+1} + c_{x+1;x^0}); \quad \delta_{x;x^0} \in \{0, 1\}; \quad (8.2)$$

being the bulk contribution, and the defect term is

$$h_{0;1} = h_{1;0} = \frac{1}{2}; \quad h_{0;0} = h_{1;1} = \frac{1}{2} \frac{1}{1 - \frac{1}{2}}. \quad (8.3)$$

Here  $c_x^y, \hat{c}_x$  are the creation and annihilation operators of fermions at site  $x$ , satisfying the usual anticommutation relations  $\{c_x^y, \hat{c}_x\} = \delta_{xx^0}$ .

For  $\gamma = 1$  the Hamiltonian (8.1) reduces to a standard hopping model, and the defect is said to be purely transmissive. In contrast, for  $\gamma = 0$  the two halves are decoupled and the defect is completely reflective.

We mention that the specific structure of the defect (8.3) does not spoil the exact solvability of the model. In particular, it keeps the model free, and everything is ultimately encoded in the single particle spectrum, which turns out to be particularly simple. The single-particle energies are

$$E_q = \cos(k_q); \quad k_q = \frac{q}{2N}; \quad q = 1; \dots; 2N; \quad (8.4)$$

for any value of  $\gamma$  [53], which means that the momenta quantization is not affected by the defect. Moreover, the single-particle eigenstates of  $\hat{H}$  can be related to the one in the purely transmissive case, via a specific rescaling in the left/right half chain as [53]

$$\psi_q(x) = \left( \theta(x) \psi_q^+ + (1 - \theta(x)) \psi_q^- \right) \sin(k_q x) = \frac{1}{N}; \quad (8.5)$$

with  $\theta(x)$  the Heaviside step function, and  $\psi_q^\pm = [1 - (1 - \gamma)^q \frac{1}{1 - \frac{1}{2}}]^{1/2}$ . Also, in the formal limit  $N \rightarrow \infty$ , the spectrum becomes purely continuous (say, no bound states are present), and the associated scattering problem gives rise to the following transmission/reflection probabilities [53, 218]

$$T(k) = \frac{1}{2}; \quad R(k) = \frac{1}{2}; \quad (8.6)$$

which do not depend on the momentum  $k$  of the incoming asymptotic particle. In the upcoming discussion, we will not explicitly utilize all the exact finite-size properties discussed thus far. Instead, we will focus solely on tracking the scattering properties, as they are expected to be the only relevant ones in the hydrodynamic limit.

We consider an initial state  $|j_0\rangle$ , dubbed as domain wall, as

$$|j_0\rangle = \prod_{x=N+1}^{\infty} \hat{c}_x^\dagger |1\rangle_x \prod_{x=1}^{\infty} |0\rangle_x; \quad (8.7)$$

with  $|1\rangle_x; |0\rangle_x$  being the filled/empty state at site  $x$ . This state, is locally at equilibrium, since both  $|1\rangle; |0\rangle$  are eigenstates, and a non-trivial dynamics of  $|j_0\rangle$  with the hamiltonian  $\hat{H}$  occurs due to the hopping across the interface. We focus on the hydrodynamic limit of the protocol, where the system size is infinite ( $N \rightarrow \infty$ ) and we consider the scaling limit

$$x; t \rightarrow \infty; \quad x = t \text{ fixed}; \quad (8.8)$$

corresponding to a large-scale ballistic dynamics. In this limit, we regard the position  $x$  as a continuous variable, and the (single-particle) momentum  $k$  belongs to the first Brillouin zone  $k \in [-\frac{\pi}{2}; \frac{\pi}{2}]$ . The 'essential' local information of the microscopic state  $|j_0\rangle$  is ultimately encoded in the local fermionic occupation number

$$n_0(x; k) = \begin{cases} 1; & \text{if } x = 0 \text{ and } k = \frac{\pi}{2}; \\ 0; & \text{otherwise} \end{cases} \quad (8.9)$$

In the absence of the defect ( $\epsilon = 1$ ), the evolution is completely understood in terms of Euler equations. These amount to characterize the time-evolved state  $|\psi_t\rangle = e^{-iHt} |\psi_0\rangle$  as a local occupation function  $n_t(x, k)$  satisfying

$$(\partial_t + v(k)\partial_x)n_t(x, k) = 0; \quad (8.10)$$

with  $v(k) = \sin k$  being the group velocity at momentum  $k$ . Eq. (8.10) can be simply solved as

$$n_t(x, k) = n_0(x - t \sin k; k); \quad (8.11)$$

i.e. the occupation is always equal to 0 and 1 only, and a sharp separation between these two values occur at a local Fermi contour. Intuitively, this solution encodes the fact that, in a semiclassical picture, each particle of momentum  $k$  moves freely along the system at a given velocity  $v(k)$ . While (8.11) cannot capture all the details of the microscopic state, its predictivity is related to the fact that no long-range correlations are generated in time, and distinct spatially separated regions can be always considered effectively uncorrelated. As we will see, this is not the case for a permeable defect  $\epsilon < 1$ , and dynamically generated macroscopic correlations have a huge impact on the entanglement growth. Nevertheless, as pointed out in Ref. [225], a description in terms of a local occupation function is still expected as far as the evolution of observables localized in small regions of space (say, the particle density or the current) is concerned. We provide below a semiclassical picture for the time evolution.

Let us consider a single particle localized at position  $x < 0$  far away from the defect with a given momentum  $k > 0$ . At time  $t = |x/v(k)|$  it will hit the defect, being partially scattered in two left/right moving wave packets, with probability given by the  $R(\epsilon); T(\epsilon)$  respectively<sup>1</sup>. Accordingly, for  $t > |x/v(k)|$  its contribution to the local occupation in the phase space is expected to be a sum of two delta functions, localized at the positions/momenta of the two wave packets weighted with the scattering probabilities. If we now consider a many-body state, since the system is free, it is sufficient to sum all the single-particle contributions to eventually reconstruct the dynamics. Eventually, one ends up in an ansatz for the occupation function  $n_t^{(\epsilon)}(x, k)$  that is

$$n_t^{(\epsilon)}(x, k) = \frac{1}{2} (\epsilon - x) n_t(x, k) + \frac{1}{2} (\epsilon + x) (1 - \epsilon^2) n_t(-x, -k) + n_t(x, k); \quad (8.12)$$

for the domain-wall initial state, as illustrated in Fig. 8.1. In our notations  $n_t^{(\epsilon=1)} = n_t$ , is the solution Eq. (8.11) obtained when the defect is absent.

The occupation function (8.12) gives us access to the asymptotic profiles of conserved charges as integrals over the momentum  $k$  (see [228]). For instance, the particle density profile for  $0 < x < t$  is

$$n_t^{(\epsilon)}(x) = \int \frac{dk}{2} n_t^{(\epsilon)}(x, k) = \frac{1}{2} \arccos(\epsilon - x/t); \quad (8.13)$$

For  $x < 0$ , the profile can be obtained via particle-hole symmetry, and it reads

$$n_t^{(\epsilon)}(x) = 1 - \frac{1}{2} \arccos(\epsilon + x/t); \quad t < x < 0; \quad (8.14)$$

Outside the space-time region discussed so far, i.e., for  $x > t$ , the system is basically frozen, and the occupation number is  $n_t^{(\epsilon)} = 1$  ( $n_t^{(\epsilon)} = 0$ ) on the left (right) half-chain.

<sup>1</sup>In principle, the scattering probability are  $k$  dependent, albeit this is not the case for the conformal defect we are studying.

Figure 8.1: Illustration of the evolution of the Fermi occupation function  $n_t^{(i)}(x; k)$ . The defect, located at  $x = 0$ , is represented as a yellow line. The light-grey area refers to a value of the occupation being 1. Similarly, the value in the white region is 0, in the red one is  $n_t^{(i)} = \frac{1}{2}$ , and in the blue one is  $n_t^{(i)} = 1 - \frac{1}{2}$ .

A crucial observation is that the local occupation function (8.12) for  $t \in \mathbb{1}$  assumes values which are different from 0 and 1. Consequently, the local density of entropy is non-vanishing, and long-range entanglement is generated. Physically, this phenomenology roots back to the correlations between reflected and transmitted modes originating at the defect.

## 8.2 Entanglement dynamics

We now move to our main goal, which is the characterization of the entanglement dynamics. Specifically, we focus on a spatial bipartition of the system  $A \cup B$  with a reduced density matrix  $\hat{\rho}(A) = \text{tr}_B \rho_{ij}$  of a given state  $\rho_{ij}$ . The  $n$ -Renyi entropy is

$$S_n = \frac{1}{1-n} \log \text{tr}[\hat{\rho}(A)^n] \quad (8.15)$$

that provides the entanglement entropy in the limit  $n \rightarrow 1$ , i.e.  $S_1(A; t) = -\text{tr}[\hat{\rho}_t(A) \log \hat{\rho}_t(A)]$ . A microscopic description of the entanglement dynamics is usually very demanding even in the absence of defect, due to the non-equilibrium and non-homogeneous character of the quench problem under analysis (see Ref. [54] for details regarding our protocol). However, the extensive behavior of the entropy of small regions of space is well captured by a simple semiclassical approach, which requires only the knowledge of the local occupation function. Indeed, we recall the definition of the local Yang-Yang Renyi entropy [226, 229, 231]

$$s_n(x) = \frac{1}{1-n} \int \frac{dk}{2\pi} \log [n(x; k)^n + (1 - n(x; k))^n]; \quad (8.16)$$

and for a small region of space  $A = [x_0, x_0 + dx]$  the Renyi entropy is approximately  $S_n \approx \int_{x_0}^{x_0+dx} s_n(x) dx$ . Moreover, whenever distinct points of the region  $A$  can be effectively considered uncorrelated, one expects that

$$S_n \approx \int_A dx s_n(x); \quad (8.17)$$

If there are non-zero correlations between nearby spatial points, it is possible that there are still subleading corrections to this prediction: however, the semiclassical result is expected to give the

correct leading extensive behavior in the latter case. In contrast, whenever distant points of  $A$  have non-trivial correlation, as it happens for the pairs of specular points  $(x; -x)$  in our protocol, one needs to be more careful, and the semiclassical prediction needs further modification to be predictive.

Let us first consider the simple case  $A = (-1; x_0]$  with  $x_0 < 0$ . Here, no pairs of correlated points belong to  $A$ , and one expects that Eq. (8.17) can be considered valid. In particular, we predict

$$S_n(t) = \int_A dx s_n(x; t) = \frac{N_t(A)}{1-n} \log \left( 2^n + (1-2)^n \right); \quad (8.18)$$

with

$$N_t([ -1; x_0]) = \frac{t}{1 - \frac{x_0^2}{t^2}} \arccos \frac{x_0}{t}; \quad (8.19)$$

For  $x_0 = 0$ , we get the entropy between the two half chains that is (see also Ref. [54])

$$S_n(t) = \frac{t}{(1-n)} \log \left( 2^n + (1-2)^n \right); \quad (8.20)$$

We mention that in the absence of defect, previous studies highlighted a half-system entanglement growth  $S_n(t) \sim \frac{1}{12} \frac{(n+1)}{n} \log(t)$ , arising from subleading contributions [232, 234]. This is compatible with Eq. (8.20), as (8.20) captures only the semiclassical extensive behavior, which vanishes at  $n = 1$ . Interestingly, there is a sharp transition from logarithmic to linear law that is observed even for values of  $n$  very close to unit, see Fig. 8.2. For a comparison with exact lattice calculations, and we also refer to e.g. Refs. [224, 232] for details on the numerical implementation.

Eq. (8.18) fails to capture the behaviour of entanglement for a subsystem straddling the defect because it counts also for the pairs of entangled particles which are both in  $A$ , but on different sides of the defect. To understand the failure, it is sufficient to observe that the prediction (8.18) is not symmetric under  $A \leftrightarrow B$ , which is however an exact property satisfied by  $S_n(A)$ . Such over-counting is however easily cured within the quasiparticle picture [219, 231]. In this respect, Eq. (8.18) usually overestimates the entropy in the presence of long-range correlations, and contributions with pairs of correlated particles both belonging to  $A$  have to be subtracted explicitly.

To show this mechanism, we first discuss the case  $A = [-1; x_0]$  with  $x_0 > 0$ . On one hand, we know at the microscopic level (using particle-hole symmetry and  $S_n(A; t) = S_n(B; t)$ ) that

$$S_n([-1; x_0]; t) = S_n([-1; -x_0]; t) \quad (8.21)$$

has to hold. On the other hand, according to the quasiparticle picture, we have to subtract from (8.18) the contribution coming from pairs of particles belonging to  $A$ : this comes precisely from the highly correlated region  $[-x_0; x_0]$ , and therefore the quasiparticle-picture gives us

$$S_n(A; t) = \int_{A \setminus [-x_0; x_0]} dx s_n(x; t) = \int_{(-1; -x_0]} dx s_n(x; t); \quad (8.22)$$

Indeed, both microscopic considerations and the quasiparticle picture lead to the same result, which is a non-trivial consistency check. We checked numerically the validity of these statements as shown in Fig. 8.2-(b).

This approach can be easily generalized to more complicated regions: one only needs to remove from  $A$  the (maximal) subset which have a specular image belonging to  $A$  too, and

Figure 8.2: (a) { Half-system entanglement entropy of  $A = [1; 0]$ , denoted by  $S_1(0; t)$ , for different values of  $t$  as function of time. Symbols show the numerical data while the full lines (for  $t \leq 1$ ) are given by the analytical prediction Eq. (8.20). At  $t = 1$ , the half-system entanglement entropy is  $S_1 = 1 - 6 \log(t) + \text{const}$  (dashed line) [234], and it is significantly smaller than the value obtained at  $t < 1$ . (b) { Entanglement profiles for  $A = [1; x_0]$  plotted as function of  $x_0$  at different times and fixed  $t = 0.7$ . Symbols show the numerical data while the full lines are given by Eq. (8.18). As expected from particle-hole symmetry, the profile is symmetric under  $x_0 \leftrightarrow 1 - x_0$ .

Figure 8.3: (a) Numerical results for the entanglement of the symmetric interval  $A = [x_0; x_0]$  for different values of  $x_0$  as function of time. The dashed horizontal line marks the plateau  $S_1 = 1 - 3 \log(x_0) + 2 \ln 2$  for  $\nu = 1$ . (b) Plot of  $r(t)$ , extracted as a function of time for some subsystems sizes ( $x_0 = 20, x_0^0 = 40, x_0^{00} = 60$ ) as a function of  $t$ . The full line shows the behaviour of  $c_e(t)$ , given by Eq. (8.26).

compute semiclassically the entropy of the resulting region. Similar conclusions were obtained in Ref. [226], where the steady state, corresponding to  $\nu = 1$ , was considered (albeit the defect was not conformal). In particular, Ref. [226] have shown the presence of an extensive mutual information between specular regions across the interface, related to the violation of the simple ansatz (8.17).

### 8.2.1 Subleading behavior

An interesting case we want to discuss explicitly is for  $A = [x_0; x_0]$  ( $x_0 > 0$ ), that is an interval placed symmetrically wrt the center. According to the quasi-particle picture, we simply expect

$$S_n(t) = 0 \quad (8.23)$$

This is due to the fact that no shared pairs are present between  $A$  and its complement. The vanishing of the entropy is not 'exact', and it only holds at the semiclassical level. Indeed, the 'subleading' contribution corrections are the only non-vanishing ones. For the homogeneous Hamiltonian ( $\nu = 1$ ), a useful way to incorporate quantum fluctuations in our description is established by quantum generalised hydrodynamics [224, 232, 233, 235, 239]. According to this theory, the relevant contribution to the entanglement in zero-entropy states is given by linear quantum fluctuations around the Fermi contour. We report below the predictions for the entropy at  $\nu = 1$ , which indeed coincides with the one in Refs. [233, 240] obtained via lattice methods

$$S_n([x_0; x_0]; t) = \frac{n+1}{12n} \log x_0^2 (1 - x_0^2/t^2)^3 + 2 \ln 2 \quad (8.24)$$

with  $\ln 2$  a known non-universal amplitude [241, 242] ( $\ln 2 \approx 0.6931$ ). For  $t > x_0$ , Eq. (8.24) predicts a saturation of the half-system entanglement to the value  $S_1([x_0; x_0]; t > x_0) = 1 - 3 \log(x_0) + 2 \ln 2$ . Crucially, the growth of the stationary value as a function of the subsystem size is logarithmic, namely subextensive.

Numerical results for the lattice model reveal a similar behaviour for the half-system entanglement even in the presence of the defect  $2(0; 1)$ , see Fig. 8.3-(a). In particular, in the large time limit, the entropy is expected to grow logarithmically in the subsystem size, namely

$$S_1([x_0; x_0]; 1) \sim \frac{r(\epsilon)}{3} \log(x_0) + \dots \quad (8.25)$$

Here  $r(\epsilon)$  is just a dimensionless parameter which depends on  $\epsilon$ , and we fit numerically. The perfect collapse in Fig. 8.3-(b) of the fitted  $r(\epsilon)$  for different pairs  $x_0; x_0^0$  is in agreement with the conjectured behaviour of Eq. (8.25).

Surprisingly, we found that  $r(\epsilon)$  is numerically consistent with the effective central charge appearing in the critical ground-state entanglement of free fermions with defects [218] given by

$$c_e(\epsilon) = \frac{6}{2} (1 + \epsilon) \text{Li}_2(\epsilon) + (1 - \epsilon) \text{Li}_2(\epsilon^{-1}) + \frac{h}{2} (1 + \epsilon) \log(1 + \epsilon) + (1 - \epsilon) \log(1 - \epsilon) \log \epsilon; \quad (8.26)$$

that satisfies  $c_e(0) = 0$  and  $c_e(1) = 1$ . Clearly, both  $r(\epsilon)$  and  $c_e(\epsilon)$ , but we are not sure if universal very small discrepancies at finite  $\epsilon$ . Our conjecture is that  $c_e(\epsilon) = r(\epsilon)$ ; moreover, we claim that an underlying (defect) CFT could be able to describe the protocol we consider in our work in the context of quantum generalized hydrodynamics, similarly as it happens in the homogeneous case ( $\epsilon = 1$ ). We hope to come back to this problem in the future.

### 8.3 Concluding remarks

We conclude this chapter with some final remarks. We have shown that long-range correlations are generated in the dynamics of a domain wall initial state whenever a single localised defect is present. In particular, a linear growth of entropy is observed, which is entirely due to the permeable defect. We have provided some analytical predictions in the case of a conformal defect for a free fermionic chain, and we think that the underlying mechanism is similar for other defects/systems as long as the ballistic spreading dominates the dynamics.

This observation has severe consequences for any possible formulation of large-scale hydrodynamic theory in the presence of defects, since, as far as I know, there are no systematic ways to keep track of these long-range correlations. In particular, the quasi-particle picture presented here, that is a variation of [219], is far from being a theory or a method, and it only applies to some case-by-case protocols: e.g., in the way it is formulated, it is not even predictive for the global quench of Chapter 7, where the same microscopic Hamiltonian has been considered.

We are confident that, even for free fermions, the local occupation numbers  $n_t(x; k)$  alone cannot be sufficient to describe the evolution of some observables: this is the case of entropy, but also for correlation functions between specular points. Moreover, we believe that even (strictly) local observables might not be described quantitatively with a self-consistent equation for  $n_t(x; k)$ . For example, one could naively argue that the Euler equations with properly chosen boundary conditions at  $x = 0$ , could be sufficient to describe the evolution of  $n_t(x; k)$ . However, this is probably not the case: if one considers a highly correlated initial state, quantum interference between left/right particles moving particles hitting the defect is expected to have a huge impact on the macroscopic dynamics, and it is probably not captured by any semiclassical approach. For example, it is not clear to us, how to study systematically the time-reversal of the protocol considered in this chapter.

## Chapter 9

# Outlook

We point out some possible directions deserving further investigation. While we think that the whole story about symmetry resolution has been more or less understood both for finite spin systems and for quantum field theories with a clear lattice realization, a unifying theory regarding the symmetries of (algebra of) observables and their relation to quantum entanglement seems to be missing: some important steps have been provided in [243, 244].

This is far more than a mere mathematical curiosity, as for many relevant systems the usual notion of tensor product of two Hilbert spaces, associated with complementary classes of observables, simply does not apply, and it is not even clear how to formulate a good notion of symmetry resolution for those systems. For example, for lattice gauge theories the algebra of gauge-invariant observables is not realized as a tensor product due to the appearance of sectors [245]. Also, semilocal observables that have proven to play a crucial role in thermalization (see [246]) do not have a local realization in the corresponding microscopic Hilbert space. Moreover, we emphasize that, strictly speaking, systems with infinite degrees of freedom, that is the case for spin systems in infinite lattices, quantum field theory, gravity, are not even described by separable Hilbert spaces, while they can be understood as von Neumann algebras of type II and III (see Ref. [137] for a review). For the aforementioned reasons, we would like to understand better the relation between entanglement and symmetry from the point of view of the algebra of observables, rather than overfocus on their representation over 'abstract' Hilbert spaces.

Finally, from our point of view, it seems that the understanding of the dynamics of quantum many-body systems, particularly concerning the ballistic spreading of quantum correlations, is disappointingly lacking. Specifically, as we have demonstrated through two specific protocols involving free systems, the presence of long-range correlations can play a significant role, especially in the context of global quenches or defects. In the case of interacting systems, the situation may be even more challenging, as interactions can introduce additional sources of long-range correlations. There, while it may be tempting to describe quantum systems solely in terms of their local (generalized) Gibbs ensemble, it is evident that this perspective is profoundly unsatisfactory when entanglement (and more generally, non-local observables) comes into play. Surprisingly, even if tons of dynamical protocols have been considered in the last decades, the emergence and the importance of those long-range correlations have been mostly overlooked. Recent works, in the context Mesoscopic Fluctuation Theory, pointed out their explicit presence for both free [223] and interacting systems [247, 248] and their role in the dynamics of observables. We also mention that the so-called quantum generalized hydrodynamics, as formulated and applied in Refs. [236], does not solve the aforementioned issues, as it primarily addresses "quantum corrections" arising from short-range correlations.

In summary, two fundamental questions demand attention: how can we quantify systematically correlations between distant points and comprehend their dynamics within a mesoscopic hydrodynamic framework, and how can we establish their relationship with the expectation values of observables at intermediate times?

# Acknowledgments

After 4 years of PhD, I have no doubt that the main lesson I learned about Science is what is made of: beyond any equation, any plot, and any theory there are people with their own idea, feelings, beliefs, and prejudices. Most of the work pursued to write this thesis would have been nonexistent without the help, discussions and support from all the people I encountered during my path.

I would first thank my supervisor, Pasquale, for his guidance in these years. I am in debt with my collaborators Paola, Sara, Viktor, Michele, Cecilia, Olalla, Lucia, Riccarda, Pantelis, Stefano, Federico, Andrea, Carlo, Mario, Guido, Alessandro. I am particularly grateful with Olalla, Viktor and Benoit: my personal growth (if present ?) is mostly due to the experience I had abroad as a visitor. Your kind hospitality will always be remembered with a deep sense of gratitude.

Trieste and SISSA have a special place in my hearth: this wonderful experience has been possible thanks to all my friends, who stood me when I was down, and, most importantly, when I was not. A special thanks go to Elaheh, who always encouraged me and believed in me. I cannot give a meaning to these years, without thinking about all these beautiful people I encountered.

So Long, and Thanks for All the Fish (D.A.).



# Bibliography

- [1] L. Capizzi, P. Ruggiero, and P. Calabrese, "Symmetry resolved entanglement entropy of excited states in a CFT", *J. Stat. Mech.* **2007**, 073101 (2020).
- [2] D. X. Horvath, L. Capizzi, and P. Calabrese, "U(1) symmetry resolved entanglement in free 1+1 dimensional field theories via form factor bootstrap", *JHEP* **05**, 197 (2021).
- [3] L. Capizzi and P. Calabrese, "Symmetry resolved relative entropies and distances in conformal field theory", *JHEP* **10**, 195 (2021).
- [4] L. Capizzi, D. X. Horvath, P. Calabrese, and O. A. Castro-Alvaredo, "Entanglement of the 3-state Potts model via form factor bootstrap: total and symmetry resolved entropies", *JHEP* **05**, 113 (2022).
- [5] L. Capizzi, O. A. Castro-Alvaredo, C. De Fazio, M. Mazzoni, and L. Santamaria-Sanz, "Symmetry resolved entanglement of excited states in quantum field theory. Part I. Free theories, twist fields and qubits", *JHEP* **12**, 127 (2022).
- [6] L. Capizzi, C. De Fazio, M. Mazzoni, L. Santamaria-Sanz, and O. A. Castro-Alvaredo, "Symmetry resolved entanglement of excited states in quantum field theory. Part II. Numerics, interacting theories and higher dimensions", *JHEP* **12**, 128 (2022).
- [7] L. Capizzi, M. Mazzoni, and O. A. Castro-Alvaredo, "Symmetry resolved entanglement of excited states in quantum field theory. Part III. Bosonic and fermionic negativity", *JHEP* **06**, 074 (2023).
- [8] L. Capizzi, S. Murciano, and P. Calabrese, "Renyi entropy and negativity for massless Dirac fermions at conformal interfaces and junctions", *JHEP* **08**, 171 (2022).
- [9] L. Capizzi, S. Murciano, and P. Calabrese, "Renyi entropy and negativity for massless complex boson at conformal interfaces and junctions", *JHEP* **11**, 105 (2022).
- [10] L. Capizzi and V. Eisler, "Entanglement evolution after a global quench across a conformal defect", *SciPost Phys.* **14**, 070 (2023).
- [11] L. Capizzi and V. Eisler, "Zero-mode entanglement across a conformal defect", *J. Stat. Mech.* **2305**, 053109 (2023).
- [12] L. Capizzi, S. Scopa, F. Rottoli, and P. Calabrese, "Domain wall melting across a defect", *EPL* **141**, 31002 (2023).
- [13] L. Capizzi, G. Giachetti, A. Santini, and M. Collura, "Spreading of a local excitation in a quantum hierarchical model", *Phys. Rev. B* **106**, 134210 (2022).
- [14] R. Bonsignori, L. Capizzi, and P. Panopoulos, "Boundary Symmetry Breaking in CFT and the string order parameter", *JHEP* **05**, 027 (2023).

- [15] L. Capizzi, S. Murciano, and P. Calabrese, "Full counting statistics and symmetry resolved entanglement for free conformal theories with interface defects", (2023).
- [16] L. Capizzi, C. Vanoni, P. Calabrese, and A. Gambassi, "A hydrodynamic approach to Stark localization", (2023).
- [17] E. Schrödinger, "Discussion of probability relations between separated systems", in *Mathematical proceedings of the cambridge philosophical society*, Vol. 31, 4 (Cambridge University Press, 1935), pp. 555{563.
- [18] A. Einstein, B. Podolsky, and N. Rosen, "Can quantum-mechanical description of physical reality be considered complete?", *Phys. Rev* **47**, 777 (1935).
- [19] J. Bromberg, "Twentieth century-the born-einstein letters. correspondence between albert einstein and max and hedwig born from 1916 to 1955 with commentaries by max born.", *The British Journal for the History of Science* **6**, 222{223 (1972).
- [20] R. P. Feynman, "Simulating physics with computers, 1981", *International Journal of Theoretical Physics* **21**, <https://doi.org/10.1007/BF02650179> (1981).
- [21] P. W. Shor, "Algorithms for quantum computation: discrete logarithms and factoring", in *Proceedings 35th annual symposium on foundations of computer science* (Ieee, 1994), pp. 124{134.
- [22] S. Wiesner, "Conjugate coding", *ACM Sigact News* **15**, 78{88 (1983).
- [23] C. H. Bennett, G. Brassard, C. Crépeau, R. Jozsa, A. Peres, and W. K. Wootters, "Teleporting an unknown quantum state via dual classical and einstein-podolsky-rosen channels", *PRL* **70**, 1895 (1993).
- [24] X.-G. Wen, "Topological orders in rigid states", *International Journal of Modern Physics B* **4**, 239{271 (1990).
- [25] D. C. Tsui, H. L. Stormer, and A. C. Gossard, "Two-dimensional magnetotransport in the extreme quantum limit", *PRL* **48**, 1559 (1982).
- [26] R. B. Laughlin, "Anomalous quantum hall effect: an incompressible quantum fluid with fractionally charged excitations", *PRL* **50**, 1395 (1983).
- [27] S. Ostlund and S. Rommer, "Thermodynamic limit of density matrix renormalization", *PRL* **75**, 3537 (1995).
- [28] S. Rommer and S. Ostlund, "Class of ansatz wave functions for one-dimensional spin systems and their relation to the density matrix renormalization group", *PRB* **55**, 2164 (1997).
- [29] U. Schollwöck, "The density-matrix renormalization group in the age of matrix product states", *Annals of physics* **326**, 96{192 (2011).
- [30] R. Orús, "A practical introduction to tensor networks: matrix product states and projected entangled pair states", *Annals of physics* **349**, 117{158 (2014).
- [31] J. D. Bekenstein, "Black holes and entropy", *Phys. Rev. D* **7**, 2333 (1973).
- [32] S. W. Hawking, "Black hole explosions?", *Nature* **248**, 30{31 (1974).
- [33] S. Ryu and T. Takayanagi, "Holographic derivation of entanglement entropy from the anti-de sitter space/conformal field theory correspondence", *PRL* **96**, 181602 (2006).

- [34] S. Ryu and T. Takayanagi, "Aspects of holographic entanglement entropy", *Journal of High Energy Physics* **2006**, 045 (2006).
- [35] J. Maldacena, "The large-N limit of superconformal field theories and supergravity", *International journal of theoretical physics* **38**, 1113(1133 (1999).
- [36] E. Chitambar, D. Leung, L. Marcinska, M. Ozols, and A. Winter, "Everything you always wanted to know about locc (but were afraid to ask)", *Communications in Mathematical Physics* **328**, 303(326 (2014).
- [37] E. H. Lieb and M. B. Ruskai, "A fundamental property of quantum-mechanical entropy", *PRL* **30**, 434 (1973).
- [38] E. H. Lieb and M. B. Ruskai, "Proof of the strong subadditivity of quantum-mechanical entropy", *Les rencontres physiciens-mathématiciens de Strasbourg-RCP259*, 36(55 (1973).
- [39] M. A. Nielsen and I. Chuang, *Quantum computation and quantum information*, 2002.
- [40] A. De Pasquale, P. Facchi, V. Giovannetti, G. Parisi, S. Pascazio, and A. Scardicchio, "Statistical distribution of the local purity in a large quantum system", *J. Phys. A: Math. Theor.* **45**, 015308 (2011).
- [41] S. Dutta and T. Faulkner, "A canonical purification for the entanglement wedge cross-section", *JHEP* **2021**, 1(49 (2021).
- [42] G. Vidal and R. F. Werner, "Computable measure of entanglement", *Phys. Rev. A* **65**, 032314 (2002).
- [43] M. B. Plenio, "Logarithmic negativity: a full entanglement monotone that is not convex", *PRL* **95**, 090503 (2005).
- [44] L. Amico, R. Fazio, A. Osterloh, and V. Vedral, "Entanglement in many-body systems", *Rev. Mod. Phys.* **80**, 517 (2008).
- [45] J. Eisert, M. Cramer, and M. B. Plenio, "Colloquium: area laws for the entanglement entropy", *Rev. Mod. Phys.* **82**, 277 (2010).
- [46] P. Calabrese and J. Cardy, "Entanglement entropy and conformal field theory", *J. Phys. A* **42**, 504005 (2009).
- [47] J. L. Cardy, O. A. Castro-Alvaredo, and B. Doyon, "Form factors of branch-point twist fields in quantum integrable models and entanglement entropy", *J. Stat. Phys.* **130**, 129(168 (2008).
- [48] P. Calabrese, J. Cardy, and B. Doyon, "Entanglement entropy in extended quantum systems", *J. Phys. A: Math. Theor.* **42**, 10.1088/1751-8121/42/50/500301 (2009).
- [49] A. Lukin, M. Rispoli, R. Schittko, M. E. Tai, A. M. Kaufman, S. Choi, V. Khemani, J. Leonard, and M. Greiner, "Probing entanglement in a many-body localized system", *Science* **364**, 256(260 (2019).
- [50] J. C. Xavier, F. C. Alcaraz, and G. Sierra, "Equipartition of the entanglement entropy", *Phys. Rev. B* **98**, 041106 (2018).
- [51] M. Goldstein and E. Sela, "Symmetry-resolved entanglement in many-body systems", *Phys. Rev. Lett.* **120**, 200602 (2018).
- [52] C. L. Kane and M. P. A. Fisher, "Transmission through barriers and resonant tunneling in an interacting one-dimensional electron gas", *Phys. Rev. B* **46**, 15233(15262 (1992).

- [53] I. Peschel and V. Eisler, "Exact results for the entanglement across defects in critical chains", *J. Phys. A: Math. Theor.* **45**, 155301 (2012).
- [54] V. Eisler and I. Peschel, "On entanglement evolution across defects in critical chains", *EPL* **99**, 20001 (2012).
- [55] K. Sakai and Y. Satoh, "Entanglement through conformal interfaces", *JHEP* **12**, 001 (2008).
- [56] P. Calabrese and J. Cardy, "Quantum quenches in 1+1 dimensional conformal field theories", *J. Stat. Mech.: Theor. Exp.* **2016**, 10.1088/1742-5468/2016/06/064003 (2016).
- [57] N. Lorenz and S. Rachel, "Spin-resolved entanglement spectroscopy of critical spin chains and Luttinger liquids", *J. Stat. Mech.* **2014**, 10.1088/1742-5468/2014/11/P11013 (2014).
- [58] E. Cornfeld, M. Goldstein, and E. Sela, "Imbalance entanglement: symmetry decomposition of negativity", *Phys. Rev. A* **98**, 032302 (2018).
- [59] C. Callan and F. Wilczek, "On geometric entropy", *Commun. Math. Phys.* **133**, 55 (1994).
- [60] P. Calabrese and J. L. Cardy, "Entanglement entropy and quantum field theory", *J. Stat. Mech.* **0406**, P06002 (2004).
- [61] V. G. Knizhnik, "Analytic Fields on Riemann Surfaces. 2", *Commun. Math. Phys.* **112**, 567 (1987).
- [62] L. J. Dixon, D. Friedan, E. J. Martinec, and S. H. Shenker, "The Conformal Field Theory of Orbifolds", *Nucl. Phys. B* **282**, 13 (1987).
- [63] O. A. Castro-Alvaredo and B. Doyon, "Bi-partite entanglement entropy in integrable models with backscattering", *J. Phys. A* **41**, 275203 (2008).
- [64] O. A. Castro-Alvaredo and B. Doyon, "Bi-partite entanglement entropy in massive 1+1-dimensional quantum field theories", *J. Phys. A* **42**, 504006 (2009).
- [65] D. X. Horvath and P. Calabrese, "Symmetry resolved entanglement in integrable field theories via form factor bootstrap", *JHEP* **11**, 131 (2020).
- [66] S. Murciano, G. Di Giulio, and P. Calabrese, "Entanglement and symmetry resolution in two dimensional free quantum field theories", *JHEP* **08**, 073 (2020).
- [67] D. X. Horvath, P. Calabrese, and O. A. Castro-Alvaredo, "Branch Point Twist Field Form Factors in the sine-Gordon Model II: Composite Twist Fields and Symmetry Resolved Entanglement", *SciPost Phys.* **12**, 088 (2022).
- [68] B. Berg, M. Karowski, and P. Weisz, "Construction of Green Functions from an Exact S Matrix", *Phys. Rev. D* **19**, 2477 (1979).
- [69] A. N. Kirillov and F. A. Smirnov, "A Representation of the Current Algebra Connected With the SU(2) Invariant Thirring Model", *Phys. Lett. B* **198**, 506 (1987).
- [70] F. Smirnov, *Form factors in completely integrable models of quantum field theory* Advanced series in mathematical physics (World Scientific, 1992).
- [71] G. Del no, P. Simonetti, and J. L. Cardy, "Asymptotic factorization of form-factors in two-dimensional quantum field theory", *Phys. Lett. B* **387**, 327 (1996).
- [72] C. Efthimiou and A. LeClair, "Particle-field duality and form factors from vertex operators", *Commun. Math. Phys.* **171**, 10.1007/BF02104677 (1995).

- [73] M. Karowski and P. Weisz, "Exact Form-Factors in (1+1)-Dimensional Field Theoretic Models with Soliton Behavior", *Nucl. Phys. B* **139**, 455{476 (1978).
- [74] E. Marino, B. Schroer, and J. Swieca, "Euclidean functional integral approach for disorder variables and kinks", *Nucl. Phys. B* **200**, 473{497 (1982).
- [75] D. Bianchini and O. A. Castro-Alvaredo, "Branch Point Twist Field Correlators in the Massive Free Boson Theory", *Nucl. Phys. B* **913**, 879{911 (2016).
- [76] H. Casini, C. D. Fosco, and M. Huerta, "Entanglement and alpha entropies for a massive Dirac field in two dimensions", *J. Stat. Mech.* **0507**, P07007 (2005).
- [77] O. A. Castro-Alvaredo, C. De Fazio, B. Doyon, and I. M. Szecsenyi, "Entanglement content of quantum particle excitations. Part I. Free field theory", *JHEP* **10**, 039 (2018).
- [78] H. Casini and M. Huerta, "Entanglement entropy in free quantum field theory", *J. Phys. A* **42**, 504007 (2009).
- [79] M. Sato, T. Miwa, and M. Jimbo, "Holonomic Quantum Fields. 4.", *Publ. Res. Inst. Math. Sci. Kyoto* **15**, 871{972 (1979).
- [80] I. S. Gradshteyn and I. M. Ryzhik, Table of integrals, series, and products (Academic press, 2014).
- [81] H. M. Wiseman and J. A. Vaccaro, "Entanglement of indistinguishable particles shared between two parties", *Phys. Rev. Lett.* **91**, 097902 (2003).
- [82] M. Kiefer-Emmanouilidis, R. Unanyan, J. Sirker, and M. Fleischhauer, "Bounds on the entanglement entropy by the number entropy in non-interacting fermionic systems", *SciPost Phys.* **8**, 083 (2020).
- [83] M. Kiefer-Emmanouilidis, R. Unanyan, M. Fleischhauer, and J. Sirker, "Evidence for unbounded growth of the number entropy in many-body localized phases", *Phys. Rev. Lett.* **124**, 243601 (2020).
- [84] M. Kiefer-Emmanouilidis, R. Unanyan, M. Fleischhauer, and J. Sirker, "Slow delocalization of particles in many-body localized phases", *Phys. Rev. B* **103**, 024203 (2021).
- [85] O. Blondeau-Fournier and B. Doyon, "Expectation values of twist fields and universal entanglement saturation of the free massive boson", *J. Phys. A: Math. Theor.* **50**, 10.1088/1751-8121/aa7492 (2016).
- [86] E. Cornfeld and E. Sela, "Entanglement entropy and boundary renormalization group flow: Exact results in the Ising universality class", *Phys. Rev. B* **96**, 075153 (2017).
- [87] S. L. Lukyanov and A. B. Zamolodchikov, "Exact expectation values of local fields in quantum sine-Gordon model", *Nucl. Phys. B* **493**, 571{587 (1997).
- [88] L. Chim and A. B. Zamolodchikov, "Integrable field theory of q state Potts model with  $0 < q < 4$ ", *Int. J. Mod. Phys. A* **7**, 5317{5336 (1992).
- [89] M. Sato, T. Miwa, and M. Jimbo, "Studies on Holonomic Quantum Fields. 1.", *Publ. Res. Inst. Math. Sci. Kyoto* **14**, 223{267 (1978).
- [90] A. B. Zamolodchikov, "Integrals of Motion in Scaling Three State Potts Model Field Theory", *Int. J. Mod. Phys. A* **3**, 743{750 (1988).
- [91] G. Del no and J. Cardy, "Universal amplitude ratios in the two-dimensional q-state potts model and percolation from quantum field theory", *Nucl. Phys. B* **519**, 551{578 (1998).

- [92] A. B. Zamolodchikov and A. B. Zamolodchikov, "Factorized s-matrices in two dimensions as the exact solutions of certain relativistic quantum field theory models", *Annals of Physics* **120**, 253{291 (1979).
- [93] L. D. Faddeev, "Quantum completely integral models of field theory", *Sov. Sci. Rev. C* **1**, 107{155 (1980).
- [94] V. A. Fateev and A. B. Zamolodchikov, "Parafermionic Currents in the Two-Dimensional Conformal Quantum Field Theory and Selfdual Critical Points in  $Z(n)$  Invariant Statistical Systems", *Sov. Phys. JETP* **62**, 215{225 (1985).
- [95] G. Del no, "Fields, particles and universality in two dimensions", *Annals Phys.* **360**, 477{519 (2015).
- [96] R. Koberle and J. A. Swieca, "Factorizable  $Z(N)$  models", *Phys. Lett. B* **86**, 209{210 (1979).
- [97] P. Di Francesco, P. Mathieu, and D. Senechal "Conformal Field Theory, Graduate Texts in Contemporary Physics (Springer-Verlag, New York, 1997).
- [98] O. Castro-Alvaredo, B. Doyon, and E. Levi, "Arguments towards a c-theorem from branch-point twist elds", *J. Phys. A Math. Theor.* **44**, 10.1088/1751-8113/44/49/492003 (2011).
- [99] E. Levi, "Composite branch-point twist elds in the Ising model and their expectation values", *J. Phys. A* **45**, 275401 (2012).
- [100] D. Bianchini, O. A. Castro-Alvaredo, B. Doyon, E. Levi, and F. Ravanini, "Entanglement Entropy of Non Unitary Conformal Field Theory", *J. Phys. A* **48**, 04FT01 (2015).
- [101] D. Bianchini, O. A. Castro-Alvaredo, and B. Doyon, "Entanglement Entropy of Non-Unitary Integrable Quantum Field Theory", *Nucl. Phys. B* **896**, 835{880 (2015).
- [102] O. A. Castro-Alvaredo, "Massive Corrections to Entanglement in Minimal  $E_8$  Toda Field Theory", *SciPost Phys.* **2**, 008 (2017).
- [103] O. A. Castro-Alvaredo, M. Lencsés, I. M. Szecsenyi, and J. Viti, "Entanglement Oscillations near a Quantum Critical Point", *Phys. Rev. Lett.* **124**, 230601 (2020).
- [104] O. A. Castro-Alvaredo, C. De Fazio, B. Doyon, and I. M. Szecsenyi, "Entanglement Content of Quasiparticle Excitations", *Phys. Rev. Lett.* **121**, 170602 (2018).
- [105] O. A. Castro-Alvaredo, C. De Fazio, B. Doyon, and I. M. Szecsenyi, "Entanglement content of quantum particle excitations. Part II. Disconnected regions and logarithmic negativity", *JHEP* **11**, 058 (2019).
- [106] O. A. Castro-Alvaredo, C. De Fazio, B. Doyon, and I. M. Szecsenyi, "Entanglement Content of Quantum Particle Excitations III. Graph Partition Functions", *J. Math. Phys.* **60**, 082301 (2019).
- [107] O. A. Castro-Alvaredo and B. Doyon, "Bi-partite entanglement entropy in massive QFT with a boundary: The Ising model", *J. Stat. Phys.* **134**, 105{145 (2009).
- [108] O. A. Castro-Alvaredo and E. Levi, "Higher particle form factors of branch point twist elds in integrable quantum field theories", *J. Phys. A Math. Theor.* **44**, 255401 (2011).
- [109] E. Levi, O. A. Castro-Alvaredo, and B. Doyon, "Universal corrections to the entanglement entropy in gapped quantum spin chains: a numerical study", *Phys. Rev. B* **88**, 094439 (2013).

- [110] O. Blondeau-Fournier, O. A. Castro-Alvaredo, and B. Doyon, "Universal scaling of the logarithmic negativity in massive quantum field theory", *J. Phys. A* **49**, 125401 (2016).
- [111] O. A. Castro-Alvaredo, M. Lenc es, I. M. Szecsenyi, and J. Viti, "Entanglement Dynamics after a Quench in Ising Field Theory: A Branch Point Twist Field Approach", *JHEP* **12**, 079 (2019).
- [112] V. A. Fateev, V. V. Postnikov, and Y. P. Pugai, "On scaling fields in  $Z(N)$  Ising models", *JETP Lett.* **83**, 172{178 (2006).
- [113] B. Estienne, Y. Ikhlef, and A. Morin-Duchesne, "Finite-size corrections in critical symmetry-resolved entanglement", *SciPost Phys.***10**, 054 (2021).
- [114] A. Belin, L.-Y. Hung, A. Maloney, S. Matsuura, R. C. Myers, and T. Sierens, "Holographic Charged Renyi Entropies", *JHEP* **12**, 059 (2013).
- [115] P. Caputa, G. Mandal, and R. Sinha, "Dynamical entanglement entropy with angular momentum and  $U(1)$  charge", *JHEP* **11**, 052 (2013).
- [116] P. Caputa, M. Nozaki, and T. Numasawa, "Charged Entanglement Entropy of Local Operators", *Phys. Rev. D* **93**, 105032 (2016).
- [117] J. S. Dowker, "Conformal weights of charged Renyi entropy twist operators for free scalar fields in arbitrary dimensions", *J. Phys. A* **49**, 145401 (2016).
- [118] J. S. Dowker, "Charged Renyi entropies for free scalar fields", *J. Phys. A* **50**, 165401 (2017).
- [119] H. Shapourian, K. Shiozaki, and S. Ryu, "Partial time-reversal transformation and entanglement negativity in fermionic systems", *Phys. Rev. B* **95**, 165101 (2017).
- [120] H. Shapourian, P. Ruggiero, S. Ryu, and P. Calabrese, "Twisted and untwisted negativity spectrum of free fermions", *SciPost Phys.***7**, 037 (2019).
- [121] B. Doyon, "Bipartite entanglement entropy in massive two-dimensional quantum field theory", *Phys. Rev. Lett.* **102**, 031602 (2009).
- [122] V. A. Fateev and A. B. Zamolodchikov, "Integrable perturbations of  $Z_N$  parafermion models and the  $O(3)$  sigma model", *Phys. Lett. B* **271**, 91{100 (1991).
- [123] A. Jafarizadeh and M. A. Rajabpour, "Bipartite entanglement entropy of the excited states of free fermions and harmonic oscillators", *Phys. Rev. B* **100**, 165135 (2019).
- [124] J. Zhang and M. Rajabpour, "Excited state Renyi entropy and subsystem distance in two-dimensional non-compact bosonic theory. part i. single-particle states", *JHEP* **2020**, 10.1007/JHEP12(2020)160 (2020).
- [125] J. Zhang and M. A. Rajabpour, "Universal Renyi entanglement entropy of quasiparticle excitations", *EPL* **135**, 60001 (2021).
- [126] J. Zhang and M. A. Rajabpour, "Corrections to universal Renyi entropy in quasiparticle excited states of quantum chains", *J. Stat. Mech.***2109**, 093101 (2021).
- [127] J. Zhang and M. Rajabpour, "Excited state Renyi entropy and subsystem distance in two-dimensional non-compact bosonic theory. part ii. multi-particle states", *JHEP* **2021**, 10.1007/JHEP08(2021)106 (2021).
- [128] J. Zhang and M. Rajabpour, "Entanglement of magnon excitations in spin chains", *JHEP* **2022**, 10.1007/JHEP02(2022)072 (2022).

- [129] J. Angel-Ramelli, "Entanglement Entropy of Excited States in the Quantum Lifshitz Model", *J. Stat. Mech.* **2101**, 013102 (2021).
- [130] G. Mussardo and J. Viti, "Large  $L$  Limit of the entanglement entropy", *Phys. Rev. A* **105**, 032404 (2022).
- [131] J. Mölter, T. Barthel, U. Schollwöck, and V. Alba, "Bound states and entanglement in the excited states of quantum spin chains", *J. Stat. Mech.* **1410**, P10029 (2014).
- [132] F. C. Alcaraz, M. I. Berganza, and G. Sierra, "Entanglement of low-energy excitations in Conformal Field Theory", *Phys. Rev. Lett.* **106**, 201601 (2011).
- [133] B. Pozsgay and G. Takacs, "Form factors in finite volume I: form factor bootstrap and truncated conformal space", *Nucl. Phys. B* **788**, 167{208 (2008).
- [134] B. Pozsgay and G. Takacs, "Form factors in finite volume. II. Disconnected terms and finite temperature correlators", *Nucl. Phys. B* **788**, 209{251 (2008).
- [135] P. Fonseca and A. Zamolodchikov, "Ward identities and integrable differential equations in the Ising field theory", (2003).
- [136] D. Bernard and A. LeClair, "Differential equations for sine-gordon correlation functions at the free fermion point", *Nucl. Phys. B* **426**, 534{558 (1994).
- [137] E. Witten, "Aps medal for exceptional achievement in research: invited article on entanglement properties of quantum field theory", *Rev. Mod. Phys.* **90**, 045003 (2018).
- [138] M. I. Berganza, F. C. Alcaraz, and G. Sierra, "Entanglement of excited states in critical spin chains", *J. Stat. Mech.* **1201**, P01016 (2012).
- [139] L.-Y. Hung, R. C. Myers, and M. Smolkin, "Twist operators in higher dimensions", *JHEP* **10**, 178 (2014).
- [140] A. Svesko, "Extending charged holographic Renyi entropy", *Class. Quant. Grav.* **38**, 135024 (2021).
- [141] J. Long, "Area law of connected correlation function in higher dimensional conformal field theory", *JHEP* **02**, 110 (2021).
- [142] I. Peschel, "Calculation of reduced density matrices from correlation functions", *J. Phys. A: Math. Gen.* **36**, L205 (2003).
- [143] H. Casini and M. Huerta, "Entanglement and alpha entropies for a massive scalar field in two dimensions", *J. Stat. Mech.* **0512**, P12012 (2005).
- [144] H. Araki, "Relative Entropy of States of Von Neumann Algebras", *Publ. Res. Inst. Math. Sci. Kyoto* 1976, 809{833 (1976).
- [145] H. Casini, E. Teste, and G. Torroba, "Relative entropy and the RG flow", *JHEP* **03**, 089 (2017).
- [146] P. Ruggiero and P. Calabrese, "Relative Entanglement Entropies in 1+1-dimensional conformal field theories", *JHEP* **02**, 039 (2017).
- [147] S. Murciano, P. Ruggiero, and P. Calabrese, "Entanglement and relative entropies for low-lying excited states in inhomogeneous one-dimensional quantum systems", *J. Stat. Mech. Theory Exp.* 2019, 034001 (2019).
- [148] P. Fries and I. A. Reyes, "Entanglement and relative entropy of a chiral fermion on the torus", *Phys. Rev. D* **100**, 105015 (2019).

- [149] Y. O. Nakagawa, G. Sarosi, and T. Ugajin, "Chaos and relative entropy", *JHEP* **07**, 002 (2018).
- [150] S. Hollands, "Relative entropy for coherent states in chiral CFT", *Lett. Math. Phys.* **110**, 713(733) (2020).
- [151] Y. O. Nakagawa and T. Ugajin, "Numerical calculations on the relative entanglement entropy in critical spin chains", *J. Stat. Mech.* **1709**, 093104 (2017).
- [152] H. Casini, S. Grillo, and D. Pontello, "Relative entropy for coherent states from Araki formula", *Phys. Rev. D* **99**, 125020 (2019).
- [153] D. L. Jaeris, A. Lewkowycz, J. Maldacena, and S. J. Suh, "Relative entropy equals bulk relative entropy", *JHEP* **06**, 004 (2016).
- [154] H. Casini, I. Salazar Landea, and G. Torroba, "The g-theorem and quantum information theory", *JHEP* **10**, 140 (2016).
- [155] D. D. Song and E. Winstanley, "Information erasure and the generalized second law of black hole thermodynamics", *Int. J. Theor. Phys.* **47**, 1692(1698) (2008).
- [156] H. Casini, "Relative entropy and the Bekenstein bound", *Class. Quant. Grav.* **25**, 205021 (2008).
- [157] N. Lashkari, "Relative Entropies in Conformal Field Theory", *Phys. Rev. Lett.* **113**, 051602 (2014).
- [158] N. Lashkari, "Modular Hamiltonian for Excited States in Conformal Field Theory", *Phys. Rev. Lett.* **117**, 041601 (2016).
- [159] G. Sarosi and T. Ugajin, "Relative entropy of excited states in two dimensional conformal field theories", *JHEP* **07**, 114 (2016).
- [160] G. Sarosi and T. Ugajin, "Relative entropy of excited states in conformal field theories of arbitrary dimensions", *JHEP* **02**, 060 (2017).
- [161] T. Ugajin, "Mutual information of excited states and relative entropy of two disjoint subsystems in CFT", *JHEP* **10**, 184 (2017).
- [162] H. Casini, M. Huerta, and R. C. Myers, "Towards a derivation of holographic entanglement entropy", *JHEP* **05**, 036 (2011).
- [163] J. Bhattacharya, M. Nozaki, T. Takayanagi, and T. Ugajin, "Thermodynamical Property of Entanglement Entropy for Excited States", *Phys. Rev. Lett.* **110**, 091602 (2013).
- [164] R. Bousso, Z. Fisher, J. Koeller, S. Leichenauer, and A. C. Wall, "Proof of the Quantum Null Energy Condition", *Phys. Rev. D* **93**, 024017 (2016).
- [165] M. Fagotti and F. H. L. Essler, "Reduced density matrix after a quantum quench", *Phys. Rev. B* **87**, 245107 (2013).
- [166] J. Zhang, P. Calabrese, M. Dalmonte, and M. A. Rajabpour, "Lattice Bisognano-Wichmann modular Hamiltonian in critical quantum spin chains", *SciPost Phys. Core* **2**, 007 (2020).
- [167] J. Zhang, P. Ruggiero, and P. Calabrese, "Subsystem trace distance in low-lying states of (1 + 1)-dimensional conformal field theories", *Journal of High Energy Physics* **2019**, 10.1007/JHEP10(2019)181 (2019).
- [168] J. de Boer, V. Godet, J. Kastikainen, and E. Keski-Vakkuri, "Quantum hypothesis testing in many-body systems", *SciPost Phys. Core* **4**, 019 (2021).

- [169] J. Zhang, P. Ruggiero, and P. Calabrese, "Subsystem Trace Distance in Quantum Field Theory", *Phys. Rev. Lett.* **122**, 141602 (2019).
- [170] P. Calabrese, J. Cardy, and E. Tonni, "Entanglement entropy of two disjoint intervals in conformal field theory", *J. Stat. Mech.* **0911**, P11001 (2009).
- [171] P. Calabrese, J. Cardy, and E. Tonni, "Entanglement entropy of two disjoint intervals in conformal field theory II", *J. Stat. Mech.* **1101**, P01021 (2011).
- [172] Z. Li and J.-j. Zhang, "On one-loop entanglement entropy of two short intervals from OPE of twist operators", *JHEP* **05**, 130 (2016).
- [173] T. Dupic, B. Estienne, and Y. Ikhlef, "Entanglement entropies of minimal models from null-vectors", *SciPost Phys.* **4**, 031 (2018).
- [174] A. Klemm and M. G. Schmidt, "Orbifolds by Cyclic Permutations of Tensor Product Conformal Field Theories", *Phys. Lett. B* **245**, 53{58 (1990).
- [175] T. Palmai, "Excited state entanglement in one dimensional quantum critical systems: Extensivity and the role of microscopic details", *Phys. Rev. B* **90**, 161404 (2014).
- [176] T. Palmai, "Entanglement Entropy from the Truncated Conformal Space", *Phys. Lett. B* **759**, 439{445 (2016).
- [177] E. M. Brehm and M. Broccoli, "Correlation functions and quantum measures of descendant states", *JHEP* **04**, 227 (2021).
- [178] L. Taddia, J. C. Xavier, F. C. Alcaraz, and G. Sierra, "Entanglement entropies in conformal systems with boundaries", *Phys. Rev. B* **88**, 075112 (2013).
- [179] L. Taddia, F. Ortolani, and T. Palmai, "Renyi entanglement entropies of descendant states in critical systems with boundaries: conformal field theory and spin chains", *J. Stat. Mech.* **1609**, 093104 (2016).
- [180] L. S. Levitov and G. B. Lesovik, "Charge distribution in quantum shot noise", *JETP Letters* **58**, 230{235 (1993).
- [181] I. Klich and L. Levitov, "Quantum Noise as an Entanglement Meter", *Phys. Rev. Lett.* **102**, 100502 (2009).
- [182] D. Gioev and I. Klich, "Entanglement Entropy of Fermions in Any Dimension and the Widom Conjecture", *Phys. Rev. Lett.* **96**, 100503 (2006).
- [183] R. Bonsignori, P. Ruggiero, and P. Calabrese, "Symmetry resolved entanglement in free fermionic systems", *J. Phys. A* **52**, 475302 (2019).
- [184] J. Cardy and P. Calabrese, "Unusual Corrections to Scaling in Entanglement Entropy", *J. Stat. Mech.* **1004**, P04023 (2010).
- [185] S. Fraenkel and M. Goldstein, "Symmetry resolved entanglement: exact results in 1d and beyond", *J. Stat. Mech. Theory Exp.* **2020** (2019).
- [186] J. Zhang and P. Calabrese, "Subsystem distance after a local operator quench", *JHEP* **02**, 056 (2020).
- [187] I. Peschel and V. Eisler, "Reduced density matrices and entanglement entropy in free lattice models", *J. Phys. A: Math. Theor.* **42**, 504003 (2009).
- [188] R. Balian and E. Brezin, "Nonunitary bogoliubov transformations and extension of wick's theorem", *Nuovo Cim. B* **64**, 37{55 (1969).

- [189] M. Fagotti and P. Calabrese, "Entanglement entropy of two disjoint blocks in XY chains", *J. Stat. Mech.* **1004**, P04016 (2010).
- [190] C. Bachas, J. de Boer, R. Dijkgraaf, and H. Ooguri, "Permeable conformal walls and holography", *JHEP* **06**, 027 (2002).
- [191] E. M. Brehm and I. Brunner, "Entanglement entropy through conformal interfaces in the 2D Ising model", *JHEP* **09**, 080 (2015).
- [192] C. Holzhey, F. Larsen, and F. Wilczek, "Geometric and renormalized entropy in conformal field theory", *Nucl. Phys. B* **424**, 443{467 (1994).
- [193] J. Cardy and E. Tonni, "Entanglement hamiltonians in two-dimensional conformal field theory", *J. Stat. Mech.* **1612**, 123103 (2016).
- [194] V. Alba, P. Calabrese, and E. Tonni, "Entanglement spectrum degeneracy and the Cardy formula in 1+1 dimensional conformal field theories", *J. Phys. A* **51**, 024001 (2018).
- [195] K. Ohmori and Y. Tachikawa, "Physics at the entangling surface", *J. Stat. Mech.* **1504**, P04010 (2015).
- [196] M. Gutperle and J. D. Miller, "Entanglement entropy at CFT junctions", *Phys. Rev. D* **95**, 106008 (2017).
- [197] C. Bachas, I. Brunner, and D. Roggenkamp, "Fusion of Critical Defect Lines in the 2D Ising Model", *J. Stat. Mech.* **1308**, P08008 (2013).
- [198] C. Bachas, I. Brunner, and D. Roggenkamp, "A worldsheet extension of  $O(d,d;Z)$ ", *JHEP* **10**, 039 (2012).
- [199] P. Calabrese, M. Mintchev, and E. Vicari, "Entanglement Entropy of Quantum Wire Junctions", *J. Phys. A* **45**, 105206 (2012).
- [200] K. Shiozaki, H. Shapourian, K. Gomi, and S. Ryu, "Many-body topological invariants for fermionic short-range entangled topological phases protected by antiunitary symmetries", *Phys. Rev. B* **98**, 035151 (2018).
- [201] H. Shapourian and S. Ryu, "Entanglement negativity of fermions: monotonicity, separability criterion, and classification of few-mode states", *Phys. Rev. A* **99**, 022310 (2019).
- [202] H. Shapourian and S. Ryu, "Finite-temperature entanglement negativity of free fermions", *J. Stat. Mech.* **1904**, 043106 (2019).
- [203] V. Eisler and Z. Zimboras, "On the partial transpose of fermionic gaussian states", *New J. Phys.* **17**, 053048 (2015).
- [204] S. Murciano, R. Bonsignori, and P. Calabrese, "Symmetry decomposition of negativity of massless free fermions", *SciPost Phys* **10**, 111 (2021).
- [205] E. Cornfeld, E. Sela, and M. Goldstein, "Measuring Fermionic Entanglement: Entropy, Negativity, and Spin Structure", *Phys. Rev. A* **99**, 062309 (2019).
- [206] S. Murciano, V. Vitale, M. Dalmonte, and P. Calabrese, "Negativity hamiltonian: an operator characterization of mixed-state entanglement", *Phys. Rev. Lett.* **128**, 140502 (2022).
- [207] P. Calabrese, J. Cardy, and E. Tonni, "Entanglement negativity in quantum field theory", *Phys. Rev. Lett.* **109**, 130502 (2012).

- [208] P. Calabrese, J. Cardy, and E. Tonni, "Entanglement negativity in extended systems: A field theoretical approach", *J. Stat. Mech.* **1302**, P02008 (2013).
- [209] M. Gruber and V. Eisler, "Time evolution of entanglement negativity across a defect", *J. Phys. A: Math. Theor.* **53**, 205301 (2020).
- [210] P. Ruggiero, V. Alba, and P. Calabrese, "Negativity spectrum of one-dimensional conformal field theories", *Phys. Rev. B* **94**, 195121 (2016).
- [211] P. Calabrese, M. Mintchev, and E. Vicari, "The entanglement entropy of one-dimensional gases", *Phys. Rev. Lett.* **107**, 020601 (2011).
- [212] P. Calabrese, M. Mintchev, and E. Vicari, "The Entanglement entropy of 1D systems in continuous and homogenous space", *J. Stat. Mech.* **1109**, P09028 (2011).
- [213] B. Bellazzini and M. Mintchev, "Quantum Fields on Star Graphs", *J. Phys. A* **39**, 11101{11118 (2006).
- [214] P. Calabrese, P. Le Doussal, and S. N. Majumdar, "Random matrices and entanglement entropy of trapped fermi gases", *Phys. Rev. A* **91**, 012303 (2015).
- [215] E. Vicari, "Quantum dynamics and entanglement in one-dimensional fermi gases released from a trap", *Phys. Rev. A* **85**, 062324 (2012).
- [216] J. Zinn-Justin, "Quantum field theory and critical phenomena, Vol. 77, International Series of Monographs on Physics (Oxford University Press, Apr. 2021).
- [217] X. Wen, Y. Wang, and S. Ryu, "Entanglement evolution across a conformal interface", *J. Phys. A Math. Theor.* **51**, 10.1088/1751-8121/aab561 (2018).
- [218] V. Eisler and I. Peschel, "Entanglement in fermionic chains with interface defects", *Ann. Phys. (Berlin)* **522**, 679 (2010).
- [219] P. Calabrese and J. Cardy, "Evolution of Entanglement Entropy in One-Dimensional Systems", *J. Stat. Mech.: Theor. Exp.* **4**, 10.1088/1742-5468/2005/04/P04010 (2005).
- [220] M. Fagotti and P. Calabrese, "Evolution of entanglement entropy following a quantum quench: Analytic results for the XY chain in a transverse magnetic field", *Phys. Rev. A* **78**, 10.1103/PhysRevA.78.010306 (2008).
- [221] V. Alba and P. Calabrese, "Entanglement and thermodynamics after a quantum quench in integrable systems", *Proc. Natl. Acad. Sci.* **114**, 10.1073/pnas.1703516114 (2016).
- [222] R. Modak, V. Alba, and P. Calabrese, "Entanglement revivals as a probe of scrambling in finite quantum systems", *J. Stat. Mech.: Theor. Exp.* **2020**, 083110 (2020).
- [223] G. D. V. Del Vecchio, B. Doyon, and P. Ruggiero, "Entanglement entropy entropies from ballistic fluctuation theory: the free fermionic case", arXiv preprint arXiv:2301.02326 (2023).
- [224] S. Scopa, A. Krajenbrink, P. Calabrese, and J. Dubail, "Exact entanglement growth of a one-dimensional hard-core quantum gas during a free expansion", *Journal of Physics A: Mathematical and Theoretical* **54**, 10.1088/1751-8121/ac20ee (2021).
- [225] M. Ljubotina, S. Sotiriadis, and T. Prosen, "Non-equilibrium quantum transport in presence of a defect: the non-interacting case", *SciPost Phys.* **6**, 004 (2019).
- [226] S. Fraenkel and M. Goldstein, "Extensive Long-Range Entanglement in a Nonequilibrium Steady State", (2022).

- [227] G. Gouraud, P. L. Doussal, and G. Schehr, "Stationary time correlations for fermions after a quench in the presence of an impurity", arXiv preprint arXiv:2211.15447 (2022).
- [228] T. Antal, Z. Racz, A. Rakos, and G. M. Schatz, "Transport in the XX chain at zero temperature: emergence of  $\alpha$  at magnetization profiles", *Phys. Rev. E* **59**, 4912{4918 (1999).
- [229] V. Alba, B. Bertini, and M. Fagotti, "Entanglement evolution and generalised hydrodynamics: interacting integrable systems", *SciPost Phys.* **7**, 005 (2019).
- [230] B. Bertini, K. Klobas, V. Alba, G. Lagnese, and P. Calabrese, "Growth of Renyi Entropies in Interacting Integrable Models and the Breakdown of the Quasiparticle Picture", *Phys. Rev. X* **12**, 031016 (2022).
- [231] V. Alba and P. Calabrese, "Quench action and Renyi entropies in integrable systems", *Phys. Rev. B* **96**, 115421 (2017).
- [232] F. Ares, S. Scopa, and S. Wald, "Entanglement dynamics of a hard-core quantum gas during a Joule expansion", *J. Phys. A* **55**, 375301 (2022).
- [233] S. Scopa, P. Calabrese, and J. Dubail, "Exact hydrodynamic solution of a double domain wall melting in the spin-1/2 XXZ model", *SciPost Phys.* **12**, 207 (2022).
- [234] J. Dubail, J.-M. Stephan, J. Viti, and P. Calabrese, "Conformal field theory for inhomogeneous one-dimensional quantum systems: the example of non-interacting Fermi gases", *SciPost Phys.* **2**, 002 (2017).
- [235] M. Collura, A. De Luca, P. Calabrese, and J. Dubail, "Domain wall melting in the spin- $\frac{1}{2}$  XXZ spin chain: Emergent Luttinger liquid with a fractal quasiparticle charge", *Phys. Rev. B* **102**, 180409 (2020).
- [236] P. Ruggiero, P. Calabrese, B. Doyon, and J. Dubail, "Quantum generalized hydrodynamics", *Phys. Rev. Lett.* **124**, 140603 (2020).
- [237] S. Scopa and D. X. Horvath, "Exact hydrodynamic description of symmetry-resolved Renyi entropies after a quantum quench", *J. Stat. Mech.* **2208**, 083104 (2022).
- [238] P. Ruggiero, Y. Brun, and J. Dubail, "Conformal field theory on top of a breathing one-dimensional gas of hard core bosons", *SciPost Phys.* **6**, 051 (2019).
- [239] P. Ruggiero, P. Calabrese, B. Doyon, and J. Dubail, "Quantum generalized hydrodynamics of the tonks-girardeau gas: density fluctuations and entanglement entropy", *J. Stat. Mech. Theory Exp.* **55**, 024003 (2021).
- [240] M. Gruber and V. Eisler, "Entanglement spreading after local fermionic excitations in the XXZ chain", *SciPost Phys.* **10**, 005 (2021).
- [241] B. Jin and V. Korepin, "Quantum spin chain, toeplitz determinants and shur-hartwig conjecture", *JSTAT* **116**, 10.1023/B:JOSS.0000037230.37166.42 (2003).
- [242] P. Calabrese and F. H. L. Essler, "Universal corrections to scaling for block entanglement in spin-1/2 xx chains", *J. Stat. Mech.: Theor. Exp.* **2010**, P08029 (2010).
- [243] H. Casini, M. Huerta, J. M. Magan, and D. Pontello, "Entropic order parameters for the phases of qft", *Journal of High Energy Physics* **2021**, 1{98 (2021).
- [244] H. Casini, S. Grillo, and D. Pontello, "Relative entropy for coherent states from araki formula", *Phys. Rev. D* **99**, 125020 (2019).

- [245] H. Casini, M. Huerta, and J. A. Rosabal, "Remarks on entanglement entropy for gauge fields", *Phys. Rev. D* **89**, 085012 (2014).
- [246] E. Ilievski, J. Nardis, B. Wouters, J.-S. Caux, F. Essler, and T. Prosen, "Complete generalized gibbs ensembles in an interacting theory", *PRL* **115**, 10.1103/PhysRevLett.115.157201 (2015).
- [247] B. Doyon, G. Perfetto, T. Sasamoto, and T. Yoshimura, "Ballistic macroscopic fluctuation theory", arXiv preprint arXiv:2206.14167 (2022).
- [248] B. Doyon, G. Perfetto, T. Sasamoto, and T. Yoshimura, "Emergence of hydrodynamic spatial long-range correlations in nonequilibrium many-body systems", arXiv preprint arXiv:2210.10009 (2022).